NASA Contractor Report 191058

LOX/Hydrocarbon Rocket Engine Analytical Design Methodology Development and Validation

Jerry L. Pieper and Richard E. Walker
Aerojet Propulsion Division
Sacramento, California

May 1993

Prepared for
Lewis Research Center
Under Contract NAS3–25556

NASA
National Aeronautics and
Space Administration

LOX/HYDROCARBON ROCKET ENGINE ANALYTICAL DESIGN METHODOLOGY DEVELOPMENT AND VALIDATION

(Contract NAS 3-25556)

Final Report

VOLUME I
EXECUTIVE SUMMARY AND TECHNICAL NARRATIVE

Prepared
For

NASA/Lewis Research Center
21000 Brookpark Road
Cleveland, Ohio 44135

Prepared By:

J.L. Pieper
Project Engineer

Approved By:

Bryce L. Reimer
Program Manager

Aerojet Propulsion Division
P.O. Box 13222
Sacramento, California 95813-6000

ACKNOWLEDGEMENT

The analytical Design Methodology development activity described in this report was performed by the Combustion Analysis Group within the Aerojet Propulsion Division (APD) Engineering Analysis Department. Mr Jeff Muss was the principal investigator for the development of the ROCket Combustor Interactive Design (ROCCID) computer code. Dr. Thong Van Nguyen and Yuriko Jones contributed to the development and checkout of the combustion stability design iteration within ROCCID. Mr. Curtis Johnson of Software and Engineering Associates (SEA) Inc. developed the Interactive Front End (IFE) computer code contained within ROCCID. The SEA Inc. work was performed under subcontract to APD and their contribution is gratefully acknowledged. Numerous analysis models, developed and available throughout the industry, have been used within the ROCCID computer program. A description of these models, the source for their development and the contracting agency are included in this report. These analysis models are the engine of ROCCID and this industry-wide contribution is gratefully acknowledged.

The ROCCID validation effort was conducted by design, fabrication and test teams within the Aerojet organization. The design team consisted of Jim Price, Dick Walker, Jeff Muss, Roger Ishikawa, Fred Inouye, Ernie Demeter and Lance Myers. The fabrication operation in support of this program was successfully planned, coordinated and monitored by Lance Myers of Aerojet's Development Operations. Subcontract management was ably performed by Ray Haynes and Craig Duey of Aerojet. A special note of appreciation is due Lance Myers and Ken Gustafson who performed the critical copper injector faceplate brazing process for the two injector cores. The test team consisted of Jim Wilkins, Paul Hill, Jack Standen and Carl Vickers who were responsible for the successful test program in the Aerojet E-Area test zone and Dick Walker, Jeff Muss, Thong Nguyen and Karen Niija for test analysis. A special thanks to Glenn Dunn who provided the project engineering skills during the critical test phase.

Aerojet project managers for this program included Marvin Young, Art Kobayashi, Reed Jenkins and Bryce Reimer and their contributions are gratefully acknowledged. Finally, the contributions of the NASA Lewis Review Team consisting of Mark Klem, program manager, Kevin Breisacher and Richard Priem are appreciated and contributed to the success and quality of the ROCCID Methodology, hardware designs and validation test plan.

TABLE OF CONTENTS

		Page
ACKNOWLEDGEMENT		iii
I.	INTRODUCTION	1
II.	EXECUTIVE SUMMARY	3
III.	CONCLUSIONS AND RECOMMENDATIONS	35
IV	TECHNICAL NARRATIVE	38
	A. Data/Stability Model Survey	38
	B. The Rocket Combustor Interactive Design Methodology	45
	C. Application of the ROCCID Methodology	56
	D. ROCCID Validation Test Plan Development	66
	E. Validation Hardware Design	91
	F. Hardware Fabrication	108
	G. Validation Testing	118
	H. Test Analysis and ROCCID Methodology Assessment	153
V.	REFERENCES	174

FIGURE LIST

Figure No.		Page
1	Major Components of ROCCID Include the Interactive Front End, the Point Analysis Evaluation and the Point Design Evaluation	4
2	Facility Operating Limitations	11
3	Expected Combustion Stability for the ROCCID Validation Hardware	15
4	The ROCCID Test Validation Engine Assembly Installed on Test Stand E-4	16
5	The Injector Core With Its Faceplate Installed for Brazing	18
6	The OFO Triplet Element Was Designed to ROCCID Specification	19
7	ROCCID Validation Test Points	20
8	Overview of Test Logic	22
9	ROCCID Validation Test Results Indicate Stable and Unstable Operating Regions	26
10	ROCCID Predicted a Somewhat Larger Zone of Unstable Operation Than Was Observed Experimentally	27
11	Comparison of Unanchored ROCCID Predictions and Test Results-Isp-Based ERE	30
12	Comparison of Unanchored ROCCID Predictions and Test Results-C* Efficiency	30
13	Good Agreement Observed Between Predicted and Measured Chamber Static Pressure Profiles at Near Stoichrometric Mixture Ratio	31
14	Poor Agreement Observed Between Predicted and Measured Chamber Static Pressure Profiles at Very Low and High Mixture Ratio	32
15	ROCCID Injector Cold Flow Propellant Spray Fan Formation	34
16	ROCCID Performs a Majority of the Combustor Design Iterations to Meet Combustion Stability and Performance Requirements	46
17	Major Components of ROCCID Include the Interactive Front End, Point analysis, and Point Design Evaluation	48
18	Illustration of the Growth Coefficient λ in Terms of Traditional Combustion Stability Transfer Function Format	52
19	Facility Operating Limitations	58
20	Like Doublet Injector Stability Prediction, Chamber Pressure - 1250 psia; Length = 17 in., No Damping	62
21	Fine Triplet 1L Mode Stability Map Showing Values of λ at Various Points as Well as Points Predicted to Be Extremely Stable	62
22	Fine Triplet 1T Mode Stability Map Showing Values of λ at Various Points as Well as Points Predicted to Be Extremely Stable	62

FIGURE LIST (Continued)

Figure No.		Page
23	Fine Triplet 2T Mode Stability Map Showing Values of λ at Various Points as Well as Points Predicted to Be Extremely Stable	63
24	Fine Triplet 1T Mode Stability Map Showing Values of λ at Various Points as Well as Points Predicted to Be Extremely Stable	63
25	Variation of Growth Coefficient λ With N and τ	63
26	Overview of Test Logic	70
27	Block 1 Test Logic and Success Criteria (Chamber With 1/4 Wave Damping)	72
28	Block 1 Tests Will Define Stable Operating Region With an Acoustic Cavity and Evaluate Chug and L Mode Instabilities	74
29	Block 1 - Test Series A Logic	75
30	Block 1 - Test Series B Logic	76
31	Block 1 - Test Series C Logic	77
32	Stability Predictions at Low Chamber Pressure Show Large Influence of Injection Coupling	78
33	Block 1 - Test Series D Logic	80
34	Block 2A - Test Series Logic	81
35	Block 2A - Tests Will Define Stable and Unstable Operating Regions Without an Acoustic Cavity	83
36	Block 3 Test Logic	86
37	Block 3A Tests Were Planned to Reconfirm Stable Operating Regions With an Acoustic Cavity and Define Regions of Unstable Operation With the Cavity	88
38	The Drawing Tree for the ROCCID Test Validation Thrust Chamber	92
39	The Engine Assembly for ROCCID Test Validation	93
40	The ROCCID Test Validation Engine Assembly Installed on Test Stand E-4	95
41	The Injector Assembly Used an Existing Fuel Manifold and Injector Core and a New Injector Faceplate	96
42	The Injector Flange and Outer Fuel Manifold was Available From a Previous Phillips Laboratory Program	97
43	An Existing Injector Core was Used	98
44	The LOX/Hydrocarbon Injector Assembly is Test Proven	99
45	A 105-Element OFO Injector Pattern Defined Using ROCCID is Incorporated into a Zirconium Copper Faceplate	101
46	The OFO Triplet Element Was Designed to ROCCID Specification	102
47	A New Thrust Chamber Design was Prepared to Meet ROCCID Validation Requirements	103

FIGURE LIST (Continued)

Figure No.		Page
48	A New Silica Phenolic Liner was Created to Match ROCCID Design Criteria	104
49	A Bituned 1/4 Wave Tube Acoustic Cavity Insert Design	106
50	Bomb Adaptor Design With a Thermal Protection Enhancement	107
51	Provision for Instrumentation Required for Validation	109
52	The Injector Core With its Faceplate Installed for Brazing	111
53	The Injector Core Shown With the LOX Inlet Attached	112
54	Bitune - Cavity Configuration Comparison of Actual and Intended Acoustic Cavities for ROCCID Testing	113
55	Blocked - Cavity Configuration	114
56	Monotune Cavity Configuration	115
57	Water Cold Flow Tests Were Conducted to Verify Element Impingement and Flow Resistance	117
58	Overview of Test Logic	121
59	Measured Injector Kw Values Were Consistent Between Tests	128
60	Total Kw Values Were Consistent Between Tests	129
61	Test Operating Conditions	130
62	Calculated Performance Efficiency for Tests With Valid Steady-State Measurements	131
63	Average Acoustic Cavity Gas Temperature Measurements	132
64	Calculations Show Little Effect of Actual Cavity	136
65	Oscillation Component of Chamber Pressure Measured by PCHF1	138
66	Evolution of the Amplitude and Frequency of PCHF1 Measured Chamber Pressure	139
67	Power Spectral Density Analysis of PCHF1 Measured Chamber Pressure	140
68	Waterfall Plot Shows a Resonance at 2T Frequency Appeared and Then Disappear Quickly.	141
69	Power Spectral Density Analysis of Chamber Pressure Show the Existence of a 2T Resonance	142
70	Chamber Pressure Oscillation With 1L Mode During Transient Start-Up of Test 17	144
71	Power Spectral Density Analysis of Chamber Pressure During Transient Start-Up of Test 17 Showed 1L Resonant Frequency of Approximately 1300 Hz	145

FIGURE LIST (Continued)

Figure No.		Page
72	Evolution of the Amplitude and Frequency of Chamber Pressure in Test 21 Shows an Instability Began With a 2T Resonance then Switched to a 1T Resonance	146
73	Power Spectral Analysis for the Early Part of Instability Indicated 2T Resonance	147
74	Evolution of the Amplitude and Frequency of Chamber Pressure in Test 40 Shows the Instability Began With a 1T Mode, Switched to a 2T Mode, Then Switched Back to the 1T Mode	149
75	Higher Resolution Plot of the Evolution of the Amplitude and Frequency of Chamber Pressure in Test 40	150
76	Mean Chamber Pressure and Cavity Temperature vs Time in Test 40	151
77	Power Spectral Analysis of Chamber Pressure Indicated 2T Resonance	152
78	Mean Chamber Pressure vs Time in Test 19, Typical of Unstable-Combustion Tests Which were Shutdown Early by CSM	154
79	Pc-MR Stability Map	155
80	DOP-DFP Stability Map	155
81	Comparison of Unanchored ROCCID Predictions and Test Results - C* Efficiency	158
82	Comparison of Unanchored ROCCID Predictions and Test Results - Isp-Based ERE	159
83	Good Agreement Observed Between Predicted and Measured Chamber Static Pressure Profiles at Near Stoichiometric Mixture Ratio	161
84	Poor Agreement Observed Between Predicted and Measured Chamber Static Pressure Profiles at Very Low and High Mixture Ratio	162
85	Comparison of ROCCID and Injector Characterization Program Engine Propellant Spray Fan Formation	164
86	Comparison of Unanchored ROCCID Predictions and Test Results Marginal Chug Pc	167
87	ROCCID Validation Test Results Indicate Stable and Unstable Operating Regions	170
88	ROCCID Predicted a Somewhat Larger Zone of Unstable Operation Than Was Observed Experimentally	171

TABLE LIST

Table No.		Page
1	Existing Steady-State Combustion Models Were Evaluated for Use in ROCCID	6
2	Combustion Stability Models Are Included for All Aspects of Stability Modeling	8
3	Injectors Compared Against Rating Criteria	13
4	Planned and Actual Test Conditions	21
5	Comparison Between Calculated Results and Test Data	24
6	Measured and Predicted Validation Engine Performance	29
7	Analyses Model Evaluation Criteria Has Been Developed	40
8	Computer Code Evaluation Summary	41
9	Database Review and Selection	43
10	Combustion Stability Models Are Included for All Aspects of Stability Modeling	50
11	Element Characteristics for Several Conventional Liquid Rocket Injector Elements Modeled Within ROCCID	55
12	Comparison of Selected Nominal Design Parameters	59
13	Injectors Compared Against Rating Criteria	64
14	ROCCID Validation Test Series	67
15	ROCCID Validation Test Matrix	68
16	Block 1 Tests Are Conducted With an Acoustic Cavity	73
17	Block 2A Tests Were Conducted With No Acoustic Damping Damping to Verify Predicted Stable/Unstable Operating Regions	82
18	Block 2B Tests Were Conducted Without an Acoustic Cavity to Provide Data for Acoustic Cavity Redesign	85
19	Block 3 Tests Were Made to Confirm stable Operation With an Acoustic Cavity	87
20	Combustion Stability Data Acquisition Requirements	89
21	Thrust Chamber Performance Data Acquisition Requirements	90
22	ROCCID - Subcomponents	110
23	ROCCID Injector Cold Flow Admittance Values (lbm/sec/psid$^{1/2}$)	118
24	Planned and Actual Test Conditions	120
25	ROCCID Validation Test Data	122
26	Summary of Stable-Combustion Test Results	133
27	Summary of Unstable-Combustion Test Results	134
28	Measured and Predicted Valadation Engine Performance	157
29	ROCCID Calculated Chug Results ROCCID Version 30 July 1991 - Date: 23 October 1991	166
30	Comparison Between Calculated Results and Test Data	168

I. INTRODUCTION

During the past three decades, enormous amounts of resources have been expended in the design and development of Liquid Oxygen/Hydrocarbon and Hydrogen (LOX/HC and LOX/H_2) rocket engines. A significant portion of these resources have been used to develop and demonstrate the performance and combustion stability for each new engine. During these efforts, many analytical and empirical models have been developed that characterize design parameters and combustion processes that influence performance and stability. Many of these models are suitable as design tools, but they have not been assembled into an industry-wide usable analytical design methodology.

An objective of this program was to assemble existing performance and combustion stability models into a usable methodology capable of producing high performing and stable LOX/Hydrocarbon and LOX/Hydrogen propellant booster engines. In the first phase of this program, we focused on developing an analytical design methodology to perform the design tradeoffs leading to an optimized high-performing and stable combustion device. This design methodology, the Rocket Combustor Interactive Design (ROCCID), contains previously developed and available analysis models for characterizing the effects of all critical design and operating parameters on the performance and combustion stability of liquid propellant combustors.

This methodology was released for industry use in May 1991 (Ref. 1) after undergoing a Beta test by potential users, including propulsion contractors, government facilities and interested Universities.

Concurrently, a validation plan for demonstration of the ROCCID capabilities and identification of its shortfalls and limitations was developed. The methodology was applied to develop a combustor design and a detailed test plan was formulated to verify the performance and combustion stability of the combustor compared to that predicted by the ROCCID Methodology.

The validation hardware consisted of a thrust chamber for operation with LOX/RP-1 propellants and containing an injector assembly with 105 OFO triplet elements and a combustion chamber with a silica phenolic liner. The thrust chamber was designed for operation up to chamber pressures of 1,750 psia and over a wide range of mixture ratio (e.g., 1.0 to 10.0). A copper insert was provided to permit operation with and without an acoustic resonator. The basic hardware design is fashioned after a test proven thrust chamber developed and hot fired during a successful program conducted by Aerojet for the Air Force Astronautics Laboratory (Contract F04611-85-C-0100).

Hot fire tests were performed with this thrust chamber resulting in 27 valid tests for direct comparison with the ROCCID methodology predictions. Test results and comparison with the ROCCID based predictions are included in this report.

This program was conducted by the Aerojet Propulsion Division under Contract NAS 3-25556 from the NASA Lewis Research Center. This program was conducted over the period from December 1988 through November 1991. Mark Klem was the NASA program manager during this entire effort.

II. EXECUTIVE SUMMARY

Up to this time, there has been no industry standard methodology to aid in the design and analysis of combustion stable, high performance liquid propellant rocket engine combustion chambers. While NASA design guidelines for injectors, chambers, and stability devices (NASA SP-8089, 8087, and 8113, respectively) were available, designers used their own methodology for developing design features and evaluating effects of design or operating parameter changes on combustion stability and efficiency. This was usually a time consuming process, requiring extensive designer and analysis specialist interaction, and generally dependent upon expensive experimental evaluations with many design iterations.

This problem was addressed during this effort through the development of a user friendly and interactive computer based analytical design methodology for creation of liquid propellant combustor designs that produce both high performance and stable operation. This ROCket Combustor Interactive Design (ROCCID) methodology consists of an assembly of existing industry-wide performance and combustion models linked with an interactive computer logic that allows the user to design a combustor to meet desired performance levels and combustion stability margins.

The development of ROCCID provides a design and analysis tool to reduce future engine development costs. Propulsion contractors and university research centers benefit through access to the best available analysis codes and improved design efficiency from the use of properly linked and adequately documented analysis tools. Efficiency will evolve from a standardization of the combustor design approach. Government agencies also benefit by having a valid tool for evaluation of proposed designs, realistic assessment of performance goals, and effective system optimization early in a development program. ROCCID is already in use in support of the STME engine for the NLS where the consortium formed for that development program has recommended its use.

Methodology Overview

The structure of ROCCID is illustrated in Figure 1. ROCCID contains three main components which are:

1. An interactive front end (IFE) that provides guidance to the user for input setup, input and output control and the generation and maintenance of library files for replay and restart, propellant properties and combustion gas properties.

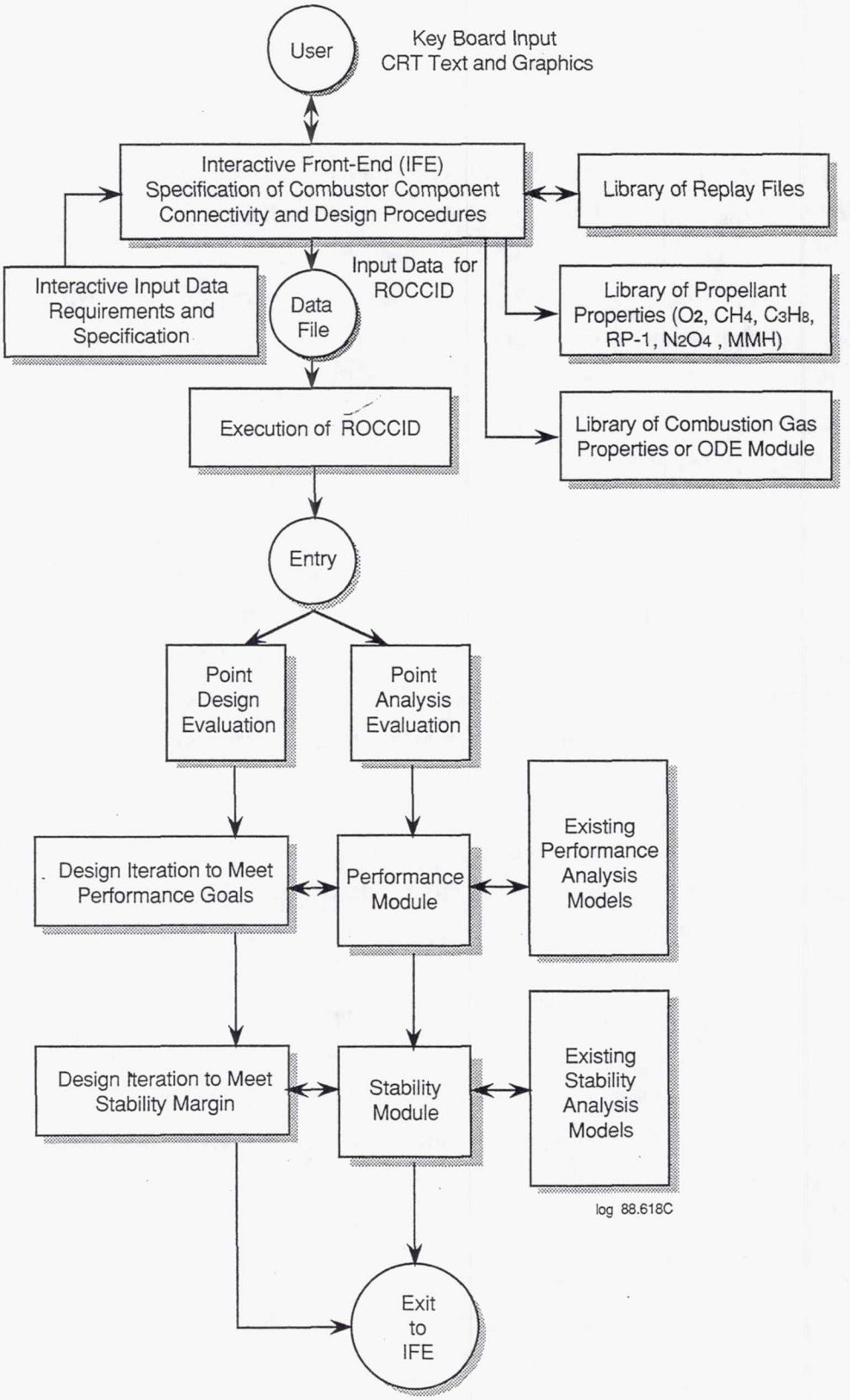

Figure 1. Major Components of ROCCID Include the Interactive Front End, The Point Analysis Evaluation and the Point Design Evaluation

2. A point analysis option that provides performance and combustion stability analysis of existing combustor designs.

3. A point design option that creates the essential combustor design features for a high performance and stable rocket engine from specified requirements.

Both the point analysis and point design options use a library of performance and combustion analysis models selected from an existing and industry-wide inventory. These analysis models are contained within ROCCID in a modular format. This permits the user to access specific models for a specialized sub-analysis or to use two or more models that perform similar functions to define and resolve uncertainties in the particular area of the analysis. Modular construction also permits easier and less costly methodology upgrading as new analysis models are developed or refined.

A steady-state combustion analysis including propellant atomization, vaporization and mixing supplies key input into the performance and stability analyses. Specific models that were reviewed and selected for use in the ROCCID steady-state combustion analysis are described in Table 1.

Four models/correlations for propellant dropsize are included for standard injector elements from showerhead, doublet and triplet impinging elements and shear and swirl concentric tube (coaxial) elements. Dropsizes from all applicable correlations are calculated and displayed for comparison. A user may select any of the calculated values for the steady state combustion analysis or provide another estimated value in their place. Propellant (fuel or oxidizer) vaporization is calculated using the generalized length correlation developed by Priem and Heidmann. Propellant mixing is based on the use of a unielement mixing efficiency value determined from cold flow measurements and adjusted for interelement mixing effects. Currently, this value is supplied by the user, but guidelines for its selection are included.

The combustion stability analysis is made with a large array of models used to calculate the chamber admittance and the burning response magnitudes. These models provide the capability to estimate combustion stability margin for all common types of combustor instabilities including chugging and chamber acoustic coupled (high frequency) modes. ROCCID displays the stability analysis results in terms of the calculated growth coefficient (λ) for the particular acoustic mode of concern. This growth coefficient represents the amount

TABLE 1. EXISTING STEADY-STATE COMBUSTION MODELS WERE EVALUATED FOR USE IN ROCCID

I. Atomization

Model/ Correlation	Developed By Developed For	Approach	Applicable Injection Element Type(s)	Advantages/Disadvantages	Used in ROCCID
Priem TR-67	NASA-LeRC In-House	Derived Empirically From LOX/Heptane Tests	Showerhead, Doublet, Triplet	Propellant Properties Effects Included, Historical Data Base, Limited Off-Design Capability	Yes, as Option
Aerojet Impingement Model	Aerojet NASA-LeRC	Potential Flow/Boundary Layer Breakup Calculation	Doublet, Triplet	Mechanistic, Simple Off-Design Capability Total Time Lags Calculated	Yes, as Option
PLC	Aerojet NASA MSFC	Potential Flow/Boundary Layer Breakup for Gas/Liquid Concentric Tube Elements	Shear Coaxial; Swirl Coaxial	Mechanistic, but Little Historical Basis	Yes, as Option
CICM	Rocketdyne NASA MSFC	Uses Empirical Coefficients for LOX Breakup and Intra-Element Mixing	Shear Coaxial	JANNAF Reference but Difficult to Incorporate and Limited Historical Base	No
SDER	Rocketdyne Phillips Laboratory	Uses Empirical Dropsize Correlations From Hot Wax Experiments	Doublet, Triplets	JANNAF Reference but Contains Known Correlation Problems	No
Dropmix	WJSA Phillips Laboratory	Empirical Dropsize Correlations	Doublet, Triplet; Shear Coaxial	Improved Correlations Over SDER	Yes, as Option

II. Vaporization

Model	Developed By Developed For	Approach	Applicable Propellants & Operating Conditions	Advantages/Disadvantages	Used in ROCCID
SDER	Rocketdyne Phillips Laboratory	Simultaneous Solution of 2-Phase Equations for Gas Flow and Drop Acceleration and Vaporization	All Hydrocarbons with Definable Properties. Sub-Critical and Super-Critical Pressures	Contains Fatal Calculation Problems	No
PCDER	WJSA Phillips Laboratory	Same as SDER	Same As Above	Improved Version of SDER-Runs on PC	No, but Could Be Used Outside ROCCID
Generalized Length	NASA-LeRC In-House	Simplified Correlation of Mechanistic Vaporization Model Calculations	Derived from Subcritical Pressure Results but Has Been Applied Successfully to Supercritical Conditions	Simple, Fast Calculation; Excellent Historical Basis	Yes

III. Mixing

Model	Developed By Developed For	Approach	Applicable Injection Elements	Advantages/Disadvantages	Used in ROCCID
LISP SDER	Rocketdyne Phillips Laboratory	Uses Spray Coefficients Derived from Unielement Cold Flow Tests	Doublet and Triplet Built-In Coefficients	Spray Coefficients Derived From Cavitating Flow Invalid, Time-Consuming Set-Up	No
Dropmix	WJSA Phillips Laboratory	Uses Intra-Element Mixing Efficiency Based on Cold Flow Data Base	All for which Em Correlation Is Available	Simple, Fast Calculation	Yes, as Option
Two Stream Based on Em	Aerojet NASA MSFC	Uses Intra-Element or Inter-Element Em Based on Cold Flow or Hot Fire	All for which Em Correlation Is Available	Simple, Fast Calculation	Yes, as Option
Hersch Turbulent Mixing	NASA-LeRC In-House	Based on Turbulence Intensity	All	Simple, but Does Not Account for Intra-Element and Combustion Effects	No

log 891.232A

of amplification required by the chamber to achieve the condition where the driving required to support the waveform exactly equals the driving response present within the system. Thus a value of $\lambda = 0$ represents a neutral stability condition, $\lambda > 0$ represents an unstable condition and $\lambda<0$ represents a stable operating condition.

The effects of damping devices such as acoustic cavities (1/4 wave tube and helmholtz) and baffles are also considered by these models. A listing of the combustion stability models considered for ROCCID is provided in Table 2.

The performance of the combustor is defined by its energy release efficiency. This accounts for combustion efficiency limitations resulting from incomplete propellant vaporization and/or mixing. The energy release efficiency is calculated using the JANNAF simplified performance procedure as contained in CPIA 246 and the propellant vaporization and mixing limitations from the steady-state combustion analysis. An input file for use in the TDK/BLM computer analysis is also generated that can be used for a rigorous performance analysis of the complete rocket engine as described in CPIA 246.

The design requirements for combustor cooling are established using techniques outside of ROCCID. These requirements may include estimates of fuel film cooling required for chamber and baffle walls, dump cooling off baffle tips, and bulk temperature increases resulting from regenerative cooling of the nozzle chamber and resonator/baffle components. This information is used to calculate the propellant injection temperatures, injection orifice requirements and the local flow injection mixture ratios. This method of accounting for temperature limits of the injector/thrust chamber materials with ROCCID was selected to keep the focus on the combustion stability and performance issues while providing a useful and practical combustor design tool.

Capabilities and Limitations

ROCCID has been specifically formulated to be applicable to combustor designs for LOX/HC, LOX H_2, and N_2O_4/MMH propellants. Propellant and combustion gas properties for LOX/RP-1, LOX/CH_4, LOX/C_3H_8, LOX/H_2, and N_2O_4/MMH are included. Both gas/liquid and liquid/liquid propellant injection are considered. Conventional impinging like doublet and triplet (OFO and FOF) elements, impinging unlike double elements, non-impinging showerhead and coaxial tube elements with or without liquid stream swirl are treated. Injection element

TABLE 2. COMBUSTION MODELS ARE INCLUDED FOR ALL ASPECTS OF STABILITY MODELING

I. CHAMBER RESPONSE

Model	Developed By Developed For	Approach	Applicable Design Features	Advantages/ Disadvantages	Used in ROCCID
HIFI	Aerojet Phillips Laboratory	Linear Perturbation Technique With Mean and Fluctuating Components for Dependent Gas Dynamic Variables	Acoustic Resonators	Mechanistic, Burning Rate and Injection Coupled Extensive Application History	Yes
DIST3D	Colo State Phillips Laboratory	Calculates Baffle Damping Using a Turbulent Boundary Layer Model for Viscous Dissipation	Baffle Height and Blade Distribution Acoustic Resonators as Secondary Damping	Distributed Combustion, Mechanistic, Radial Baffles Only	Yes
FDORC	Colo State Phillips Laboratory	Piecewise Distributed Combustion With Arbitrarily Located Resonators	1/4 Wave Tube and Helmholtz Resonators and Liners	Distributed Combustion, Resonator Location, Mechanistic	Yes

II. BURNING RESPONSE

Model/ Correlation	Developed By Developed For	Approach	Applicable Injector Types	Advantages/ Disadvantages	Used in ROCCID
Reardon-Smith N/τ Correlations	Reardon-Smith JANNAF	Correlation of Empirical N/τ Using a Sensitive Time Lag Model	Doublets, Triplets; Coaxial	Simple Historical Data Base, Non-Mechanistic	Yes, as Option
CRP	Aerojet Phillips Laboratory	Uses Agosta-Hammer Non-Linear Vaporization Response Model	All for Which a Representative Dropsize Exists	Mechanistic, but Can Require Long Run Times	Yes, as Option
Empirical/Damp Growth Rate Correlation	Aerojet Phillips Laboratory	Use Observed Damp or Growth Rates to Infer Combustion Response	All for Which Empirical Growth or Damp Rates Exist	Requires Experimental Data Base but Is a Means for Anchoring Stability Model	Yes, as a Means for Increasing N/τ Data Base

III. INJECTOR RESPONSE

Model/ Correlation	Developed By Developed For	Approach	Applicable Injector Types	Advantages/ Disadvantages	Used in ROCCID
LFCS	Aerojet Phillips Laboratory	Wenzel & Szuch Lumped Parameter	All with Definable Total Timelag	Simple, Good Track Record for Chug Instability	No
INJ	Aerojet NASA-LeRC	Lumped Parameter Analysis with Spacially Varying Acoustic Wave in the Chamber	All with Definable Total Timelag	Computes Injector Response Based on Element Timelag. Dependent on Good Injection Model	Yes
Lewis Non-Linear	NASA-LeRC In-House	Modification of Feiler and Heldmann Feed System Coupled Instability Model to Include Manifold Acoustic Effects	Concentric Tube Elements	Include Flow Response Due to Manifold Acoustics if Important	Yes

log 891.255A

zones for the injector core, barrier and fuel film cooling can be included. For the point design option, design parameters such as contraction ratio (CR) and chamber length (L') are internally defined to provide the best tradeoff between performance and combustion stability. A simple tradeoff between nozzle length and chamber length is also included to optimize engine delivered specific impulse for an envelope limited system. Acoustic damping devices are also recommended and their design features specified to provide the required combustion stability margin. Design tradeoffs for a throttling engine are also performed.

The point design option features an optimization of the injector element design through user interactive operation. Guidelines are provided to aid in injector element selection for a particular application. The quantity of elements and the injector orifice size are calculated through a series of trade studies to satisfy: (1) performance and high frequency combustion stability requirements, (2) chug stability and pressure drop constraints including throttling requirements and (3) basic injection area and combustion chamber size limitations.

This ROCCID methodology has been prepared with certain limitations in order to simplify its construction and guarantee its timely and affordable development. For example, no supersonic nozzle effects are included. Nozzle design and engine specific impulse are determined outside of ROCCID. Precombusted fuel (stage combustion cycle) is not presently considered. Mass addition from ablation, igniters, gas generator dump or transpiration cooling is not modeled. A flat faced injector with one element type in each zone (core, barrier, etc.) is assumed. As previously noted, cooling requirements are defined outside ROCCID, but their effects on performance and stability are considered.

The computer code for ROCCID is operational on VAX 8600 series computers at both Aerojet Propulsion Division in Sacramento and NASA Lewis Research Center in Cleveland. This program was also operational on a SUN computer at SEA, Inc., in Carson City. Interactive graphics for a Tektronics 41XX terminal are also provided. The code has been constructed without machine dependent instructions (except for graphics), but operation on other systems remains to be verified.

ROCCID Demonstration and Verification

The capabilities of ROCCID were demonstrated by using this newly developed methodology to create several combustor configurations some of which were subsequently

designed, fabricated and test fired. These tests results were compared to the performance and combustion stability predictions made by ROCCID during the design formulation. This comparison provided a general assessment of ROCCID capabilities and a means to identify the strength and weaknesses of the methodology.

The propellant combination of LOX/RP-1 was selected for study using ROCCID and for eventual hot fire testing to validate ROCCID capabilities. This propellant was selected because historically, it has proven to be a difficult propellant to provide both stable combustion and high performance.

Normal design propellant injection temperatures of 174.4°R for liquid oxygen and ambient condition (515°R) for RP-1 were selected. These conditions represent normal propellant storage temperatures within the Aerojet test facility and therefore are the most cost effective test conditions.

A nominal design mixture ratio of 2.8 was selected since this approximates an optimum performance design from a thrust chamber performance viewpoint. Note that this mixture ratio value was selected for design purposes only. The effects of mixture ratio variation on a fixed design were evaluated using ROCCID and mixture ratio was a key operating parameter for validation testing.

Thrust chamber size is a key design parameter, particularly from a combustion stability standpoint. The chamber diameter has a direct effect on the resonant frequency of acoustic modes within the chamber. Large chambers appropriate for booster engine application (Dc = 17.5 to 44 in.), have lower resonant frequencies that are more likely to couple with typical combustion responses. On the other hand, subscale chamber diameters of 5.5 and 7.68 in. have been successfully used in the past for combustion stability investigations (see Section IV,C.). For this study, a nominal baseline chamber diameter of 7.68 in. was selected since it is a proven "subscale" design and residual hardware was available.

A contraction ratio of 2:1 that corresponds to a throat diameter of 5.43 in. and nominal design chamber pressure of 1250 psi were selected to provide a large operating chamber pressure variation within the existing hardware and test facility capabilities. The operational envelope of the validation hardware within the Aerojet E-4 test facility is shown in Figure 2. A variation in mixture ratio from approximately 1 to 10 was possible at the nominal chamber pressure of 1250

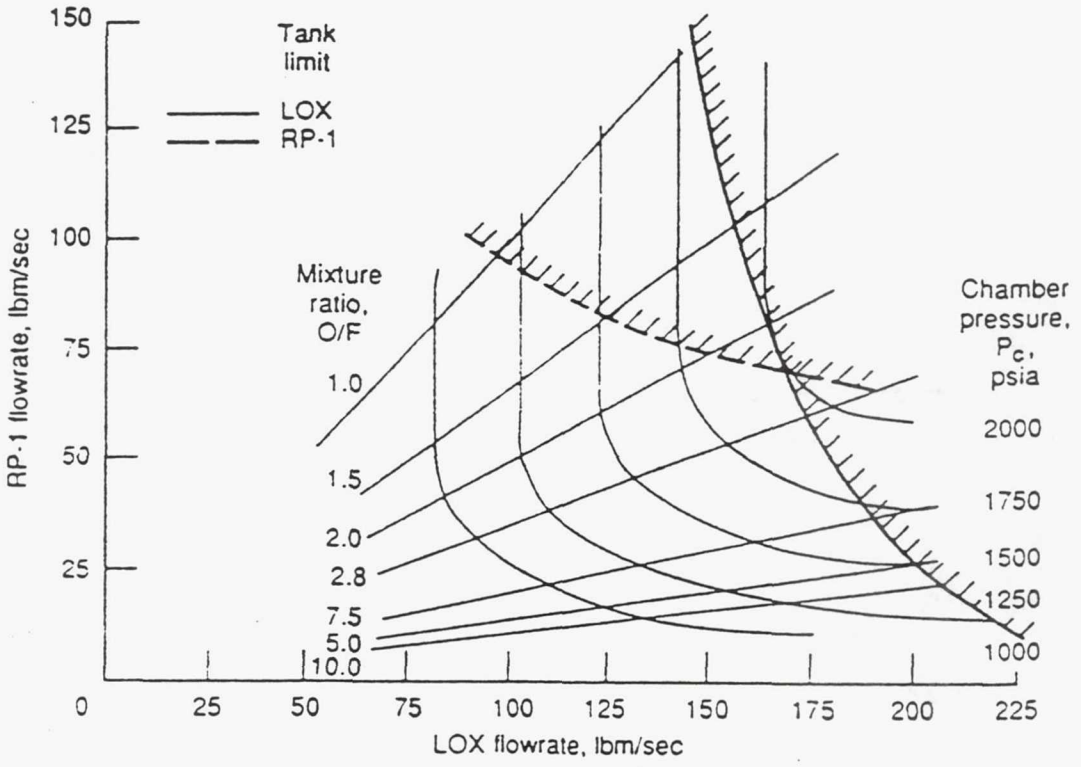

Figure 2. Facility Operating Limitations

psi. A maximum chamber pressure of approximately 1800 psi was achievable at the nominal mixture ratio. The mixture ratio excursion range diminishes as chamber pressure is increased because of the facility run tank pressure limits.

Impinging injector designs were selected for this evaluation since they are most appropriate for liquid/liquid injection. Specifically, the like doublet and OFO triplet elements, both of which are included in ROCCID, were evaluated. The OFO triplet element was selected over the FOF since the propellant density and mixture ratio will result in equal orifice diameters with an OFO element but not with the FOF triplet. From experience, equal orifice diameters are desirable with a triplet element to provide optimum mixing and atomization.

Three injector designs, fine triplet, coarse triplet, and like-on-like doublet, were selected to be evaluated by ROCCID for detail design and testing. Initially, the point design option of ROCCID was used to size the injectors for the nominal operating conditions. Thereafter, the analysis portion of ROCCID was used to perform trade studies on the initial designs. The experience gained from past experimental results were also applied to the analysis. Also from past experience, certain model combinations in ROCCID were used because they produced good results. HIFI was used to analyze the chamber response. Combination of Smith-Readon and Aerojet N/τ correlations were used to analyze the burning response. INJ was used to analyze the injector response.

The injector orifice sizes (diameter) evaluated were 0.090 in. for the fine triplet, 0.159 in. for the coarse triplet, and 0.100 in. LOX and 0.065 in. fuel for the like-on-like doublet. The predicted performance efficiencies for all three injectors were greater than 97 percent so performance did not become a critical concern in the selection process.

Criteria were established to select the best injector design for use in the validation of ROCCID. Because of limited resources, only one thrust chamber design could be selected for design and testing. The criteria were established on the basis of providing the best test of the capabilities of ROCCID. The criteria are provided in Table 3.

The chug stability limits of the three injectors were defined using ROCCID. The fine triplet and the doublet have low chug thresholds at about 300 psi. The coarse triplet has a more undesirable chug threshold at about 600 psi. Considered that the nominal operating pressure is 1250 psi, this higher chug pressure limit for the coarse triplet does not allow for much leeway in throttling the engine to find stable and unstable high frequency stability regions.

The high frequency stability characteristics of the three injectors were also predicted using ROCCID. The coarse triplet was found to be the most stable injector design without acoustic

TABLE 3.

INJECTORS COMPARED AGAINST RATING CRITERIA

Rating Criteria	Injector Configuration		
	Fine O-F-O Triplet	Coarse O-F-O Triplet	Like-on-like; One Doublet
Largest negative and positive growth coefficients for least damped mode without acoustic damping	Most unstable	Most stable	Unstable
Best sensitivity of combustion stability to P_c and O/F	Significant variation with 2T and 1T; stable operation with O/F and P_c	Much larger variation in P_c and O/F required to drive unstable	Good sensitivity with O/F for 1T mode
Greatest change from existing data base	N_c, 39 to 105 D_o, 0.125 to 0.090	N_c, 39 to 48 D_o, 0.125 to 0.159	N_c, 105 to 123 D_o, 0.059 to 0.065
Capable of stabilization at nominal operating conditions using an acoustic cavity	Three types of cavities evaluated	Stable without an acoustic cavity	1T monotune cavity judged to be sufficient
Best confidence in modeling drop size and mixing efficiency	r_m reasonable; E_m good	r_m reasonable; E_m good	r_m reasonable; E_m reasonable
Ease of incorporating design features into existing hardware	New faceplate only	New faceplate and injector core	New faceplate and injector core
Preferred rating	6 of 6	3 of 6	2 of 6

Indicates preferred characteristic

damping devices. From a flight hardware designer's point of view, this would be an excellent design. However, since our validation criteria require both stable and unstable operation for verification, the coarse triplet injector design was not sufficient for ROCCID validation. If resources were available, this design would be a good choice for a secondary, very stable, alternate test series to demonstrate ROCCID's capability to stabilize the thrust chamber through injector design changes (i.e., combustion response).

The doublet was predicted to be stable except for the first tangential mode. The doublet looked very promising because it was predicted to have a region of operation where it could be driven stable and unstable by changing the mixture ratio. The doublet was also predicted to be stable using acoustic damping devices, which would allow validation of the models for damping devices. The major drawback of the doublet was that it is very similar to previously tested designs. Since this was a validation of the predictive capability of the models in ROCCID, using an injector so close to previously tested hardware made this injector a secondary choice.

The fine triplet design was predicted to be unstable in several different modes with varying operating conditions. Figure 3 shows ROCCID predictions of stability changes over the operating map. The first longitudinal (1L) mode is stable until lower chamber pressures are reached. The first tangential (1T), second tangential (2T), and first radial (1R) modes are unstable over wide changes in operating conditions. An orifice diameter change from 0.09 to 0.10 in. was evaluated to determine the effect of orifice diameter on stability. The increase in orifice diameter did not improve stability margin sufficiently to provide any significant advantages. Damping devices were predicted to be very effective in damping the unstable modes. Also, this design was very different from previously tested hardware in terms of number of elements and orifice size.

Table 3 also provides a rating of the candidate injector designs. Using the criteria in Table 3, the fine triplet injector was the best choice to validate the models contained within ROCCID. The fine triplet injector stability was sensitive to chamber pressure and mixture ratio variations that allowed for testing the sensitivity and predictive capabilities of the models. The fine triplet injector was sufficiently different from previously tested injectors to allow a true "a priori" prediction. As a result, this injector was selected for the validation test hardware.

The test validation engine designed using the ROCCID methodology is shown installed on the Aerojet E-4 test stand in the photograph provided as Figure 4. A picture of the injector face

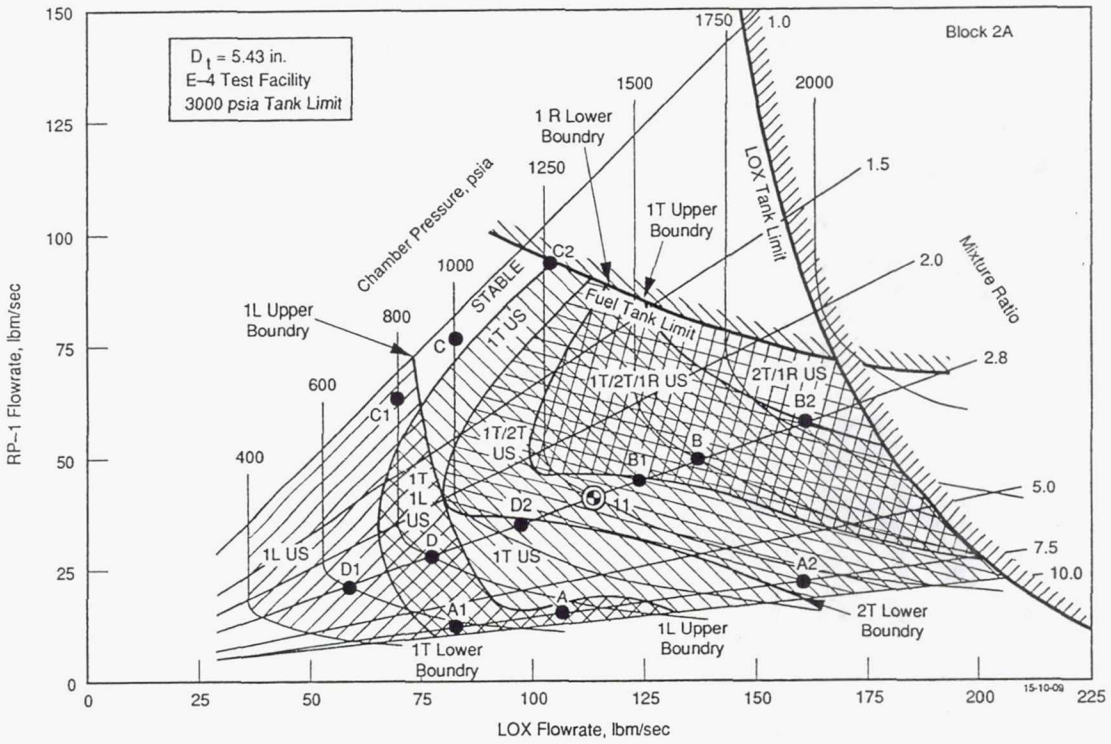

a. Predicted Stability Without an Acoustic Resonator

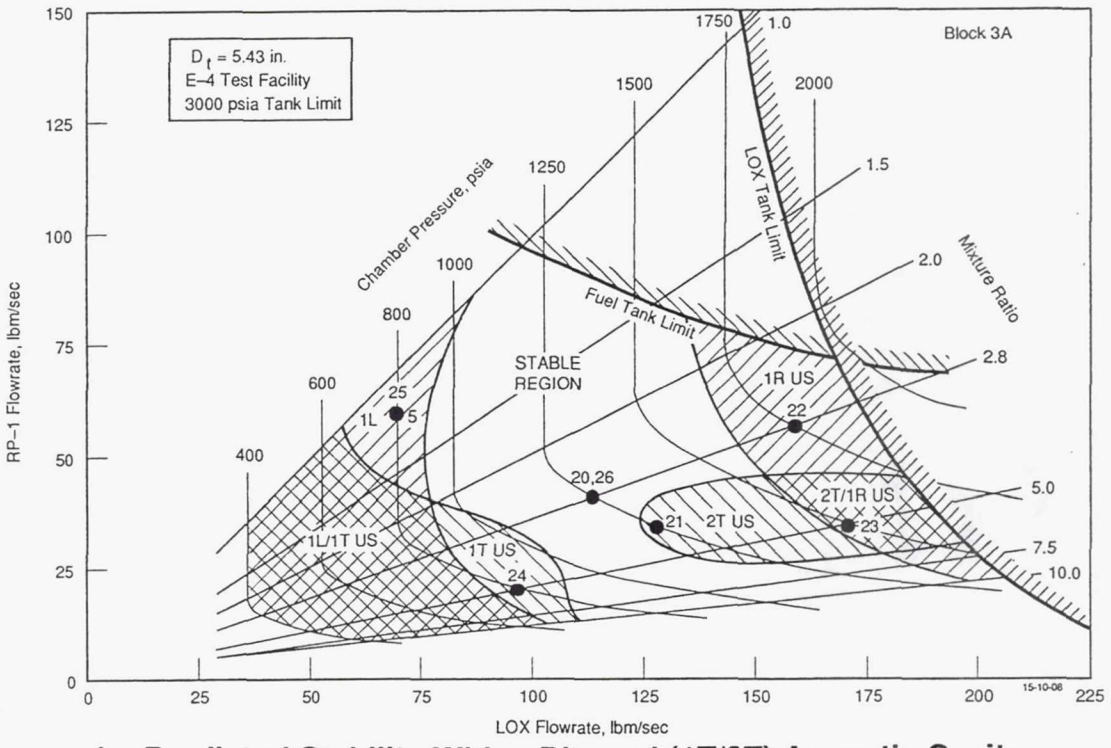

b. Predicted Stability With a Bituned (1T/2T) Acoustic Cavity

Figure 3. Expected Combustion Stability For the ROCCID Validation Hardware

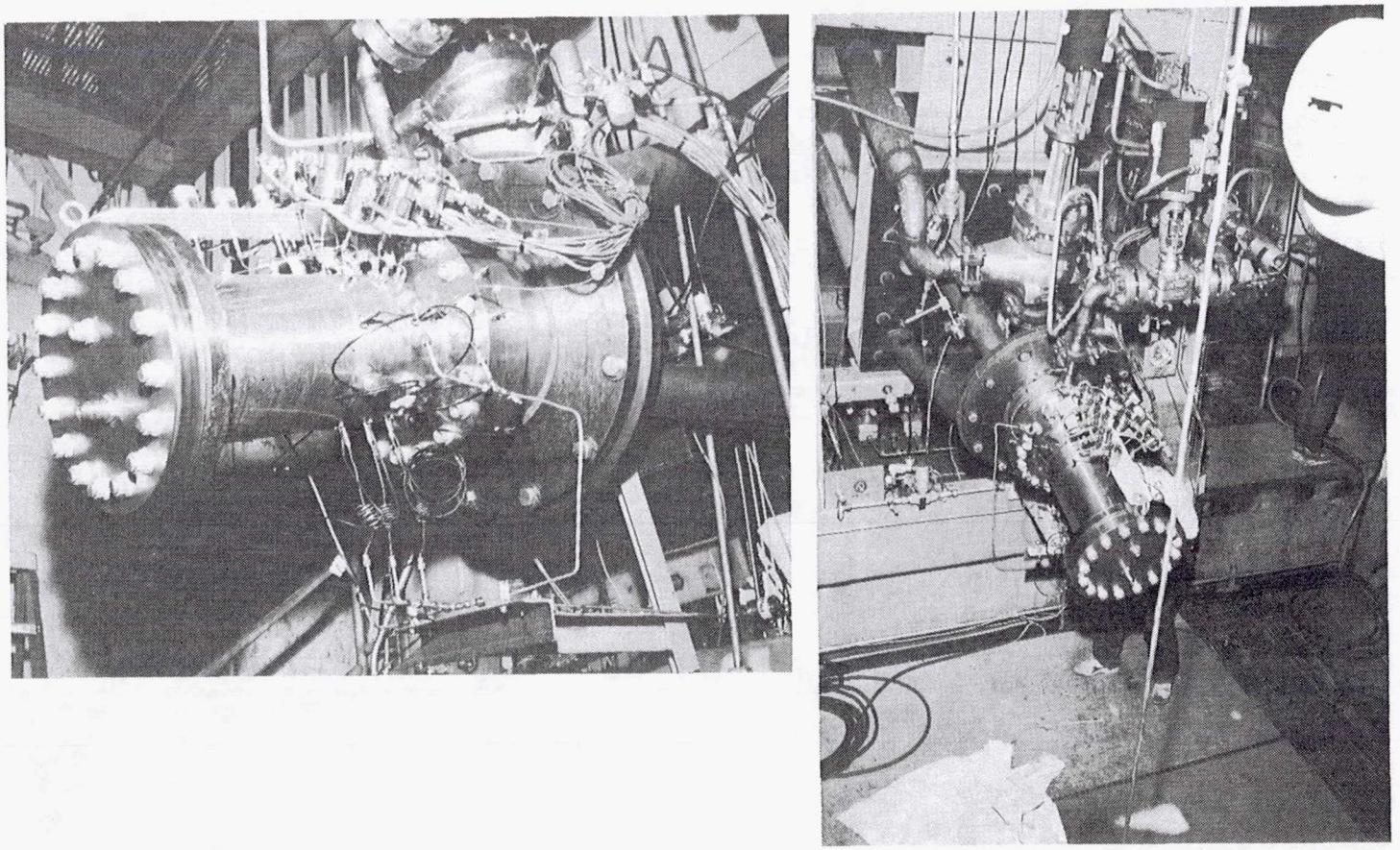

Figure 4. The ROCCID Test Validation Engine Assembly Installed on Test Stand E-4

is shown on Figure 5 and the OFO triplet element drawing is shown on Figure 6. The injector contained 105 OFO triplet elements with equal 0.090 in. diameter oxidizer and fuel orifices and a 35 deg impingement half angle.

Validation Test Results

Validation tests were successfully conducted in the Spring of 1991 in the Aerojet E-4 test facility. A total of twenty-seven tests produced useable combustion stability and/or performance data.

The actual test points are shown in Figure 7, identified by test number. The tests included eleven with a bituned acoustic cavity (Block 1 tests), eight with no cavity (Block 2 tests), and eight with a monotuned cavity (Block 3 tests). A list of individual test conditions, planned and actual, is provided on Table 4. As can be seen, the ranges of chamber pressure and mixture ratio tested correspond well to the originally intended ranges. The broad range of operating conditions provided an excellent test database for model assessment.

The testing consisted of "3 blocks" of tests. Block 1 tests were with a bituned acoustic cavity and were structured to provide test data in the most combustion stable engine configuration. These tests established performance values and mapped the regions of stable and unstable combustion. They were predicted to be the safest tests from a hardware damage standpoint since high amplitude combustion instabilities were not likely as seen in Figure 3b. This provided the most benign environment to establish start and shutdown sequences and performance values. The Block 2 tests were without any acoustic cavity and provided baseline data on chamber sound speed and an direct assessment of the benefit of the cavity used in the Block 1 tests. The Block 3 group of tests provided test data with a monotuned acoustic cavity. The tests in these three blocks are shown on Table 4.

An overview of the test logic for each of the Blocks of tests is shown on Figure 8. The path depicted by the shaded boxes was the logic path followed during the test program. The Block 1 tests with the bituned cavity were structured to meet the objectives of test series A (start, shutdown and flowrate balance verification), B (verification of stable operation at the nominal operating point, MR=2.8, Pc=1250 psia), C (verification of chug and 1L mode predictions), and D (verification of stable operation at nominal conditions). The Block 2 tests without acoustic cavities were structured to meet the objectives of test series E (verification of unstable operation

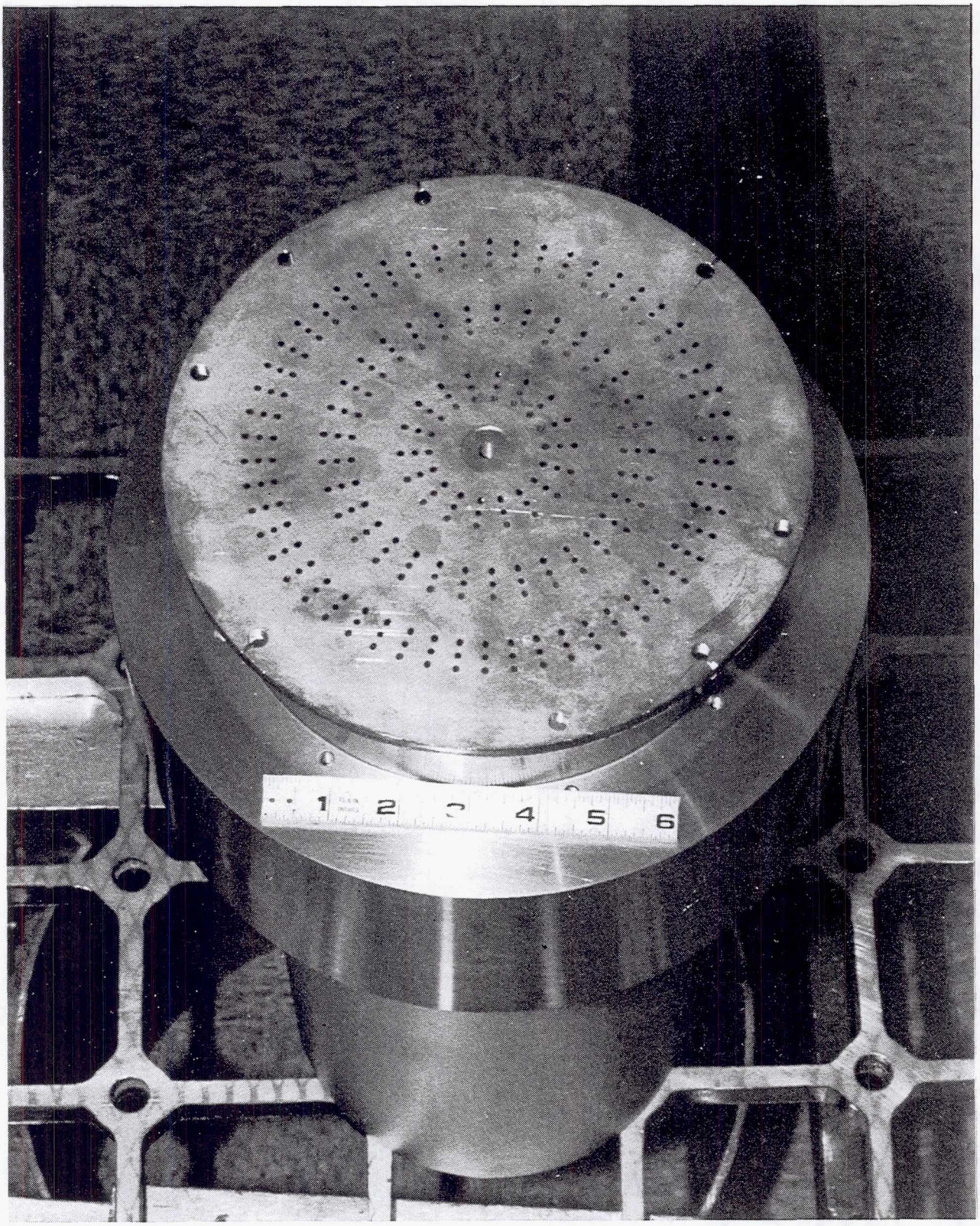

Figure 5. The Injector Core With Its Faceplate Installed for Brazing

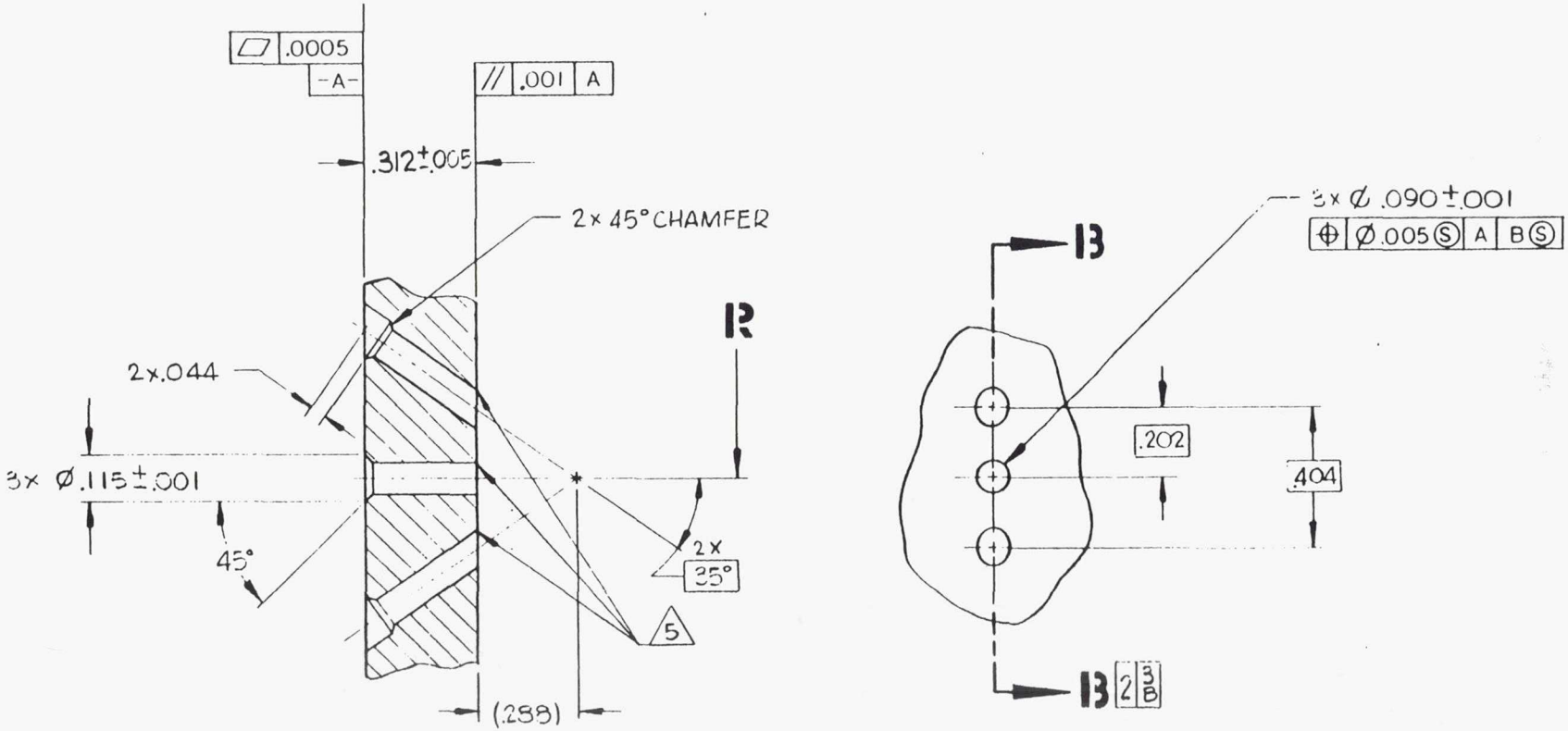

Figure 6. The OFO Triplet Element Was Designed to ROCCID Specification

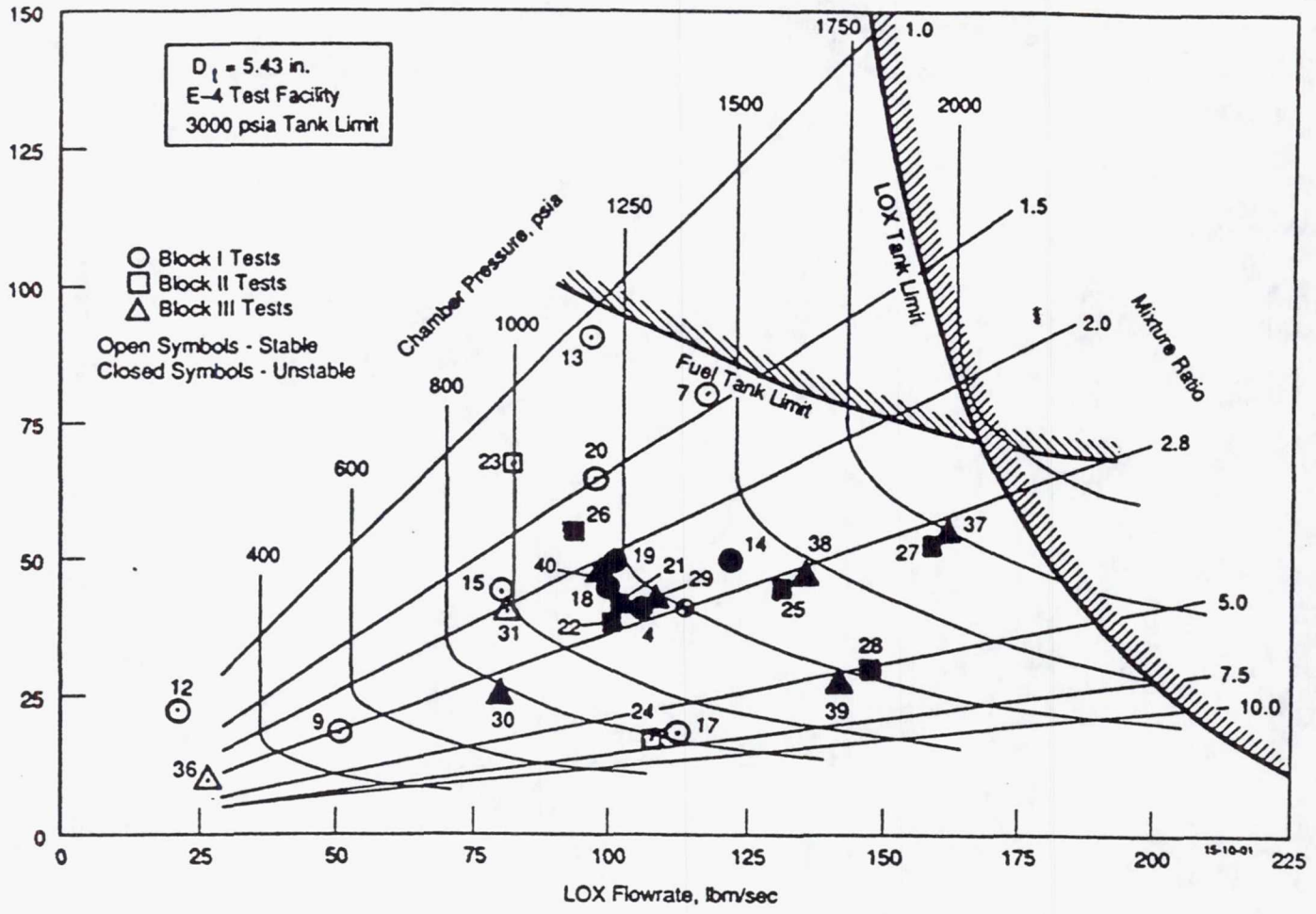

Figure 7. ROCCID Validation Test Points

TABLE 4. PLANNED AND ACTUAL TEST CONDITIONS

		Planned Conditions		Actual Conditions	
Test No.	Block	Chamber Pressure psia	Mixture Ratio	Chamber Pressure psia	Mixture Ratio
4	I	1250	2.80	1177	2.59
7	I	1500	1.50	1441	1.45
9	I	500	2.80	505	2.94
12	I	300	2.80	250	1.01
13	I	1250	1.20	1210	1.13
14	I	1500	2.80	1358	2.67
15	I	1000	2.00	969	1.93
17	I	800	7.50	792	6.74
18	I	1250	2.80	1165	2.35
19	I	1250	2.20	1220	2.06
20	I	1250	1.50	1193	1.50
21	II	1250	2.80	1222	2.67
22	II	1250	2.80	1092	2.52
23	II	1000	1.20	1004	1.25
24	II	800	7.50	788	6.71
25	II	1500	2.80	1410	2.86
26	II	1250	1.50	1130	1.70
27	II	1750	2.80	1706	3.03
28	II	1250	5.00	1260	5.15
29	III	1250	2.80	1208	2.55
30	III	800	2.80	791	3.09
31	III	1000	2.00	953	2.09
36	III	250	2.80	249	3.31
37	III	1750	2.80	1735	3.05
38	III	1500	2.80	1467	3.07
39	III	1250	5.00	1235	5.60
40	III	1250	2.20	1174	2.23

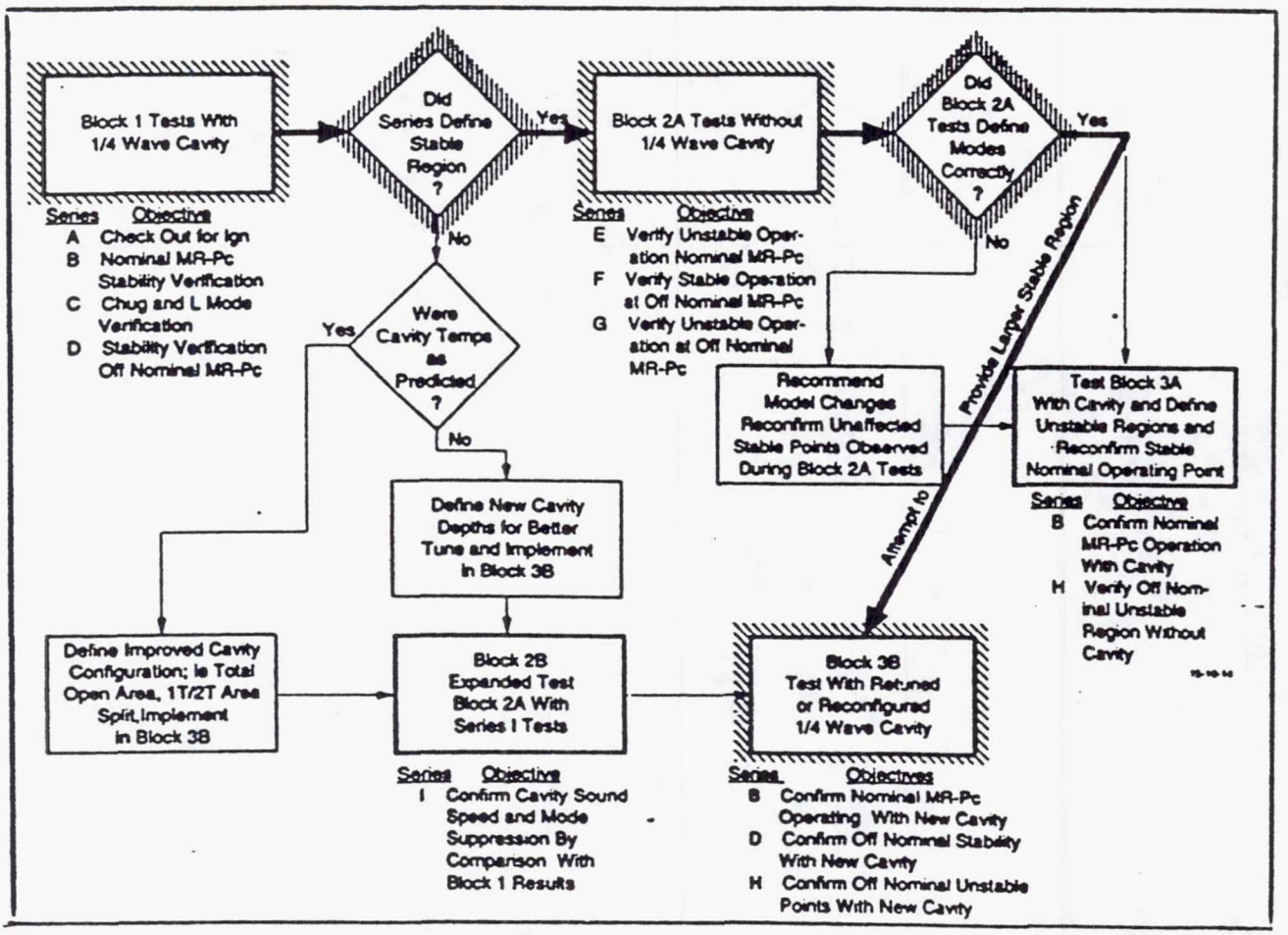

Figure 8. Overview of Test Logic

without acoustic cavities at the nominal design point), F (verify stable operation without acoustic cavities at off nominal conditions, and G (verify unstable operation without acoustic cavities at off nominal conditions). The Block 3B tests with a reconfigured (monotuned) acoustic cavity were conducted since the original bitune cavity did not provide as large a region of stable operation as originally desired.* This block of tests met objectives B (confirm nominal MR-Pc operation with a new cavity tune), D (confirm off nominal stability with a new cavity), and H (confirm off nominal unstable points with a new cavity).

Acoustic Mode Stability

The ROCCID methodology was used to recalculate the combustion stability for the tests where the acoustic cavity design was inadvertently changed (Block 1 and Block 3). Pretest predictions using ROCCID for the configuration without a cavity were still valid. The ROCCID calculations of combustion stability for each test condition are summarized in Table 5. Test results are also shown in Table 5 for comparison.

The eleven Block 1 tests with a bituned acoustic cavity covered a range of chamber pressures from 250 to 1442 psia and mixture ratios from 0.54 to 6.74. Seven of these tests were stable and four had spontaneous first tangential mode instabilities that ranged from peak-to-peak amplitudes of 46 to 103% of the steady-state chamber pressure. Four of these stable tests had the combustion process disturbed by bombs to promote combustion instabilities. Bomb over pressures ranged from 5 to 67%. Two stable tests were low chamber pressure tests for chug stability evaluation and were not bombed and one test had a bomb intended but did not produce a measurable overpressure. The ROCCID methodology correctly predicted all of the four tangential mode unstable tests but only two of the seven stable tests. In some cases, ROCCID predicted instability in the 1L mode, but no instabilities in this mode were observed.

The eight Block 2 tests without an acoustic cavity had chamber pressures from 788 to 1706 psia and mixture ratios from 1.25 to 6.71. Only two of these tests were stable, the lowest and highest mixture ratio tests. Both these tests had bomb over pressures of 5 and 11%. Of the six unstable tests all were in the first tangential mode and all were correctly predicted to be

---

* Subsequently, an error in the design of the acoustic cavity block was found that resulted in a significantly larger radial entrance to the cavity. The larger entrance resulted in an effectively shorter cavity and higher cavity gas temperature that considerably reduced damping near the first tangential frequency (See Figures 54, 55, and 56).

TABLE 5.

COMPARISON BETWEEN CALCULATED RESULTS AND TEST DATA

ROCCID Version 30-JUL-91
Date: 08-OCT-91

Operating Condition			Calculated Results (3)												Test Results					
			Chug		Longitudinal		1T		2T		1R		3T		1st Resonance		2nd Resonance		3rd Resonance	
Test	Pc	Mr	Pc,psia(1)	F,Hz	Al,1/s(2)	F,Hz	Al,1/s	F,Hz	Al,1/s	F,Hz	Al,1/s	F,Hz	Al,1/s	F,Hz	Al,1/s	F,Hz	Al,1/s	F,Hz	Al,1/s	F,Hz
4	1178	2.59	302	705	-822	1441	-67	3148	156	4868	-478	5891	-2100	0	153	3303	n/a	6548	n/a	9680
7	1441	1.45	258	608	-933	1566	-267	3627	1137	5122	500	6060	-144	6104	n/a	Stable	n/a	n/a	n/a	n/a
9	505	2.94	257	645	267	1246	-2100	0	-2100	0	-2100	0	-2100	0	n/a	Stable	n/a	n/a	n/a	n/a
12	250	1.01	83	744	-2100	0	-2100	0	-2100	0	-2100	0	-2100	0	n/a	Stable	n/a	n/a	n/a	n/a
13	1210	1.13	117	763	-600	1451	-100	3004	-2100	0	-2100	0	-2100	0	n/a	Stable	n/a	n/a	n/a	n/a
14	1460	2.67	288	694	-1100	2972	278	3130	-56	5009	467	5883	-400	5926	38	3303	n/a	6548	n/a	9910
15	969	1.93	280	662	-1167	1294	200	3550	394	5068	-2100	0	-2100	0	n/a	Stable	n/a	n/a	n/a	n/a
17	795	6.74	76	658	-200	1379	100	2594	-2100	0	-2100	0	-2100	0	-38	Stable	n/a	n/a	n/a	n/a
18	1165	2.35	291	696	-867	1442	-133	3153	533	4839	-367	5867	-2100	0	67	3185	n/a	6489	n/a	9733
19	1220	2.06	303	704	-833	1461	-122	3221	336	5060	-300	6012	-507	7629	37	3185	48	6548	n/a	9733
20	1193	1.50	171	744	-867	1440	278	3224	500	5049	-267	6044	-2100	0	-666	Stable	n/a	n/a	n/a	n/a
21	1222	2.67	274	670	-1178	1535	0	3057	1000	5039	-33	6243	-2100	0	84	3362	n/a	6784	n/a	10205
22	1092	2.52	303	710	-1022	1422	78	3180	178	5086	-2100	0	-2100	0	37	3303	47	6725	n/a	10087
23	1004	1.25	142	759	-1100	1768	133	3009	-2100	0	-2100	0	-2100	0	n/a	Stable	n/a	n/a	n/a	n/a
24	788	6.71	82	681	-67	1383	-189	2647	-2100	0	-2100	0	-2100	0	-73	Stable	n/a	n/a	n/a	n/a
25	1410	2.86	277	689	-1100	2998	100	3141	533	5379	-122	6258	100	6856	128	3244	129	6607	n/a	9969
26	1130	1.70	269	633	-1122	1395	-33	3229	67	5647	133	6556	-293	7418	220	3126	86	6282	n/a	9556
27	1755	3.03	281	684	-1574	3075	0	3597	67	5103	667	6585	667	6907	114	3274	n/a	6725	n/a	9379
28	1260	5.15	118	683	-1133	2758	100	3176	667	4611	-256	5712	-2100	0	n/a	3126	n/a	6400	n/a	9497
29	1208	2.55	282	676	-933	1473	-211	3209	67	5136	133	6418	-400	6868	56	3155	n/a	6430	n/a	9556
30	791	3.09	258	654	100	1705	100	3102	-2100	0	-2100	0	-2100	0	29	2949	n/a	5781	n/a	8700
31	953	2.09	281	670	-767	1826	500	3570	233	5156	-2100	0	-2100	0	n/a	Stable	n/a	n/a	n/a	n/a
36	249	3.31	224	600	-2100	0	-2100	0	-2100	0	-2100	0	-2100	0	n/a	Stable	n/a	n/a	n/a	n/a
37	1738	3.05	257	657	-1678	3039	-100	3604	67	5382	567	6604	522	6927	n/a	3008	n/a	4424	n/a	n/a
38	1467	3.07	260	671	-1289	3034	-122	3134	26	5022	733	6213	-152	6924	55	3185	n/a	6430	n/a	9703
39	1214	5.60	85	651	-1167	2697	67	3135	533	4549	-511	5855	-2100	0	37	2065	n/a	n/a	n/a	n/a
40	1180	2.23	274	670	-933	1459	-167	3232	167	5197	300	6447	-278	7244	94	2772	67	5250	n/a	10500

(1) Chamber pressure below which chug instability is predicted for given test mixture ratio.
(2) AL is the growth coefficient calculated by ROCCID as illustrated in Figure 18.
(3) Calculated results using ROCCID as described in Section IV H.

unstable by the ROCCID methodology. The methodology predicted one of the stable tests correctly (the low Pc chug test) but did not correctly predict the other.

Block 3 testing consisted of 8 tests with a monotuned cavity that were conducted over a chamber pressure range from 249 to 1735 psia and a mixture ratio range from 2.09 to 5.60. Six tests were unstable as predicted by ROCCID and two tests were stable, only one of which was predicted stable by ROCCID.

The combustion stability test results from all three test blocks are shown in Figure 9 as a function of measured chamber pressure and mixture ratio. An approximate correlation for the stable/unstable transition as a function of chamber pressure and mixture ratio is also provided and compared to the ROCCID prediction. From these results, no change in this transition boundary was discernable with the use of the improperly tuned acoustic cavities. Some additional damping was evident when these acoustic cavities were used, however, based on the reduction in the amplitude of the instability measured with acoustic cavities compared to that measured without cavities. Also, a reduced experimental growth coefficient was estimated from tests with the acoustic cavities compared to tests without cavities. Similar trends were predicted by ROCCID as noted in Table 5.

A comparison of the experimentally observed stability transition boundary (from Figure 9) to that predicted by ROCCID (1T lower boundary from Figure 3a) is shown in Figure 10. From this comparison, the zone of unstable operation expected based on the ROCCID results was somewhat larger than the experimentally determined zone. Interestingly, however, a close correlation between the ROCCID prediction and the observed test results was achieved near the design mixture ratio of 2.8. This may indicate that the stability analysis models provide better predictions at mixture ratios near "nominal" values where a majority of the historical database was generated and upon which the models were developed and verified.

Nonacoustic (Chug Stability)

All tests were chug stable at the tested operating conditions. A few tests briefly encountered chug instabilities during the early part of the start-up transient where the chamber pressures were extremely low. These instabilities, however, disappeared quickly as the mean chamber pressure increased to its steady-state value. These tests results confirmed the chug predictions made using the ROCCID methodology.

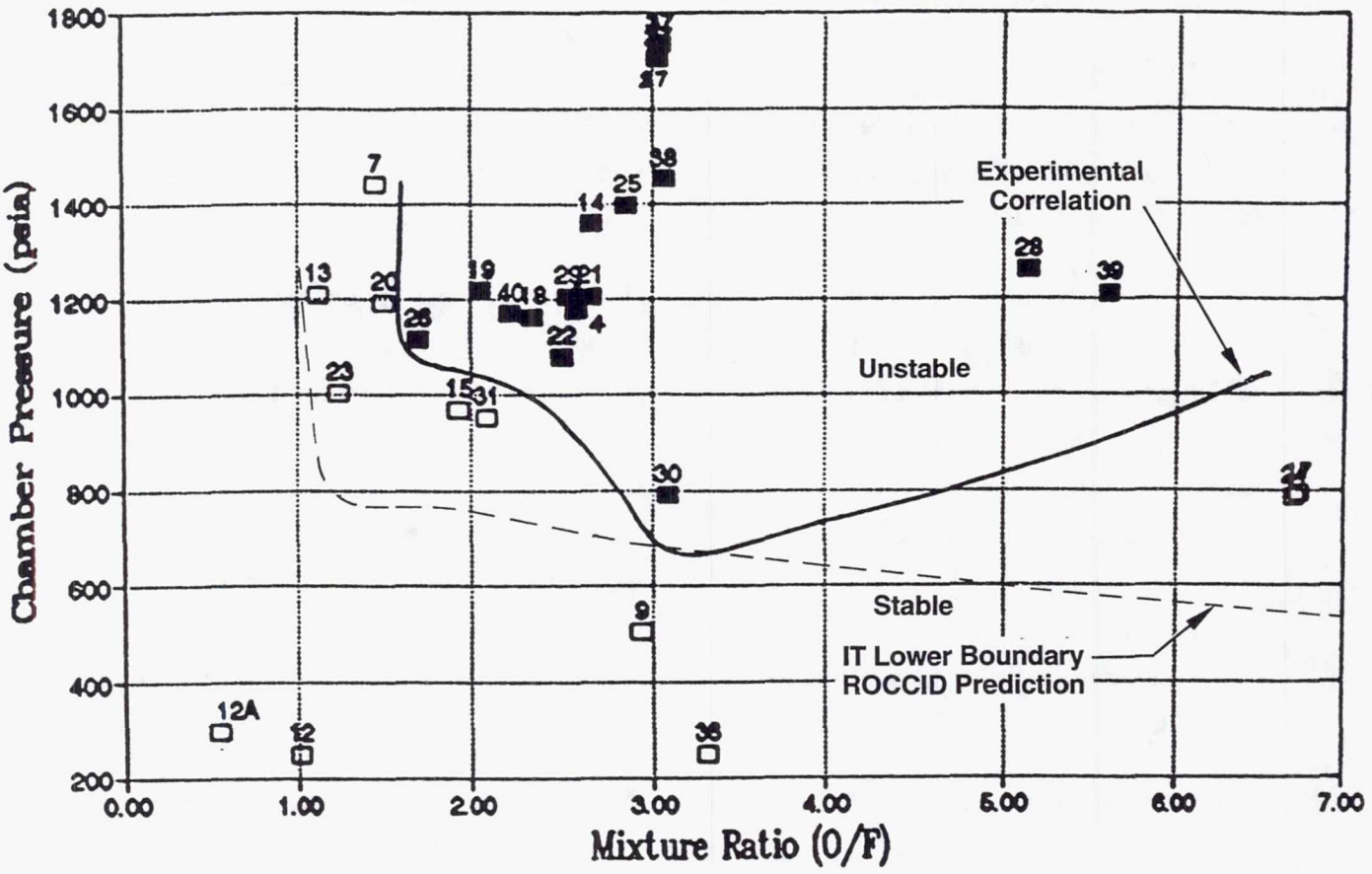

open symbol: stable
solid symbol: unstable
number 1-20: test with bituned cavities
number 21-28: test with blocked cavities
number 29-40: test with a monotuned cavity

Figure 9. ROCCID Validation Test Results Indicate Stable and Unstable Operating Regions

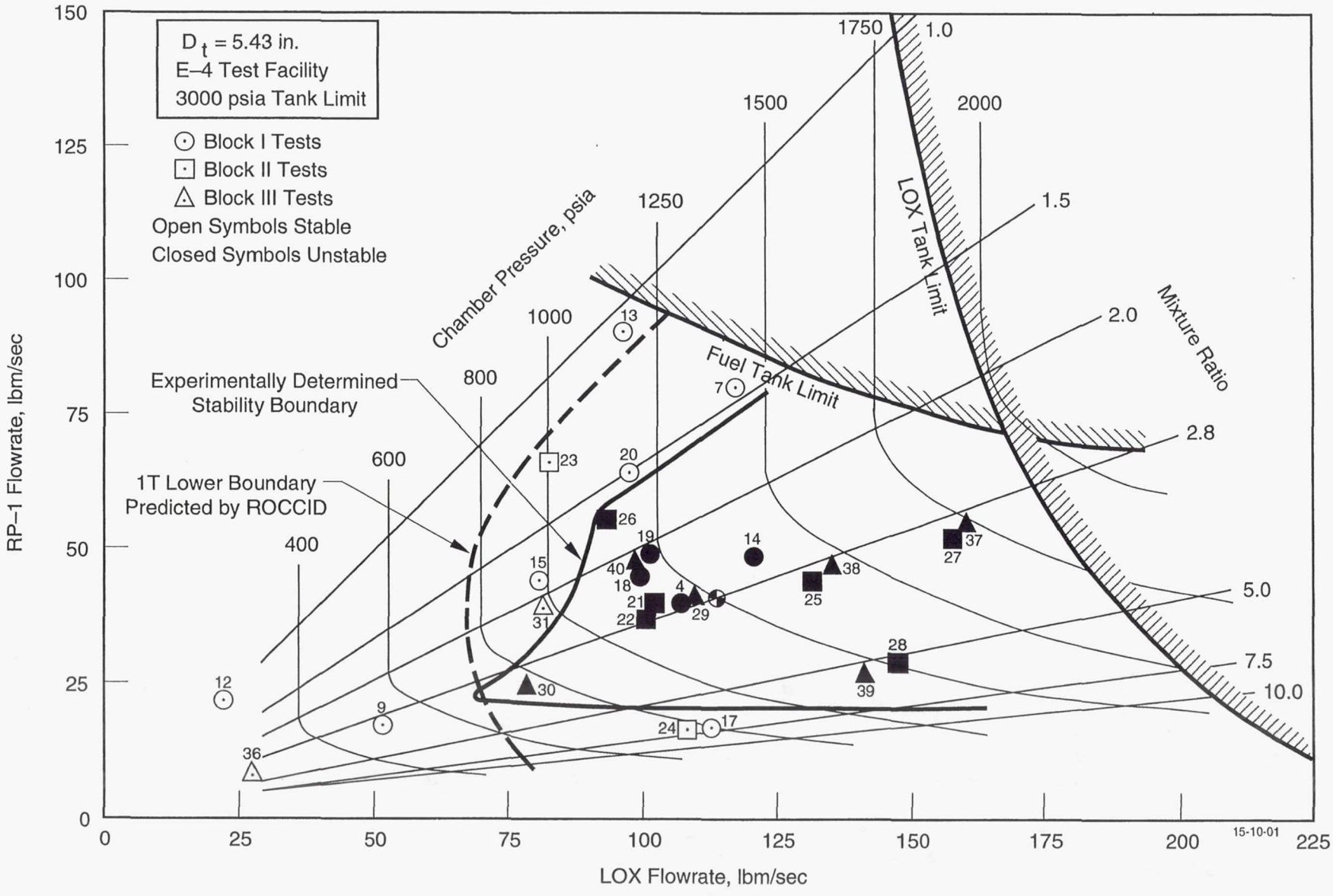

Figure 10. ROCCID Predicted a Somewhat Large Zone of Unstable Operation Than Was Observed Experimentally

Performance

The test measured performance efficiency based on either characteristic velocity (%C*) or specific impulse (energy release efficiency or ERE) was 5 to 7% lower than that predicted by the ROCCID analysis. A comparison of the predicted and measured performance in terms of the percent C* and the thrust based energy release efficiency (ERE) is shown on Table 6. The trends of both the measured and predicted performance with mixture ratio are shown on Figures 11 and 12 for ERE and %C*, respectively. In addition to the measured data showing significantly lower performance than the predictions, the mixture ratio for minimum efficiency is somewhat different between the predicted and measured values. The predicted minimum efficiency is 97.8% and occurs at a mixture ratio of 2.2, while the measured minimum (91%C*, 93% ERE) is at a mixture ratio of approximately 2.9. The ROCCID code predicts a vaporization efficiency of 99.8% and a mixing efficiency of 98% at a mixture ratio of 2.2.

The vaporization efficiency at near stoichiometric mixture ratios appears reasonable based on a comparison between the predicted and measured static pressure profiles in the combustion chamber. A typical pressure profile comparison at near nominal conditions is shown on Figure 13. However, at very low or high mixture ratios the ROCCID code over predicts the vaporization rate, as can be seen from the comparison between the predicted and measured chamber static pressure profiles shown on Figure 14. This over prediction is probably a result of the generalized length correlation used for vaporization estimates that is based on data and calculations assuming typical stoichiometric combustion temperatures. The generalized length model in ROCCID may need to be modified to reflect the lower vaporization rates at off nominal conditions either by using a more mechanistic model, or by modifying the generalized length correlation by including a combustion temperature correction factor.

Since the vaporization efficiency at near stoichiometric mixture ratio appears valid, the lower experimental efficiency must be the result of a lower mixing efficiency. The performance mixing efficiency was calculated by ROCCID from an input unielement E_m of 0.77 obtained from previously conducted cold flow tests. A unielement to multielement correlation from DROPMIX was used by ROCCID to determine the multielement E_m (.87) for the 105 element OFO injector. A better match of the prediction to the data is obtained, however, if a multielement E_m of .75 is used, which would be indicative of no interelement mixing improvement.

TABLE 6. MEASURED AND PREDICTED VALIDATION ENGINE PERFORMANCE

			Calculated		Measured	
Test	Pc	Mr	Eta-C*	ERE	Eta-C*	ERE
4	1178	2.59	0.983	0.983	0.801	0.842
7	1441	1.45	0.990	0.989	0.975	0.972
9	505	2.94	0.988	0.988	0.994	0.987
12	250	1.01	0.981	0.980	0.863	0.792
13	1210	1.13	1.003	1.004	1.049	1.010
14	1460	2.67	0.985	0.985	0.932	0.948
15	969	1.93	0.980	0.981	0.968	0.951
17	795	6.74	0.991	0.991	1.025	1.015
18	1165	2.35	0.979	0.979	0.978	0.997
19	1220	2.06	0.979	0.980	0.994	1.000
20	1193	1.50	0.983	0.982	0.955	0.948
21	1222	2.67	0.984	0.984	0.934	0.928
22	1092	2.75	0.980	0.980	0.836	0.924
23	1004	1.25	1.014	1.016	0.961	0.937
24	788	6.71	0.990	0.990	0.956	0.947
25	1410	2.86	0.987	0.987	0.908	0.926
26	1130	1.70	0.983	0.983	0.736	0.753
27	1755	3.03	0.990	0.990	0.890	0.938
28	1260	5.15	0.994	0.994	0.904	0.946
29	1208	2.55	0.982	0.982	0.927	0.915
30	791	3.09	0.991	0.990	0.919	0.921
31	953	2.09	0.978	0.979	0.843	0.663
36	249	3.31	0.990	0.990	0.931	0.899
37	1738	3.05	0.990	0.990	0.918	0.927
38	1467	3.07	0.991	0.990	0.920	0.963
39	1214	5.60	0.994	0.994	0.945	0.916
40	1180	2.23	0.978	0.978	0.874	0.886

Note: Efficiencies greater than 1.00 are suspect and are probably the result of interpolation accuracies for calculated values or test measurement accuracies for measured values. See Section IV H.

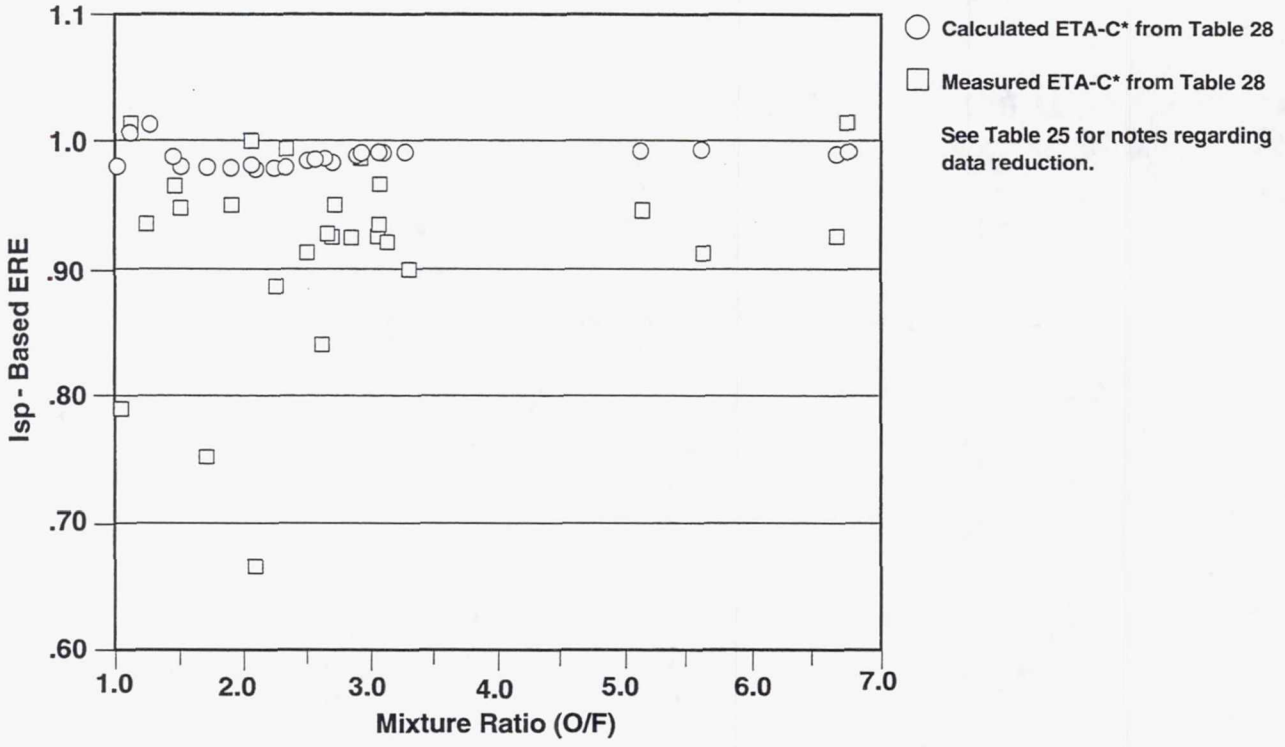

Figure 11. Comparison of Unanchored ROCCID Predictions and Test Results – Isp-Based ERE

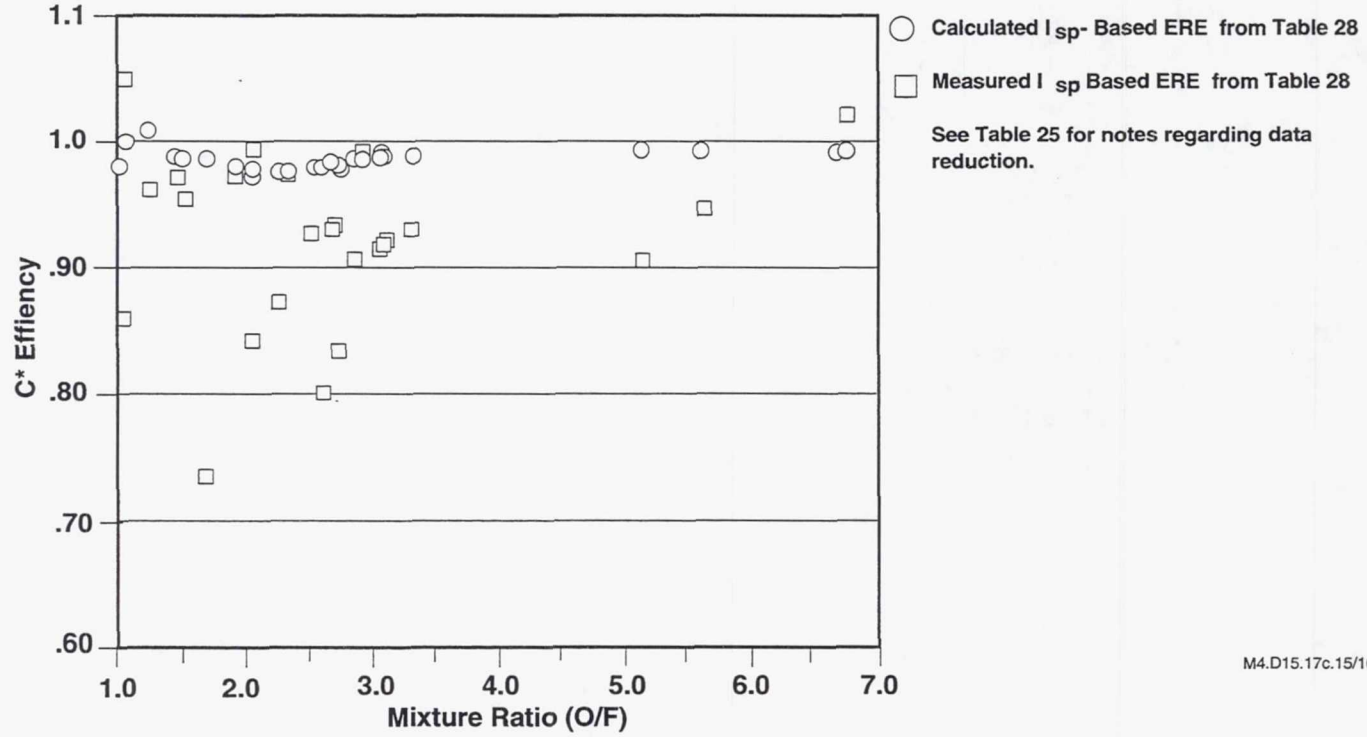

Figure 12. Comparison of Unanchored ROCCID Predictions and Test Results C* Efficiency

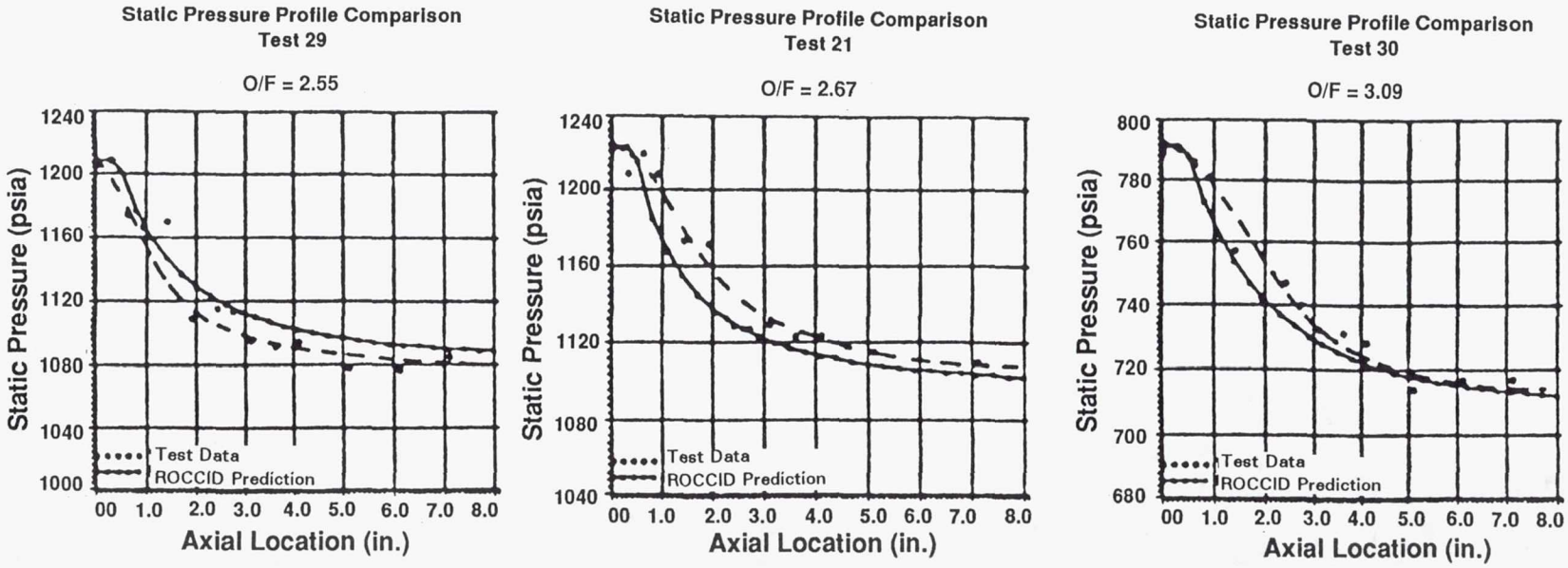

Figure 13. Good Agreement Observed Between Predicted and Measured Chamber Static Pressure Profiles at Near Stoichiometric Mixture Ratio

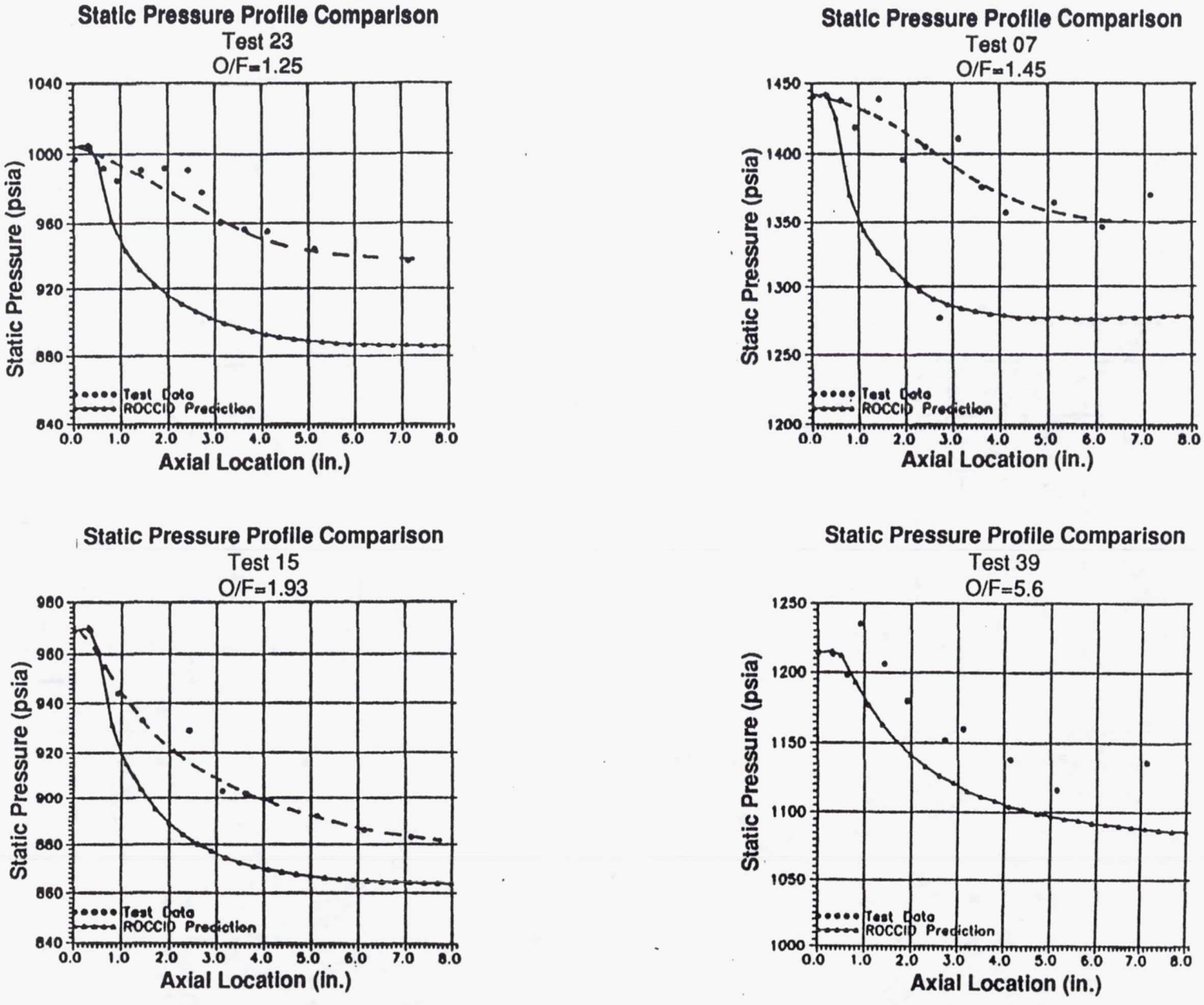

Figure 14. Poor Agreement Observed Between Predicted and Measured Chamber Static Pressure Profiles at Very Low and High Mixture Ratios

Cold flow testing, shown in the photograph of Figure 15, indicated that the propellant spray fan formation from individual elements is not complete before adjacent elements begin to restrict the fans* . This may cause a multielement mixing efficiency to be actually lower than the unielement mixing efficiency. To confirm this, it is recommended that both unielement and multielement cold flow tests be conducted to measure the cold flow mixing efficiencies. The correlation currently in the DROPMIX code indicates an increase in multielement Em for a given unielement Em as the pattern fineness increases. This correlation should be used with caution for very fine patterns and an expanded element mixing database covering a wide range of element pattern densities and element types using both cold flow and hot fire data should be generated. At a minimum, both unielement and multielement Em's should be determined from cold flow testing for designs that are outside of the DROPMIX database.

The validation test program has shown that ROCCID is a good tool that can be effectively used to perform first cut combustor design and parametric analyses. The testing showed some limitations within the methodology such as uncertain combustion response calculations, a constrained interelement mixing correlation and an apparent over prediction of the propellant vaporization rate at very off-nominal mixture ratio. However, the ROCCID stability predictions were conservative in that ROCCID tended to predict less stable operation than what was obtained and the overprediction in performance efficiency probably could have been found through relatively simple multielement cold flow mixing tests. An overall assessment of the ROCCID methodology and the results achieved during the validation test program are provided in the following section, III Conclusions and Recommendations.

* Cold flow visualization tests of OFO triplet elements as a function of element spacing have been performed by the NASA Lewis Research Center and results supporting this observation are presented in NASA Technical Memorandum 105750 (AIAA-92-3226).

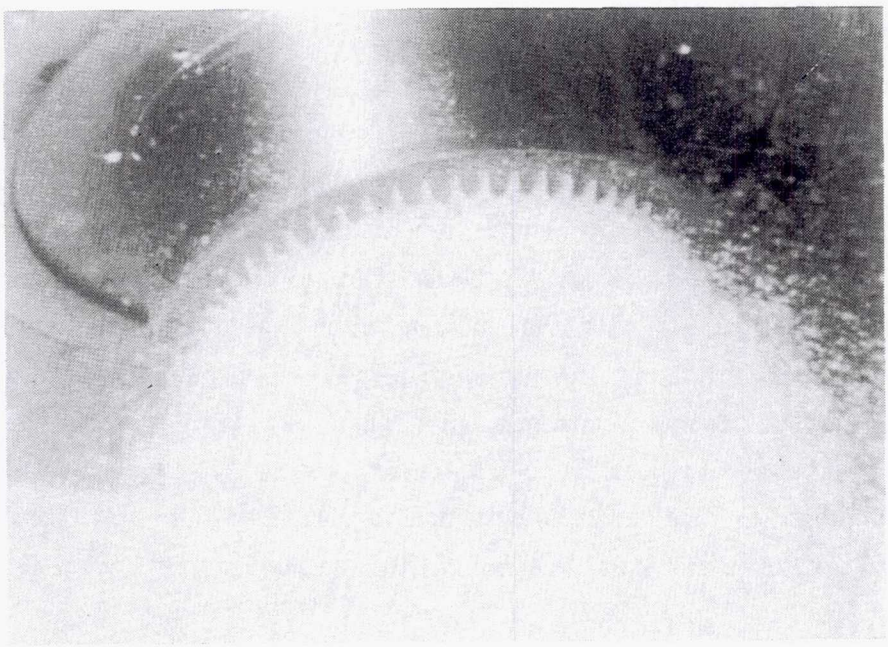

Figure 15. ROCCID Injector Cold Flow Propellant Spray Fan Formation

III. CONCLUSIONS AND RECOMMENDATIONS

A computerized design methodology has been developed for use in designing efficient and stable combustors for LOX/Hydrocarbon and LOX/Hydrogen rocket engines. This Combustor Analytical Interactive Design Methodology (ROCCID) is unique in several respects. First, it contains an ordered assemblage of industry-wide analysis models that are used to define the effects of design and operating parameters on combustor performance and stability. Second, all practical and available analysis models and correlations are included even when redundant capabilities exist. This allows the user to directly compare the results of available techniques and select the method that appears to be the most applicable for a specific application. It also provides a means to identify design and operational uncertainties based on the differences predicted by available techniques. Third, these analysis models and correlations are contained in a modular format so that model updates and new models can be incorporated into the methodology as they are developed. Last, ROCCID is designed to be user friendly and contains an interactive front end for input formulation and checking, file generation, and output display.

Validation tests using hardware with critical design features determined from the ROCCID methodology has demonstrated both the utility and capability of the methodology and identified some of its shortcomings. ROCCID high frequency (acoustic coupled) instability predictions proved to be conservative in that the experimental zone of instability was somewhat smaller, in terms of operating chamber pressure and mixture ratio, than that predicted from the ROCCID methodology. Nonetheless, the general unstable character of the combustion chamber without acoustic damping was adequately predicted from a design selection standpoint. In this case, use of the ROCCID methodology would have led to improved stability margin through the incorporation of acoustic damping devices to increase chamber damping and/or a change in the injector design to reduce the predicted combustion response.

In spite of the relatively good correlation between the ROCCID predictions and the validation test results, determination of the combustion response remains a highly empirical and analyst dependent process. The adequacy of a-priori specification of the combustion response can be a function of the element type and design, the propellants and the available experimental database. While some analytical approaches, such as CRP and the NASA Lewis Injection Coupling Model have been developed, their application has been relatively limited and generally involved in correlation of tested designs. Clearly, further advancement in the modeling and characterization of the combustion response is essential for improvement in the overall predictive capability of liquid propellant combustion stability.

However, since the whole sensitive time lag methodology, upon which ROCCID is based, is built upon empirical correlations and analytical approaches that have been verified, refined and/or anchored with empirical data generated over the past thirty to thirty-five years, it is not obvious that additional improvements in any specific modeling area would result in an overall improvement in the combustion stability characterization. For example, the chamber response modeling does not account for the acoustic energy damping provided by the chamber wall and the propellant spray. Improvements in this area may be able to be incorporated into the chamber response model to make it more physically representative. Yet since, the combustion response, n, has been "backed out" from experimental results using chamber response models without the wall and spray damping considerations, its use with the improved chamber response models may actually result in a degradation in the predictative capability of the methodology.

Chug stability limits appeared to be adequately defined. The predicted longitudinal instability at lower chamber pressure was not observed at steady-state conditions but was observed during the start transient. Thus injection pressure drop requirements can be adequately defined using the ROCCID methodology.

Performance efficiency was overpredicted by ROCCID. In this case, it appears that the interelement mixing efficiency was overpredicted by a basically empirical correlation. The propellant vaporization appeared to be adequately predicted at near nominal mixture ratios but was overpredicted at very off-nominal mixture ratios where the driving temperature (combustion temperature) is significantly reduced. In this sense, the validation test result can be used to extend the empirical limits of the ROCCID models for very off-nominal mixture ratio operation with LOX/RP-1 propellants. Additionally, future improvements may result from emerging computational fluid dynamic (CFD) modelling that can, as a minimum, be used to validate or improve existing and primarily empirical based techniques while using ROCCID as a parametric design tool to home in on specific areas to study with CFD.

ROCCID will provide significant cost savings for the design and development of rocket engine combustion chambers. Standardization of the design and analysis approach and the availability and use of all the best combustion analysis models and correlations ensure cost efficiency improvements. ROCCID is a low cost design tool in that it results in relatively low CPU usage, doesn't require high performance computers such as a CRAY, is portable to different computer platforms and provides, through its built-in model connectivity and interactive front-end, increased parametric design and analysis capability with decreased engineering hours. Savings

of 50% or greater in manhours are estimated when using ROCCID once the analyst is familiar with its operation and capabilities.

Further validation and continued wide application experience will provide additional means to identify strengths and limitations in the methodology. Isolation of weaknesses will provide for focused improvements in the methodology and an evolution to a proven and robust combustor analytical design technology that can serve the industry while sophisticated and mechanistically based computational methods are developed.

IV. TECHNICAL NARRATIVE

The LOX/Hydrocarbon Rocket Engine Analytical Design Methodology Development and Validation was a three year program conducted by the Aerojet Propulsion Division under contract NAS 3-25556 from the NASA Lewis Research Center. This program consisted of two major efforts: first, the development of an analytical design methodology for liquid propellant rocket engines that uses existing industry analysis computer programs and empirical correlations, and second, the validation and critical evaluation of this methodology through its application for the design of a test demonstration thrust chamber and prediction of its combustion stability and performance characteristics. The capability of this methodology was demonstrated through fabrication and testing of this thrust chamber over a wide range of mixture ratio and chamber pressure while obtaining detailed measurements of its operation for comparison to the performance and combustion stability forecasts developed using the methodology.

These activities were completed during eight technical tasks, the results of which are summarized in this final report. Task 1.0 consisted of a survey of existing industry analysis models for use in the methodology and existing stability and performance databases for evaluation of these models. Development of the methodology, which was named the ROCket Combustor Interactive Design (ROCCID) methodology, was completed during Task 2.0 and a limited release of a test (beta) version of the computer code was made. The newly developed ROCCID methodology was applied to illustrate the effects of critical design parameters and operating conditions on combustion chamber performance and combustion stability during Task 3.0 to provide a basis for the selection of these parameters for hardware design to validate the methodology. Task 4.0 consisted of the development of a detailed test plan and thrust chamber performance and combustion stability predictions for validation testing of the newly developed ROCCID methodology. Validation hardware design and hardware fabrication were completed during Tasks 5.0 and 6.0, respectively. Finally, hot fire testing of the validation hardware was completed during Task 7.0, and data analysis and comparison of test results with the ROCCID predictions was provided in Task 8.0. A summary of these task results are contained in the following subsections.

A. DATA/STABILITY MODEL SURVEY

A survey of existing analysis models and available databases containing combustion stability and performance measurements was conducted to identify and acquire analysis models that perform critical analytical characterization or empirical correlation of important combustion

processes that influence the combustion stability and performance of a rocket engine combustor. Models reviewed covered three general areas of combustion analysis; (1) steady-state combustion, which models the propellant injection, atomization, vaporization and mixing processes, (2) combustion stability, which models the non-steady injection, combustion and chamber response of a combustor design and (3) performance, which defines the combustion efficiency of the energy release processes.

Evaluation criteria were developed to provide a means for rating and selecting analysis models for further review and comparison with the selected combustion databases. The evaluation criteria used to rate various analysis models are provided in Table 7. The first three criteria were considered most important since a failure to meet any of these three requirements would mean that a particular model was unacceptable for use in the analytical design methodology. For this reason, the relative value of these criteria range from 0 to 1.0 and these are used as multipliers in the overall rating value equation also shown in Table 7. A zero value for the A, B, and C evaluation criteria will result in a zero value for the overall rating value. In this case it is clear that a model is unacceptable for use in the advanced methodology. Conversely, a value of 1.0 for all three of these criteria means that selection of the model for further evaluation will be made on the basis of the remaining three evaluation criteria.

The remaining three evaluation criteria, D, E, and F, have relative values between 1 and 10. The higher the relative value for a particular model, the better that model meets the evaluation criteria. Note that the average relative value of the D, E, and F evaluation criteria are used in defining the overall rating.

A list of 18 models that were evaluated for further study is contained in Table 8. These models are grouped in three categories: (1) Steady State Combustion, (2) Combustion Stability, and (3) Engine Performance. The table provides our subjective assessment of the relative value for each of the six evaluation criteria for each model. An overall assessment is included using the overall rating value equation from Table 7. The final column in Table 8 indicates if a model is recommended for further evaluation by correlation with existing industry databases. A favorable recommendation is made if the overall rating value is 5.0 or greater.

The set of recommended models included in Table 8 is sufficient to build a complete analytical design methodology with only one exception. The ability to model combustion instability coupling with nonlinear feed system acoustics is not contained in the set of recommended

TABLE 7. ANALYSIS MODEL EVALUATION CRITERIA HAVE BEEN DEVELOPED

EVALUATION CRITERIA	RELATIVE VALUE
A. It is applicable to LOX/Hydrocarbon Booster Engine Designs?	0 Is not applicable 1.0 Fully acceptable
B. Is it a functional code? Does it provide useful results over a wide range of design and operating conditions	0 Not operational/limited range 1.0 Fully operational/wide ranging
C. Is it available for industry use?	0 Proprietary and unavailable 1.0 Available through the CPIA or Cosmic
D. Is it a mechanistically based analysis tool? Can it provide means to tradeoff design parameters to arrive at an optimum overall combustor design?	1.0 Purely empirical based with a low degree of design parameter influence 10.0 Analytically based with a high degree of design parameter influence
E. Is there relevant industry experience with the analysis tool? Is it a JANNAF reference program or has it been compared with a JANNAF Program?	1.0 Not widely used within the industry and not used as a primary design tool 10.0 JANNAF reference program
F. Is it practical? Can it be used intelligently by the designer/ analyst? Is the computer run time practical?	1.0 Long running with abstract and difficult to define I/O parameters 10.0 Quick running with straight foreward I/O parameters

$$\text{Overall Rating Value} = (A)(B)(C)\left[\frac{(D) + (E) + (F)}{3}\right]$$

TABLE 8. COMPUTER CODE EVALUATION SUMMARY

Code	Applicable (A)	Functional (B)	Available (C)	Mechanistic (D)	History of Use (E)	Practical (F)	Overall Assessment ABC[(D+E+F)/3]	Recommended for Further Correlation*
Steady State Combustion								
• SDER/CICM	1.0	0.8	1.0	8	10	3	5.6	Yes
• PCDER/Dropmix	1.0	1.0	0.9	8	6	8	6.6	Yes
• Inject	1.0	1.0	0.8	7	8	8	6.1	Yes
• PLC	1.0	0.8	0.8	6	4	8	3.8	No
• SEA/RPL Perf.	1.0	1.0	0.8	8	5	5	4.8	No
Stability								
• LFCS	1.0	1.0	0.9	7	8	10	7.5	Yes
• n-τ Correlations	1.0	1.0	1.0	3	6	10	6.3	Yes
• HIFI	1.0	1.0	0.9	8	8	10	7.8	Yes
• FDORC	1.0	1.0	0.9	9	6	8	6.9	Yes
• CRP	1.0	1.0	0.9	8	5	6	5.7	Yes
• DIST2(3)D	1.0	0.8	0.9	8	5	8	5.0	Yes
• Lewis Non-lin Injection	1.0	1.0	0.2	7	5	6	1.2	No
• SEA Non-Lin. Instab.	1.0	0.5	0.2	7	5	6	0.6	No
• GENSTA	1.0	0.5	0.5	9	3	6	1.5	No
• Rocketdyne ANALOG	1.0	0.5	0.0	5	3	1	0.0	No
Performance								
• Rocket	1.0	1.0	0.8	7	6	10	6.1	Yes
• TDK/BLM	1.0	1.0	1.0	10	10	6	8.7	Yes
• AUTOCOM	1.0	0.2	0.2	7	3	6	0.2	No

*Recommended model if overall assessment ≥ 5

models. This deficiency was eliminated through the development of non-linear injection model (Leinj) similar to the approach described in Reference 2.

Existing combustion performance and stability databases listed in Table 9 were also reviewed as a source for data and design information for further model evaluation. Four of the eleven data bases reviewed were selected for this evaluation.* These sets cover a range of hydrocarbon fuels (and hydrogen) injector elements (impinging and concentric tube) acoustic damping devices and operating conditions (Pc, O/F, Dchb, Tfuel, etc.). Most importantly, they contain stable and unstable operating characteristics and performance data that can be compared to model calculations.

Unfortunately, not all of the 11 recommended models were evaluated and compared to the existing data bases. Model availability, computational flaws, inefficient run times, ill-defined input and extensive and previously documented model evaluations were reasons for exclusion of some models. Nonetheless, a complete set of models were available to calculate combustor performance and combustion stability. In any case, several critical model correlations such as spray dropsize or burning response were available and were compared to each other and to data base measurements.

Performance model evaluations were made by comparing calculated combustor efficiency (energy release or C*) to test based published values. Calculated variations in efficiency with key combustor design parameters such as injector element configuration and chamber length and operating parameters such as fuel type and mixture ratio were compared with experimentally determined trends. combustion stability models were evaluated by comparing predicted stable or unstable operation with documented results from the selected data bases. Chug, burning coupled and injection coupled instabilities were modeled and acoustic mode and frequency predicted. Injection element type, chamber size, acoustic damping devices (resonators and baffles) and fuel type are parameters that were included in this evaluation.

Results from the performance model evaluation have shown that combustor efficiency can be predicted to within 1 to 2% over a wide range of design and operating conditions. Injector designs producing high efficiency, such as the impinging OFO triplet element, were well

* Subsequently, data anomalies have been discovered in the LeRC in-house data base (NASA TM 79319) and further use of this data base is not recommended pending its correction.

TABLE 9. DATA BASE REVIEW AND SELECTION

Data Base	Contract Number	Element Type	Fuel Type	Data Stability	Available	Comments	Recommended Data Base
OX/HC Injector Characterization	F04611-85-C-0100	OFO,LOL	RP-1, C3H8,CH4	S and US	Yes	Damping Device DesignVariations	Yes
LOX/HC Instability Investigation	NAS 3-24612	Shear Coax	CH4	S and US	Yes	CH4 Temperature Ramping	Yes
Characterization of LOX/HC Propellants	NAS 9-15958	OFO	C3H4, C3H70H	S	Yes	Low Chamber Pressure	No
Injectors for HC Fuels	LeRC inhouse	LOL, OFO, FOOF	RP-1,LNG, JP-10	S and US	Yes NASA TM 79319	Low Chamber Pressure	Yes *
ATC LOX/CH4 (Main) Injector	NAS 8-33205	Swirl Coax	CH4	S	Yes	Poor Instrumentation	No
Rkdn LOX/CH4 (Main) Injector	NAS 8-33206	Shear Coax	CH4	S		Poor Instrumentation	
LOX Cooling Study	LeRc inhouse	OFO	RP-1	S and US	Unknown	Only 1 instability	No
F-1	NASw-16	LOL,OFO	RP-1	S and US	No	Few tests on many designs	No
Atlas/Thor	AF04(647)-318	LOL	RP-1	S	No	Few tests on many designs	No
Carbon Deposition	NAS 8-34715	OFO,FOF	RP-1, C3H8,CH4	S	Yes	Predominantly low MR	No
High Density Fuel	NAS 3-21030	TLOL,PAT	RP-1	S and US	Yes	Platelet designs	No
LOX/RP-1 (Main) Injector	NAS 8-33651	PAT	RP-1	S and US		Platelet designs	
LOX/H2 Temperature Ramping	LeRC inhouse	Shear Coax	H2	S and US	Yes NASA TND-3373, 4733,4515, and 5373	Excellent Variation of critical design parameters	Yes

* Subsequent Data Base Anomalies Noted. Not Recommended Until Corrections Are Provided

characterized. Moderate to low performance designs, such as the like doublet with little or no intentional unlike propellant fan impingement, were not as well characterized because of deficiencies in modeling their propellant mixing inefficiencies. The injection process of gas/liquid concentric tube element injectors was found to be not well characterized. However, because of the volatility of liquid oxygen (the fuel is injected at a temperature above its critical value with this injection concept) the vaporization lag produced with concentric tube injector is relatively small and therefore less sensitive to LOX atomization model assumptions. Similarly, the intra-element mixing process of this element is not well characterized but mixing inefficiencies have been overcome by maintaining small mixing distances through the use of relatively small elements. Performance model limitations could become more significant for this element type with the use of higher molecular weight fuels (e.g., methane vs hydrogen) and larger (fewer and lower cost) injection elements.

The propellant vaporization rate or the droplet heating rate (for liquids above their critical pressure) appears to be adequately characterized using the simplified "generalized length" correlation developed by Priem in NASA TR-67. This is particularly true in light of the uncertainties in the propellant atomization models. Use of generalized length correlation will greatly streamline the propellant vaporization calculations and improve the efficiency of the methodology.

Stability model evaluations compare surprisingly well with the selected data base results. This is particularly true for the liquid/liquid impinging element injector designs with and without acoustic damping devices. The stabilizing effects of both baffles and acoustic cavities were well characterized when compared with test results. Burning rate coupled instabilities were predicted with likely acoustic modes and frequencies corresponding closely with experimental results for different chamber sizes, element designs and orifice sizes. The burning response was found to contribute the largest uncertainty in the model predictions of this mode instability. Burning response, based on the empirical pressure index (n) and sensitive time lag (τ) correlations, has been previously characterized as accurate to within only $\pm 25\%$. Nevertheless, when used with stability model chamber admittance predictions, good insight into combustion stability of individual designs was achieved. An analytically based combustion response model (CRP) also appears promising although its application in this evaluation was somewhat limited.

The combustion stability of the LOX/CH_4 shear coaxial element combustor was not well characterized using available models. Model characterization of the combustion stability was improved by using the experimental results to infer or anchor the model(s) of the element injection process. In this case, the combustion stability could be shown to be injection rate coupled rather than burning rate coupled and therefore a strong function of the fuel injection velocity (mixture ratio and methane density). Improvement in the concentric tube injection process modeling is essential before good a priori predictions of its combustion stability can be made. Details of the performance and stability model correlations are provided in Reference 3.

Finally, the models and correlations evaluated were reassessed on the basis of the model evaluation results and a complete set of models was recommended for incorporation into the rocket combustor analytical design methodology. In many cases, more than one model or correlation was recommended to provide the same capability or function so the user has options for model selection and may produce comparative solutions (predictions) upon which to base his design decisions and assessment of critical design and operating parameters. A listing of the models included in ROCCID is provided in the following subsection.

B. THE ROCKET COMBUSTOR INTERACTIVE DESIGN METHODOLOGY

The design and/or evaluation of a liquid propellant rocket engine combustion chamber is normally achieved through an interactive process consisting of inter-dependent design analyses. These design analyses cover a multitude of disciplines including aerodynamics, thermodynamics, combustion, hydraulics, heat transfer and structural analysis. Many subcomponents are involved in creating a combustion chamber design including an injector and associated propellant manifolds, a combustion chamber and its associated cooling schemes, a supersonic expansion nozzle, an ignition system for non-hypergolic propellants and possibly acoustic damping devices such as resonators and/or baffles for combustion stability control.

A flow chart containing a description of the first order analyses and design iteration for the combustion design process is shown in Figure 16. A portion of this methodology, noted with a dashed line boundary in Figure 16, has been developed into a user friendly interactive computerized methodology. This methodology, entitled ROCket Combustor Interactive Design or ROCCID, contains the design and analysis logic and computer analysis modules to define the combustion stability and steady state performance of a combustor.

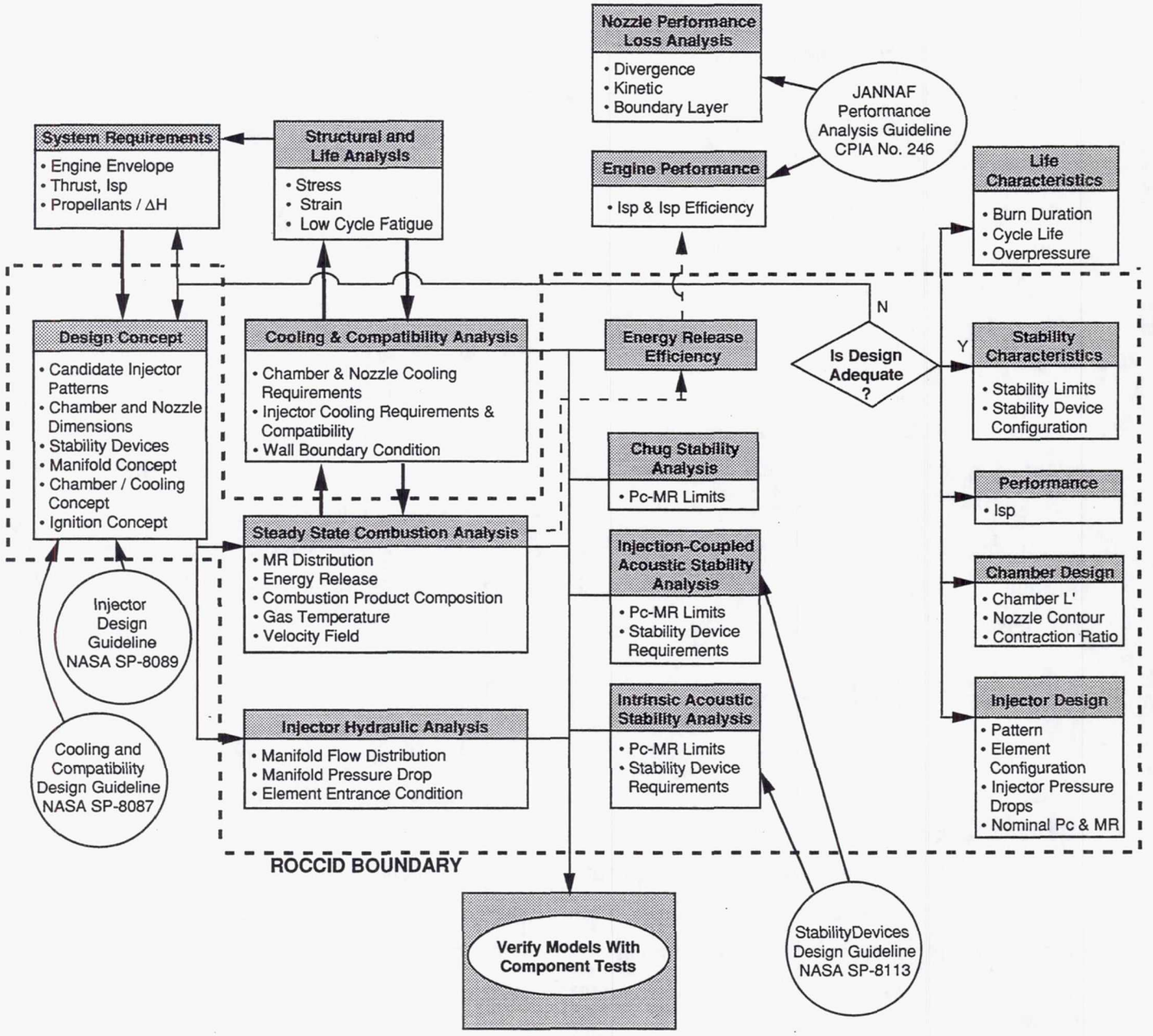

Figure 16. ROCCID Performs a Majority of the Combustor Design Iterations to Meet Combustion Stability and Performance Requirements

The structure of ROCCID is illustrated in Figure 17. ROCCID contains three main components including:

(1) An interactive front end (IFE) that assists the user with input setup, generation of plots of model output data, maintenance of combustion gas properties and logic for controlling file structure for the reuse and restart of computer runs.

(2) A point analysis option that provides performance and combustion stability analysis of existing combustor designs.

(3) A point design option that creates essential design features of a combustor that satisfies specified performance and combustion stability requirements.

Both the point analysis and point design options use a library of performance and combustion analysis models that were selected from existing appropriate codes. These analysis models are contained within ROCCID in a modular format. This permits the user to access specific models for a specialized subanalysis or to use two or more models that perform similar functions to define and resolve uncertainties in that particular area of the analysis. Modular construction also permits easier and less costly upgrades to the methodology as new analysis models are developed.

The IFE is a menu driven preprocessor constructed using an extensive library of interactive subroutines. Each input character is checked in the IFE for validity. Warnings are displayed when input errors are sensed. Replay files that contain all case input are created and maintained. These files can be edited and used as input for a subsequent session. The user may repeatedly alter the input until the desired result is achieved. Required propellant properties for both the injected fuel and oxidizer and their resulting combustion gas are internally generated and maintained in files. The "MIPROPS" data base, generated by the National Bureau of Standards (NBS), is used to obtain properties for LOX, H_2, CH_4 and C_3H_8. RP-1, N_2O_4, and MMH properties have also been included using special curve fit correlations. Finally, combustion gas properties are obtained using the One Dimensional Equilibrium (ODE) code developed by the NASA Lewis Research Center.

Upon completion of the input deck, the user may execute either the point analysis or point design options. These options contain many interactive decision points for the user. Upon

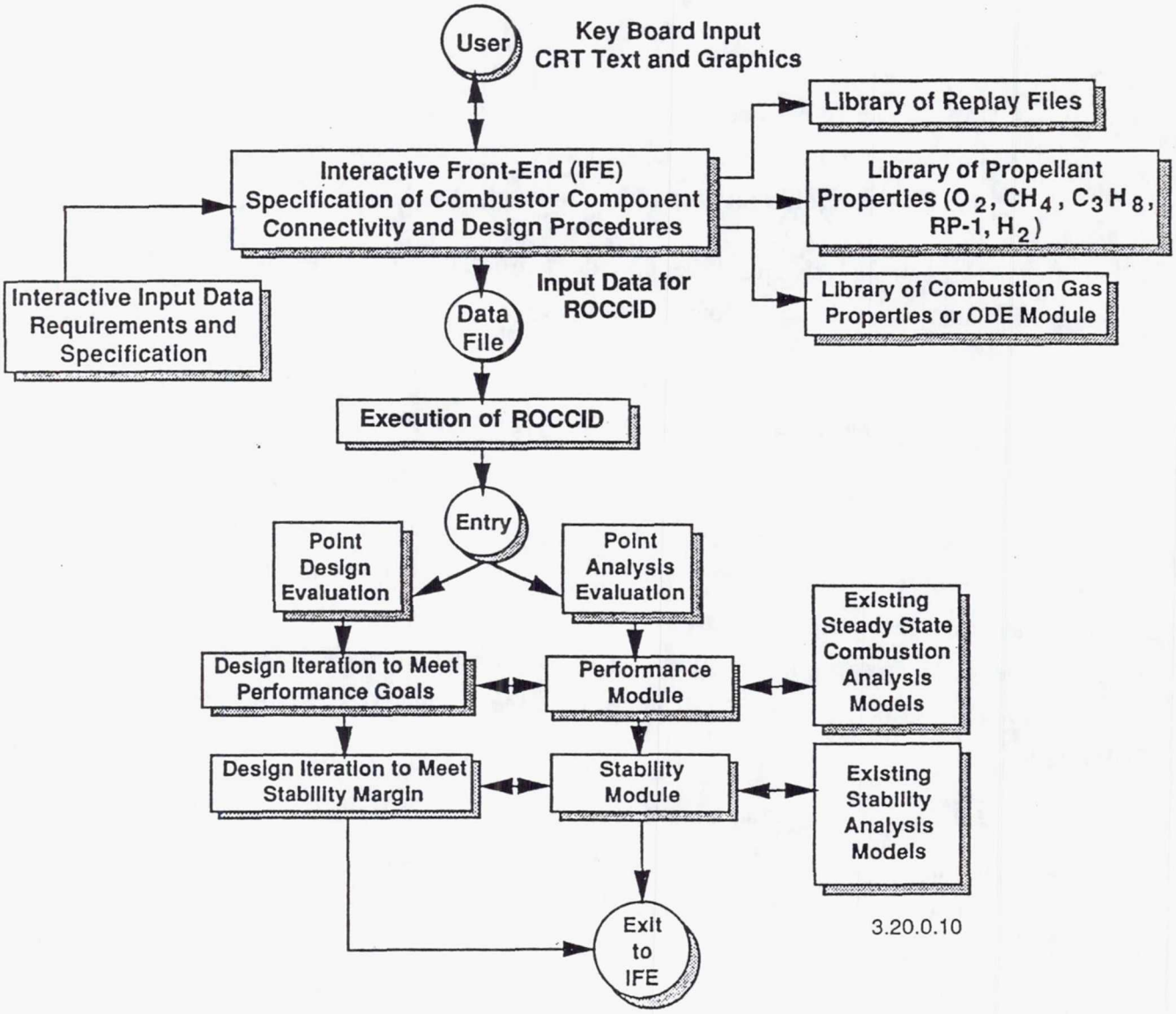

Figure 17. Major Components of ROCCID Include the Interactive Front End, Point Analysis, and Point Design Evaluation

completion of the analysis or user termination, the run stream returns to the IFE to monitor the results, record, print pertinent information, and prepare input for the next run.

The performance of the combustor is defined by the energy release efficiency. This accounts for combustion efficiency limitations resulting from incomplete propellant vaporization and/or mixing. The energy release efficiency is calculated using the JANNAF simplified performance procedure (Ref 4) and the propellant vaporization and mixing limitations from the steady-state combustion analysis. An input file for use in the TDK/BLM performance analysis of the complete engine is also generated.

A steady-state combustion analysis including propellant atomization, vaporization, and mixing supplies key input to the performance and stability analyses. Four models/correlations for propellant dropsize are included for standard injector elements including showerhead, doublet and triplet impinging elements, and shear and swirl coaxial elements. Drop sizes from all applicable correlations are calculated and displayed for comparison. A user may select any of the calculated values for performance and stability analyses or provide another estimated value. Propellant vaporization is calculated using the generalized length correlation (Ref 5). Propellant mixing is based on the use of a unielement mixing efficiency value determined previously from cold flow measurements and adjusted for interelement mixing effects.

The combustion stability analysis can be made with a large array of models used to calculate the chamber admittance and the burning and injector responses magnitudes. These models provide the capability to estimate combustion stability margin for all common types of combustor instabilities including chugging and chamber acoustic coupled (high frequency) modes. The effects of damping devices such as acoustic cavities and baffles are also considered by these models. A summary of the combustion stability models available within the ROCCID is provided in Table 10.

The chug stability characteristics are determined by calculating an acoustic chamber response without damping devices. This response is compared to a lumped parameter or acoustic injection response (user option) to determine the marginal chamber pressure for the on-set of chug stability. The injection response is determined as a function of operating pressure by evaluating combustor operation through flowrate reduction at a constant mixture ratio.

TABLE 10.

COMBUSTION STABILITY MODELS ARE INCLUDED FOR ALL ASPECTS OF STABILITY MODELING

I. CHAMBER RESPONSE

Model	Developed By Developed For	Approach	Applicable Design Features	Advantages/ Disadvantages	Used in ROCCID
HIFI	Aerojet AFAL	Linear Perturbation Technique With Mean and Fluctuating Components for Dependent Gas Dynamic Variables	Acoustic Resonators	Mechanistic, Burning Rate and Injection Coupled Extensive Application History	Yes
DIST3D	Colo State AFAL	Calculates Baffle Damping Using a Turbulent Boundary Layer Model for Viscous Dissipation	Baffle Height and Blade Distribution Acoustic Resonators as Secondary Damping	Distributed Combustion, Mechanistic, Radial Baffles Only	Yes
FDORC	Colo State AFAL	Piecewise Distributed Combustion With Arbitrarily Located Resonators	1/4 Wave Tube and Helmholtz Resonators and Liners	Distributed Combustion, Resonator Location, Mechanistic	Yes

II. BURNING RESPONSE

Model/ Correlation	Developed By Developed For	Approach	Applicable Injector Types	Advantages/ Disadvantages	Used in ROCCID
Reardon-Smith N/τ Correlations	Reardon-Smith JANNAF	Correlation of Empirical N/τ Using a Sensitive Time Lag Model	Doublets, Triplets; Coaxial	Simple Historical Data Base, Non-Mechanistic	Yes, as Option
CRP	Aerojet AFAL	Uses Agosta-Hammer Non-Linear Vaporization Response Model	All for Which a Representative Dropsize Exists	Mechanistic, but Can Require Long Run Times	Yes, as Option
Empirical/Damp Growth Rate Correlation	Aerojet AFAL	Use Observed Damp or Growth Rates to Infer Combustion Response	All for Which Empirical Growth or Damp Rates Exist	Requires Experimental Data Base but Is a Means for Anchoring Stability Model	Yes, as a Means for Increasing N/τ Data Base

III. INJECTOR RESPONSE

Model/ Correlation	Developed By Developed For	Approach	Applicable Injector Types	Advantages/ Disadvantages	Used in ROCCID
LFCS	Aerojet AFAL	Wenzel & Szuch Lumped Parameter	All with Definable Total Timelag	Simple, Good Track Record for Chug Instability	No
INJ	Aerojet NASA-LeRC	Lumped Parameter Analysis with Spacially Varying Acoustic Wave in the Chamber	All with Definable Total Timelag	Computes Injector Response Based on Element Timelag. Dependent on Good Injection Model	Yes
Lewis Non-Linear	NASA-LeRC In-House	Modification of Feiler and Heldmann Feed System Coupled Instability Model to Include Manifold Acoustic Effects	Concentric Tube Elements	Include Flow Response Due to Manifold Acoustics if Important	Yes

M10/D5/LOX-3

High frequency stability is calculated using the sensitive time lag approach. Analysis models are available to calculate the chamber response with or without acoustic damping devices and both burning and injection responses. Table 10 identifies the three models currently available to estimate the chamber response. The HIFI model (Ref. 6) developed by Aerojet calculates the chamber response for chambers without acoustic damping devices or with monotuned or bituned 1/4 wave tube or helmholtz acoustic resonators. A second model, DIST3D (Ref. 7), developed by Colorado State University is also available. This model calculates the chamber response including damping generated from radially oriented baffles. Acoustic resonators are also modeled as secondary damping devices. A third model, FDORC (Ref. 8), is also available. This model calculates chamber response for piecewise distributed combustion with arbitrarily located 1/4 wave tube or Helmholtz resonators.

Multiple approaches are also available to calculate both the burning response and the injection response as noted in Table 10. Pressure interaction index sensitive time lag (N/τ) correlations developed by Reardon are included for the impinging doublet and triplet elements and the concentric tube (coax) element. In addition, a combustion response model (Ref. 9) recently developed by Aerojet is included. This model is based on the Agosta-Hammer non-linear vaporization response model. Two models are also available to calculate the injection response of the system. The first model (INJ) bases the response on element injection timelags including atomization and partial vaporization. The second model (developed by Priem and Breisacher) is appropriate for shear concentric tube elements and includes the effects of acoustic waves in the fuel and LOX injection manifold (or LOX tube) in the injection response.

ROCCID displays the stability analysis results in terms of the calculated growth coefficient (λ) for the particular acoustic mode of concern. This growth coefficient represents the amount of amplification required by the chamber to achieve the condition where the driving required to support the waveform exactly equals the driving response present within the system. Thus a value of $\lambda = 0$ represents a neutral stability condition, $\lambda > 0$ represents an unstable condition and $\lambda < 0$ represents a stable operating condition.

The growth coefficient, in terms of the traditional combustion instability transfer function format, is illustrated in Figure 18. Three typical situations are illustrated in this example. Figure 18 (a) illustrates results of a traditional stability analysis where the region formed by overlapped chamber response and combustion response curves indicate the potential for an instability. However, this traditional analysis does not include a survey of chamber

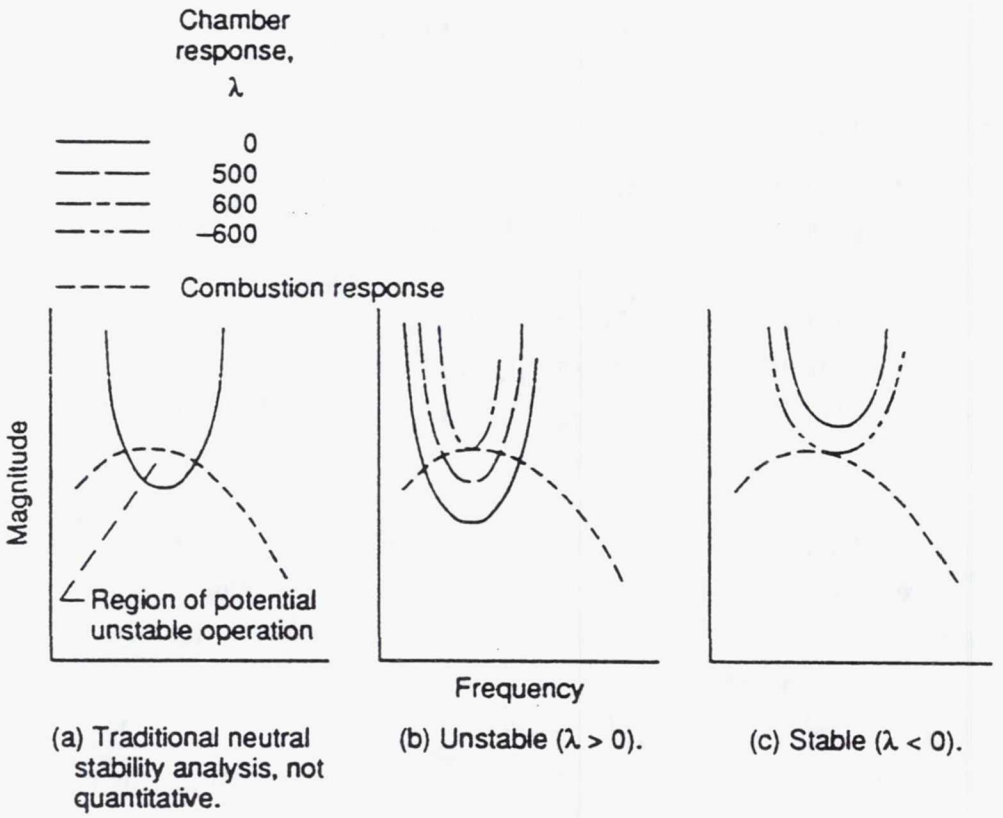

Figure 18. Illustration of the Growth Coefficient, λ, in Terms of Traditional Combustion Stability Transfer Function Format

admittances that would lead to a growth coefficient value that would provide zero stability margin, i.e., chamber response and combustion response curves being tangent at some point. The growth coefficient at this zero margin point provides a quantitative assessement stability. Figures 18 (b) and (c) illustrate unstable and stable quantitative predictions, respectively, where the growth coefficient is used to define the relative stability based on the rate of pressure amplitude growth ($\lambda > 0$) or decay ($\lambda<0$). The following is the exponential relationship used to define λ:

$$A/A_0 = e^{\lambda \Delta t}$$

where A/A_0 is the pressure amplitude ratio chamber over the period, Δt (sec).

The resultant growth coefficient can be related to the damp time required for dynamic stability as defined in CPIA 247, by defining a growth coefficient ($\lambda_{CPIA\ 247}$) required to achieve a 10:1 overpressure damping within the damp time specified from CPIA 247. That is:

$$\lambda_{CPIA\ 247} = 1n\ (0.1)/t_{damp,\ CPIA\ 247}$$

where

$$t_{damp,\ CPIA\ 247} = 1.250/\sqrt{f}\ \ (1/sec),$$

and

f = frequency of the unstable oscillation

Reducing results in the following relationship:

$$\lambda_{CPIA\ 247} = -1.842\ \sqrt{f}\ (1/sec)$$

Note that $\lambda_{CPIA\ 247}$ will always be negative, indicating a damped system, and will be a function of the frequency (mode) of the damped oscillation. Therefore, if the growth coefficient is equal to or less than $\lambda_{CPIA\ 247}$ the system is dynamically stable. Conversely, if the growth coefficient is greater than $\lambda_{CPIA\ 247}$ the system is not dynamically stable.

The design requirements for combustor cooling are established using techniques outside of ROCCID. These requirements may include estimates of fuel film cooling required for chamber and baffle walls, dump cooling of baffle tips, and bulk temperature increases resulting

from regenerative cooling of the nozzle, chamber, and resonator/baffle components. This information is used to calculate the propellant injection temperatures, injection orifice requirements, and the local flow injection mixture ratios.

Capabilities and Limitations

ROCCID has been specifically formulated to be applicable to combustor designs for LOX/HC and LOX/H_2 propellants. Propellant and combustion gas properties for LOX-RP-1, LOX/CH_4, LOX/C_3H_8, LOX/H_2, and N_2O_4/MMH are internally calculated. Both gas/liquid and liquid/liquid propellant injection are considered. Conventional impinging like doublet and triplet (OFO and FOF) elements, unlike doublet elements, non-impinging showerhead and shear and swirl coaxial elements are modelled. The injector can consist of a mixed element pattern, including core, baffle, barrier and fuel film/cavity cooling elements. Different element types can exist in different zones (i.e., baffle core, barrier). However, in any one zone only one element type may exist and doublet elements must be in matched pairs of oxidizer and fuel.

The point design option permits the user to constrain some design parameters, such as contraction ratio (CR) and chamber length (L'), thereby focusing on the best trade-off between performance and combustion stability. A simple trade-off between nozzle length and chamber length is also included to optimize engine delivered specific impulse for an envelope limited system. Acoustic damping devices are also recommended and their design features specified to provide the required combustion stability margin. Design trade-offs for a throttling engine are also performed.

The point design option features an optimization of the injector element design. The guidelines in Table 11 are provided to aid the user in injector element type selection for a particular application. The quantity of elements and the injector orifice size are calculated through a series of trade studies to satisfy performance and high frequency combustion stability requirements, chug stability and other user-specified constraints.

ROCCID has been prepared with certain limitations in order to simplify its construction and guarantee is timely and affordable initial development. No supersonic nozzle effects are currently included. The nozzle design and engine specific impulse must be determined outside of ROCCID. Precombusted fuel (staged combustion cycle) is not presently considered. Mass addition from ablation, igniters, gas generator dump or transpiration cooling is not modelled. As

TABLE 11. Element Characteristics for Several Conventional Liquid Rocket Injector Elements Modeled Within ROCCID

Injection ElementType	Propellant State Application	Key Design Parameters	Atomization	Mixing	Performance	Combustion Stability		Compatibility
						Characteristic	Control Method	
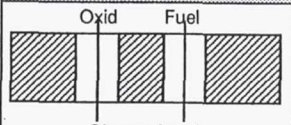 Showerhead	Liquid/Liquid Gas/Liquid Gas/Gas	• Orifice Size • Injection Velocity • Chamber Gas Density	Poor But Well Characterized	• Very Poor • Used Generally for Film or Barrier Cooling	• Very Poor	• Generally Detuned From Chamber Acoustic Modes	Not Generally Required	• Very Good When Used as Fuel Film Coolant Injection • Potential for LOX Impingement on Chamber Walls
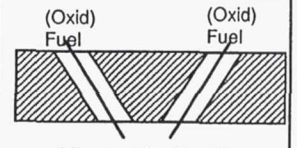 Like-on-Like Doublet	Liquid/Liquid Gas/Liquid Gas/Gas	• Orifice Size • Like Impingement Angle • Unlike Impingement Angle • Spray Overlap	• Good • Independent of Momentum Ratio and Relative Orifice Size	• Very Sensitive to Unlike Impingement Angle • Insensitive to Conditions or Relative Orifice Size • Generally Requires Inter-Element Mixing for High Em	• Good for Wide Range of Applications when Proper Unlike Impingement Angle & Thrust/Element Are Used	• Burning Rate Coupled • Non-Linear	• Multiple Chamber Acoustic Damping • Derate Performance by Increasing Thrust/Element	• Very Good with Proper Spray Orientation • May Require Film Cooling Between Elements
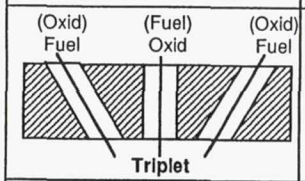 Triplet	Liquid/Liquid Gas/Liquid Gas/Gas	• Orifice Size • Relative Orifice Size	• Superior • Sensitive to Relative Orifice Size	• Excellent Intra-Element Mixing with Equal Orifice Diameter • Sensitive to Design Operating Conditions with Unequal Orifice Size	• Excellent for Limited Design Conditions (Equal Orifice Size) • Best for Maximum Thrust/Element	• Burning Rate Coupled • Non-Linear	• Maximize Thrust/Element • Chamber Acoustic Damping	• Good with Proper Spray Orientation • Generally Requires Film or Barrier Cooling Particularly, with the OFO Configuration
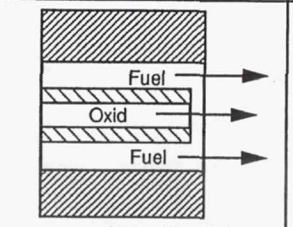 Shear Coaxial	Gas/Liquid Gas/Gas	• LOX Tube Size • Velocity Ratio • Tube Recess • Fuel Injection Velocity	• Moderate • Controlled by Shear • Not Well Characterized	• Intra-Element Controlled • Element Size Limited	• Excellent with Limited Thrust/Element • Fuel-to-Oxygen Velocity Ratio Sensitive	• Injection Coupled • Linear • Total Time Lag Sensitive	• Injection Velocity and Velocity Ratio • Limit Operating Region • Chamber/Manifold Acoustic Damping	• Generally Good - Potential for LOX Impingement on Chamber Walls
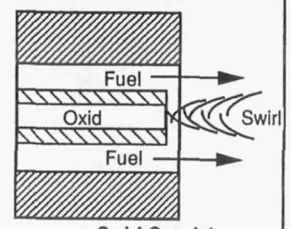 Swirl Coaxial	Gas/Liquid Gas/Gas	• LOX Tube Size • Degree of Swirl • Fuel Injection Velocity	• Good • Controlled by LOX Swirl and Fuel Shear • Not Well Characterized	• Intra-Element Controlled • Improved Over Shear Coaxial Element	• Excellent • Less Restricted Thrust/Element Constraint	• Injection Coupled • Linear • Total Time Lag Sensitive	• Injection Velocity, Velocity Ratio and LOX Swirl Angle • Limit Operating Condition • Chamber Acoustic Damping	• High Potential for LOX Impingement on Chamber Walls • Increased Sensitivity to Operating Conditions

log 89.464C

previously noted, cooling requirements are defined outside ROCCID, but their effects on performance and stability are considered.

ROCCID has been developed and is operational on VAX 8600 series computers at both Aerojet and NASA Lewis Research Center. It has also been operated on a SUN4/SPARC architecture computer at SEA, Inc. Interactive graphics for Tektronix 40XX and 41XX terminals are also provided. The code has been constructed without machine dependent instructions, but operation on other computer systems remains to be verified. A complete description of the ROCCID methodology and a user's manual for its operation is provided in References 10 and 11.

C. APPLICATION OF THE ROCCID METHODOLOGY

The creation of a combustor design consists of an evolutionary process where design requirements and operational goals are used to establish design parameters for the injector and combustion chamber. Iterations to the set of critical design parameters are performed to meet performance goals while providing for stable combustion. ROCCID has been used to examine the sensitivity and influence of several injector and combustor design parameters on the predicted combustor performance and combustion.

The propellant combination of LOX/RP-1 was selected for study using ROCCID and for eventual hot fire testing to validate ROCCID capabilities. This propellant was selected because historically, it has proven to be a difficult propellant to provide both stable combustion and high performance.

Nominal design propellant injection temperatures of 174.4°R for liquid oxygen and ambient conditions (515°R) for RP-1 were selected. These conditions represent normal propellant storage temperatures within the Aerojet test facility and therefore were the most cost effective test conditions.

A nominal design mixture ratio of 2.8 was selected since this approximates an optimum performance design from a thrust chamber performance viewpoint. Note that this mixture ratio value was selected for design purposes only. The effects of mixture ratio variation on a fixed design were evaluated using ROCCID and mixture ratio was a key operating parameter for validation testing.

Thrust chamber size was also a key design parameter, particularly from a combustion stability standpoint. The chamber diameter has a direct effect on the resonant frequency of acoustic modes within the chamber. large chambers approrpriate for booster engine application(Dc = 17.5 to 44 in.), have lower resonant frequencies that are more likely to couple with typical combustion responses. On the other hand, subscale chamber diameters of 5.5 and 7.68 in. have been successfully used in the past for combustion stability investigations (Refs. 12 and 13). For this study, a nominal baseline chamber diameter of 7.68 in. was selected since it is a proven "subscale" design and residual hardware was available from the test program in Ref. 13.

A contraction ratio of 2:1 that corresponds to a throat diameter of 5.43 in. and a nominal design chamber pressure of 1250 psi were selected to provide a large operating chamber pressure variation within the existing hardware and test facility capabilities. The operational envelope of the validation hardware for the Aerojet E-4 test facility is shown in Figure 19. A variation in mixture ratio from approximately 1 to 10 was possible at the nominal chamber pressure of 1250 psi. A maximum chamber pressure of approximately 1800 psi could be achieved at the nominal mixture ratio. The mixture ratio excursion range diminishes as chamber pressure is increased due to the facility run tank pressure limits.

Impinging injector designs were selected for this evaluation since they are most appropriate for liquid/liquid injection. Specifically, the like doublet and OFO triplet elements, both of which are included in the ROCCID methodology were evaluated. The OFO triplet element was selected over the FOF since the propellant density and mixture ratio resulted in equal orifice diameters with an OFO element but not with the FOF triplet. From experience, equal orifice diameters are desirable with a triplet element to provide optimum mixing and atomization.

A summary of the selected design parameters for this study is presented in Table 12. Design parameters from two recent combustion stability investigations in Refs. 12 and 13, are also provided for comparison purposes.

Downselect Criteria

Criteria were established to select the injector for use in the validation of ROCCID. Because of limited resources, one and at best two different thrust chamber designs could be selected for design and testing. The following criteria were established on the basis of providing the best test of the capabilities of ROCCID:

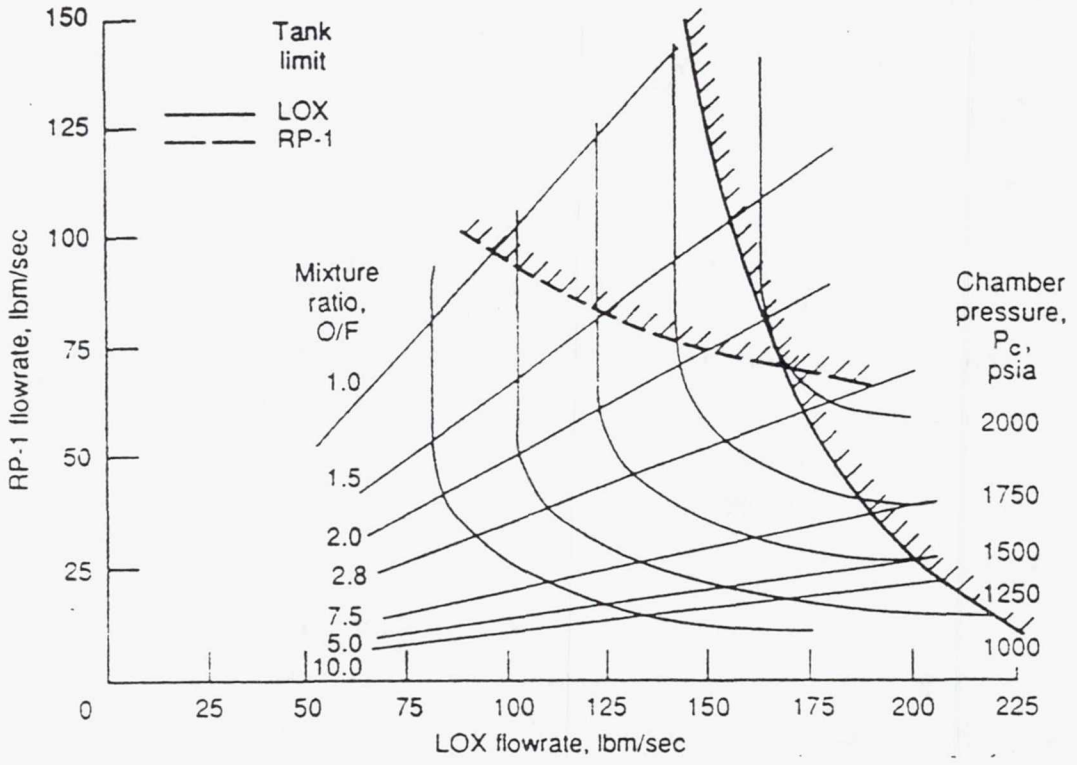

Figure 19. Facility Operating Limitations

TABLE 12. COMPARISON OF SELECTED NOMINAL DESIGN PARAMETERS

	Combustion Stability Investigation		
	NAS 3-25556[1]	F04611-85-C-0100[2]	NAS 3-24612[3]
Propellant Combination	LOX/RP-1	LOX/RP-1	LOX/CH_4
Mixture Ratio	$2.8 \pm$ TBD	2.9 ± 0.3	$3.5^{-1.6}_{+0.2}$
Injection Temperature LOX °R Fuel °R	 174 515	 174 530 ± 20	 174 530 to 438
Chamber Pressure (psia)	$1250 \pm$ TBD	2000^{+100}_{-1300}	2000^{+100}_{-500}
Chamber Diameter (in.)	7.68	7.68	5.66
Throat Diameter (in.)	5.43	4.43	3.31
Contraction Ratio	2:1	3:1	2.92:1
Chamber Length (in.)	TBD	8.5, 13, 20	14
Nominal Thrust Level (lbf)	52,000	54,000	30,000
Total Flowrate (lbm/sec)	$160 \pm$ TBD	180^{+10}_{-90}	90^{+7}_{-15}
Injection Element Type	OFO Triplet Like Doublet	OFO Triplet Like Doublet	Shear Coaxial

(1) LOX/Hydrocarbon Rocket Engine Analytical Design Methodology Development and Validation
(2) Oxygen/Hydrocarbon Injector Characterization (Ref 13)
(3) LOX/Hydrocarbon Combustion Instability Investigation (Ref 12)

(1) Largest negative and positive growth coefficients for the most stable and unstable modes without acoustic damping.

(2) Highest sensitivity of combustion stability to chamber pressure and mixture ratio.

(3) Greatest design change from existing data base.

(4) Capable of stabilization at nominal operating conditions using an acoustic cavity.

(5) Highest confidence in modelling dropsize and mixing efficiency.

(6) Ease of incorporating design features into existing hardware.

Selection of the Injector

Three injector designs, a fine triplet, a coarse triplet, and a like-on-like doublet, were selected to be evaluated by ROCCID for detail design and testing. Initially, the point design option ROCCID was used to size the injectors for the nominal operating conditions. Thereafter, the analysis portion of ROCCID was used to perform trade studies on the initial designs. The experience gained from the experimental results of Ref. 13 was also applied to the analysis. Also from past experience, certain model combinations in ROCCID were used because they produced good results. HIFI was used to analyze the chamber response. Smith-Reardon and N/τ correlations were used to analyze the burning response. INJ was used to analyze the injector response.

The injector orifice sizes evaluated were 0.090 in. for the fine triplet, 0.159 in. for the coarse triplet, and 0.100 in. LOX and 0.065 in. fuel for the like-on-like doublet. The predicted performance efficiencies for all three injectors were greater than 97 percent so performance did not become a critical concern in the selection process.

An extensive number of stability predictions were generated and only a portion will be discussed in the following section. References 14 and 15 should be examined for more details.

The chug stability of the three injectors was analyzed. The fine triplet and the doublet had low chug thresholds at about 300 psi. The coarse triplet had a more undesirable

chug threshold at about 600 psi. Considering that the nominal operating pressure is 1250 psi, this higher chug pressure limit for the coarse triplet would not allow for much leeway in throttling the engine to find stable and unstable high frequency stability regions.

The high frequency stability characteristics of the three injectors were also analyzed. The coarse triplet was found to be the most stable injector design (λ less than -37 in all modes) without acoustic damping devices. From a flight hardware designer's point of view, this would be an excellent design. However, since our validation criteria require both stable and unstable operation for verification, the coarse triplet injector design was not sufficient for ROCCID validation.

The doublet was found to be stable except for the first tangential mode. The doublet was very promising because it had a region of operation where it could be driven stable and unstable by changing the mixture ratio as shown in Figure 20. The doublet could be stabilized using acoustic damping devices that would allow validation of the models for damping devices. The major drawback of the doublet was that it was very similar to the design used in Ref. 13. Since this was a validation of the predictive capability of the models in ROCCID, using an injector so close to the anchored hardware made this injector a secondary choice.

The fine triplet design was predicted to be unstable in several different modes with varying operating conditions. Figures 21 to 24 show ROCCID predictions of stability changes over the operating map. The first longitudinal (1L) mode was stable at all but lower chamber pressures. The first tangential (1T), second tangential (2T), and first radial (1R) modes were predicted unstable over wide changes in operating conditions. An evaluation of an orifice diameter increase from 0.09 to 0.10 in. indicated that the stability margin did not improve sufficiently to provide any significant advantages. Damping devices were found to be very effective in damping the unstable modes. In addition, this design was very different from the hardware described in Reference 13 in terms of number of elements and orifice sizes.

Table 13 provides a rating of the candidate injector designs. It is obvious that the fine triplet injector was the best choice to validate the models contained within ROCCID. The fine triplet injector stability was predicted to be sensitive to chamber pressure and mixture ratio variations that would allow for testing the sensitivity and predictive capabilities of the models.

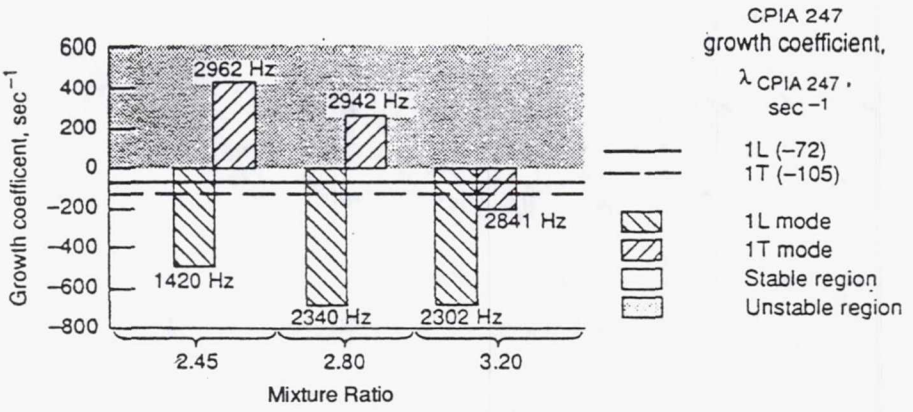

Figure 20. Like Doublet Injector Stability Prediction, Chamber Pressure - 1250 psia; Length = 17 in., No Damping

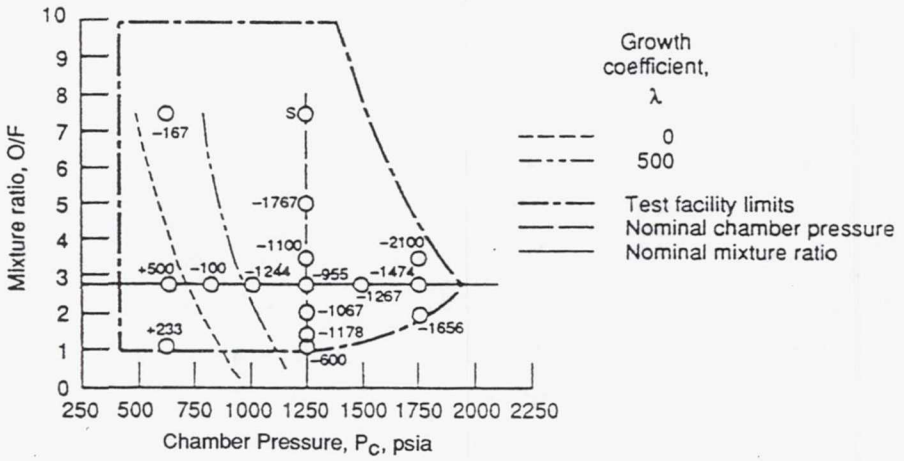

Figure 21. Fine Triplet 1L Mode Stability Map Showing Values of λ at Various Points as Well as Points Predicted to Be Extremely Stable

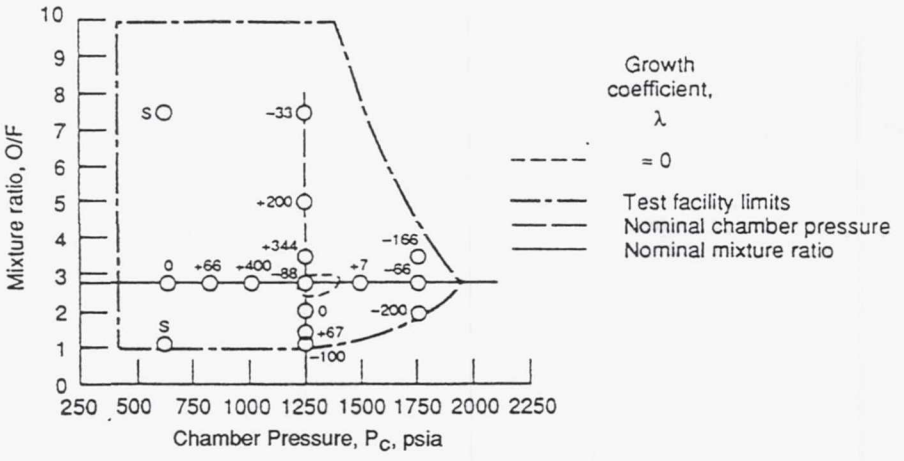

Figure 22. Fine Triplet 1T Mode Stability Map Showing Values of λ at Various Points as Well as Points Predicted to Be Extremely Stable

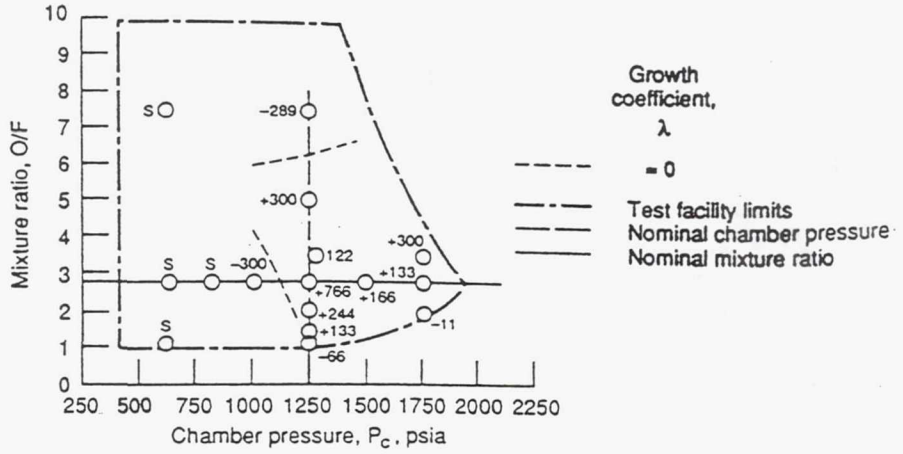

Figure 23. Fine Triplet 2T Mode Stability Map Showing Values of λ at Various Points as Well as Points Predicted to Be Extremely Stable

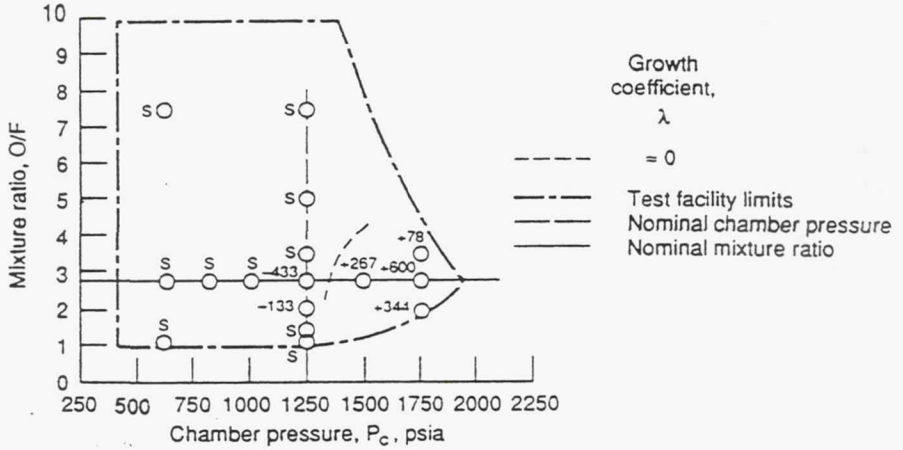

Figure 24. Fine Triplet 1R Mode Stability Map Showing Values of λ at Various Points as Well as Points Predicted to be Extremely Stable

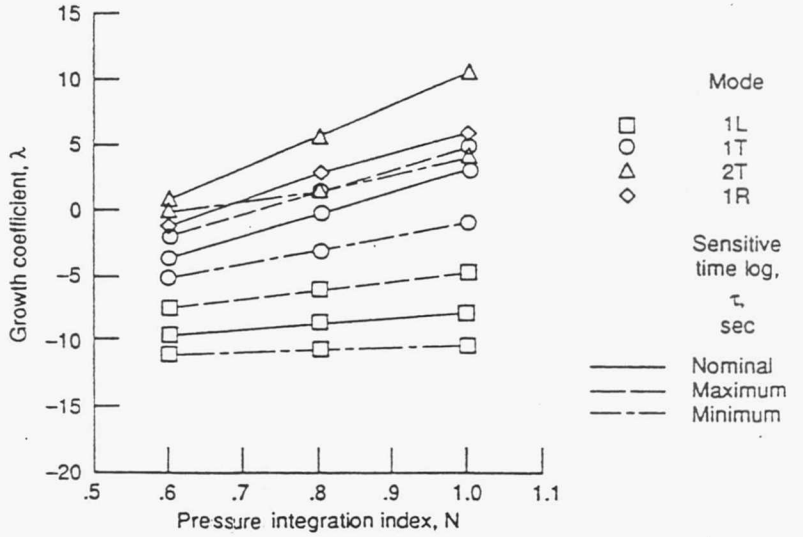

Figure 25. Variation of Growth Coefficient λ With N and τ

TABLE 13.

INJECTORS COMPARED AGAINST RATING CRITERIA

Rating Criteria	Injector Configuration		
	Fine O-F-O Triplet	Coarse O-F-O Triplet	Like-on-like; One Doublet
Largest negative and positive growth coefficients for least damped mode without acoustic damping	Most unstable	Most stable	Unstable
Best sensitivity of combustion stability to P_c and O/F	Significant variation with 2T and 1T; stable operation with O/F and P_c	Much larger variation in P_c and O/F required to drive unstable	Good sensitivity with O/F for 1T mode
Greatest change from existing data base	N_c, 39 to 105 D_o, 0.125 to 0.090	N_c, 39 to 48 D_o, 0.125 to 0.159	N_c, 105 to 123 D_o, 0.059 to 0.065
Capable of stabilization at nominal operating conditions using an acoustic cavity	Three types of cavities evaluated	Stable without an acoustic cavity	1T monotune cavity judged to be sufficient
Best confidence in modeling drop size and mixing efficiency	r_m reasonable; E_m good	r_m reasonable; E_m good	r_m reasonable; E_m reasonable
Ease of incorporating design features into existing hardware	New faceplate only	New faceplate and injector core	New faceplate and injector core
Preferred rating	6 of 6	3 of 6	2 of 6

Indicates preferred characteristic

The fine triplet injector was sufficiently different from previously tested injectors to allow a true " a priori" prediction. As a result, this injector was selected as the validation test hardware.

Growth Coefficient Uncertainty

The sensitivity of the stability predictions (in terms of the growth coefficient) to the pressure interaction index, N, and sensitive time lag, τ, were evaluated over a range of N and τ values. The ranges of N and τ values were selected based on estimates from three sources.

(1) The empirical variations in these parameters shown in Refs. 16 and 17.

(2) The calculated variation resulting from different droplet combustion mixture ratios and gas temperatures using the CRP model (Ref. 9).

(3) Variations in τ based on an estimated 1 percent uncertainty in energy release efficiency and relating that uncertainty to a change in vaporization time lag.

The three techniques yielded similar results. Based on the Ref. 16 data the uncertainly in N was estimated to be ±26% (0.90±0.20) and the uncertainty for τ was +43%, -31% (0.7 x 10^{-4} sec to 1.79 x 10^{-4} sec) (see Figures 25 (c) and (d) of Ref. 16).

The CRP model was used to evaluate assumed fuel droplet surface mixture ratios of 0.7 to 2.4 and gas temperatures of 2500 to 6500°R at the droplet surface. These analyses resulted in N values of 0.45 to 1.0 and τ values of 0.94 x 10^{-4} sec to 2.5 x 10^{-4} sec, similar to the ranges shown from Ref. 16 but slightly larger.

Additionally, a typical 1% performance uncertainty (98 ± 1%) resulting from a fuel droplet size uncertainty would yield a τ uncertainty of approximately 20%, again in the general range observed from the Smith-Reardon data.

The above variations in N and τ from Smith-Reardon at the nominal chamber pressure and mixture ratio (Pc = 1250 psi, O/F = 2.8) were evaluated using ROCCID. The results, as shown in Figure 25 indicate large variations in predicted growth coefficient, up to approximately ±600 sec^{-1} for the 2T mode if both N and τ variations are considered. However, implicit within ROCCID is a variation in τ due to engine operating conditions. Therefore, the

data scatter leading to uncertainties in τ from Refs. 16 and 17 may be due to differences in the operating condition of the engines being evaluated. If only the uncertainty in N is considered, the growth coefficient in variations are reduced to ± 25 sec^{-1} for the 1L mode, ± 350 sec^{-1} for the 1T mode, and ± 500 sec^{-1} for the 2T mode. Based on the statistical scatter in the existing empirical correlations of N and the present state of the models, these large bands of uncertainty associated with the predictions are expected.

It should be noted that there is not an equal expectation of N values within the published uncertainty band of $\pm 25\%$, which probably represents a $\pm 3\sigma$ standard deviation. If this is the case, then a statistical analysis of experimental data going into ROCCID could be performed to estimate the confidence level of the ROCCID predictions for calculated values of growth coefficient. A more detailed analytical and statistical evaluation of the data is recommended to allow a better understanding of the reasons for and consequences of the uncertainties in N and τ.

D. ROCCID VALIDATION TEST PLAN DEVELOPMENT

A plan for generation of a test data base for validation of the ROCCID Methodology was developed that consisted of nine basic test series identified as test series A-I in Table 14. These test series were developed to verify the thrust chamber start and shutdown sequence (series A), stable operation and performance with an acoustic resonator (series B and D), the chug stability predictions (series C), and unstable operation without acoustic damping (series E and G). Test series to verify stable operation without acoustic damping (series F) and unstable operation with acoustic resonators (series H) were also included to assess ROCCID's ability to forecast major combustion stability changes through operation at extreme off-nominal operating conditions. If tests with an acoustic resonator show much larger regions of unstable operation than predicted by ROCCID, a test series without an acoustic resonator (Series I) would be conducted to evaluate the instability frequency and amplitude suppressions (if any) resulting from the cavity test series to aid in cavity redesign.

A total of twenty six tests were planned, but the total number of tests and specific sequence and test series were subject to change pending program cost and schedule constraints and potential test results. A specific test matrix and test sequence for this testing is included in Table 15. The Table 15 information provides a test sequence overview. More details of the test logic and expected results are contained in the discussions of Block 1, Block 2, and Block 3 testing in subsequent paragraphs.

TABLE 14. ROCCID VALIDATION TEST SERIES

Test Series	Test Objectives	Test Procedure
A	Start, Shutdown and Balance Verification	Verify LOX/TEAL-TEB Ignition Verify RP-1 Ignition and Level II Operation Adjust Timer Settings and Level I and II Valve Positions as Required. Define System Flow Resistance Values.
B	Verify Stable Operation With Acoustic Cavities at the Nominal Design and Operating Condition.	Nominal Operating Conditions Same as Test Series E. Obtain Cavity Temperature Measurements as Required to Verify Cavity "Tune."
C	Verify Chug Stability Predictions Verify L Mode Predictions	Establish Level II Operation at a Low Pc Expected Stable Operating Point. Step Throttle Using the Thrust Chamber Control Valves to Obtain Approximately 3-5 Steady State Operating Points at Diminished Chamber Pressure.
D	Verify Stable Operation and Performance at Off-Nominal Conditions Using Acoustic Cavities	Conduct Tests at Specified Mixture Ratio and Total Flowrate to Obtain Performance Data and Verify Stable Operation Including Bomb Overpressure and Damp Rate.
E	Verify Unstable Operation Without Acoustic Damping at the Nominal Design Point	O/F Nominal = 2.8 $W_{Nominal}$ = 147 lbm/sec PC-3 Nominal = 1,250 psia D_t Nominal = 5.43 in. 6.5 Grain Bomb at FS-2.
F	Verify Stable Operation Without Acoustic Damping at Off-Nominal Conditions	Conduct Tests at Specified Mixture Ratios and Total Flowrate to Verify ROCCID Predictions of Stable Operation and Off-Nominal Performance. 6.5 Grain Bomb at FS-2.
G	Verify Unstable Operation Without Acoustic Damping at Off-Nominal Conditions	Conduct Tests at Specified Mixture Ratios and Chamber Pressures to Verify ROCCID Predictions of Unstable Operation, Instability Acoustic Mode, Frequency and Amplitudes (and Possible Growth Rate) Will Be Measured. 6.5 Grain Bomb at FS-2.
H	Verify Unstable Operation With Acoustic Cavities at Off-Tune Conditions	Same as Test Series D. Obtain Acoustic Cavity Gas Temperatures as Required to Verify Off-Tune Cavity Performance.
I	Verify Cavity Impact on Instability (Mode and Amplitude Suppression) and Confirm Cavity Sound Speed	If Block 1 Tests are Unstable, i.e. Series "B" and "D" Not Verified, Conduct Tests Without Cavity to Compare Unstable Frequencies and Amplitudes to Test With Cavities, Confirm Cavity/Chamber Sound Speed Assumption

TABLE 15. ROCCID VALIDATION TEST MATRIX

Test No.	Test Series (1)	Pc	O/F	Steady State Duration (sec)	Acoustic Cavity	Bomb @ FS-2	Block	Chamber Liner S/N	Remarks
1	A	100	N/A	N/A	Yes	No	1	1	These Block 1 Tests are Intended to Provide Checkout of Start and Shutdown Sequence, Verify Instrumentation' Adequately Define CHUG and 1L Limits and Verify Regions of Stable Operation with an Acoustic Cavity. If Stable Regions are Demonstrated Essentially as Predicted the Block 2A Test Sequence Will Be Initiated. If Not, a Reduced Block 2 (Block 2B) Series Will Be Conducted and an Acoustic Cavity Will Be Redesigned, Fabricated and Tested (During Block 3B Test Series).
2	A	1250	2.8	0.1	Yes	No	1	1	
3	B	1250	2.8	0.3	Yes	Yes	1	1	
4*	C	700	2.8	0.5	Yes	No	1	1	
5	C	500	2.8	0.5	Yes	No	1	1	
6*	D	1500	2.8	0.3	Yes	Yes	1	1	
7	D	1500	1.5	0.3	Yes	Yes	1	1	
8	D	1250	1.2	0.3	Yes	Yes	1	1	
9*	D	800	7.5	0.3	Yes	Yes	1	1	
10	D	1000	2.0	0.3	Yes	Yes	1	1	
11	E	1250	2.8	0.3	No	Yes	2A or 2B	2	Block 2A Tests if Block 1 Stability Verified, Otherwise Block 2B Tests if Block 1 Testing is Substan- tially Unstable. Use Information From Block 1 and Block 2B Tests for Acoustic Cavity Redesign as Required.
12	F	1000	1.2	0.3	No	Yes	2A or 2B	2	
13	G	800	7.5	0.3	No	Yes	2A or 2B	2	
14	G	1500	2.8	0.3	No	Yes	2A or 2B	2	
15*	G	1750	2.8	0.3	No	Yes	2A or 2B	2	
16*	F	1250	1.2	0.3	No	Yes	2A Only	2	
17*	*TBD	TBD	TBD	TBD	No	Yes	2A Only	2	
18*	TBD	TBD	TBD	TBD	No	Yes	2A Only	2	
19*	TBD	TBD	TBD	TBD	No	Yes	2A Only	2	
20	B	1250	2.8	0.3	Yes	Yes	3A or 3B	3	If Block 1 Tests are Stable Use the Same Cavity as Block 1. If Block 1 Tests are Unstable, Retune the Cavity Based on Block 1 and Block 2B Data. Block 3A Test Conditions Apply if the Same Block 1 Cavity Is Used. Otherwise the Redesigned Cavity Will Be Tested During Block 3B Series (TBD).
21	H	1250	3.5	0.3	Yes	Yes	3A/3B TBD	3	
22*	H	1750	2.8	0.3	Yes	Yes	3A/3B TBD	3	
23	H	1500	5.0	0.3	No	Yes	3A/3B TBD	3	
24	H	800	5.0	0.3	No	Yes	3A/3B TBD	3	
25*	H	800	1.2	0.3	No	Yes	3A/3B TBD	3	
26*	B	1250	2.8	0.3	No	Yes	3A/3B TBD	3	

(1) See Table VI for Test Series Description

* Identifies Tests of Lower Priority That May Be Eliminated in the Event of Unforeseen Problems That Require Additional Tests To Achieve Adequate Resutls

The testing was planned in three blocks, as shown on the overall test logic diagram, Figure 26. Block 1 tests used a 1/4 wave tube acoustic cavity and the tests were structured to meet objectives of test series A (start, shutdown, and flow rate balance verification), B (verification of stable operation at the nominal operating point, MR = 2.8, Pc = 1250 psia), C (verification of chug and L mode predictions), and D (verification of stable operation at off nominal conditions). Block 2 tests were conducted without chamber acoustic damping devices and were structured to meet the objectives of test series E (verification of unstable operation w/o damping devices at the nominal design point), F (verify stable operation w/o acoustic damping devices at off nominal conditions), and G (verify unstable operations w/o acoustic damping devices at off nominal conditions). If the Block 1 tests did not result in a significant region of stable operation a retuned or re-configured acoustic cavity would be designed, fabricated, and tested based on the Block 1 cavity temperature and stability data. In this case, the Block 2B testing (without a cavity) would be conducted to confirm undamped chamber modes at the nominal operating condition and over a range of flow rates. These tests would be used to assess the undamped configuration ROCCID predictions and the mode suppression observed in the Block 1 tests would further verify the Block 1 cavity sound speed. The tests would be conducted while the retuned cavity is being prepared for testing.

Block 3 testing, with an acoustic cavity, was used to confirm nominal operating point stability and verify predicted off nominal operating point unstable operation if, based on Block 1 tests, the original cavity tune was adequate. If the original cavity tune was not adequate to provide a substantial region of stable operation based on Block 1 tests, Block 3B tests would be used to evaluate a better cavity tune or configuration, using the ROCCID results anchored to the Block 1 data.

Tests identified with an asterisk in Table 15 are designated as lower priority than the remaining. In the event that additional unplanned tests were required to achieve any specific test objective, these tests would be considered for deletion from the test program in order to maintain control of the overall program cost.

As will be shown, each of the three blocks of tests contain 7 to 10 tests. Based on previous experience, this would allow one chamber liner to be used for each block of tests.

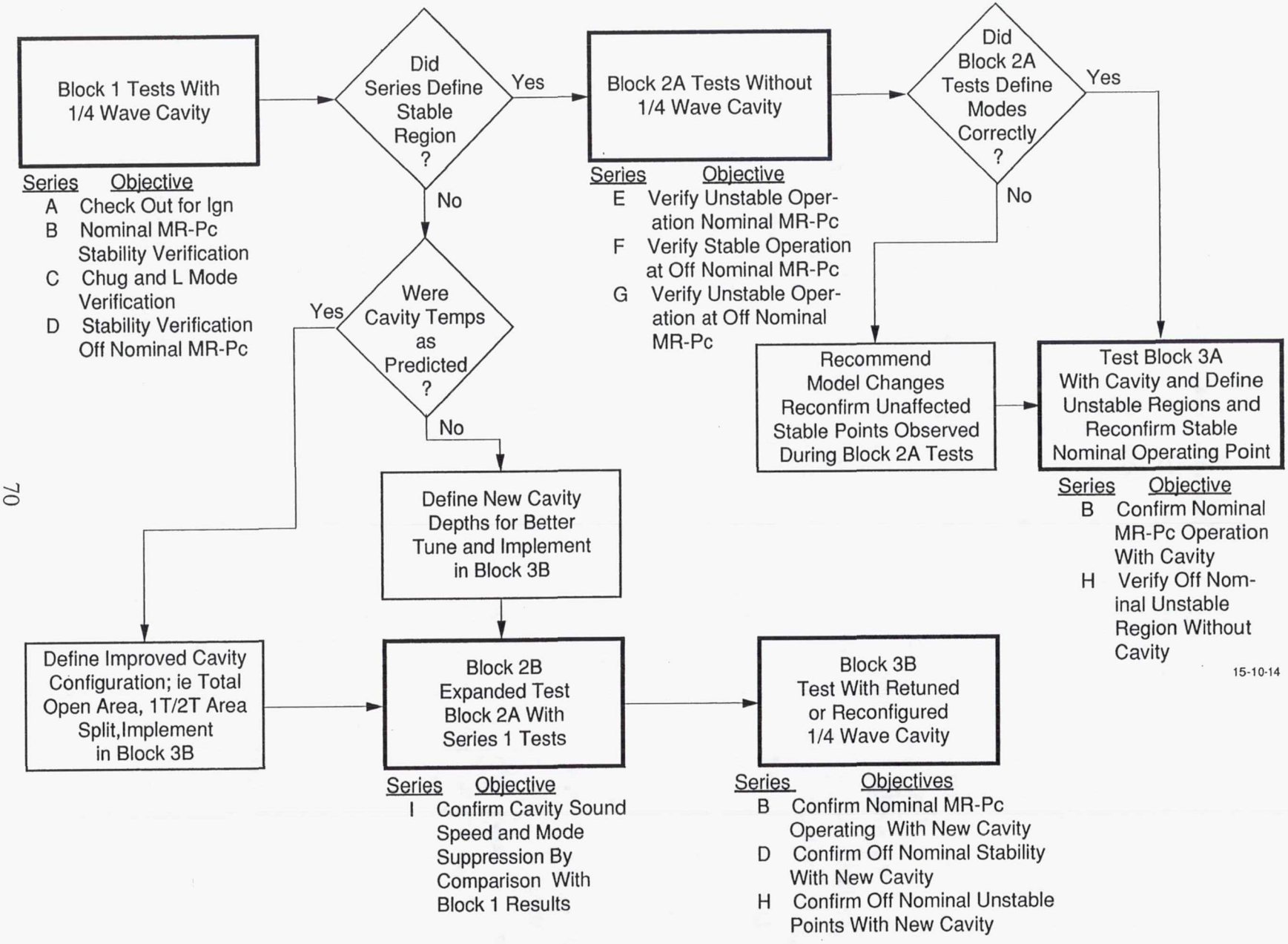

Figure 26. Overview of Test Logic

Block 1 Tests

More detailed test logic along with specific success criteria is shown on Figure 27 for the Block 1 tests. One should note that the generation of well defined test data, i.e., accurate flow rate, temperature, pressure and thrust data (and for the unstable tests accurate combustion frequency determination) were of paramount importance. These data were used not only for comparison with ROCCID model predictions but also provided the basis for updating or re-anchoring the model, should that be necessary.

The specific Block 1 test points are shown tabulated on Table 16 and shown graphically on the test facility operating map on Figure 28. The predicted regions of stable and unstable operation shown on Figure 28 were based on the ROCCID growth coefficient predictions.

The test series A logic is shown on Figure 29. Test series A verified the start and shutdown sequencing, the flow system resistances and the instrumentation (except CSMs) before proceeding onto the performance and stability tests. Two tests were allocated for this test series.

The logic for test series B, verification of nominal operating point stability, is shown on Figure 30. This was the first test of sufficient duration to verify cavity temperature estimates, provide meaningful performance data and the first test to assess bomb induced chamber pressure spikes. Four important "gates" are shown on the test logic diagram. The first gate is related to the success criteria of Figure 27 (Is the test data valid and was intended operating point achieved?) If the answer was yes the next gate would be evaluated. If the answer was no, the test data and prediction would be evaluated and a decision to retest or proceed to next gate made.

If the test was statistically stable and the bomb overpressure is less than 20% of chamber pressure, a retest would be conducted. If the test was spontaneously unstable, the mode was defined and a retest made at a more stable operating point defined from the growth coefficient predictions based on the ROCCID analysis.

The test series C logic, shown on Figure 31, was used to ensure that valid data was collected and evaluated for verification of chug and longitudinal mode instabilities. The ROCCID prediction of longitudinal mode instability was the result, to a large extent, of predictions of injection coupling. This can be seen from the response plots for MR = 2.8 and chamber pressures of 625 and 800 psia shown on Figure 32. Injection coupling with impinging

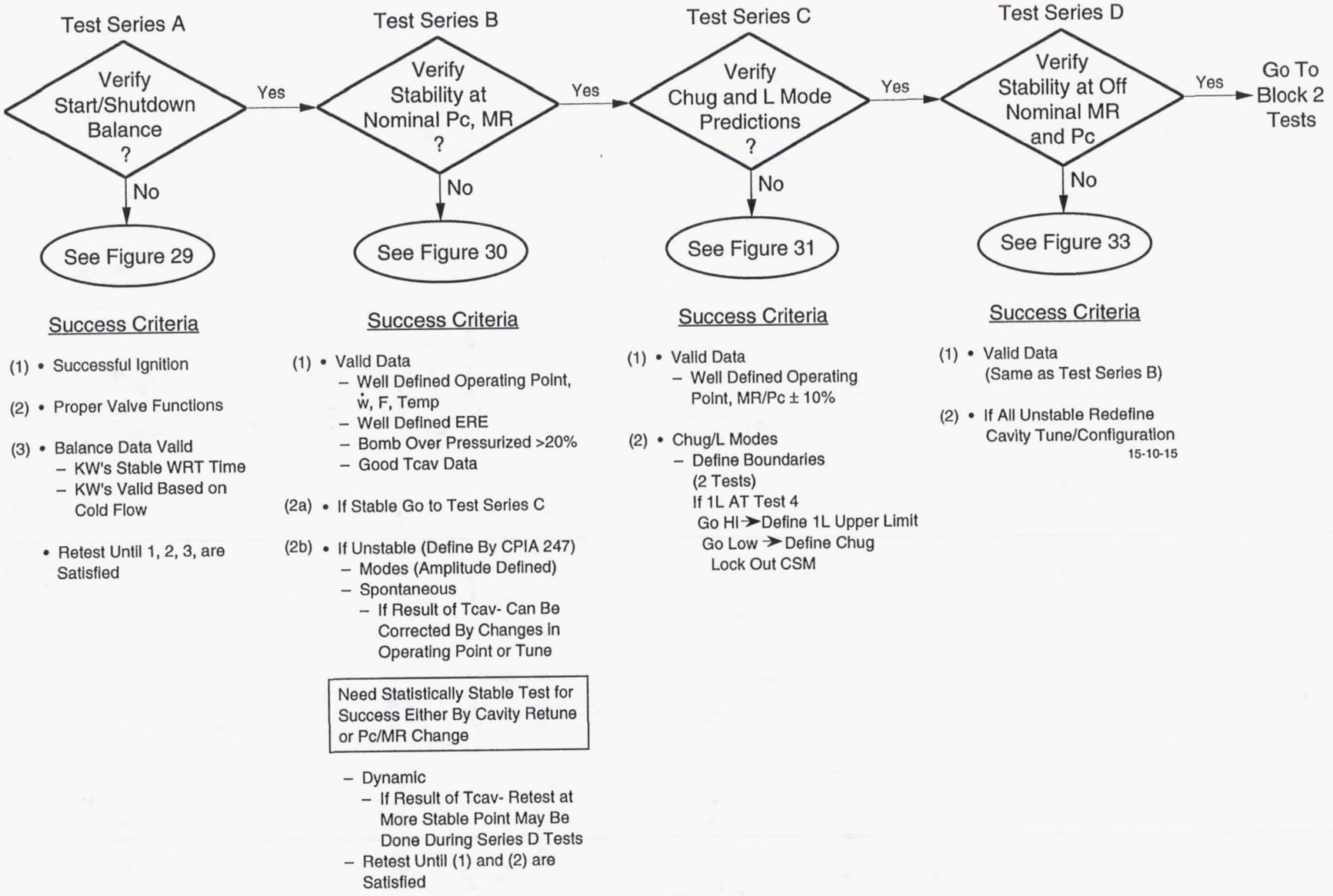

Figure 27. Block 1 Test Logic and Success Criteria (Chamber With 1/4 Wave Damping)

TABLE 16. BLOCK 1 TESTS ARE CONDUCTED WITH AN ACOUSTIC CAVITY

Objectives

- Verify Balance, Sequencing, and Instrumentation
- Verify Stability With an Acoustic Resonator
- Verify Performance
- Verify Chug Stability Limit
- Verify L Mode Stability; Contribution of Injection Coupling at Low Pc
- Verify Cavity Temperature Estimates

Test No.	Test Series	Pc	O/F	Steady State Duration (sec)	Acoustic Cavity	Bomb @ FS-2	Predicted ERE	Remarks
1	A	100	N/A	N/A	Yes	No	–	Verify TEAL/TEB Ignition
2	A	1250	2.8	0.1	Yes	No	–	Verify Level II Operation
3*	B	1250	2.8	0.3	Yes	Yes	98.6	Performance/Stability
4	C	700	2.8	0.5	Yes	No	98.5	Verify IL/Chug
5	C	500	2.8	0.5	Yes	No	98.5	Repeat Verification
6*	D	1500	2.8	0.3	Yes	Yes	98.6	Most Stable 1L
7*	D	1500	1.5	0.3	Yes	Yes	98.2	Most Stable 1T
8*	D	1250	1.2	0.3	Yes	Yes	99.6	Most Stable 2T
9*	D	800	7.5	0.3	Yes	Yes	98.8	Most Stable 1R
10*	D	1000	2.0	0.3	Yes	Yes	97.5	1L/1T Boundary, Min ERE

* Sequence Dependent on Mode of Any Instabilities

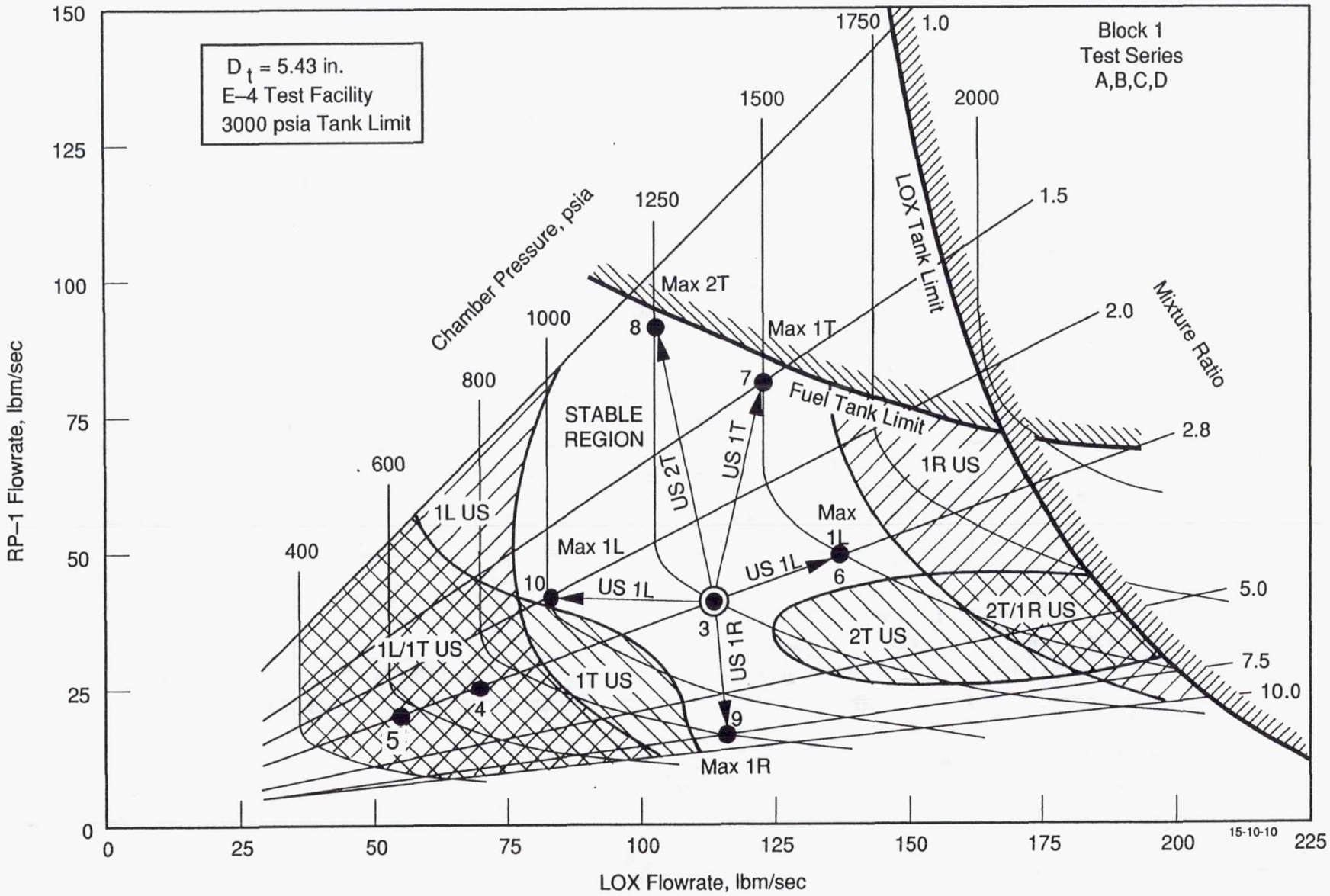

Figure 28. Block 1 Tests Will Define Stable Operating Region With an Acoustic Cavity and Evaluate Chug and L Mode Instabilities

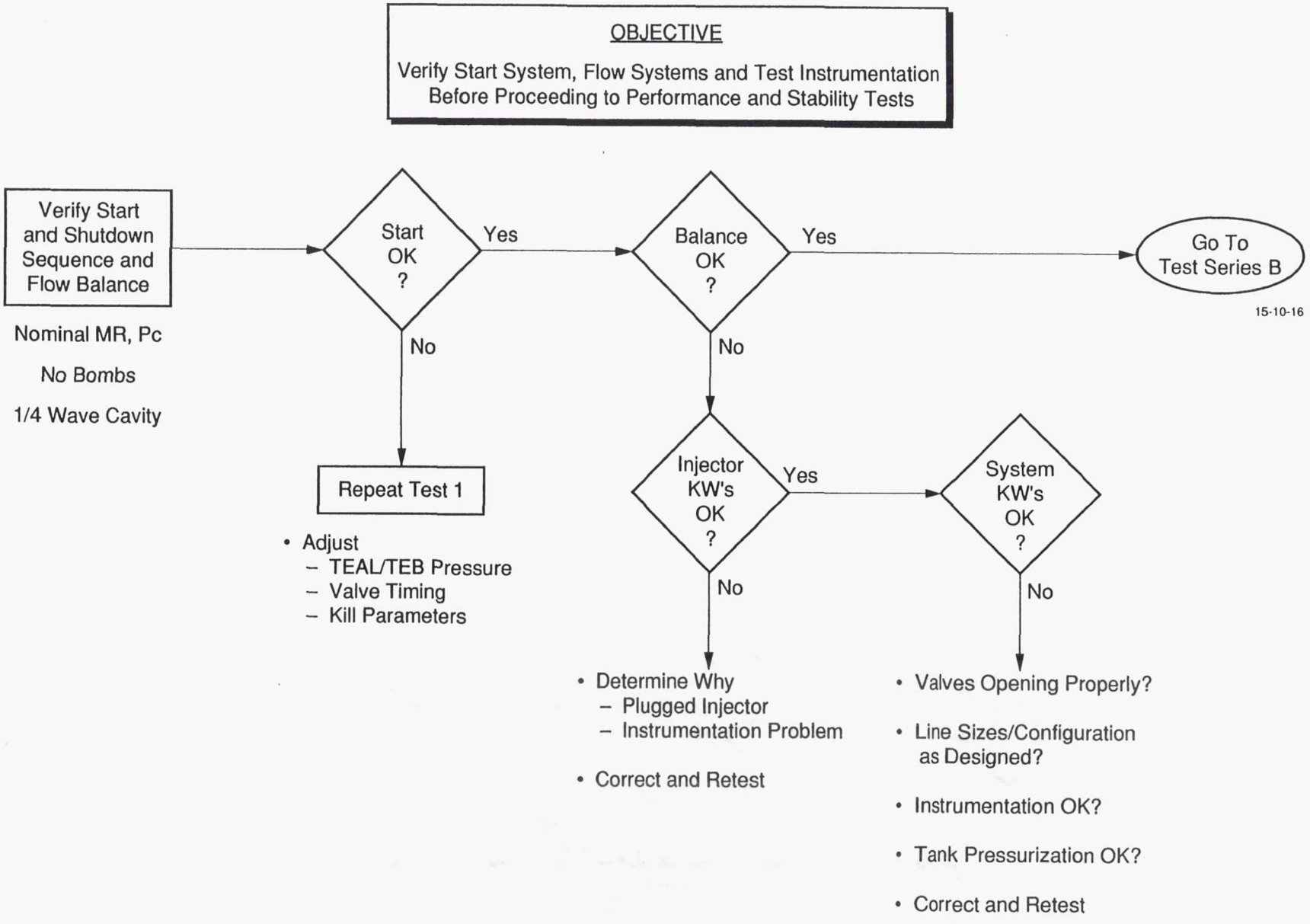

Figure 29. Block 1 – Test Series A Logic

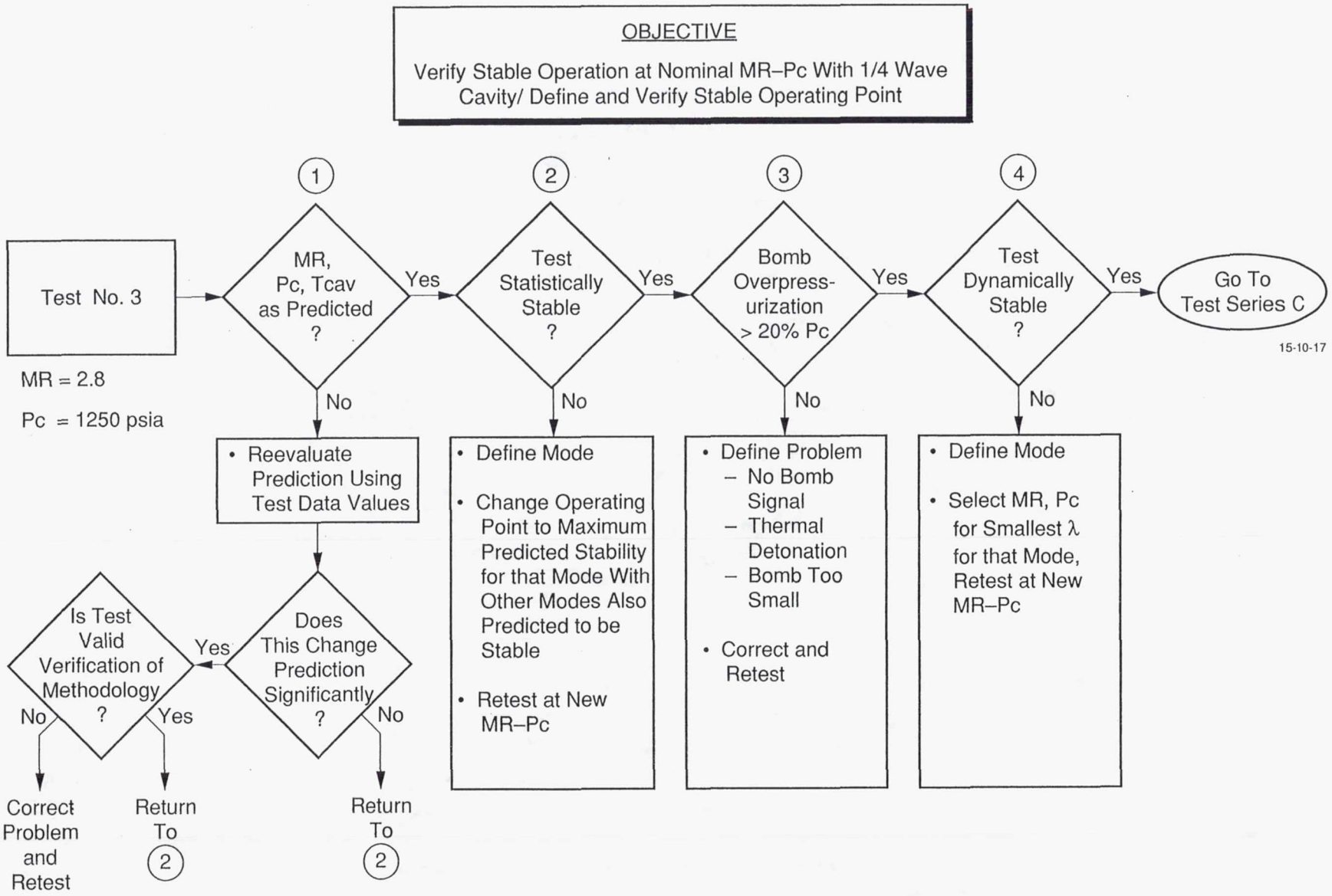

Figure 30. Block 1 – Test Series B Logic

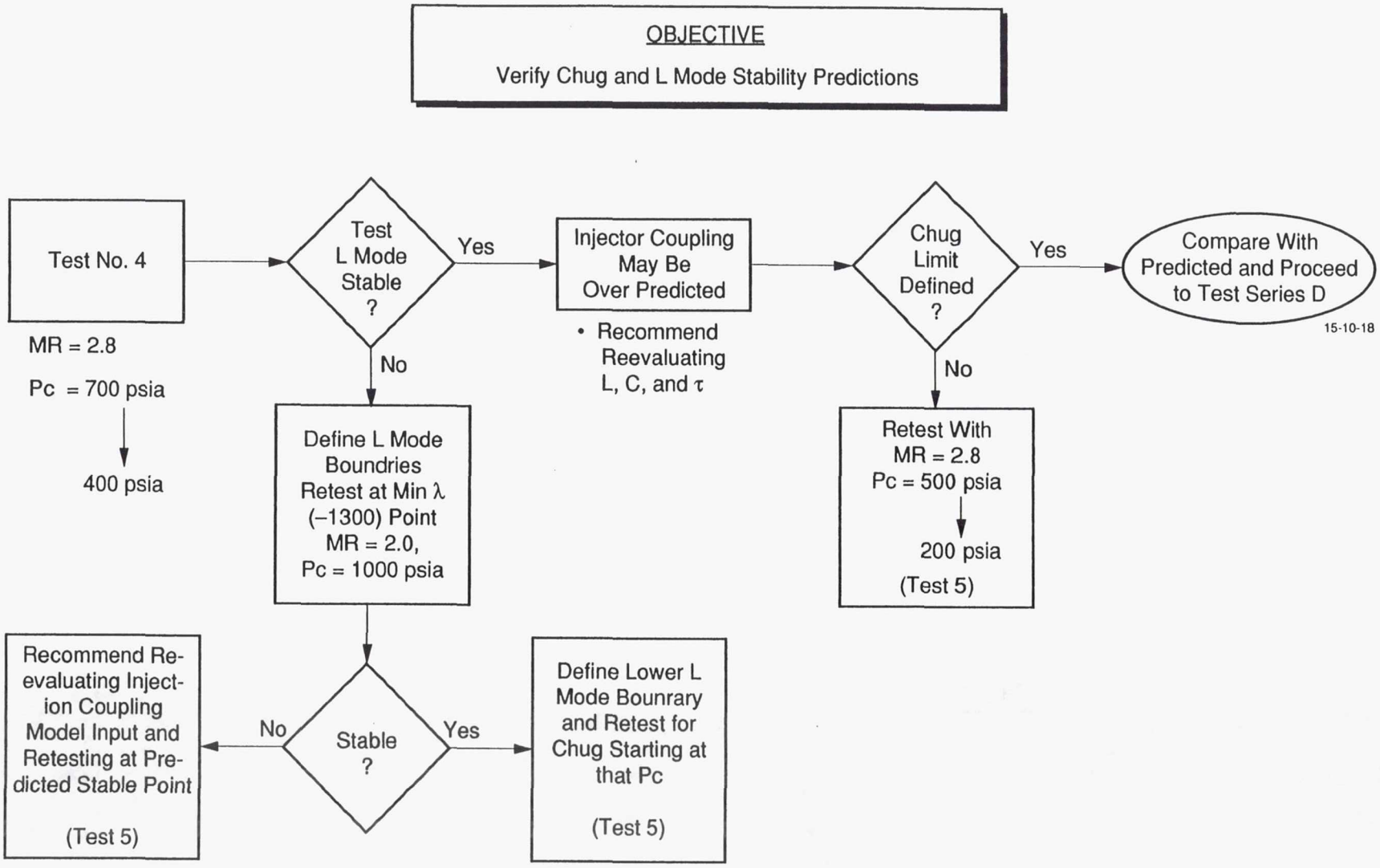

Figure 31. Block 1 – Test Series C Logic

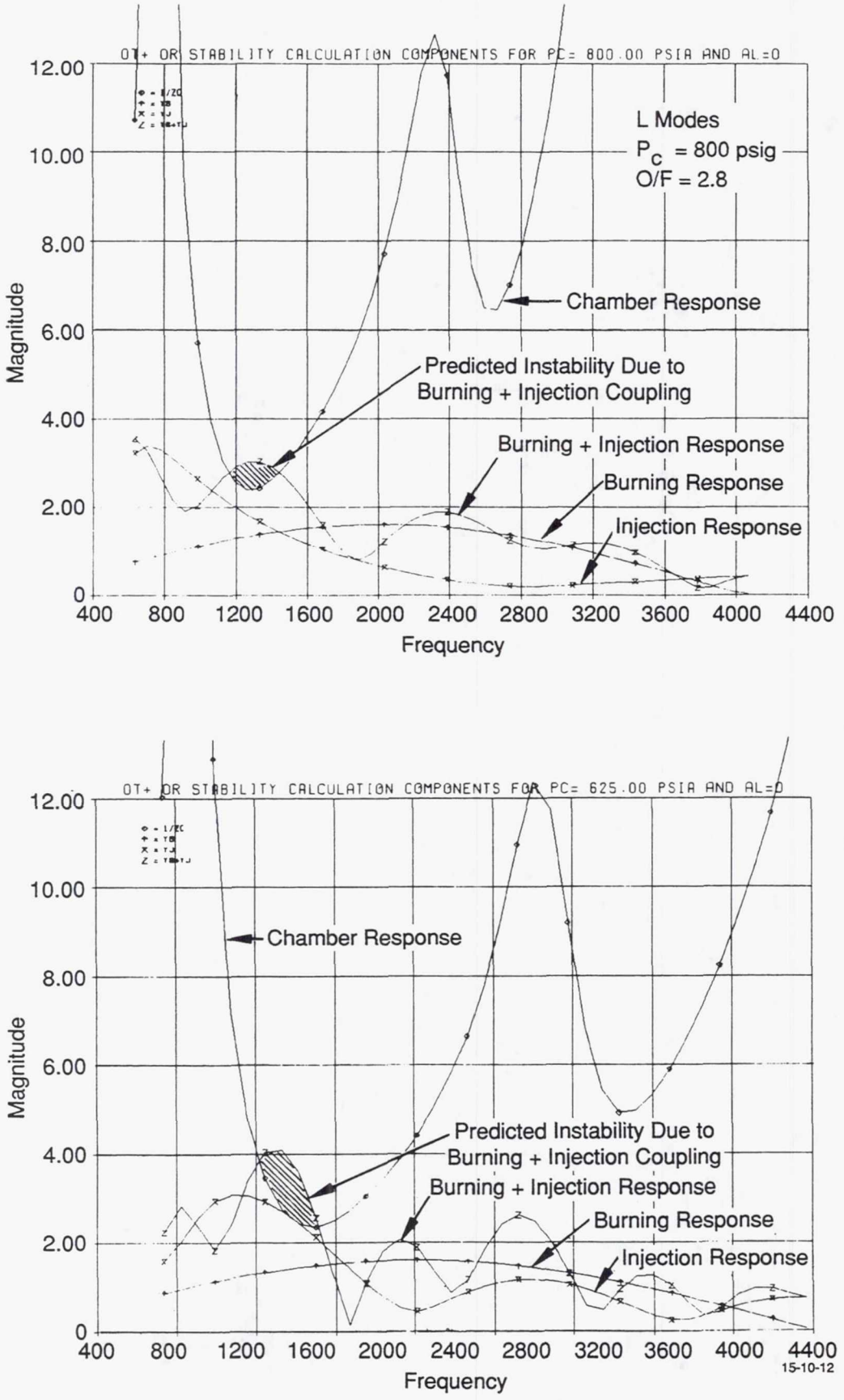

Figure 32. Stability Predictions at Low Chamber Pressure Show Large Influence of Injection Coupling

stream injectors is not well documented, and thus the comparison of the model prediction with the test data provided valuable ROCCID calibration data.

The final Block 1 test series, test series D, was structured to define the operating region of stable operation with an acoustic cavity. Test series D logic is shown on Figure 33. The series D tests were to be conducted in the order shown on Figure 28 if, as predicted, all the tests were stable. If an unstable test occurred, the mode of the instability and the appropriateness of the cavity tune (based on measured cavity gas temperature) would be defined and the growth coefficient data used to determine the most stable operating point for that mode. If a re-test at this operating point was stable, the next untested test point from Table 16 would be tested. If the re-test is unstable in the same mode as the previous test a second re-test at a maximum or minimum throttle condition would be conducted to determine the extent of the unstable region for that mode. If the re-test was unstable in a different mode from the original test, a new test point would be selected for the new mode from the growth coefficient data.

Block 2 Tests

As shown on the logic diagram of Figure 26, the Block 2 testing was conducted without an acoustic cavity. Block 2A tests were conducted to verify unstable operation without an acoustic damping device at nominal and off nominal operating conditions (test series E and G respectively) and verify stable operation at extreme off nominal conditions, test series F. The Block 2A test series logic is shown on Figure 34. Specific test conditions for these tests are shown on Table 17 and further illustrated on the test facility operating map on Figure 37.

As shown on the Figure 35 logic diagram and the specific test listing of Table 17, the first test of this series (Test #11) was at nominal mixture ratio and chamber pressure. This test was predicted to be unstable in the 1T or 2T mode. If this was verified by the test data the next test was at a predicted stable condition as shown on Table 17. If Test 11 is stable and the success criteria of Figure 27 is met, one re-test would be conducted. If this re-test was also stable, the ROCCID predictions were used to define the maximum unstable operating point and this condition was tested next. If subsequent tests were also stable the process was repeated until all the operating points with the maximum predicted growth coefficient for each mode (most unstable predicted condition) were surveyed. This resulted in a survey of a wide range of test conditions that was used for ROCCID model anchoring. If tests that were predicted to be stable were found to be unstable, another predicted stable point was tested. If a predicted

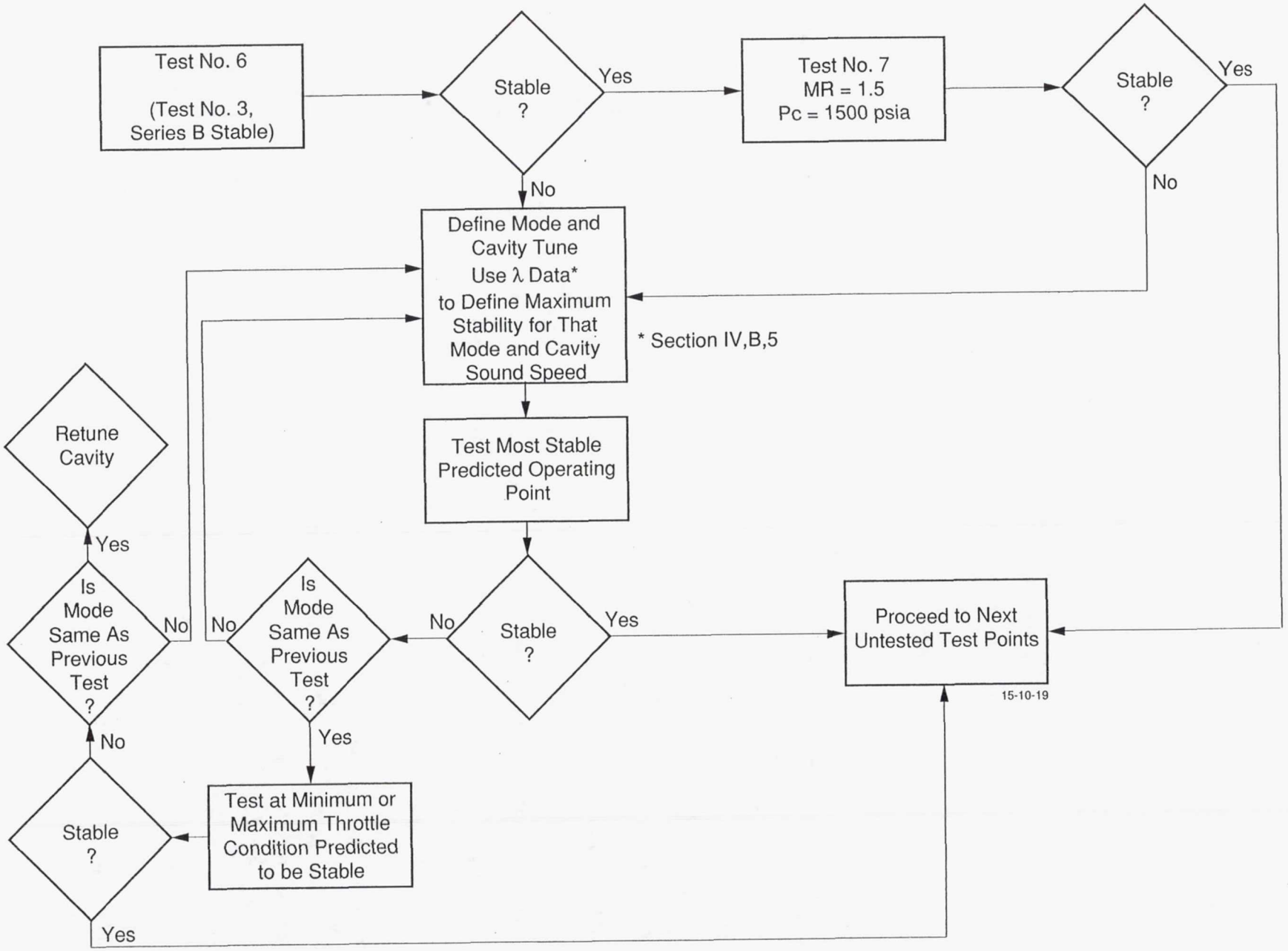

Figure 33. Block 1 – Test Series D Logic

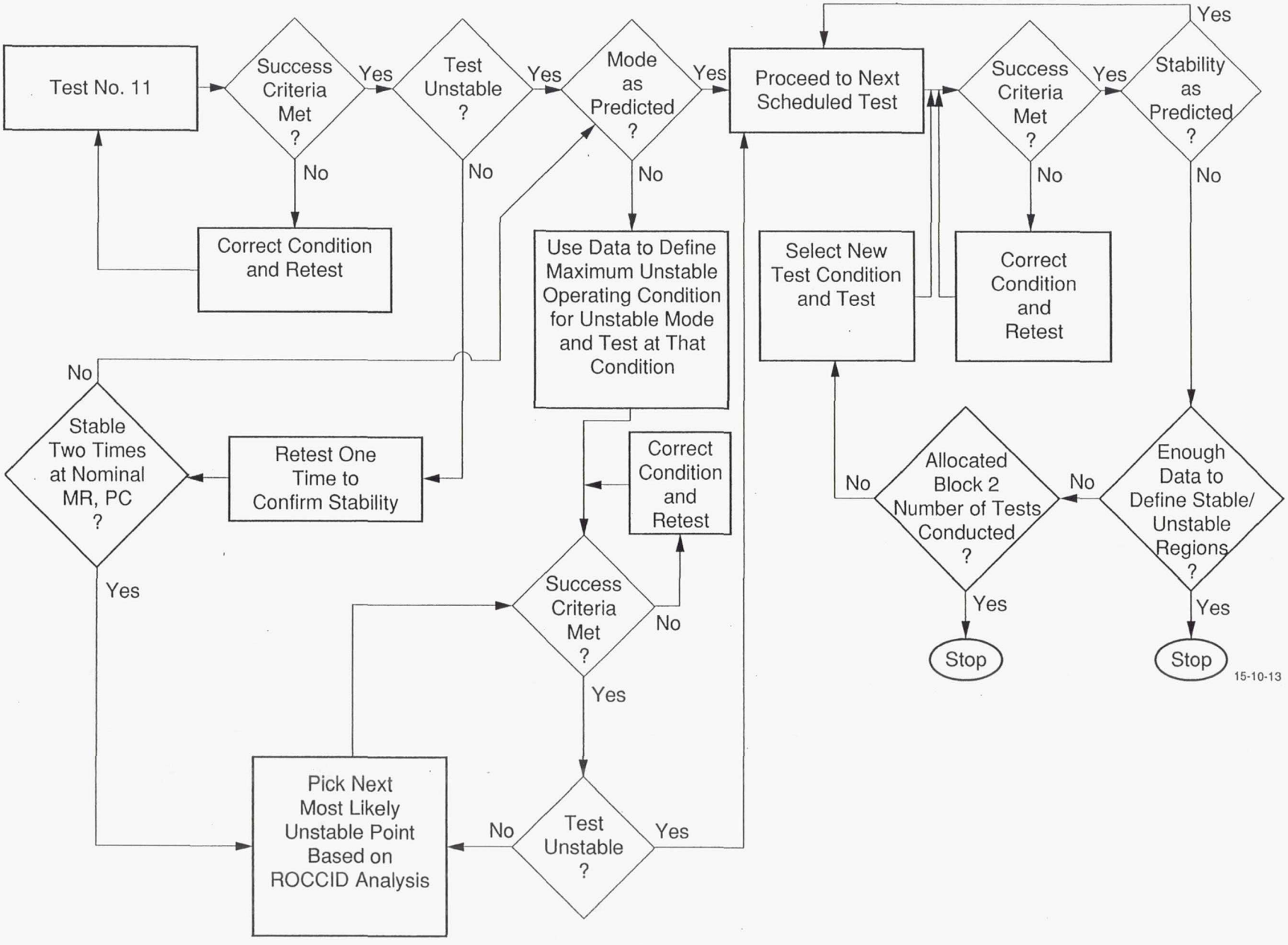

Figure 34. Block 2A Test Series Logic

TABLE 17. Block 2A Tests Were Conducted With No Acoustic Damping to Verify Predicted Stable/Unstable Operating Regions

OBJECTIVES:

Verify Unstable Operation Without Acoustic Damping, Show Changes in Unstable Modes
Verify Stable Operation At Extreme Off-Nominal Conditions

Test No.	Test Series	Pc	O/F	Steady State Duration (sec)	Acoustic Cavity	Bomb at FS-2	Remarks
11	E	1250	2.8	0.3	No	Yes	Verify U/S at Nominal
12	F	1000	1.2	0.3	No	Yes	Verify Stable W/O Damping
13	G	800	7.5	0.3	No	Yes	Verify U/S in 1T/1L, Max 1T U/S
14	G	1500	2.8	0.3	No	Yes	Verify U/S in 2T, Max 2T U/S
15	G	1750	2.8	0.3	No	Yes	Verify USIR, Max IR U/S
16	F	1250	1.2	0.3	No	Yes	Verify Stable IR
17	TBD	TBD	TBD	TBD	No	Yes	Verify Stable W/O Damping
18	TBD	TBD	TBD	TBD	No	Yes	Verify Stable W/O Damping
19	TBD	TBD	TBD	TBD	No	Yes	Verify Stable W/O Damping

Note: (1) F Throat Area Growth > 10% Replace Chamber Liner
(2) If Test Stable and Bomb Over Pressure <20% Pc Repeat Test
(3) If Thrust Area Growth <10% May Conduct Additional Tests

Test #	Repeat Test
19	11

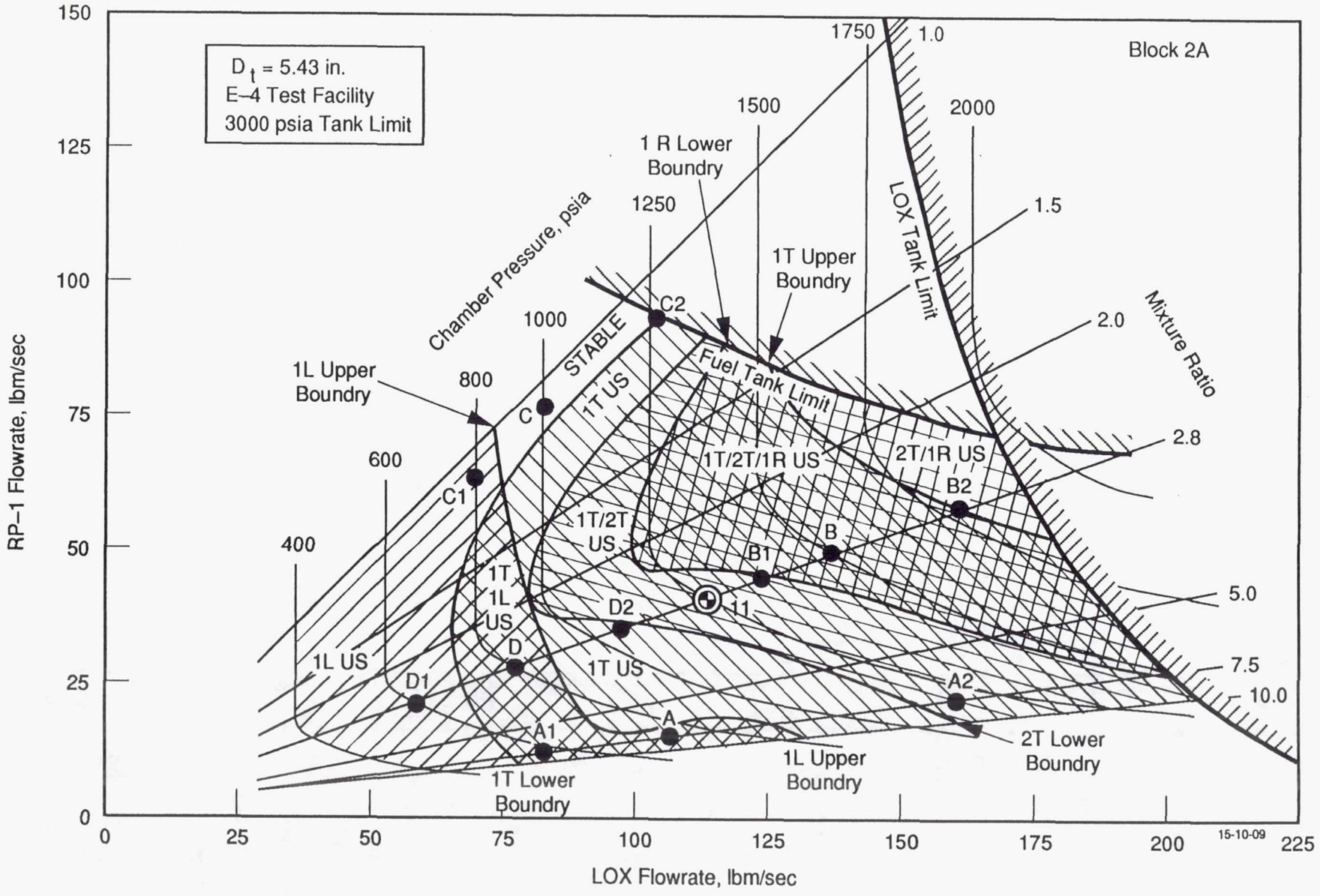

Figure 35. Block 2A Tests Will Define Stable and Unstable Operating Regions Without an Acoustic Cavity

stable point was in fact stable, the test was repeated to verify the stable result.Tests 17-19 were allocated for these tests.

If, as a result of Block 1 testing, the stable operating region with an acoustic cavity was much smaller than predicted, a retuned (different cavity depths) or reconfigured (different 1T/2T cavity numbers or % area) acoustic cavity would be made based on the Block 1 test data. In this event, the Block 2 non-cavity testing would be used to determine the amount of frequency and amplitude suppression that was achieved by the cavities by comparing the Block 1 data to data collected during the Block 2B test series. This test series is shown on Table 18.

Block 3 Tests

As shown on the logic diagram of Figure 26, the Block 3 tests would have reconfirmed the stable operating region and defined the unstable operating region with the original cavity tune from the Block 1 tests (Block 3A); or as actually happened if a new cavity configuration was required to provide stable operation, and the Block 3B tests were used to evaluate the new cavity design. The Block 3 test logic is shown on Figure 36 and the specific test points are shown on Table 19 and Figure 37.

Instrumentation Requirements and Accuracy

The objective of thrust chamber testing was to generate a data base for validation of performance and combustion stability predictions made using the ROCCID methodology. Therefore, the test hardware was heavily instrumented to provide the required data base. Instrumentation was also included to control and monitor the facility operation and thrust chamber transients and provide for test kills in the event that red lines were exceeded for specified critical parameters.

The data acquisition requirements for determination of combustion stability and performance during this testing are provided in Tables 20 and 21, respectively. Parameter ranges and accuracy requirements are specified on these tables. In some cases a single measurement was used to derive more than one parameter resulting in different measurement accuracies.

A complete list of instrumentation, range and recording device requirements was provided in the test plan (Ref. 18). The location of facility instrumentation is shown in the test

TABLE 18. Block 2B Tests Were Conducted Without an Acoustic Cavity to Provide Data for Acoustic Cavity Re-Design

OBJECTIVES:

Verify Unstable Operation Without Acoustic Damping
Verify Stable Operation at Extreme Off-Nominal Conditions

Test No.	Test Series	Pc	O/F	Steady State Duration (sec)	Acoustic Cavity	Bomb at FS-2	Remarks
11	E	1250	2.8	0.3	No	Yes	Verify U/S at Nominal
12	F	1000	1.2	0.3	No	Yes	Verify Stable Without Damping
13	G	800	7.5	0.3	No	Yes	Verify U/S at Off Nominal
14	G	1750	2.8	0.3	No	Yes	Verify U/S at Off Nominal
15	G	1500	2.8	0.3	No	Yes	Verify U/S at Off-Nominal
16	F	1250	1.2	0.3	No	Yes	Verify Stable Without Damping
17	I	TBD	TBD	0.1	No	Yes	Verify Mode Surpression
18	I	TBD	TBD	0.1	No	Yes	Verify Mode Surpression
19	I	TBD	TBD	0.1	No	Yes	Verify Mode Surpression

Note: Test 12 Near max W_F Limit
Test 13 Near Min W_F Limit
Test 14 Near Max P_c, High W_F, Wo

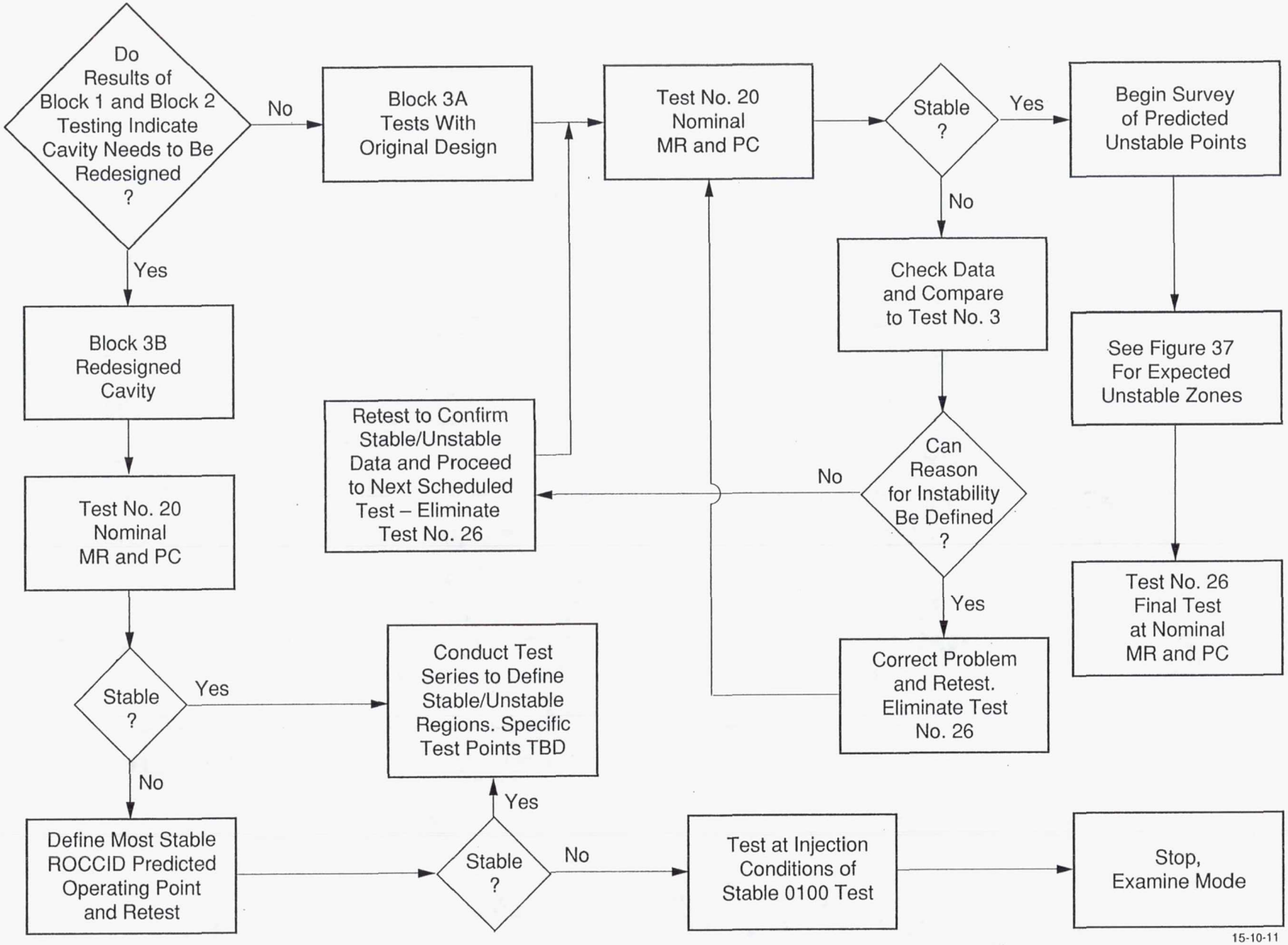

Figure 36. Block 3 Test Logic

TABLE 19. BLOCK 3 TESTS WERE MADE TO CONFIRM STABLE OPERATION WITH AN ACOUSTIC CAVITY

Objectives
- Reconfirm Stable Operation With an Acoustic Cavity
- Verify Unstable Operation at Off-Nominal Mixture Ratio
- Using Original Tune Block 3A

Test No.	Test Series	Pc	O/F	Steady State Duration (sec)	Acoustic Cavity	Bomb @ FS-2	Remarks
20	B	1250	2.8	0.3	Yes	Yes	Reconfirm Stable w/Damping
21	H	1250	3.5	0.3	Yes	Yes	Verify Cavity Detune (2T)
22	H	1750	2.8	0.3	Yes	Yes	Verify Cavity Detune (1R)
23	H	1500	5.0	0.3	Yes	Yes	Verify Cavity Detune (2T/1R)
24	H	800	5.0	0.3	Yes	Yes	Verify Cavity Detune (1T)
25	H	800	1.2	0.3	Yes	Yes	Verify Cavity Detune (1L)
26	B	1250	2.8	0.3	Yes	Yes	Reconfirm Stable W/Damping

Objectives
- Redefine Stability Map With New Tune
- With New Cavity Tune – Block 3B

Test No.	Test Series	Pc	O/F	Steady State Duration (sec)	Acoustic Cavity	Bomb @ FS-2	Remarks
20	F	1250	2.8	0.3	Yes	Yes	Reconfirm Stable w/Damping
21	H	TBD	TBD	0.3	Yes	Yes	Verify Cavity Detune
22	H	TBD	TBD	0.3	Yes	Yes	Verify Cavity Detune
23	G	TBD	TBD	0.3	Yes	Yes	Reconfirm Stable
24	F	TBD	TBD	0.3	Yes	Yes	Reconfirm Stable
25							
26							

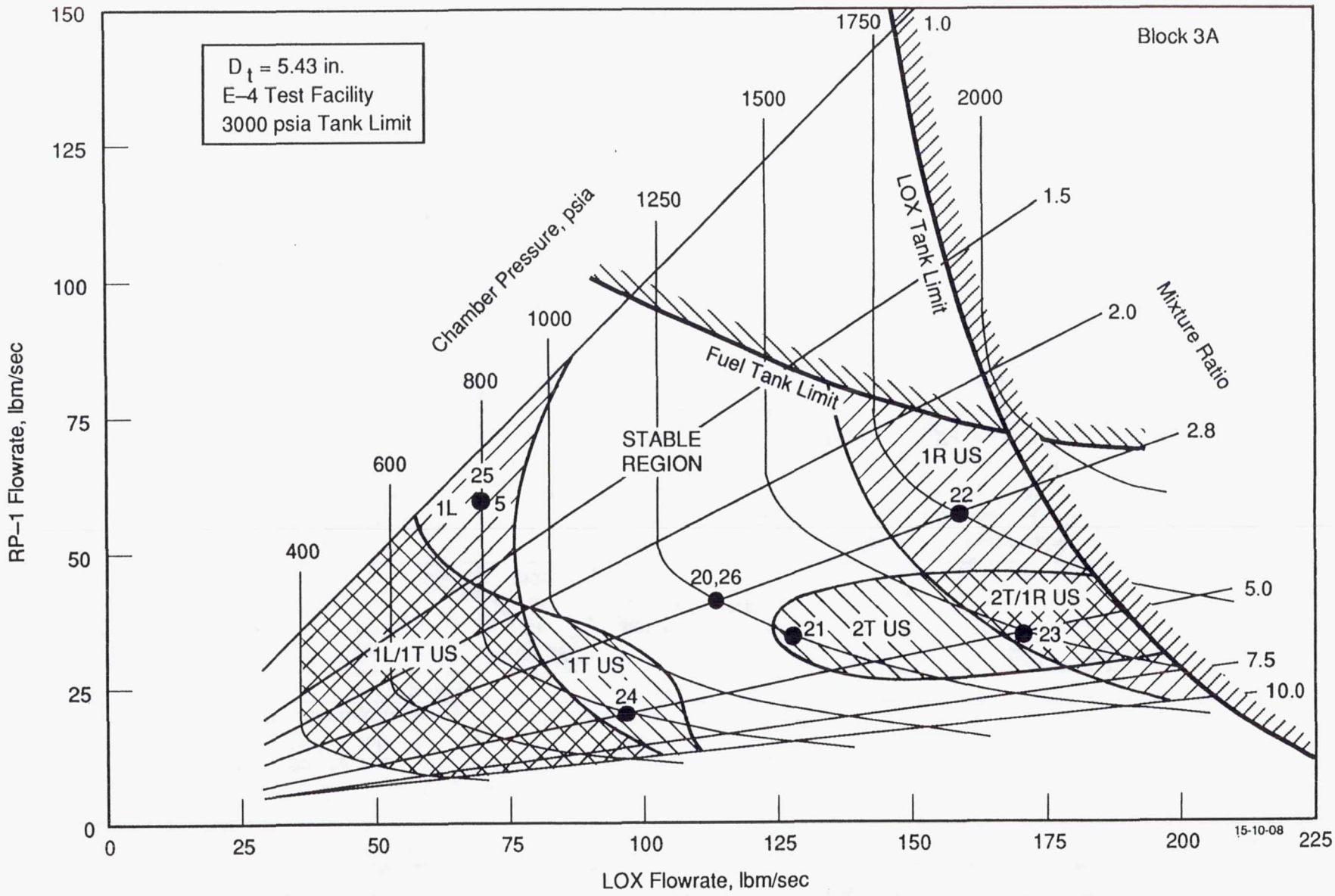

Figure 37. Block 3A Tests Were Planned to Re-Confirm Stable Operating Regions With an Acoustic Cavity and Define Regions of Unstable Operation With the Cavity

TABLE 20. COMBUSTION STABILITY DATA ACQUISITION REQUIREMENTS

1) Dynamic Chamber Pressure
   - Measurement

     Frequency: 100 to 10K hz

     Amplitude: ±100% $\overline{P}c$

     Damp & Growth Rates: psia/milliseconds
   - Location

     Minimum: 3 clock positions near the injector face and 3 axial locations at the same clock position

     Defined Consistent with CPIA 148, 170 and 247
2) Dynamic Manifold Pressure
   - Measurement

     Frequency: 100 to 5K hz

     Amplitude: ±33% $\overline{P}_{MANIFOLD}$
   - Location

     As close to orifice inlet as feasible
3) Operating Conditions
   - Static Chamber Pressure: ±2% accuracy
   - Mixture Ratio: ±3% accuracy
   - Propellant Temperature: ±10°F
   - Static Manifold Pressure: ±2%
4) Combustion Perturbation (Dynamic Rating)
   - Instantaneous
   - Minimum 25% overpressure
   - Close to the injector face
5) Acoustic Cavities (if present)
   - Gas Temperature: ±100°F
6) Accelerometer
   - Attached to the thrust chamber flange

TABLE 21. THRUST CHAMBER PERFORMANCE DATA ACQUISITION REQUIREMENTS

1) Vacuum Specific Impulse ±1%

Thrust Level: LOX Flowrate: RP-1 Flowrate:	{	Sufficient to provide overall specific impulse accuracy of ±1%
Static Chamber Pressure:		±1%
Mixture Ratio:		±2%
Tolerance Requriement is usually Propellant Temperature:		±5°F set by flowrate accuracy requirements
Expansion Area Ratio:		±2%
Ambient Pressure:		±0.1 psia
Nozzle Exit Diameter:		±.05 in.
Inert Purge Flow:		±.05% of $\dot{W}_T$ Reactive

2) Characteristic Velocity ±2% Accuracy

Chamber Pressure ±1% accuracy

LOX Flowrate: RP-1 Flowrate:	{	Accuracy requirements set by specific impulse treatment

Nozzle Throat Diameter: ±.02 in.

Mixture Ratio: ±2%

Propellant Temperature: ±5°F

Inert Purge Flow: ±.05% of $\dot{W}_T$ Reactive

3) Manifold Pressure: ±1%

4) Static Chamber Pressure Profile

Measurements sufficient to determine the total pressure loss from the injector face to the start of nozzle convergence. An array of static pressure transducers and/or ΔP gauges with in-place calibration to measure ΔP (station-to-station) of 5 to 25 psia.

facility schematic was included in the test plan. Location of the thrust chamber instrumentation was noted on the hardware drawings.

E. VALIDATION HARDWARE DESIGN

The hardware design for the test validation of the ROCCID methodology consisted of a thrust chamber that operated at moderate chamber pressure (1,250 psia) and thrust (48,000 Lbf) using LOX/RP-1 propellants. The thrust chamber was designed for short duration operation at sea level conditions adequate to experimentally determine its performance and combustion stability over a wide range of chamber pressure and mixture ratio. The drawing tree shown in Figure 38, identifies the components and their Aerojet drawing numbers that made up the engine assembly for ROCCID validation testing. A complete collection of these drawings is provided in Appendix D of Volume II of this final report and in Reference 19.

The basic hardware components were originally designed, fabricated and tested during the Oxygen/Hydrocarbon Injector Characterization Program (Contract F04611-85-C-0100) conducted over the time period from September 1985 to January 1990. The critical design features of this hardware, such as the injector element faceplate, acoustic cavities and the combustion chamber internal (gas-side) contour including throat size, contraction ratio and chamber length were redesigned using the ROCCID methodology. These changes were incorporated into a revised design disclosure (drawing package) and the hardware components were appropriately modified and refurbished for this test program. This section includes a description of this thrust chamber and its components.

1. Engine Assembly

The engine assembly for use in this test program is shown in Figure 39. Major components of this thrust chamber assembly include: (1) an injector assembly consisting of an outer flange and RP-1 manifold and an inner core with a liquid oxygen inlet and the OFO triplet injector faceplate, (2) an ablative (silica phenolic) lined combustion chamber with a high strength steel (4340) shell designed for operation at chamber pressure as high as 1,750 psia, and (3) ancillary components including a proof and leak check plate, seals, bolts, nuts and washers, bomb adapters, and acoustic cavity inserts.

This thrust chamber was designed to interface with the propellant feedsystem and thrust takeout existing in the Aerojet Propulsion Division's E-4 test stand. The fully

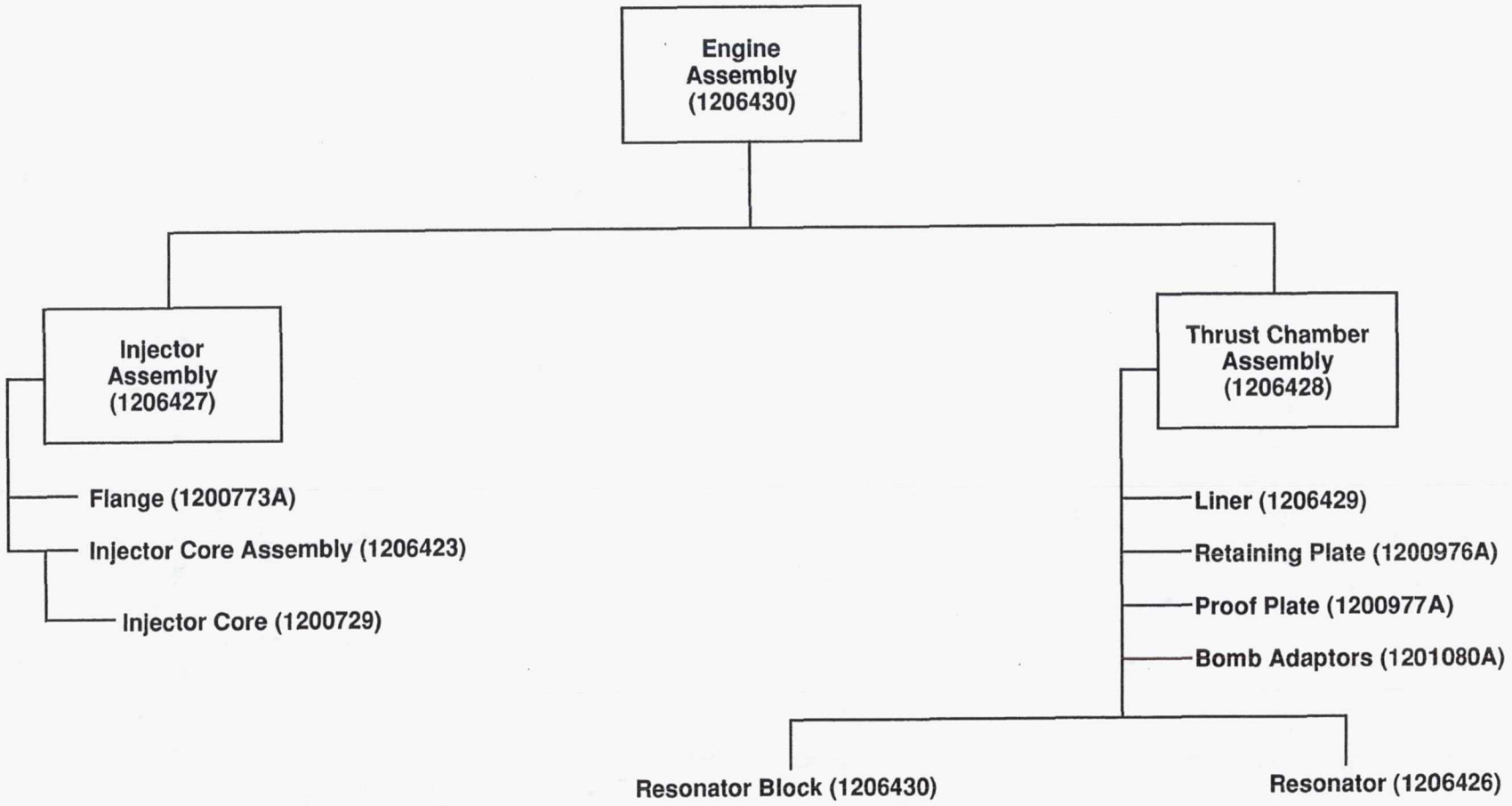

Figure 38. The Drawing Tree for the ROCCID Test Validation Thrust Chamber

M16/D14/Fig-4

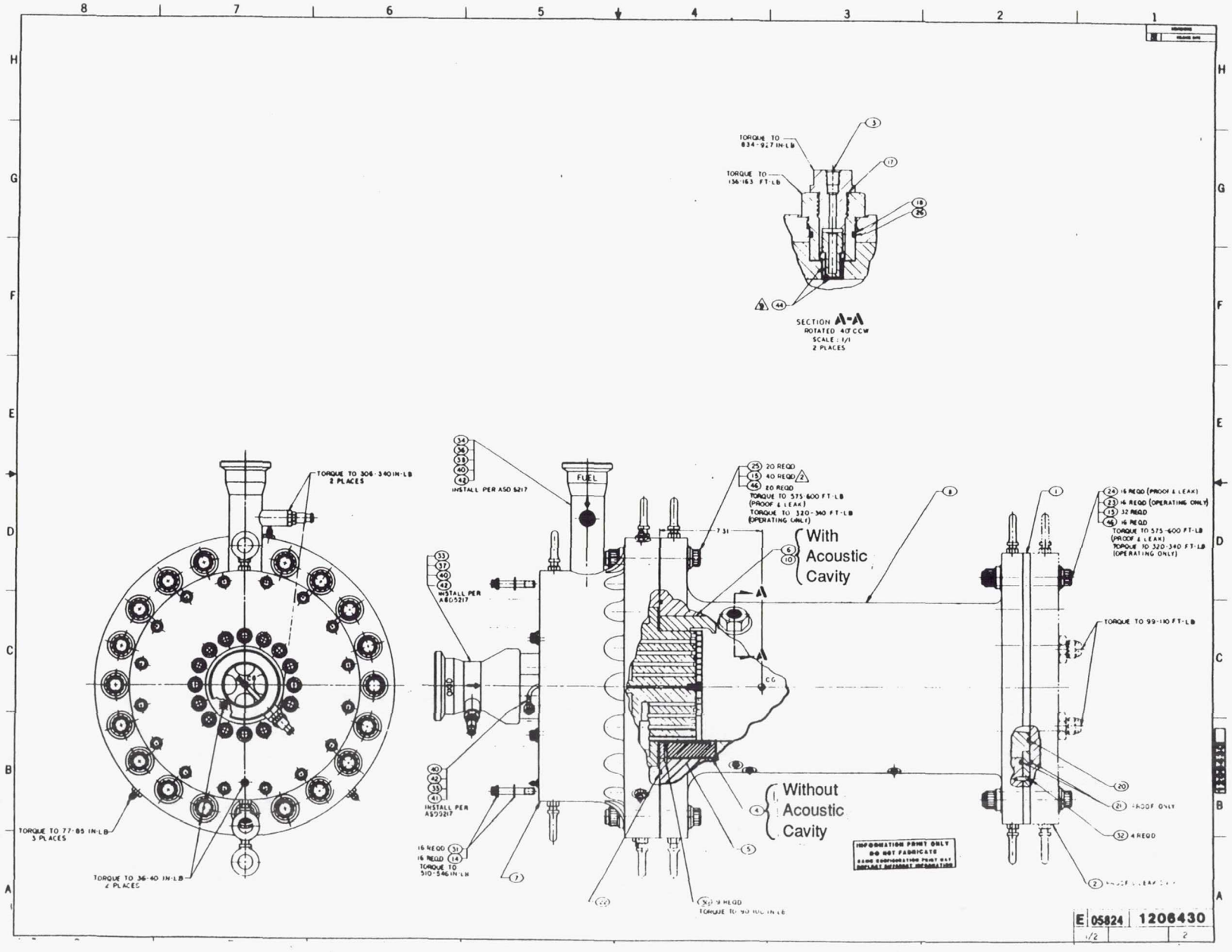

Figure 39. The Engine Assembly for ROCCID Test Validation

assembled thrust chamber weighs an estimated 1400 lbm. A photograph of a fully assembled thrust chamber on the E-4 test facility with instrumentation in place is provided in Figure 40.

The hardware design included all ports and fittings for the required instrumentation. Ports for 14 static chamber pressure transducers, 6 dynamic chamber pressure transducers, static and dynamic pressure transducers in each propellant manifold and 4 thermocouples to measure acoustic cavity gas temperatures were included. In addition, two ports were provided in the combustion chamber for the bomb adaptors that contain RDX explosives to induce chamber overpressure spikes for measurement of dynamic combustion stability characteristics.

2. Injector Assembly

A drawing of the injector assembly (P/N 1206427) is shown in Figure 41. The assembly consisted of a flange assembly (P/N 1200773-19) shown in Figure 42 and an injector core assembly (P/N 1206423) shown in Figure 43. The flange assembly contained the fuel inlet and the thrust takeout and chamber mounting surfaces. The injector core assembly contained the oxygen inlet, the fuel and oxygen downcomers, distribution channels and the injector faceplate. The injector core assembly was designed to bolt to the injector flange assembly. An assemblage of photographs showing the injector assembly and its components fabricated for previous LOX/Hydrocarbon testing is included in Figure 44.

The injector flange assembly was made from 304 stainless steel and weighs an estimated 430 lbm. This assembly was attached to the test facility using sixteen (16) 1/2 inch bolts. A 2 inch diameter Greyloc (GR 20, schedule 160) fitting was included for connection to the test facility fuel delivery system.

The injector core assembly, shown in Figure 43, consisted of an injector core made from 304 stainless steel, a schedule 160 oxidizer inlet tube with a 3 inch diameter Greyloc (GR 25, schedule 160) fitting, a zirconium copper faceplate and a stainless steel igniter line assembly. The injector assembly inserted into the flange assembly and was attached using 16 - 5/8 inch bolts. Two teflon O-ring seals provide a seal between the flange and injector core assemblies.

The injector core included a zirconium copper faceplate that was brazed to the 304 stainless steel body. The faceplate contained the fine thrust-per-element OFO triplet injector pattern that was developed using the ROCCID methodology. The 105 OFO triplet elements

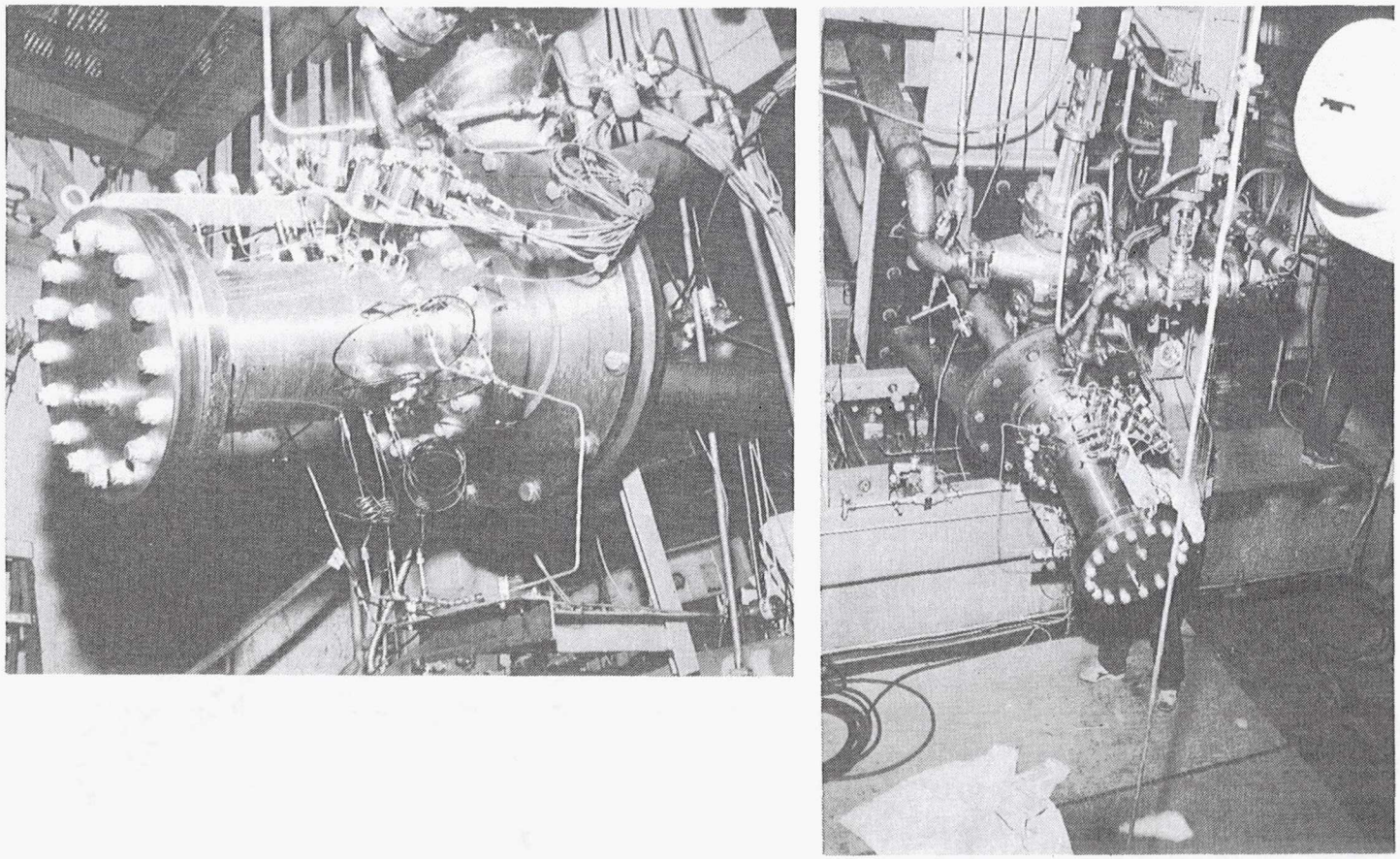

Figure 40. The ROCCID Test Validation Engine Assembly Installed on Test Stand E-4

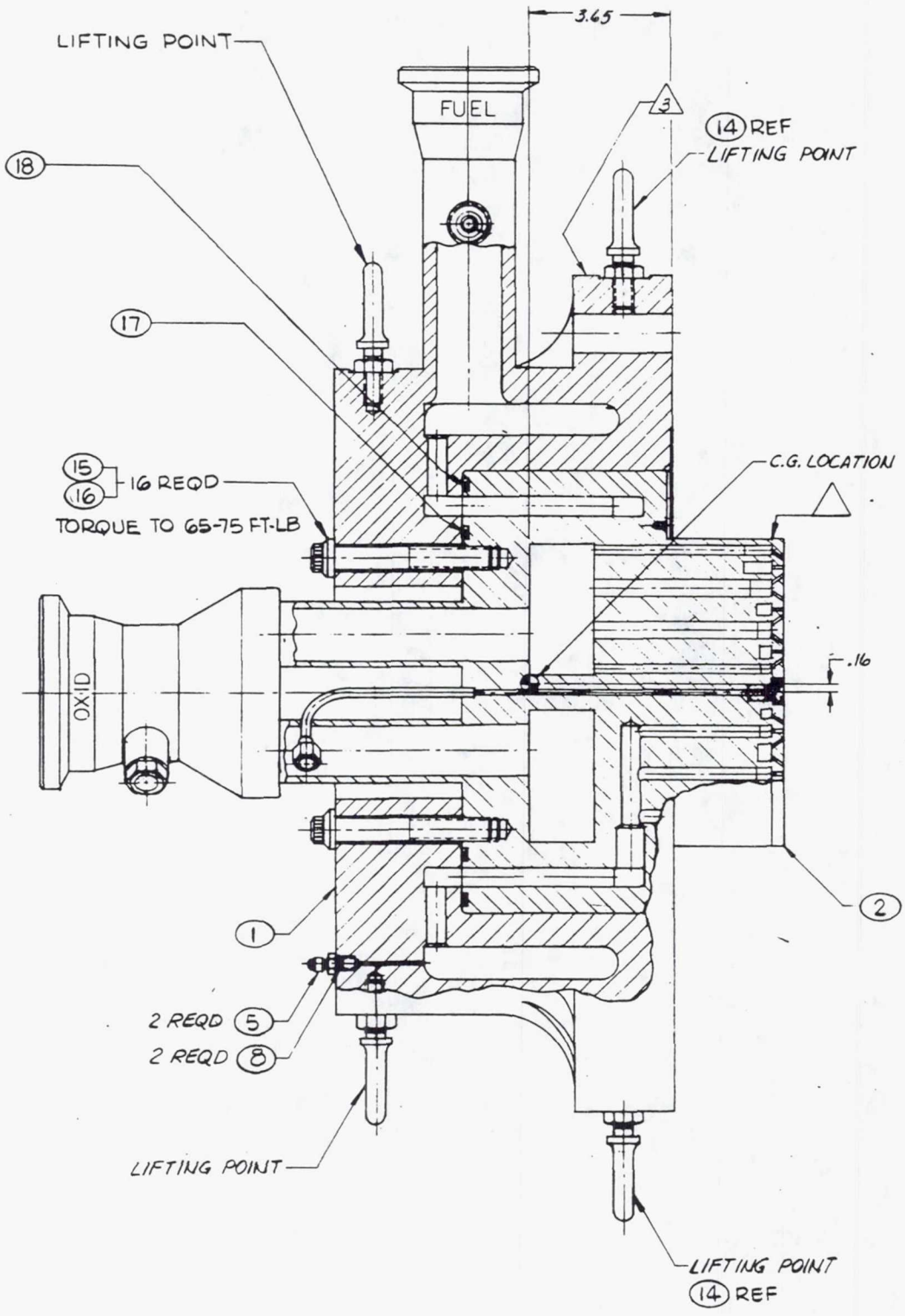

Figure 41. The Injector Assembly Used an Existing Fuel Manifold and Injector Core and a New Injector Faceplate

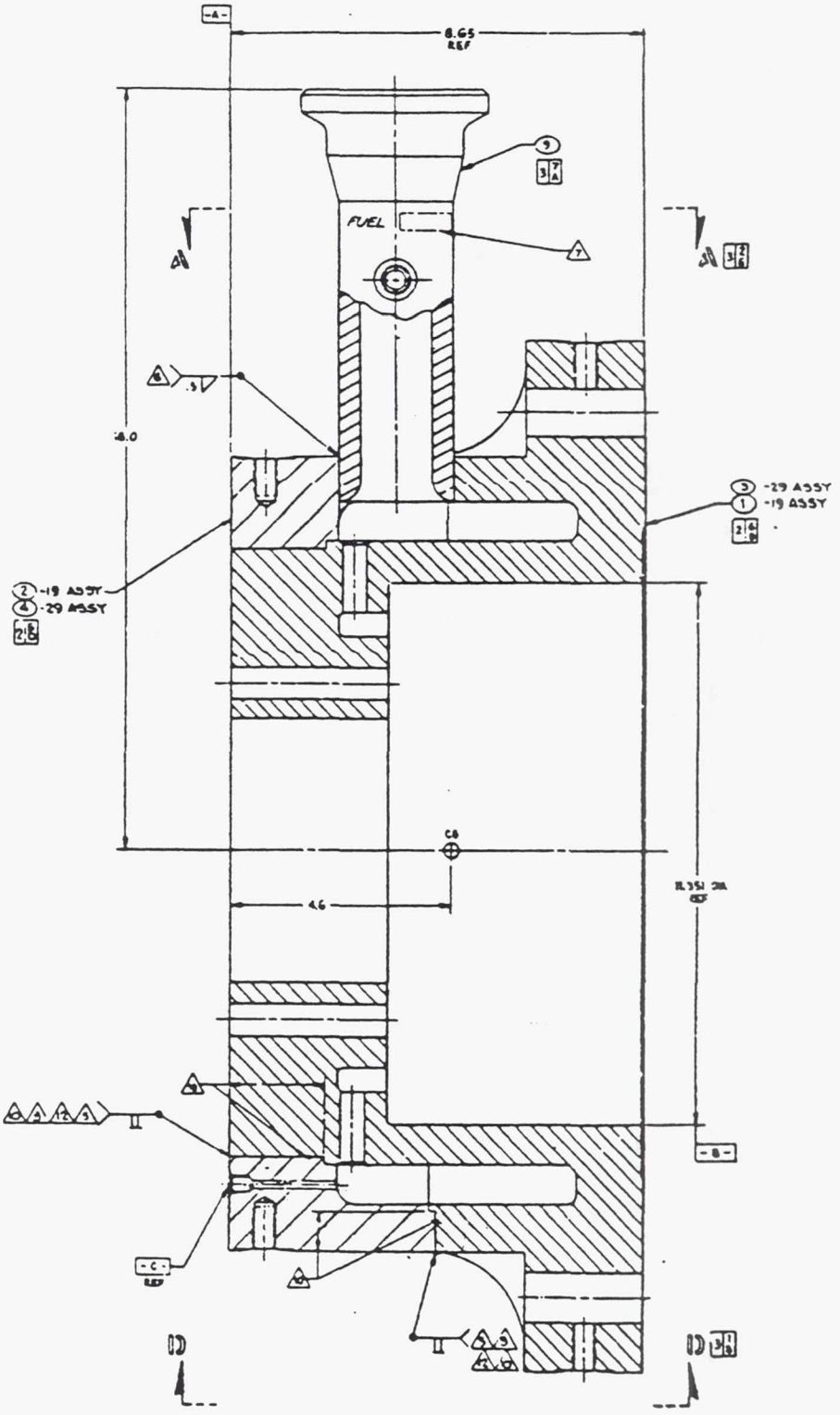

Figure 42. The Injector Flange and Outer Fuel Manifold was Available From a Previous Phillips Laboratory Program

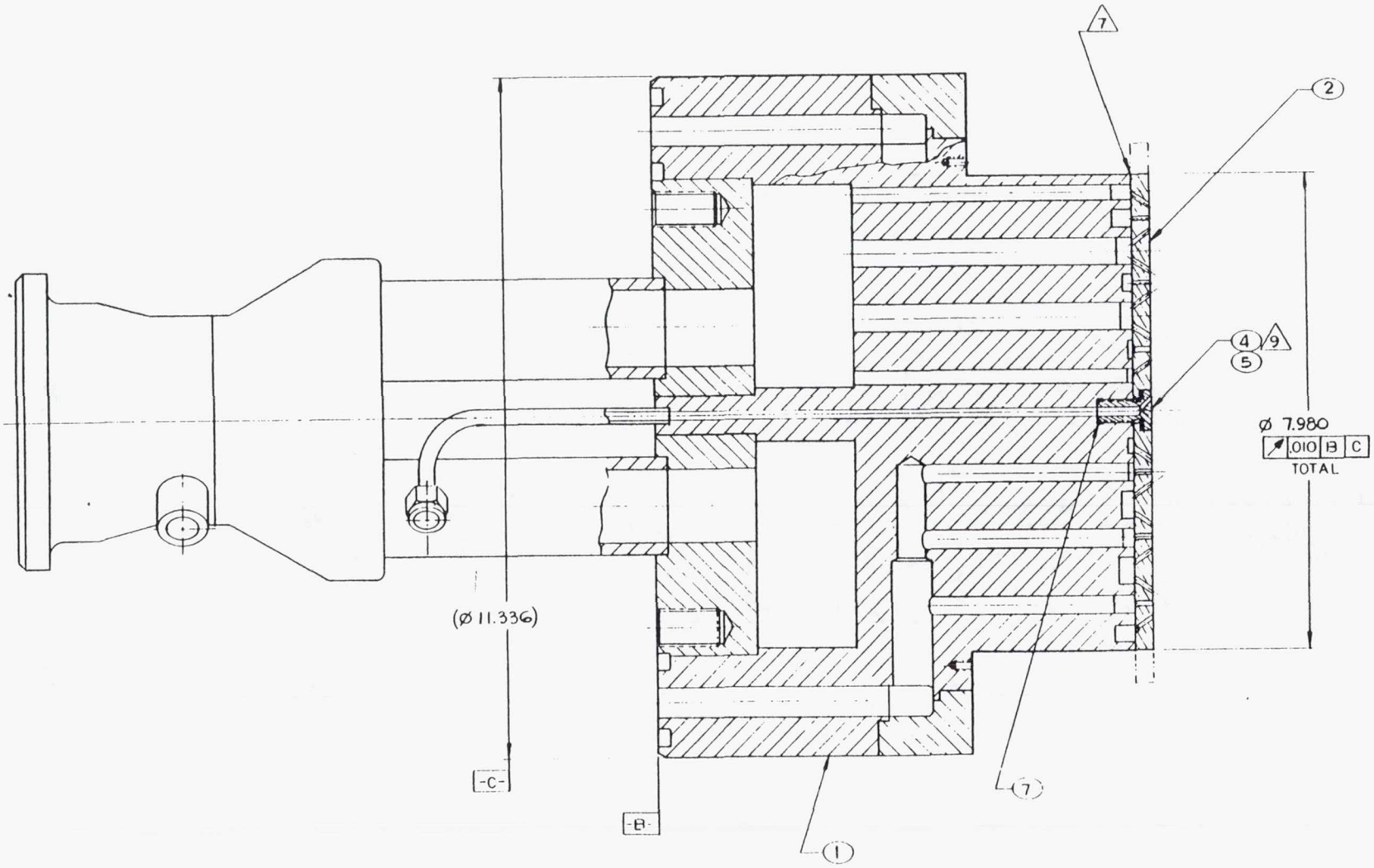

Figure 43. An Existing Injector Core Was Used

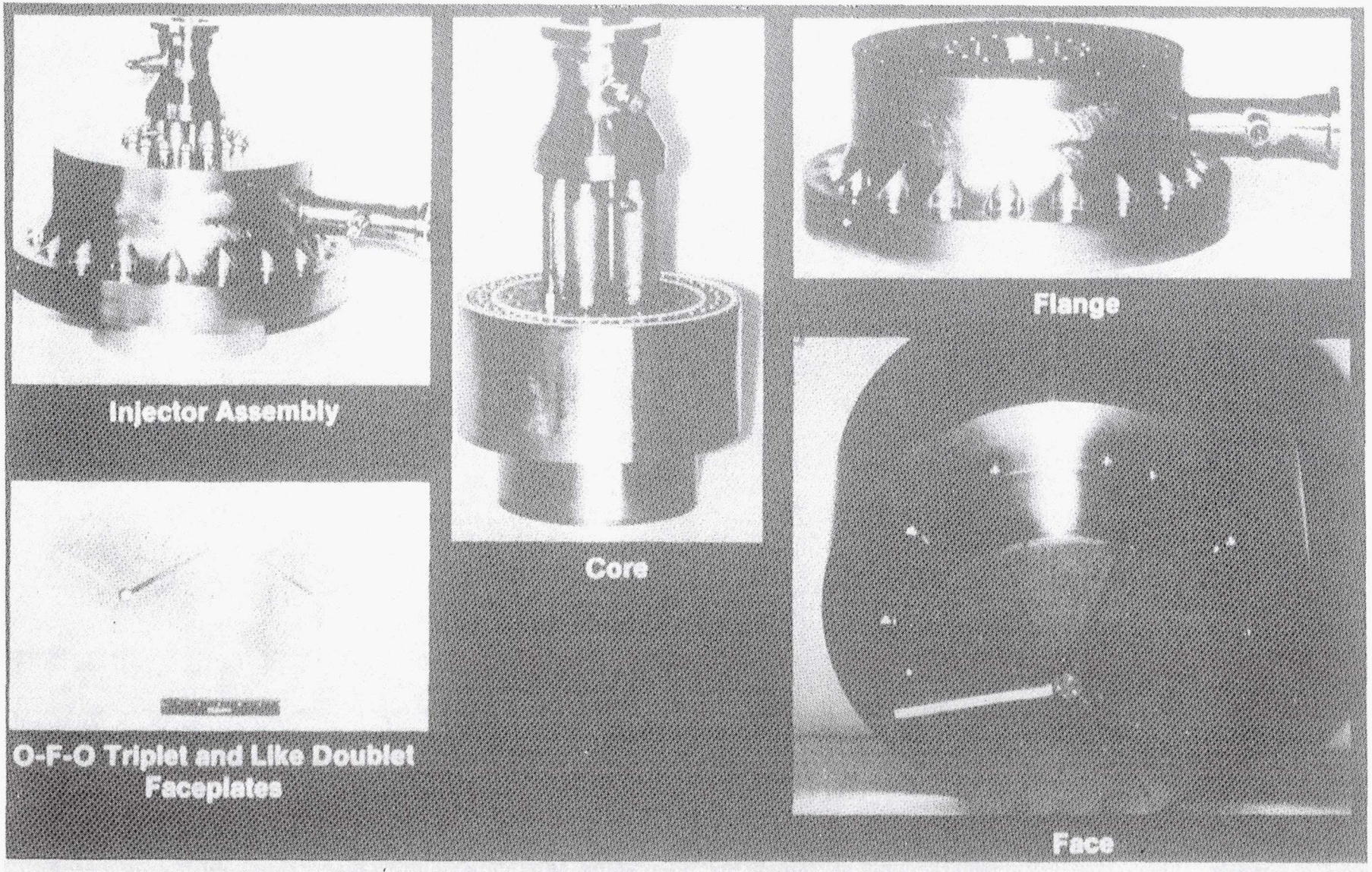

Figure 44. The LOX/Hydrocarbon Injector Assembly is Test Proven

were contained in three circular rows around a centrally located TEAL/TEB ignition port. Each OFO injector element consisted of two .090 in. diameter orifices that inject liquid oxygen on a central RP-1 stream formed from a central axially directed center .090 in. diameter orifice. A drawing of the injector faceplate showing element design details is provided in Figure 45. The .090 in. orifices were the smallest fluid flow passages in either the liquid oxygen or the RP-1 propellant circuits.

The design details of the O-F-O triplet element are provided in Figure 46. The two oxygen orifices were canted at 35° with respect to the axially directed central fuel orifice. The three orifices were aligned along a radius of the injector and spaced so that their centerlines impinge at a single point 0.288 in. off the face of the injector. The faceplate was 0.312 in. thick resulting in an orifice L/D of 3.5 for the fuel orifice and 4.3 for the oxygen orifices. The inlets to all orifices were countersunk with a 0.115 in. diameter that provided an orifice to inlet area ratio of 0.61. The backside of the copper faceplate was electropolished to round all surfaces on the orifice inlet. Cold flow tests (Ref. 13) have shown that an orifice C_D of .91 to .93 is achieved with this type of orifice geometry.

The TEAL/TEB igniter circuit contained in the injector core consisted of a flared 1/4 in. OD CRES tube that attached to the test facility using a nut attached to the tubing. The igniter runs through the center of the injector core and the TEAL/TEB was injected through a CRES igniter plug that contained 3-.124 in. ports.

3. Thrust Chamber Assembly

A drawing of the combustion chamber assembly is shown in Figure 47. The assembly consisted of a high strength 4340 steel structural shell and a single piece replaceable silica phenolic ablative liner. The weight of the thrust chamber assembly was estimated as approximately 600 lbm without the closure plate and instrumentation.

The chamber assembly was attached to the injector assembly with 20 1-inch diameter bolts. The retainer plate was attached to the steel chamber housing using 16 1-inch diameter bolts. O-ring seals were used at both the injector/chamber and chamber/retainer plate flanges to provide a hot gas seal.

The hot gas combustion chamber internal profile was formed using a silica liner, shown in Figure 48 that mated with the steel shell. The liners were inserted into the steel

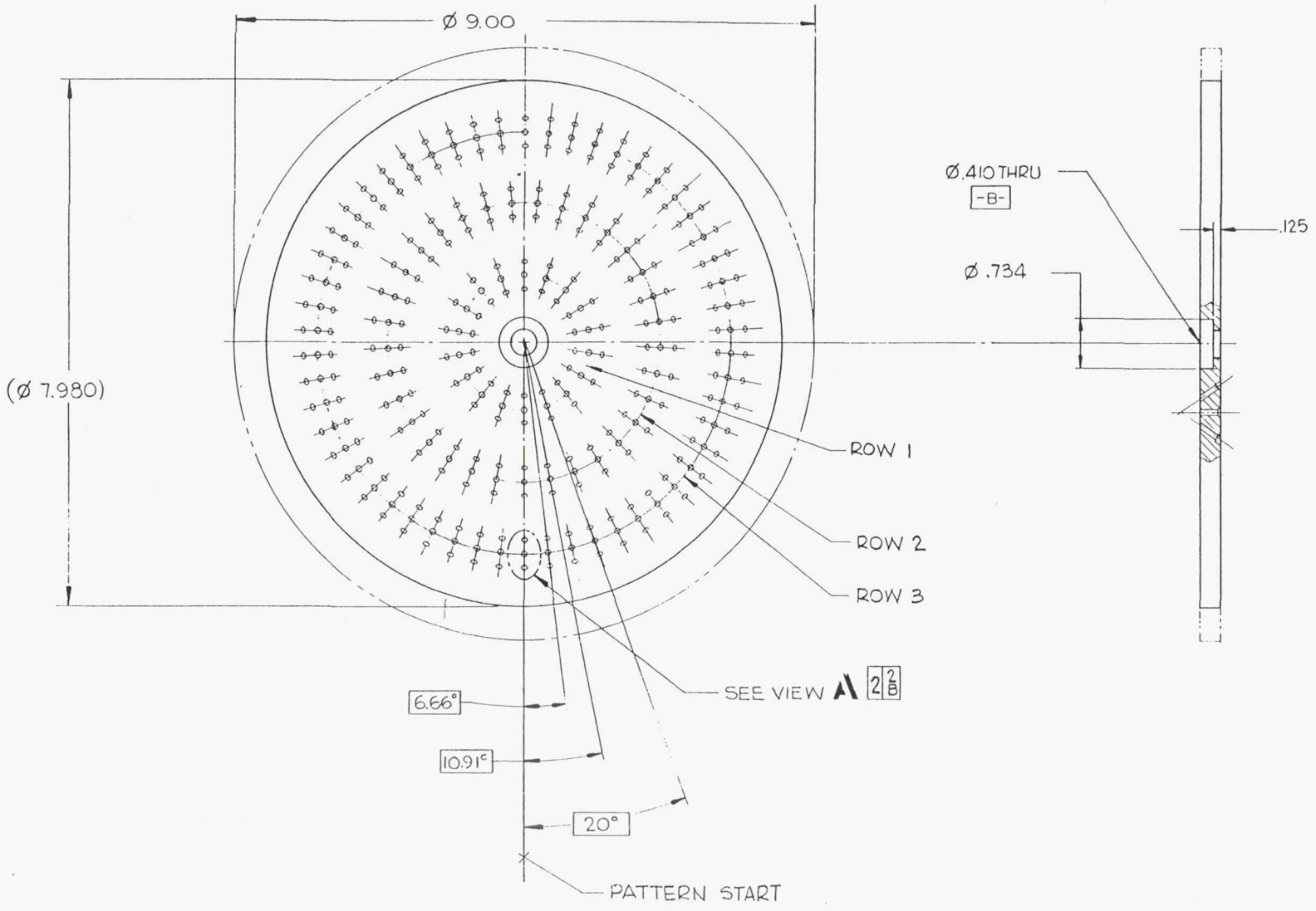

Figure 45. The 105 Element O-F-O Injector Pattern Defined Using ROCCID is Incorporated Into a Zirconium Copper Faceplate

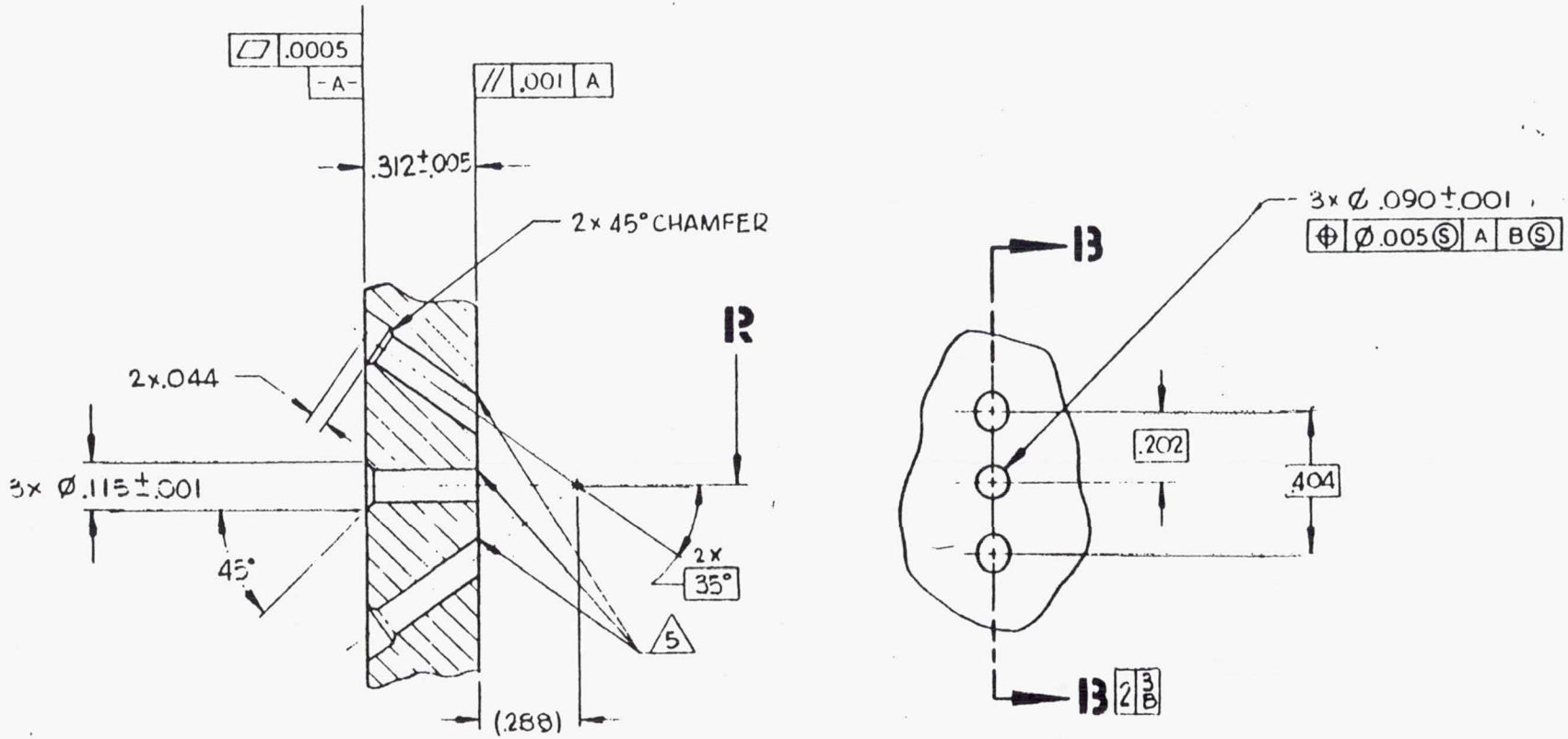

Figure 46. The OFO Triplet Element was Designed to ROCCID Specification

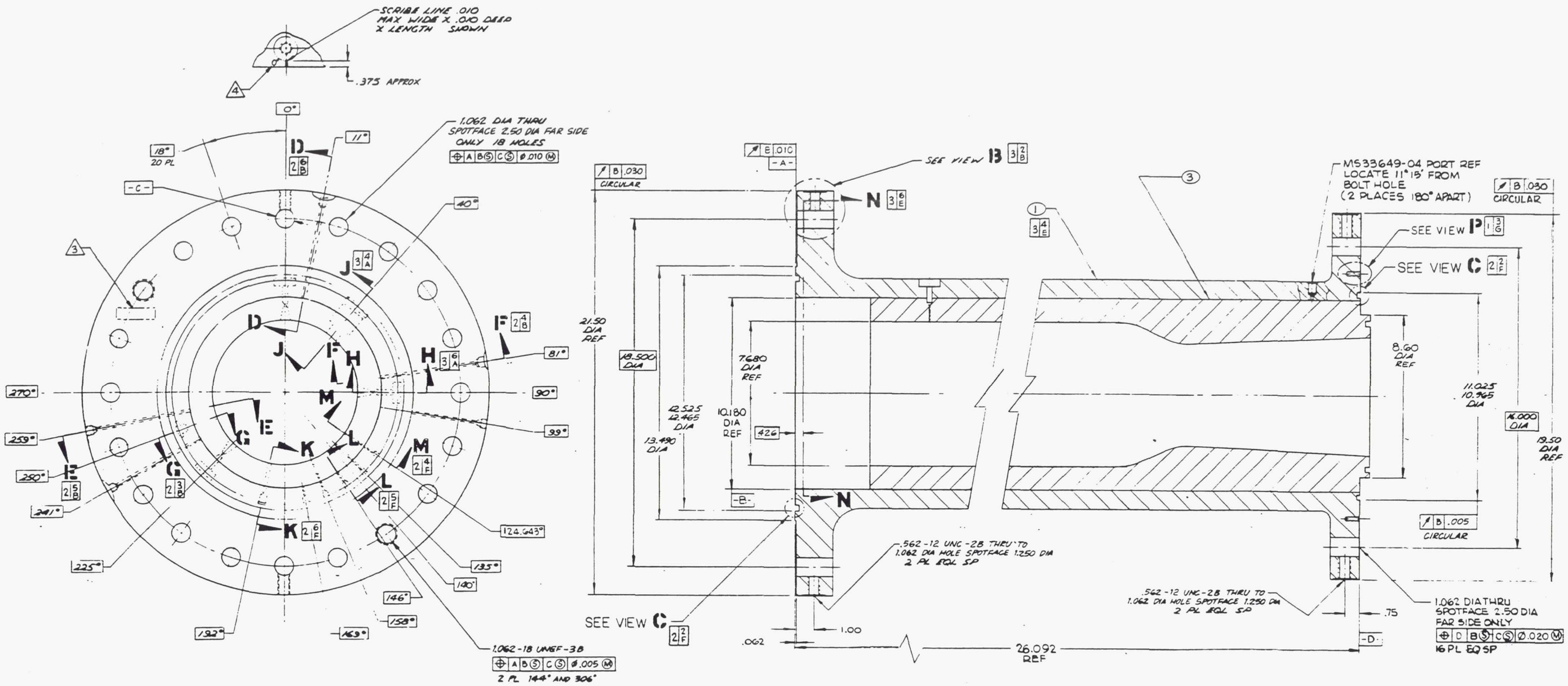

Figure 47. A New Thrust Chamber Design was Prepared to Meet ROCCID Validation Requirements

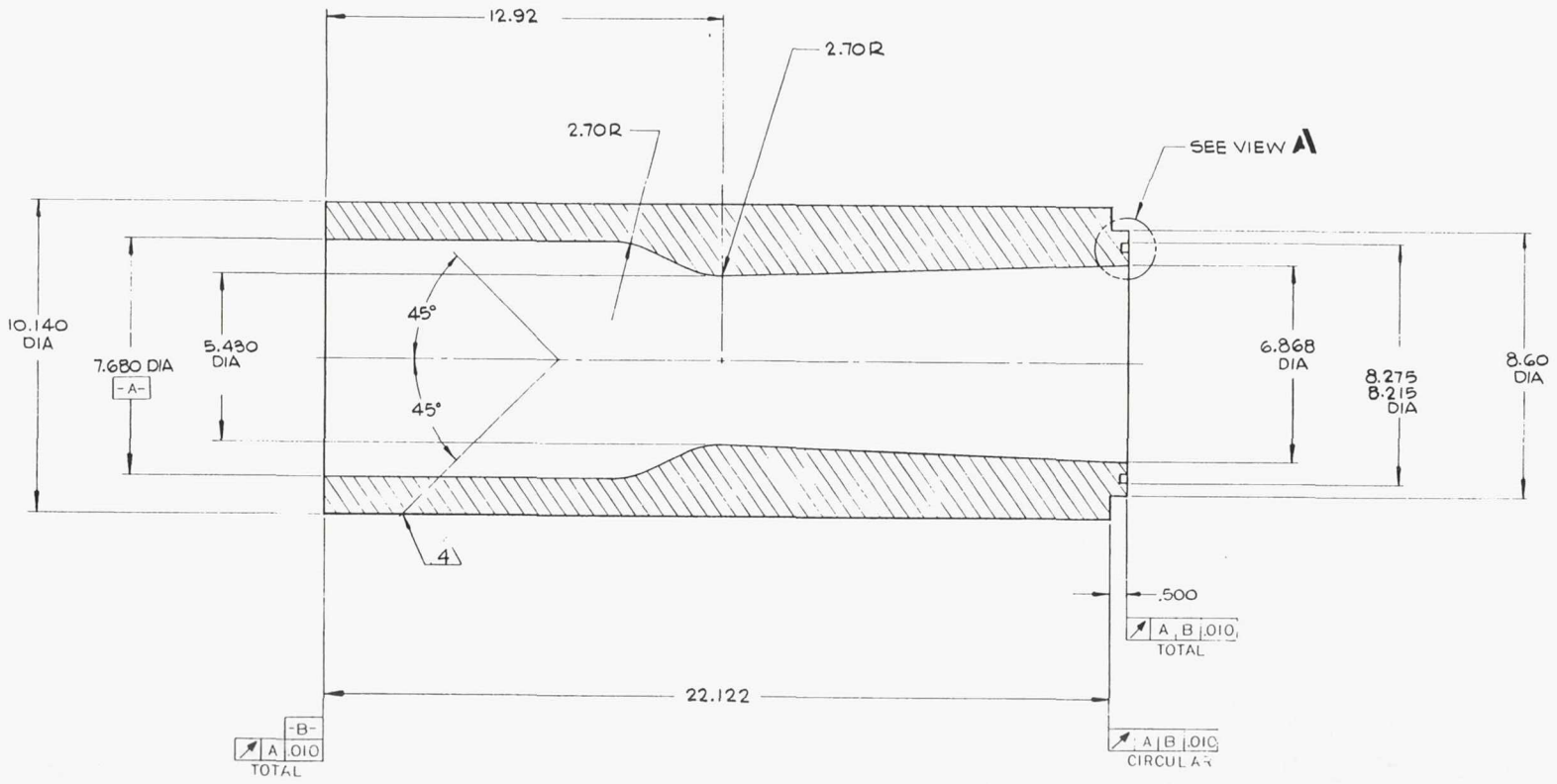

L' = 14 in. CR = 2.0 Ae/At = 1.6 D_{CH_3} = 7.68 in. D_t = 5.43 in.

Figure 48. A New Silica Phenolic Liner Design was Created to Match ROCCID Design Criteria

shell and bonded in place using RTV. A retaining ring (P/N 1200976), was also used at the aft end of the combustion chamber to locate and support the liner within the chamber shell.

The replaceable silica phenolic liner was designed with a throat diameter of 5.43 in. and a cylindrical combustion chamber with a diameter of 7.68 in. This resulted in a contraction area ratio of 2:1 (area of the nozzle inlet to the nozzle throat). A conical expansion nozzle having a 4.5° half angle was used to expand the combustion gases to a 1.6:1 expansion area ratio. The liner was designed to provide a chamber length (injector face to throat plane axial distance) of 14 in.

Previous test experience has shown that for short duration (e.g., 0.3 sec steady state) stability and performance tests that the silica phenolic material is superior in terms of durability to either the bulk graphite or carbon phenolic liners. The carbon based liners are susceptible to oxidation, particularly with the OFO injector pattern without fuel film cooling. Based on this test experience, the liners were expected to last for 6 to 10 tests before requiring replacement.

Acoustic damping in the form of an acoustic resonator was supplied using a replaceable OFHC copper ring that was installed at the head end of the combustion chamber. A bituned quarter wave acoustic cavity design using the ROCCID methodology is shown in Figure 49. The cavity tune was adjusted by changing the depth of the slots within the copper ring. A solid copper ring (without slots) was used when no acoustic damping was desired. Refer to Figure 39, which shows the installation of the cavity block (item ⑥ and ⑩) with and without acoustic cavities.

Bombs, which were used to perturb the combustion process to measure damping characteristics, were held in the combustion chamber using an adapter (P/N 1201080) shown in Figure 50. The adaptor body was fabricated from 1040 carbon steel and was threaded into the steel chamber shell in two locations. The adapter contained a carbon phenolic insert and teflon bomb holder that extended through the chamber liner to a position slightly recessed from the gas side liner surface. This recess was filled with RTV 60 to provide a measure of thermal protection to the bomb during hot-fire to preclude thermal detonation. This insert was replaceable and was designed to shield the chamber liner from the effects of the bomb. When no bomb was used, this insert was replaced with a carbon phenolic plug which filled the entire bomb cavity within the chamber liner.

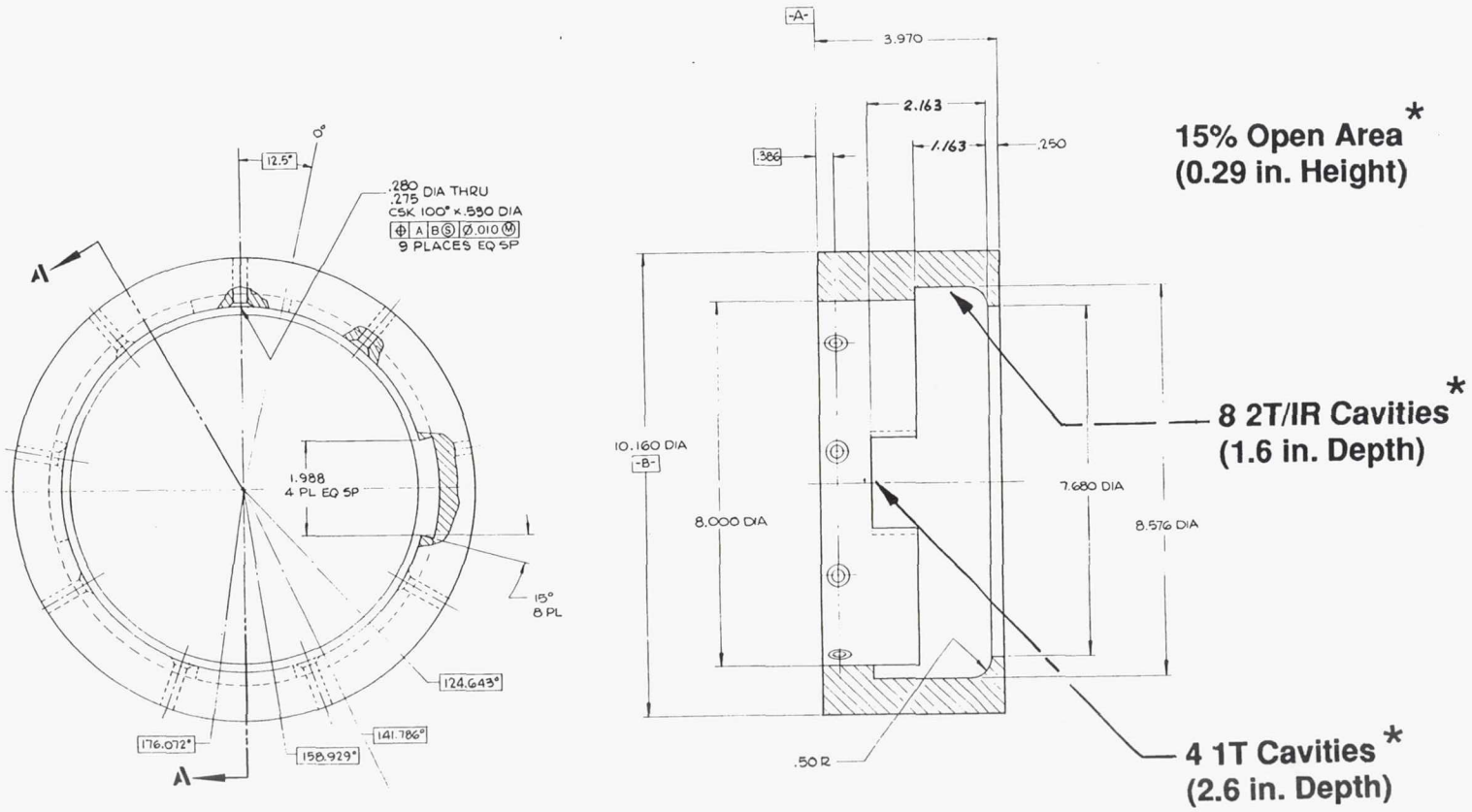

*Design Error Noted After Testing – See Figure 64

Figure 49. A Bituned 1/4 Wave Tube Acoustic Cavity Insert Design

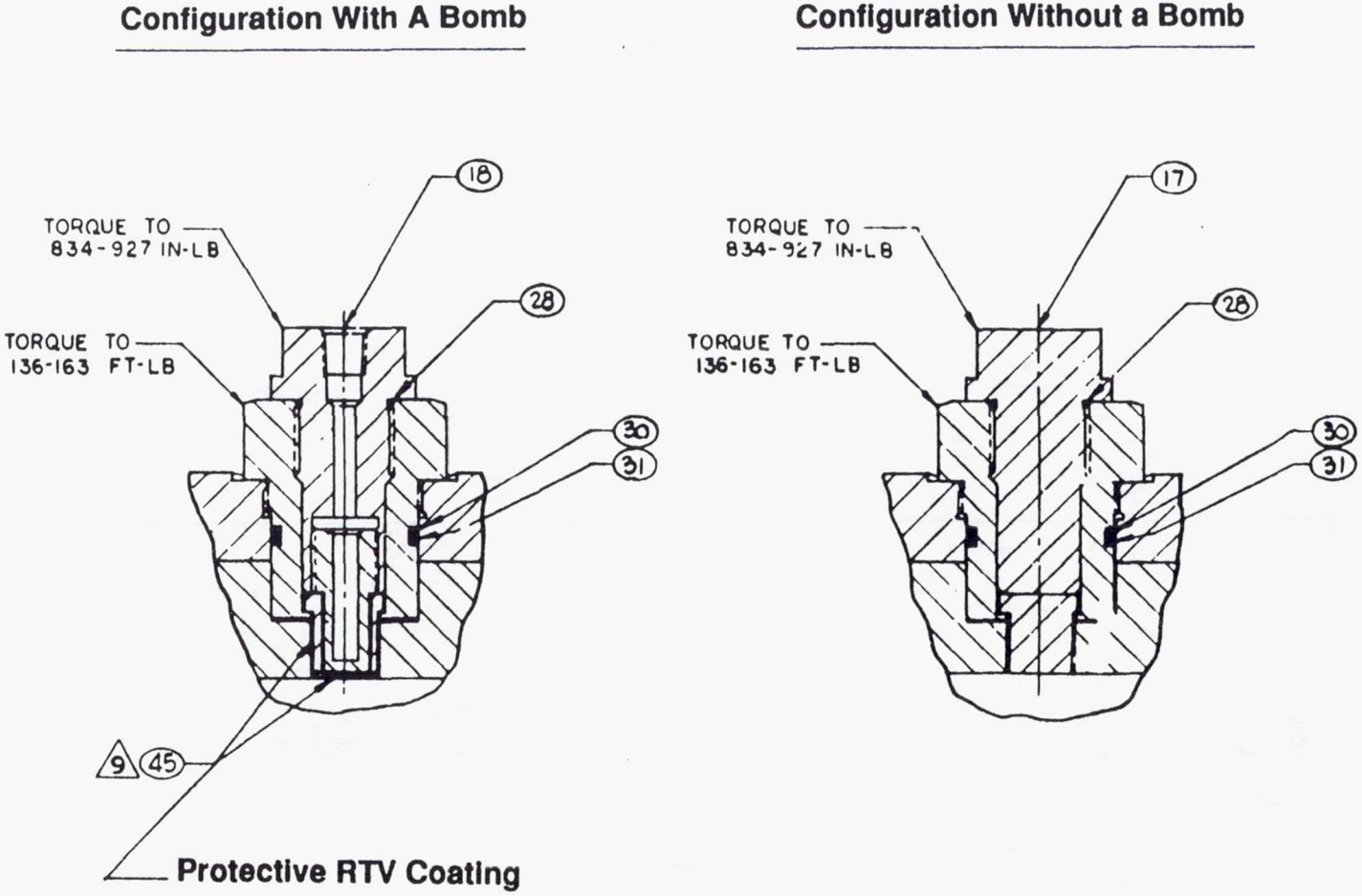

Figure 50. Bomb Adapter Design With a Thermal Protection Enhancement

The chamber contained provision for a multitude of instrumentation as shown on Figure 51. Included were 6 high frequency pressure transducer ports, 14 static pressure ports, two bomb ports, and 4 gas temperature ports. These ports were supplied in the steel shell and drilled into the replaceable silica phenolic liners after assembly.

F. HARDWARE FABRICATION

Component fabrication in support of the planned ROCCID hot fire test validation program was successfully completed over the period June 1990 through March 1991 (Reference 20). A hardware inventory necessary to support the approved test plan (Ref. 18) was obtained through rent free use of thrust chamber components from the AF 04611-85-C-0100 contract and from purchased parts and hardware fabrication subcontracts.

A complete list of components required for the ROCCID Validation Thrust Chamber Assemblies (P/N 1206430-9, -19, and -29) is provided in Table 22. Spare parts were included to enhance the probability of successfully completing the test program in a timely and cost efficient manner. For example, two identical injector cores and two chamber shells were included. The backup injector core, shown in Figures 52 and 53 was included as a risk reduction item because it was the most vulnerable component from the standpoint of survival of the combustion instabilities that were expected during validation testing. Two chamber shells were included so that replaceable liner installation could be performed on one chamber while testing was conducted with the other. Four silica phenolic ablative liners were provided for the planned 26 tests. Three acoustic resonator block assemblies were included: one machined to provide the specified 1/4 wave tube bituned cavity (P/N 1206426) and two assemblies that totally blocked the acoustic cavity region. Unfortunately, a design drafting error in the acoustic cavity blocks (PN 1206426 or 1206431) went undetected through both the design and test phases resulting in acoustic cavity configurations (both "open" and "blocked") that were far from the desired design as noted in Figures 54 to 56.

The acoustic cavity was formed from the assembly of five hardware components (the injector core, flange, chamber, liner and the acoustic block), and therefore the actual cavity and its critical dimensions that affected its "tune" were not shown on the component drawings. Therefore, inspections of individual drawings were not sufficient to reveal this design flaw. The effect of the cavity design errors on the operation of the combustion chamber and the pretest combustion stability characterization is discussed in Section VI. H of this report.

Static Chamber Pressure Measurements

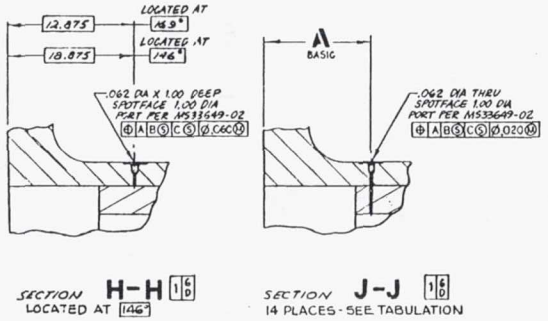

A BASIC	RADIAL LOCATION FROM -C- DATUM A BASIC	STATIC P_c
2.875	137.144°	P_c-1
3.175	154.287°	P_c-2
3.475	171.430°	P_c-3
3.775	188.573°	P_c-4
4.275	169°	P_c-5
4.775	146°	P_c-6
5.275	135°	P_c-7
5.575	158°	P_c-8
5.975	124°	P_c-9
6.475	169°	P_c-10
6.975	146°	P_c-11
7.975	135°	P_c-12
8.975	158°	P_c-13
9.975	124°	P_c-14

Cavity Gas Temperature Measurements

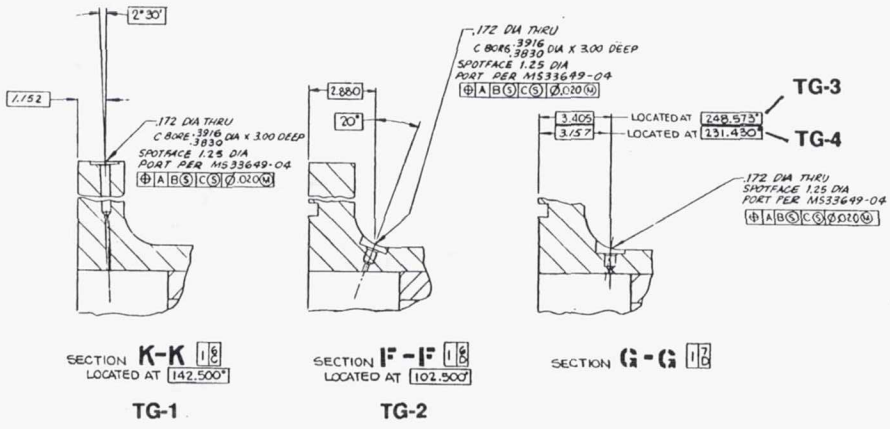

High Frequency (Kistler) Chamber Pressure Measurements

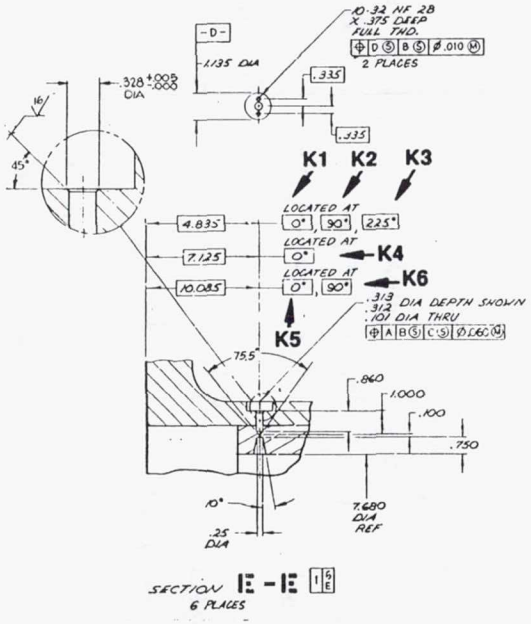

Bomb Port Locations

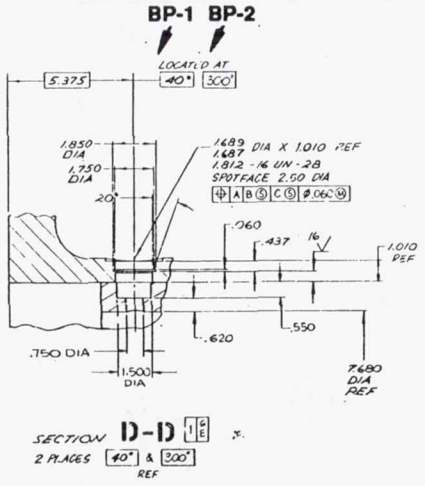

Figure 51. Provision for Instrumentation Required for Validation

TABLE 22. - ROCCID - Subcomponents

	P/N		P.O. NUMBER	DISTRIBUTION NUMBER	QTY. REQ'D PER ASSY.	TOTAL QTY. REQ'D	RESIDUAL KAE-622	COMMENTS
1	1206423-9	**INJECTOR CORE ASSY, OFO TRIPLET 3D**	L823837		1	2		.090 DIA. OFO TRIPLET 105 ELEMENT
2	1200729-9T	INJECTOR CORE PROTECTIVE CONTAINER			1	2		
3	1200729-10	IGNITER PLUG			1	4		SPARES
4	1200729-12	IGNITER, COPPER WASHER			1	9		SPARES
5	2-010S61360	O-RING, IGNITER PLUG			1	9	9	SPARES
6	AS8040K2-902	O-RING, POJ/PFJ			2			
7	MS21250-10048	BOLT, INJ. CORE/FLG.	R938705		16	24	16	
8	MS20002C10	WASHER, INJ. CORE/FLG.	"		16	24		
9	AS8040K2-445	O-RING, INJ. CORE/FLG.	R938600		1	7	3	
10	AS8040K2-450	O-RING, INJ. CORE/FLG.	"		1	7	3	
11	**1200773-49**	**INJECTOR FLANGE ASSY, 3D SUBSCALE**	L823901		1	1		304 SS WITH MAX C PLUS HIGH FREQ. PORT
12	1200773-19T	INJECTOR FLANGE PROTECTIVE CONTAINER			1	1		
13	AS8040K2-904	O-RING, DRAIN PORTS			3	6	6	
14	AS8040K2-908	O-RING, TOJ/PFJ			2			
15	NAS628H30	BOLT, THRUST MOUNT			16	28		
16	MS20002C8	WASHER, THRUST MOUNT	R938705		16	32		AN960C1816L EQUIVALENT
17	**1206428-1**	**THRUST CHAMBER, (MACH)**	L823838		1	2		4340 STEEL
18	**1206429-1**	**INSERT, THRUST CHAMBER**	L823865		1	4		SILICA PHENOLIC LINERS
19	MS9068-453	O-RING, INJ. FLG./CHB. FLANGE	R938600		1	12		
20	MS9068-450	O-RING, CHB./RETAINER	"		2	8		ONE IS REQ. FOR CLOSURE @ PROOF
21	MS21250-16072	BOLT, INJ. FLG./CHB. FLANGE			20	30	20N - 10U	
22	AN960C1616L	WASHER, FORE & AFT CHB. FLANGE			72	144	153	
23	SPS72789-1612	NUT, FORE & AFT CHB. FLANGE			36	72	72	
24	**1200976-2**	**RETAINER PLATE**	L823836		1	2		-2: 4340 STEEL & 4 RETAINING BOLT HOLES
25	NAS334CPA10	BOLT, RETAINER PLATE			4	16		
26	NAS334CPA7	BOLT,	R938705					
27	MS21250-16032	BOLT, RETAINER/CHB. FLANGE	R938655		16	32	5N - 4U	NAS636-32 EQUIVALENT
28	1200977-19	**CLOSURE PLATE**	L823838		1	1		-19: 4340 STEEL
29	MS21250-16064	BOLT, CLOSURE PLATE/CHB.	R938655		16	24		NAS636-64 EQUIVALENT
30	MS9068-444	O-RING, CLOSURE/INSERT	R938600		1	13		
31	1206426-1	**1T/2T 1/4 WAVE RESONATOR**	MHA 2585		1	1		
32	1206431-1	**BLANK RESONATOR**	"		1	2		INCLDS SPARE FOR BACKUP RESONATOR
33	NAS334CPA13	BOLT, RESONATOR RING	R938705		9	72		
34	1201080-1	BOMB INSERT, BOMB ADAPTER	MHA 2583		1	4		1040 STEEL
35	1201080-2	HOUSING, BOMB ADAPTER	MHA 2583		2	8		INCLUDES 1206430 REQ'M
36	1201080-3	THREADED PLUG, BOMB ADAPTER	MHA 2583		4			1040 STEEL
37	1201080-4	INSERT,BOMB ADAPTER	"					TEFLON
38	1201080-5	INSERT,BOMB ADAPTER	L822258					CARBON PHENOLIC
39	1201080-6	PLUG, BOMB ADAPTER	"		1	16		CARBON PHENOLIC
40	1201080-14	ADJUSTABLE INSERT, BOMB ADAPTER			1	39		TEFLON
41	1201080-15	INSERT, BOMB ADAPTER			1	39		CARBON PHENOLIC
42	MS9068-120	O-RING, BOMB INSERT	R938600		2	26		
43	MS9068-221	O-RING, HOUSING/CHAMBER	"		2	16		
44	MS28782-26	RETAINER PACKING	"		2	16		

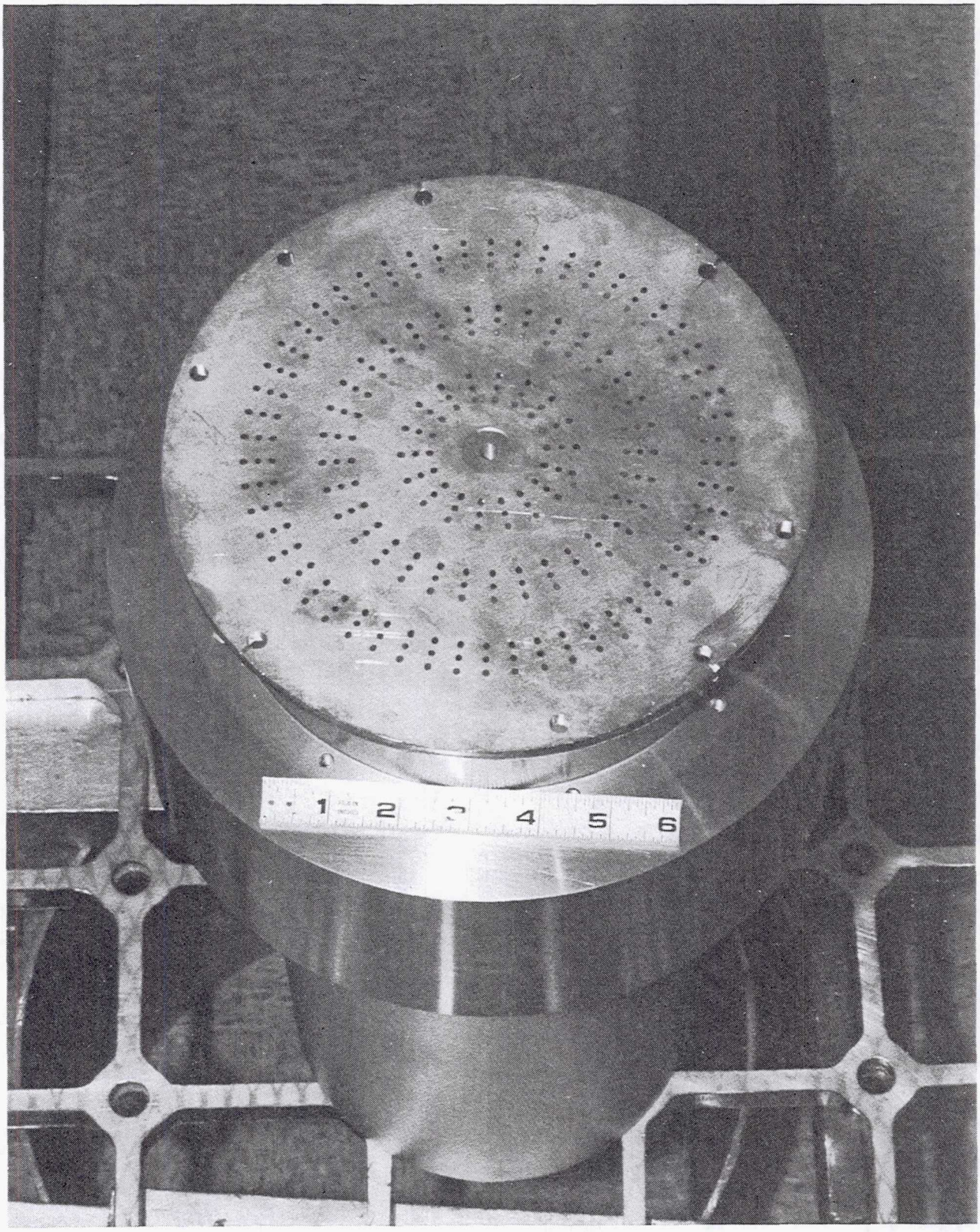

Figure 52. The Injector Core With Its Faceplate Installed for Brazing

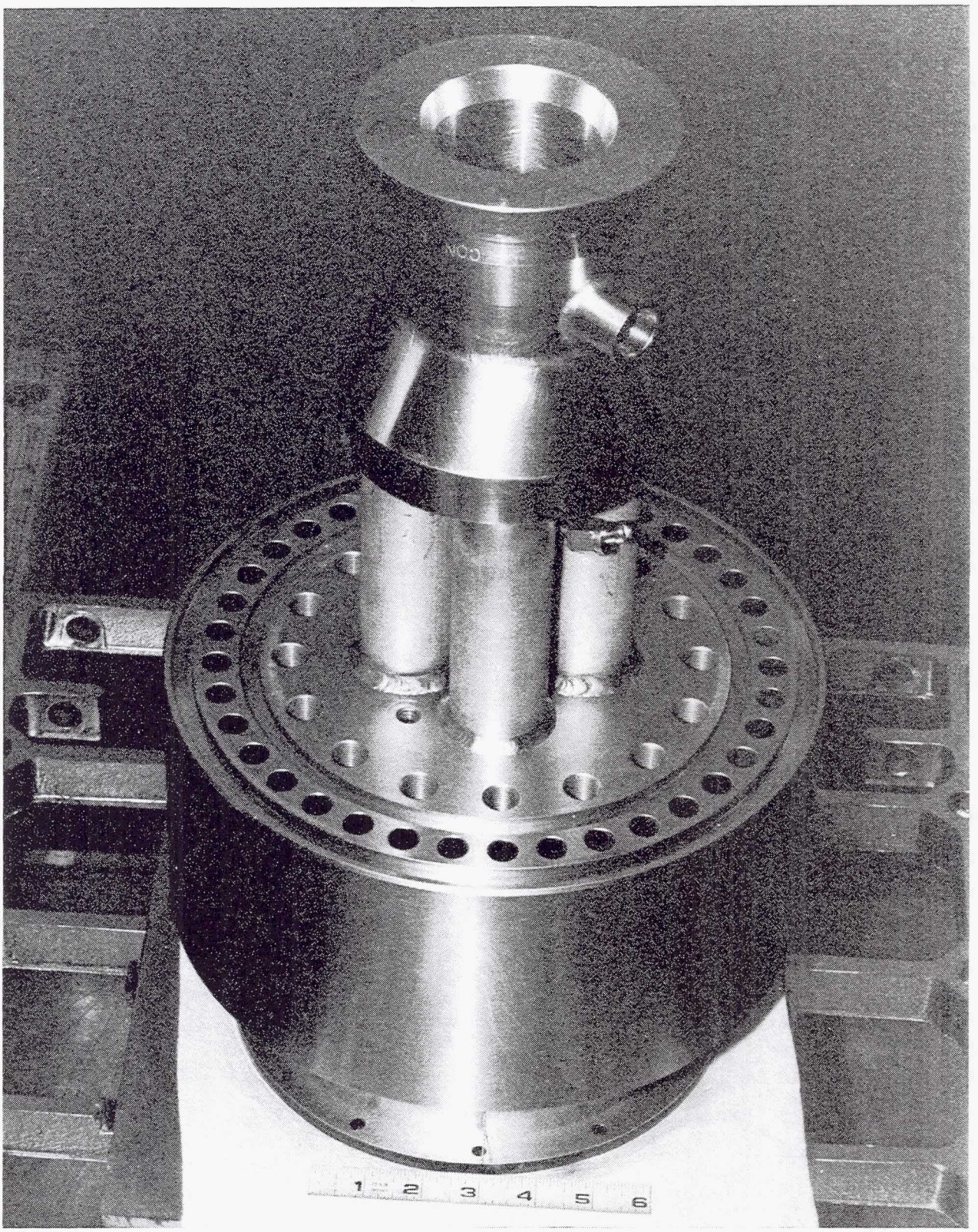

Figure 53. The Injector Core Shown With the Lox Inlet Attached

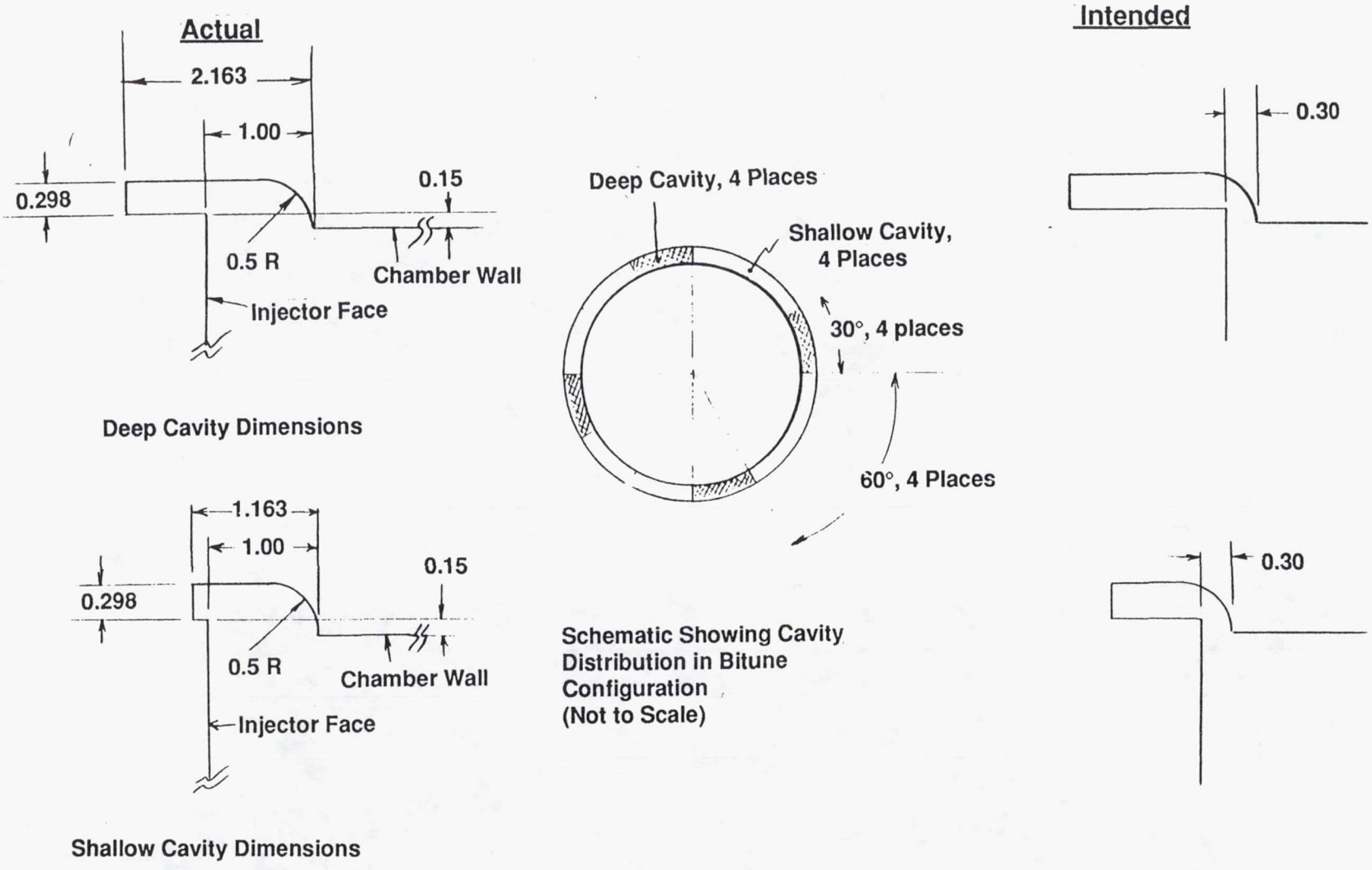

Figure 54. Bitune-Cavity Configuration Comparison of Actual and Intended Acoustic Cavities For ROCCID Testing

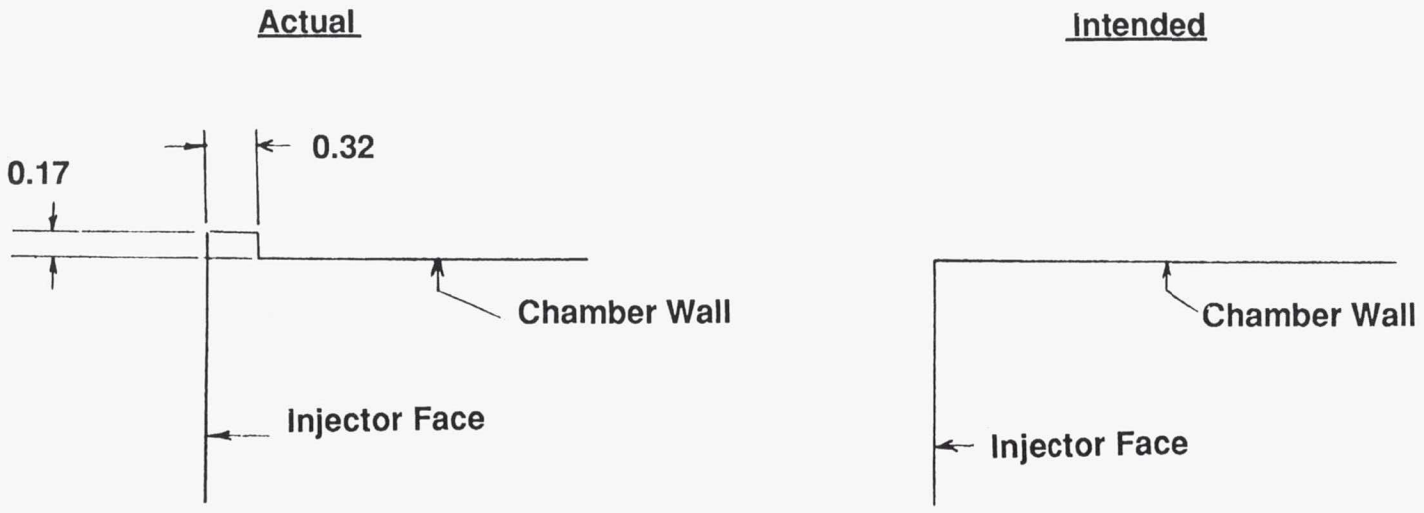

Figure 55. Blocked-Cavity Configuration

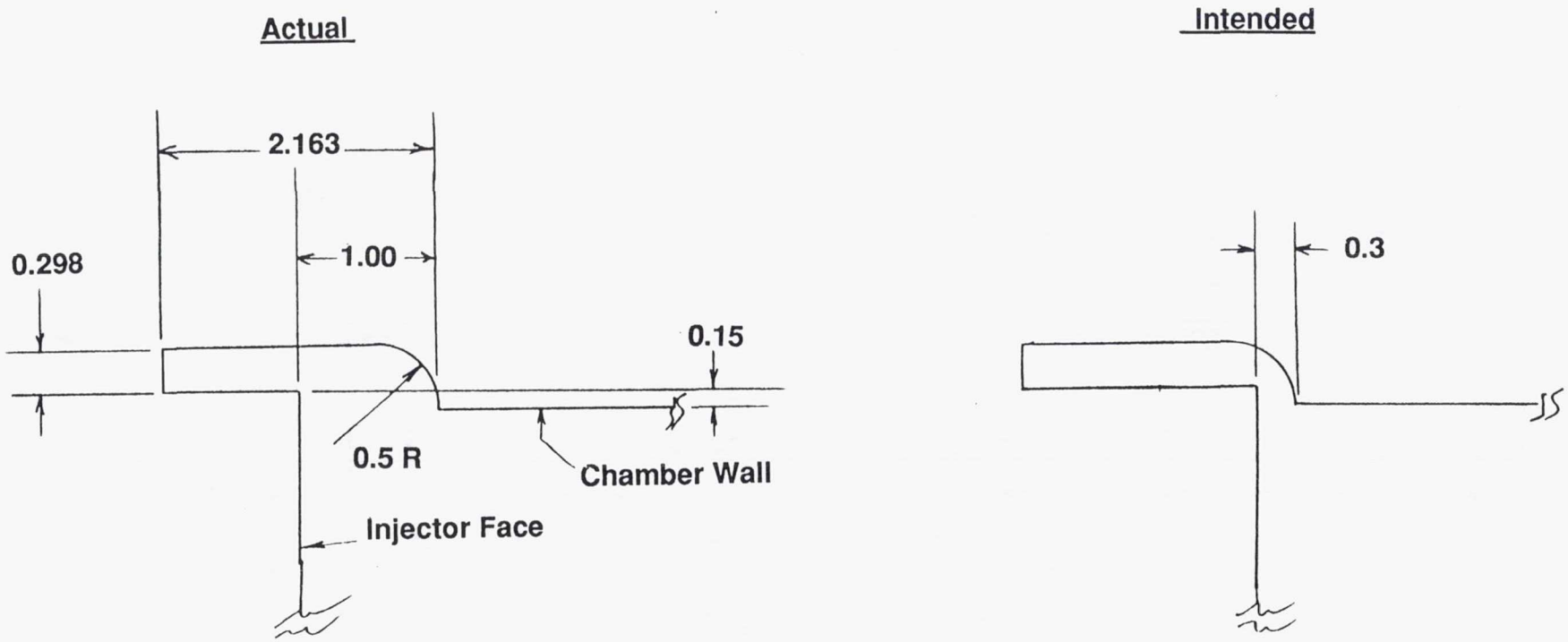

Figure 56. Monotune Cavity Configuration

Three types of verification tests were conducted to determine the adequacy of the hardware for hot fire testing.

First, the integrity of the copper faceplate braze joint to the stainless steel injector core was verified through a moderate pressure leak check using helium. During this test, the injector faceplate was sealed using a soft rubber mat and metal plate held over the face using C-clamps. The fuel circuit was filled with water and the oxygen circuit was pressurized to approximately 50 psig and held for approximately 5 minutes. No observation of helium bubbles in the water filled fuel circuit verified that the braze joints of both injector cores were leak free.

Second, all pressure containing hardware components were subjected to a proof test using filtered water at 3800 ± 100 psig and held for 5 minutes. Components that were previously verified through proof testing during the F04611-85-C-0100 contract did not require further proof verification. All proof tests were successfully conducted in the Aerojet E-Zone test facility and were witnessed by the test engineer.

Last, cold flow tests of both injector cores were conducted to verify flow resistance and the element impingement. These tests were conducted in the A-Area facility and the Production Hydrolab facility over a pressure and flowrange that precluded orifice cavitation (below approximately 50 psig). A photograph of the refurbished injector core at very low ΔP (3-5 psig) is shown in Figure 57.

The impingement process of both injector cores was visually inspected by the project engineer and the lead combustion analyst. In some cases, poor element impingement was noted, which was subsequently attributed to blocked, or partially blocked orifices resulting from inadvertent contamination from the manufacturing process. In all cases, satisfactory impingement was achieved after backflushing to remove the contamination.

Non-cavitating flow resistance (R) or admittance ($Kw = \dot{w} / (\Delta P\ Spg)^{1/2}$) values were also measured for both injector cores as summarized in Table 23.

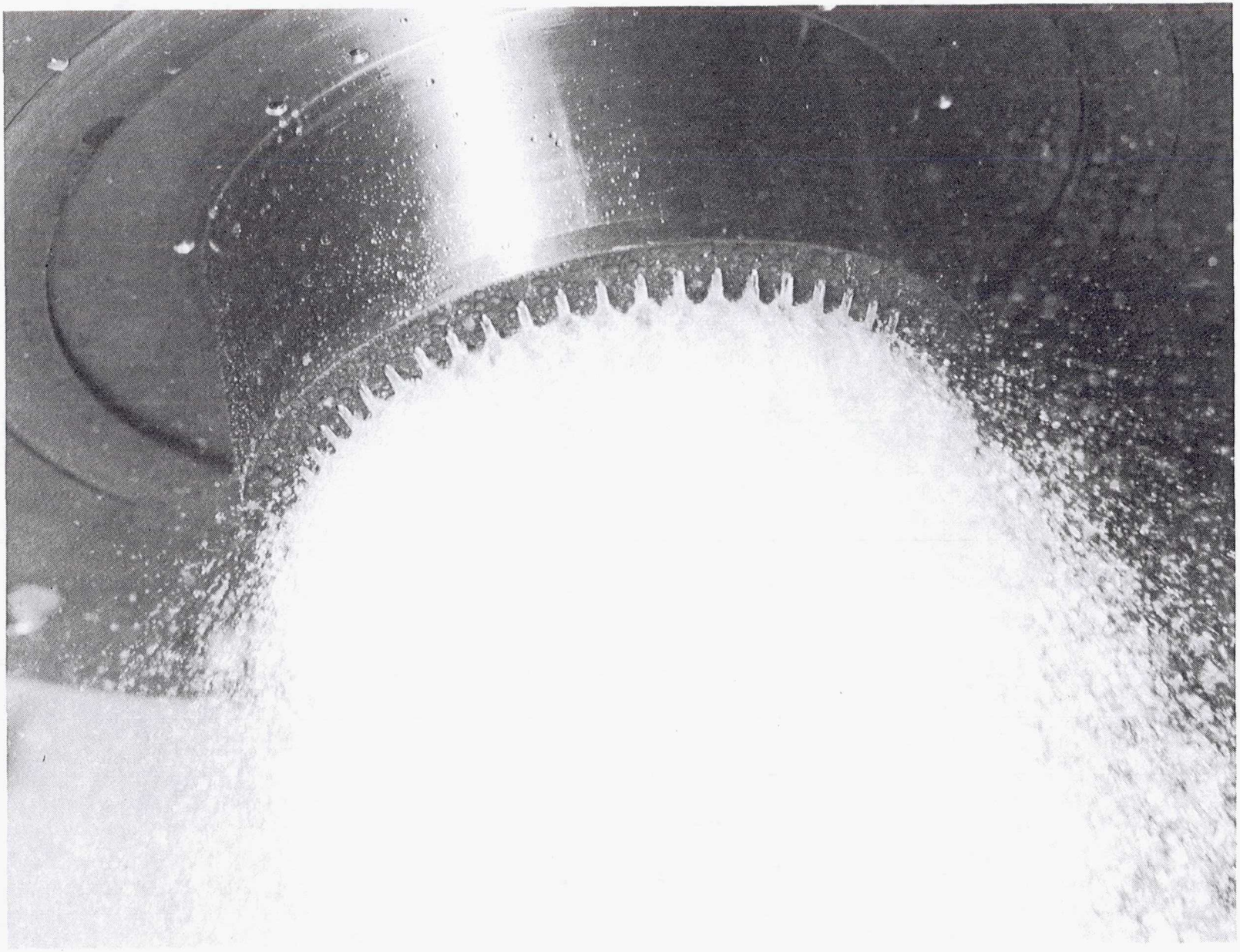

Figure 57. Water Cold Flow Tests Were Conducted to Verify Element Impingement and Flow Resistance

TABLE 23. ROCCID INJECTOR COLD FLOW ADMITTANCE VALUES (lbm/sec/(psid)$^{1/2}$)

Injector Core	Fuel Circuit	Oxygen Circuit
-0100 Refurbed New ROCCID	2.85 - 3.0	5.8 - 5.9
New Injector Core	2.95	5.7 - 5.8

These Kw values were within the expected range thus indicating that the desired high orifice C_d (> .9) was achieved.

Minor design refinements were made during the fabrication phase to facilitate the manufacturing ease and correct errors and omissions on the drawings. These changes have been incorporated into the design disclosure package using Aerojet's Advanced Drawing Change Notice (ADCN). The ADCN's prepared in support of this program are provided in Appendix E, of Volume II of this final report.

In addition to these design changes some features of the as-fabricated parts did not meet drawing requirements. In each case, these discrepancies were evaluated by the Aerojet Engineering Review Board for this program to determine that they did not affect the form, fit or function of the part. A description of the discrepancy and its disposition are recorded on Aerojet Nonconformance Reports that are included in Appendix F of Volume II of this report.

G. VALIDATION TESTING

Hot fire tests, in accordance with the approved test plan (Ref. 18), were conducted on the Aerojet E-4 test stand in the spring of 1991. The purpose of this testing was to provide a test data base with hardware designed using the ROCCID methodology for assessment of the validity and capability of the methodology and identification of its shortcomings to support future improvement efforts. A total of 40 test firings were made, from which 27 tests produced results suitable for correlation with ROCCID combustion stability and/or performance predictions.

The testing consisted of "3 blocks" of tests. Block 1 tests were with a bituned acoustic cavity and were structured to provide test data in the most combustion stable engine configuration. These tests established performance values and mapped the regions of stable and unstable combustion. They were predicted to be the safest tests from a hardware damage stand-point since high amplitude combustion instabilities were not likely. This provided the most

benign environment to establish start and shutdown sequences and performance values. The Block 2 tests were without any acoustic cavity and provided a direct assessment of the benefit of the cavity used in the Block 1 tests. The block 3, and final group of tests provided test data with a monotuned acoustic cavity. The valid tests in these three blocks are shown in Table 24.

An overview of the test logic for each of the Blocks of tests is shown on Figure 58. The path depicted by the shaded boxes was the logic path followed during the test program. The Block 1 tests with the bituned cavity were structured to meet the objectives of test series A (start, showdown and flowrate balance verification), B (verification of stable operation at the nominal operating point, MR=2.8, Pc=1250 psia), C (verification of chug and L mode predictions), and D (verification of stable operation at nominal conditions). The Block 2 tests without acoustic cavities were structured to meet the objectives of test series E (verification of unstable operation without acoustic cavities at the nominal design point), F (verify stable operation without acoustic cavities at off nominal conditions), and G (verify unstable operation without acoustic cavities at off nominal conditions). The Block 3B tests with a reconfigured (monotuned) acoustic cavity were conducted since the original bitune cavity did not provide as large a region of stable operation as originally desired. This block of tests met objectives B (confirm nominal MR-Pc operation with a new cavity tune), D (confirm off nominal stability with a new cavity), and H (confirm off nominal unstable points with a new cavity).

Table 25 is a summary of the test data. It includes directly measured data, quantities calculated from measured data, and brief comments. Tests for checking out the engine operation and unsuccessful tests were not included in the table. Plots of measured system pressures for these tests as a function of time are included in Volume II of this report.

The raw data was divided into two segments, performance data and liner data. The performance data includes the data summary period, system pressures and temperatures and thrust. If the test was of sufficient steady-state duration (>200 msec), the listed data is the period with the least variation. For the shorter tests, the data summary period typically is a single data point, and it is usually chosen to correspond with the time of maximum valve opening position. It should be noted that the flow rate values in many cases were obtained from graphical flowmeter records, since the digital time averaging tended to yield erroneous values because of transient effects in the short duration tests due to the relative location of the flowmeters and the thrust chamber.

TABLE 24. PLANNED AND ACTUAL TEST CONDITIONS

		Planned Conditions		Actual Conditions	
Test No.	Block	Chamber Pressure psia	Mixture Ratio	Chamber Pressure psia	Mixture Ratio
4	I	1250	2.80	1177	2.59
7	I	1500	1.50	1441	1.45
9	I	500	2.80	505	2.94
12	I	300	2.80	250	1.01
13	I	1250	1.20	1210	1.13
14	I	1500	2.80	1358	2.67
15	I	1000	2.00	969	1.93
17	I	800	7.50	792	6.74
18	I	1250	2.80	1165	2.35
19	I	1250	2.20	1220	2.06
20	I	1250	1.50	1193	1.50
21	II	1250	2.80	1222	2.67
22	II	1250	2.80	1092	2.52
23	II	1000	1.20	1004	1.25
24	II	800	7.50	788	6.71
25	II	1500	2.80	1410	2.86
26	II	1250	1.50	1130	1.70
27	II	1750	2.80	1706	3.03
28	II	1250	5.00	1260	5.15
29	III	1250	2.80	1208	2.55
30	III	800	2.80	791	3.09
31	III	1000	2.00	953	2.09
36	III	250	2.80	249	3.31
37	III	1750	2.80	1735	3.05
38	III	1500	2.80	1467	3.07
39	III	1250	5.00	1235	5.60
40	III	1250	2.20	1174	2.23

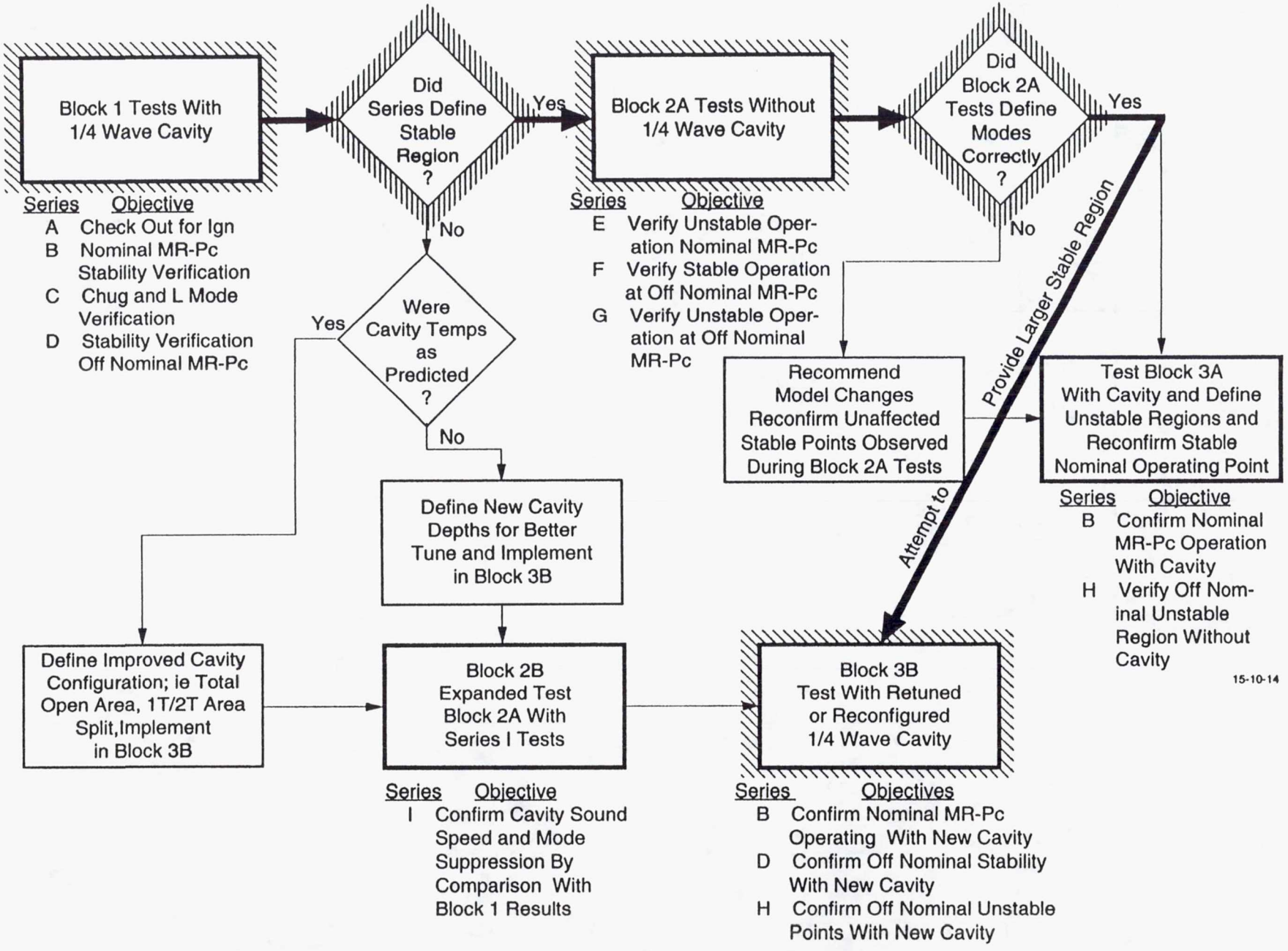

Figure 58. Overview of Test Logic

TABLE 25.

ROCCID VALIDATION TEST DATA

NASA/LeRC ROCCID Validation Testing
KFN7-D01-1J-0XX
LOX/RP-1 OPO Triplet

Printed: 09:15 AM 05-Oct-92

Test No.	4	7	9	12	12A	13	14	15	17	18	19	20	21	22
Ign. Time (sec) [Pc > 200]	1.33	1.41	1.88	1.85	1.85	1.29	1.26	1.30	1.34	1.23	1.25	1.34	1.22	1.23
PC Decay Time (sec) [Pc < 200]	1.54	2.36	2.69	2.60	2.60	1.94	1.50	1.94	1.96	1.50	1.52	1.99	2.09	1.53
PERFORMANCE MEASURED DATA														
Summary Start Time (sec)	1.492	1.753	2.469	1.994	2.394	1.723	1.403	1.723	1.636	1.367	1.379	1.765	1.644	1.362
Summary End Time (sec)	1.492	1.853	2.569	2.094	2.494	1.823	1.403	1.823	1.736	1.377	1.379	1.865	1.744	1.372
PC-1 (psia)	1178	1441	504	n/a	n/a	n/a	n/a	n/a	n/a	n/a	n/a	n/a	1222	1092
PC-2 (psia)	1177	1441	505	250	297	1210	1358	969	792	1165	1220	1193	1208	1079
PC-3 (psia)	1169	1438	501	248	295	1197	1338	955	791	1153	1213	1190	1219	1056
PC-4 (psia)	1142	1419	498	246	294	1185	1336	944	795	1161	1214	1176	1208	994
PC-5 (psia)	1104	1439	485	248	298	1197	1306	933	789	1145	1215	1179	1173	1086
PC-6 (psia)	1091	1396	n/a	n/a	n/a	n/a	n/a	n/a	n/a	n/a	n/a	n/a	1171	1027
PC-7 (psia)	1074	1405	n/a	247	296	1167	1274	929	769	1074	1141	1150	1128	1092
PC-8 (psia)	1090	1277	n/a	n/a	n/a	n/a	n/a	n/a	n/a	n/a	n/a	n/a	1127	1047
PC-9 (psia)	1059	1411	n/a	241	291	1160	1223	903	759	1031	1077	1142	1129	967
PC-10 (psia)	1051	1376	n/a	241	291	1163	1220	902	757	1034	1072	1138	1123	965
PC-11 (psia)	1049	1357	n/a	241	291	1153	1208	899	751	1029	1074	1134	1123	985
PC-12 (psia)	1056	1364	n/a	n/a	n/a	1143	1207	892	741	1016	1061	1124	1115	1002
PC-13 (psia)	1028	1346	423	237	287	1137	1186	886	736	n/a	n/a	1108	n/a	n/a
PC-14 (psia)	1049	1370	458	233	282	1130	1227	883	723	n/a	n/a	n/a	1110	1025
Last PC (psia)	1049	1346	458	233	282	1130	1186	883	723	1016	1061	1108	1110	1002
PFJ (psia)	1479	2449	542	316	590	2385	1804	1221	826	1433	1554	1903	1467	1461
Measured Thrust (lbf)	36834	44343	15068	6834	8487	36846	43082	29361	24123	36220	37347	37416	36673	36905
FMO (lb-H2O/s)	109.20	105.25	41.92	21.61	21.69	87.56	114.74	72.87	87.57	91.78	91.79	93.73	104.32	101.99
FMF (lb-H2O/s)	59.36	101.71	n/a	29.43	54.99	107.10	60.68	52.59	n/a	52.85	59.97	85.11	52.48	55.73
POT (psia)	1645	1937	572	303	301	1535	2036	1187	1132	1598	1589	1552	1657	1658
PFT (psia)	1573	2765	550	297	296	2697	1936	1314	1000	1527	1686	2134	1558	1545
POJ (psia)	1559	1821	578	263	323	1468	1918	1135	1061	1430	1503	1470	1538	1610
TOFM (F)	-289	-287	-290	-289	-289	-281	-288	-288	-289	-273	-270	-277	-270	-281
TOJ (F)	-276	-276	-280	-280	-279	-278	-268	-278	-279	-268	-269	-277	-237	-270
TFFM (F)	66	68	74	65	62	70	68	66	71	60	61	61	57	61
TFJ (F)	64	73	73	65	63	75	67	69	72	58	63	63	57	60
Tcavity-1 (F)	1154	2481	713	370	1171	n/a	575	1214	397	n/a	n/a	1717	n/a	n/a
Tcavity-2 (F)	1384	n/a	1374	1152	n/a	n/a	1859	2362	700	n/a	1593	2314	n/a	n/a
Tcavity-3 (F)	n/a	n/a	811	632	1277	2436	691	1905	611	n/a	1041	2445	n/a	n/a
Amb. Pressure (psia)	14.69	14.61	14.61	14.61	14.61	14.61	14.69	14.69	14.69	14.69	14.69	14.69	14.66	14.66
LINER DATA														
Liner S/N	1	1	1	1	1	1	1	1	1	1	1	1	2	2
Initial Throat Diam. (in)	5.416	5.451	5.480	5.502	5.502	5.531	5.481	5.512	5.495	5.540	5.532	5.543	5.433	5.461
Initial Exit Diam. (in)	6.848	6.860	6.860	6.845	6.845	6.869	6.845	6.869	6.856	6.877	6.894	6.870	6.858	6.848
Final Throat Diam. (in)	5.452	5.447	5.491	5.531	5.531	5.481	5.512	5.495	5.540	5.532	5.543	5.564	5.461	5.479
Final Exit Diam. (in)	6.860	6.863	6.865	6.869	6.869	6.845	6.869	6.856	6.877	6.894	6.870	6.889	6.848	6.851
COMMENTS														
Performance	No S.S	Good S.S.	FMF Bad	PxT Bad	PxT Bad	Good S.S.	No S.S.	Good S.S.	FMF Bad	No S.S.	No S.S.	Good S.S.	Good S.S.	Poor S.S.
Liner	None	None	None	None	None	None	None	None	None	None	None	None	None	BP Damaged

TABLE 25.

ROCCID VALIDATION TEST DATA (CONT)

NASA/LeRC ROCCID Validation Testing
KFN7-D01-1J-0XX
LOX/RP-1 OPO Triplet

Printed: 09:15 AM 05-Oct-92

Test No.	23	24	25	26	27	28	29	30	31	36	37	38	39	40
Ign. Time (sec) [Pc > 200]	1.32	1.38	1.31	1.29	1.30	1.34	1.31	1.41	1.35	2.68	1.25	1.27	1.30	1.31
PC Decay Time (sec) [Pc < 200]	1.97	2.00	1.55	1.57	1.53	1.56	1.95	1.81	2.01	3.09	1.92	1.52	1.71	2.81
PERFORMANCE MEASURED DATA														
Summary Start Time (sec)	1.725	1.798	1.451	1.485	1.430	1.460	1.635	1.593	1.804	2.916	1.605	1.391	1.495	1.643
Summary End Time (sec)	1.825	1.898	1.451	1.485	1.430	1.460	1.735	1.693	1.904	3.016	1.706	1.391	1.595	1.743
PC-1 (psia)	997	788	1382	1127	1697	1256	1205	789	944	247	1738	1463	1214	1168
PC-2 (psia)	1004	788	1397	1118	1706	1260	1208	791	951	249	1735	1456	1213	1172
PC-3 (psia)	992	787	1410	1130	1725	1258	1174	786	953	246	1731	1453	1198	1174
PC-4 (psia)	985	785	1399	1083	1687	1164	1166	781	937	249	1728	1467	1235	1153
PC-5 (psia)	991	786	1327	1122	n/a	n/a	1170	757	935	248	1710	1436	1206	1154
PC-6 (psia)	992	786	1316	1114	1643	1251	1109	742	936	236	1634	1383	1180	1125
PC-7 (psia)	991	787	1262	1085	1642	1250	1115	747	917	234	1634	1304	n/a	1123
PC-8 (psia)	978	760	n/a	1046	1574	n/a	1113	740	n/a	n/a	n/a	n/a	1152	n/a
PC-9 (psia)	960	755	1207	1126	1571	1174	1095	732	883	207	1608	1289	1160	1118
PC-10 (psia)	956	753	n/a	1082	n/a	1153	1091	731	879	233	1590	1240	n/a	1095
PC-11 (psia)	955	746	1202	1089	1531	1140	1094	728	876	232	1598	1297	1138	1099
PC-12 (psia)	944	736	1196	1066	1515	1116	1078	714	885	224	1582	1238	1116	1087
PC-13 (psia)	n/a	n/a	n/a	1068	n/a	1089	1077	717	865	206	1579	1275	1145	1108
PC-14 (psia)	936	729	1220	1096	1522	1117	1085	717	860	219	1567	1267	1136	1112
Last PC (psia)	936	729	1196	1066	1522	1117	1085	717	860	219	1567	1267	1136	1095
PFJ (psia)	1721	823	1776	1979	2242	1376	1453	894	1237	258	2222	1809	1329	1569
Measured Thrust (lbf)	30381	23967	43228	35653	53828	39874	35976	24104	22884	6924	54466	46959	38052	38022
FMO (lb-H2O/s)	78.30	94.17	121.49	94.14	150.47	137.68	98.09	71.91	75.79	23.33	154.38	131.10	141.21	103.29
FMF (lb-H2O/s)	86.00	n/a	59.40	90.27	70.02	37.49	54.24	32.52	55.16	n/a	71.68	59.56	35.23	64.92
POT (psia)	1231	1140	2068	1608	2696	2040.00	1667	990	1230	260	2698	2180	1997	1628
PFT (psia)	1963	1145	1903	2256	2451	1423.00	1551	927	1342	258	2394	1975	1376	1694
POJ (psia)	1192	1063	1951	1530	2437	1814	1563	948	1177	277	2432	2017	1780	1560
TOFM (F)	-281	-282	-285	-288	-286	-287	-288	-288	-290	-293	-287	-283	-284	-288
TOJ (F)	-273	-283	-270	-278	-274	-273	-280	-275	-280	-277	-279	-264	-277	-281
TFFM (F)	54	61	60	67	59	58	73	76	54	61	59	62	63	62
TFJ (F)	58	61	59	67	57	60	73	76	55	61	62	67	57	63
Tcavity-1 (F)	n/a	n/a	n/a	n/a	n/a	n/a	1245	1271	2111	887	1625	n/a	818	814
Tcavity-2 (F)	n/a	n/a	n/a	n/a	n/a	n/a	2169	1616	2098	1125	1956	n/a	1296	1769
Tcavity-3 (F)	n/a	n/a	n/a	n/a	n/a	n/a	n/a	1913	2060	1414	2135	n/a	961	1340
Amb. Pressure (psia)	14.56	14.56	14.56	14.70	14.70	14.70	14.24	14.24	14.49	14.49	14.56	14.56	14.59	14.59
LINER DATA														
Liner S/N	2	2	2	3	3	3	4	4	4	4	4	4	4	4
Initial Throat Diam. (in)	5.479	5.472	5.518	5.449	5.425	5.464	5.451	5.477	5.517	5.523	5.515	5.545	5.561	5.577
Initial Exit Diam. (in)	6.851	6.858	6.918	6.832	6.822	6.844	6.854	6.871	6.858	6.859	6.882	6.894	6.913	6.901
Final Throat Diam. (in)	5.472	5.518	5.534	5.425	5.464	5.472	5.477	5.517	5.523	5.515	5.545	5.561	5.577	5.574
Final Exit Diam. (in)	6.858	6.918	6.918	6.822	6.844	6.875	6.871	6.858	6.859	6.882	6.894	6.913	6.901	6.901
COMMENTS														
Performance	Good S.S.	FMF Bad	No S.S.	Poor S.S.	No S.S.	No S.S.	Good S.S.	FMF-3 bad	Good S.S.	FMF bad	Good S.S.	No S.S.	Fair S.S	Good S.S.
Liner	None	Fast Errosion	Severe Damage	None	BP Damaged	Severe Damage	None	None	None	None	Cavity Damage	None	None	Severe Damage

TABLE 25.

ROCCID VALIDATION TEST DATA (CONT)

NASA/LeRC ROCCID Validation Testing
KFN7-D01-1J-0XX
LOX/RP-1 OPO Triplet

Printed: 09:15 AM 05-Oct-92

Test No.	4	7	9	12	12A	13	14	15	17	18	19	20	21	22
CALCULATED QUANTITIES														
Ox Flowmeter Spec. Gravity	1.142	1.140	1.128	1.121	1.121	1.119	1.144	1.131	1.133	1.102	1.093	1.111	1.093	1.121
Fuel Flowmeter Spec. Gravity	0.812	0.811	0.809	0.812	0.813	0.810	0.811	0.812	0.810	0.814	0.813	0.813	0.815	0.813
WOJ (lb-LOX/s)	124.74	119.95	47.28	24.23	24.32	98.00	131.30	82.40	99.20	101.14	100.29	104.14	114.06	114.31
WFJ (lb-RP1/s)	48.17	82.48	16.07	23.89	44.69	86.75	49.19	42.68	14.72	43.00	48.78	69.22	42.75	45.32
Total Flowrate (lb-propellant/s)	172.91	202.43	63.35	48.12	69.01	184.75	180.49	125.08	113.92	144.15	149.07	173.36	156.80	159.63
Mixture Ratio	2.59	1.45	2.94	1.01	0.54	1.13	2.67	1.93	6.74	2.35	2.06	1.50	2.67	2.52
Oxidizer DPinj (psi)	381	380	73	13	26	258	458	166	266	265	283	277	316	518
Fuel DPinj (psi)	301	1008	37	66	293	1175	344	252	31	268	334	710	245	369
Oxidizer Spec. Gravity @ Inj.	1.107	1.111	1.104	1.097	1.097	1.112	1.093	1.107	1.108	1.086	1.089	1.108	1.012	1.094
Fuel Spec. Gravity @ Inj.	0.812	0.809	0.809	0.812	0.812	0.808	0.811	0.811	0.809	0.814	0.812	0.813	0.815	0.814
Oxidizer Kw,j	6.07	5.84	5.27	6.42	4.55	5.78	5.87	6.08	5.78	5.96	5.71	5.95	6.38	4.80
Fuel Kw,j	3.08	2.89	2.94	3.26	2.90	2.81	2.94	2.99	2.94	2.91	2.96	2.88	3.03	2.62
Oxidizer Kw,t (S.G. @ FMO)	5.40	5.05	5.44	n/a	n/a	5.14	5.12	5.25	5.08	4.63	4.99	5.21	5.23	4.54
Fuel Kw,t (S.G. @ FMF)	2.69	2.52	2.66	n/a	n/a	2.50	2.50	2.55	1.14	2.51	2.51	2.50	2.58	2.36
Mean Summary Data Time (sec)	1.49	1.80	2.52	2.04	2.44	1.77	1.40	1.77	1.69	1.37	1.38	1.82	1.69	1.37
S.S. Combustion Duration (sec)	0.21	0.95	0.81	0.75	0.75	0.65	0.24	0.64	0.62	0.27	0.27	0.65	0.87	0.30
Cummulative S.S. Duration (sec)	0.21	1.16	1.97	2.72	3.47	3.37	3.61	4.25	4.87	5.14	5.41	6.06	0.87	1.17
Face Stagnation Pressure (psia)	1178	1441	505	250	297	1210	1460	969	795	1165	1220	1193	1222	1092
Mean Throat Po (psia)	1101	1380	476	239	287	1158	1304	916	751	1077	1126	1138	1153	1036
Po Loss (psi)	77	61	29	11	10	52	156	53	44	88	94	55	69	56
ODE C* (ft/s)	5897	5282	5741	4435	3904	4655	5885	5831	4903	5935	5898	5369	5881	5854
C* Eta-kin. (curve fit +/- 0.4%)	0.9990	0.9935	1.0000	0.9930	0.9908	0.9923	0.9991	0.9963	1.0000	0.9980	0.9966	0.9941	0.9993	0.9988
Delivered C* (ft/s)	4719	5116	5704	3799	3177	4846	5483	5621	5028	5793	5840	5099	5486	4890
C* Efficiency	0.801	0.975	0.994	0.863	0.821	1.049	0.932	0.968	1.025	0.978	0.994	0.955	0.934	0.836
ODE ISP-vac. (sec)	258.01	230.66	250.22	195.55	169.77	202.76	256.14	253.26	213.31	257.50	256.13	233.27	257.00	255.14
ISP Eta-Kin.*Eta-Div.*Eta-B.L. (+/-0.4%)	0.9950	0.9894	0.9974	0.9888	0.9865	0.9881	0.9951	0.9922	1.0000	0.9939	0.9925	0.9899	0.9953	0.9948
Perfect Injector ISP (sec)	256.72	228.21	249.58	193.35	167.48	200.35	254.89	251.28	213.31	255.93	254.20	230.91	255.79	253.80
Pamb*Aexit (lbf)	540.81	539.99	539.95	537.67	537.67	541.41	540.34	544.18	542.16	545.52	548.15	544.37	541.53	539.91
Delivered Vacuum Thrust (lbf)	37375	44883	15608	7372	9025	37387	43622	29905	24665	36766	37895	37960	37215	37445
Delivered ISP-vac. (sec)	216.16	221.72	246.37	153.19	130.77	202.37	241.69	239.09	216.52	255.06	254.21	218.97	237.33	234.57
ISP-Based ERE	0.842	0.972	0.987	0.792	0.781	1.010	0.948	0.951	1.015	0.997	1.000	0.948	0.928	0.924
Notes:	Ograph Flows		FMF forced Kw OK, Low Pc	Kw OK, Low P	Kw OK, Low Pc		Ograph Flows PC Set for Kw		FMF forced 23% S.S. LTCF	Ograph Flows TOJ dropping	Ograph FMO			Ograph Flows TOJ dropping

TABLE 25.

ROCCID VALIDATION TEST DATA (CONT)

NASA/LeRC ROCCID Validation Testing
KFN7-D01-1J-0XX
LOX/RP-1 OPO Triplet

Printed: 09:15 AM 05-Oct-92

Test No.	23	24	25	26	27	28	29	30	31	36	37	38	39	40
CALCULATED QUANTITIES														
Ox Flowmeter Spec. Gravity	1.116	1.117	1.138	1.138	1.149	1.142	1.139	1.129	1.137	1.129	1.152	1.135	1.135	1.140
Fuel Flowmeter Spec. Gravity	0.816	0.813	0.813	0.811	0.814	0.814	0.809	0.808	0.816	0.813	0.814	0.813	0.813	0.813
WOJ (lb-LOX/s)	87.38	105.24	138.30	124.22	172.91	157.26	111.72	81.15	93.93	26.35	177.77	148.82	160.22	117.72
WFJ (lb-RP1/s)	70.14	15.68	48.32	73.23	57.00	30.53	43.87	26.28	44.99	7.95	58.33	48.42	28.63	52.78
Total Flowrate (lb-propellant/s)	157.52	120.92	186.62	197.45	229.92	187.78	155.59	107.43	138.92	34.30	236.10	197.24	188.85	170.50
Mixture Ratio	1.25	6.71	2.86	1.70	3.03	5.15	2.55	3.09	2.09	3.31	3.05	3.07	5.60	2.23
Oxidizer DPinj (psi)	188	275	541	400	731	554	355	157	224	28	694	550	545	386
Fuel DPinj (psi)	717	35	366	849	536	116	245	103	284	9	484	342	94	395
Oxidizer Spec. Gravity @ Inj.	1.096	1.117	1.099	1.111	1.115	1.104	1.117	1.096	1.113	1.091	1.127	1.085	1.113	1.120
Fuel Spec. Gravity @ Inj.	0.814	0.813	0.814	0.811	0.815	0.814	0.809	0.808	0.815	0.813	0.813	0.811	0.815	0.813
Oxidizer Kw,j	6.09	6.00	5.67	5.89	6.06	6.36	5.61	6.19	5.95	4.77	6.36	6.09	6.50	5.66
Fuel Kw,j	2.90	2.94	2.80	2.79	2.73	3.14	3.12	2.88	2.96	2.94	2.94	2.91	3.27	2.95
Oxidizer Kw,t (S.G. @ FMO)	5.49	5.31	5.05	5.33	5.13	5.27	4.89	5.42	5.29	7.48	5.35	5.23	5.45	5.18
Fuel Kw,t (S.G. @ FMF)	2.51	0.92	2.41	2.42	2.31	2.65	2.63	2.51	2.53	2.94	2.52	2.38	2.67	2.57
Mean Summary Data Time (sec)	1.78	1.85	1.45	1.49	1.43	1.46	1.69	1.64	1.85	2.97	1.66	1.39	1.55	1.69
S.S. Combustion Duration (sec)	0.65	0.62	0.24	0.28	0.23	0.22	0.64	0.40	0.66	0.41	0.67	0.25	0.41	1.50
Cummulative S.S. Duration (sec)	1.82	2.44	2.68	0.28	0.51	0.73	0.64	1.04	1.70	2.11	2.78	3.03	3.44	4.94
Face Stagnation Pressure (psia)	1004	788	1410	1130	1706	1260	1208	791	953	249	1738	1467	1235	1174
Mean Throat Po (psia)	960	751	1285	1087	1596	1175	1134	746	896	231	1634	1349	1173	1123
Po Loss (psi)	44	37	125	43	110	85	74	45	57	18	104	118	62	51
ODE C* (ft/s)	4847	4910	5833	5640	5797	5222	5908	5728	5900	5576	5795	5774	5134	5936
C* Eta-kin. (curve fit +/- 0.4%)	0.9931	1.0000	1.0000	0.9950	1.0000	1.0000	0.9988	1.0000	0.9970	1.0000	1.0000	1.0000	1.0000	0.9974
Delivered C* (ft/s)	4624	4696	5299	4132	5161	4719	5470	5261	4962	5194	5318	5315	4852	5175
C* Efficiency	0.961	0.956	0.908	0.736	0.890	0.904	0.927	0.919	0.843	0.931	0.918	0.920	0.945	0.874
ODE ISP-vac. (sec)	211.72	213.91	254.24	245.75	253.02	227.55	257.79	249.64	255.89	241.98	252.23	250.97	223.07	257.11
ISP Eta-Kin.*Eta-Div.*Eta-B.L. (+/-0.4%)	0.9889	1.0000	0.9960	0.9909	0.9964	1.0000	0.9948	0.9978	0.9929	0.9995	0.9964	0.9969	1.0000	0.9933
Perfect Injector ISP (sec)	209.38	213.91	253.23	243.50	252.12	227.55	256.44	249.08	254.08	241.85	251.33	250.20	223.07	255.39
Pamb*Aexit (lbf)	536.84	537.94	547.31	538.89	537.32	540.79	525.49	528.06	535.15	535.33	541.63	543.64	547.52	545.59
Delivered Vacuum Thrust (lbf)	30918	24505	43775	36192	54365	40415	36501	24632	23419	7459	55008	47502	38600	38567
Delivered ISP-vac. (sec)	196.28	202.66	234.57	183.30	236.46	215.22	234.61	229.28	168.58	217.46	232.99	240.84	204.39	226.20
ISP-Based ERE	0.937	0.947	0.926	0.753	0.938	0.946	0.915	0.921	0.663	0.899	0.927	0.963	0.916	0.886
Notes:		FMF forced 21% S.S. LTCFV	Ograph Flows	Ograph Flows WOJ forced	Ograph Flows	Ograph Flows	Ograph FMF	Ograph Flows	WOJ forced	FMF forced Kw OK, Low Pc		Ograph FMO	Ograph FMO PC-4 bad	FMF-3 bad

Liner data consists of liner number and the throat and exit diameters measured before and after each test. These values are typically averages of 3 measured values.

The comment section includes pertinent comments about the test, including failure of key instruments, quality of performance data, and visual changes in the liner condition. The comments are frequently about the failure of the fuel flowmeter, that was caused by interference from the camera sequencer and was most prevalent at low fuel flow rates.

The calculated data includes propellant flow rates, injector and total system flow admittances (Kw's) and combustion efficiencies. Propellant flow rates were calculated using the reported equivalent water flow rates and the propellant specific gravities, which are function of both temperature and pressure. The pressures at the flowmeters were assumed to be equal to the tank pressure less 75 psi, which is estimated to be the line loss.

The pretest throat and exit diameters were used to calculate the throat area and the contraction and expansion ratios for performance calculations. The throat stagnation pressure is the average of the values computed using two techniques. The first technique utilizes the last static pressure measurement, the contraction ratio and an assumed ratio of specific heat of 1.135, to calculate an isentropic throat stagnation pressure. The second technique utilizes a correlation developed by J. Ito of Aerojet:

$$P_{o,throat} = Pc - 0.25*Pc/CR^{0.18}$$

where CR is the chamber contraction ratio and Pc is the chamber static pressure.

C* and ISP-based energy release (ERE) efficiencies were calculated as the ratio of the delivered to the perfect injector estimated values. In both cases, the perfect injector values were calculated using the TDK/BLM computer program TDK (Ref. 21) with kinetic, boundary layer and divergence losses from the one dimensional equilibrium (ODE) values accounted for.

The "delivered" C*'s were computed from the throat stagnation pressures, throat areas, and total propellant flow rates. The throat area used was the pretest measured value. Test-to-test throat diameter changes were small, less than 5% from first to last test for each of the three chamber liners used during the testing. The delivered vacuum ISP's were calculated using the measured thrust, propellant flow rates, nozzle exit area and ambient pressure.

Calculations using techniques different from that described above are noted at the bottom of Table 25. Most common of these notes is that one or both of the flow rates were taken from the graphical data. In a few cases where the fuel flowmeter was interfered with by the camera sequencer, the mean injection Kw was used to estimate a fuel flow rate, and thus mixture ratio. The injection and total Kw's values are fairly consistent between tests as can be seen in Figures 59 and 60. The fuel and oxygen injection Kw were found to be approximately 2.94 and 6.01, respectively. Good test-to-test correlation of the Kw's indicated that the measurements of propellant flow rates, and the resulting mixture ratio were consistent.

Figure 61 shows the PC and MR for each of the tests. The C* and ISP based efficiency values from tests that achieved sufficient steady-state duration to allow good measurements are plotted against mixture ratio on Figure 62. In most cases C* and ERE efficiencies agree within 1%, and greater agreement could be achieved by iterating on the throat diameter, rather than just using the pretest dimension, and by including a throat Cd term. Some of the scatter may also be due to lumping tests of markedly different chamber pressure into the same plot, although the influences of chamber pressure on the efficiencies were expected to be small.

The measured cavity temperature data is plotted as a function of mixture ratio in Figure 63. The temperature is the average value of the temperatures measured at three different locations in each test. The temperature data, including values that are still in transient in several tests, were scattered as can be seen from the figure. As a result, these data were not sufficient to provide reasonable accurate speed of sound estimates inside the cavities.

All tests were chug stable at the steady-state operating conditions. In tests 25, 28, and 38, chug instabilities with a small amplitude oscillation at 500 Hz occurred during the early portion of the transient start-up where chamber pressures were very low. These low frequency oscillations lasted approximately 15 to 40 msec and quickly disappeared as the chamber pressures rose to steady-state values. During the later part of the transient start-up periods, acoustic instabilities with higher amplitude and higher frequencies began to appear.

A summary of the stable-combustion test results is provided in Table 26 and a summary of the unstable-combustion test results is provided in Table 27. Both tables list test number, test series number (corresponding to Table 25) inferring a particular cavity configuration used, chamber and manifold pressures, propellant flow rates, and injected mixture

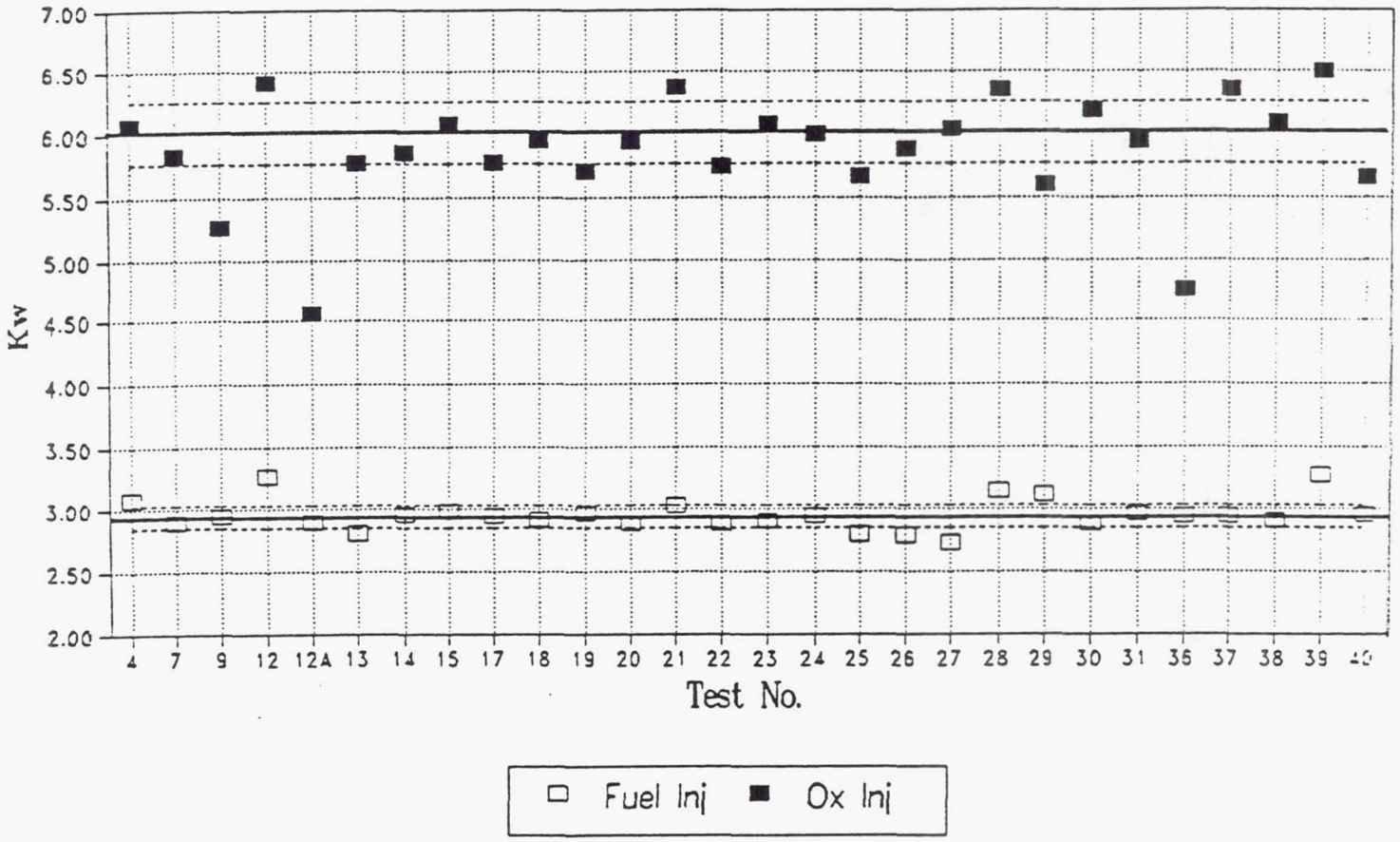

Figure 59. Measured Injector Kw Values Were Consistent Between Tests

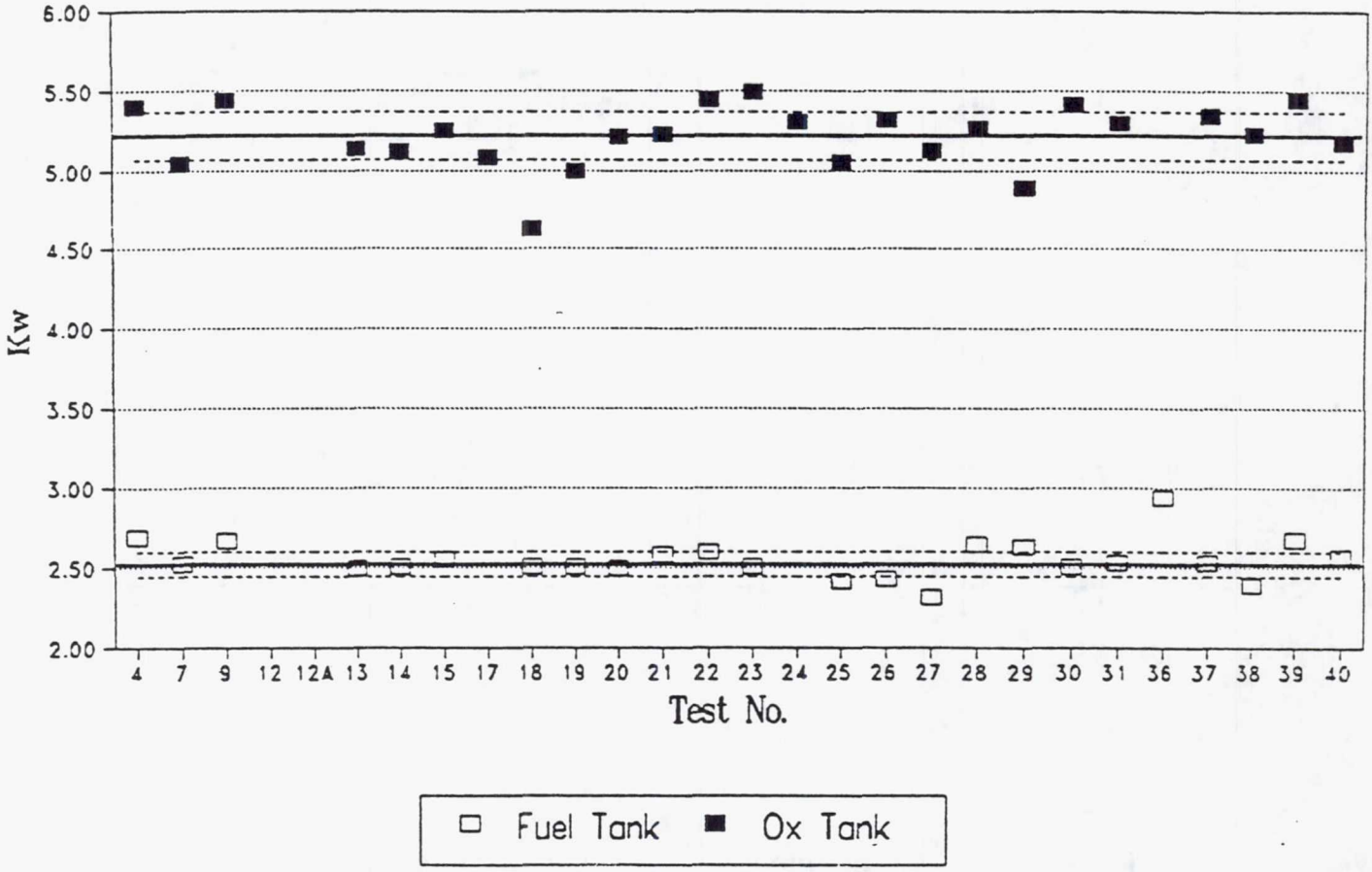

Figure 60. Total Kw Values Were Consistent Between Tests

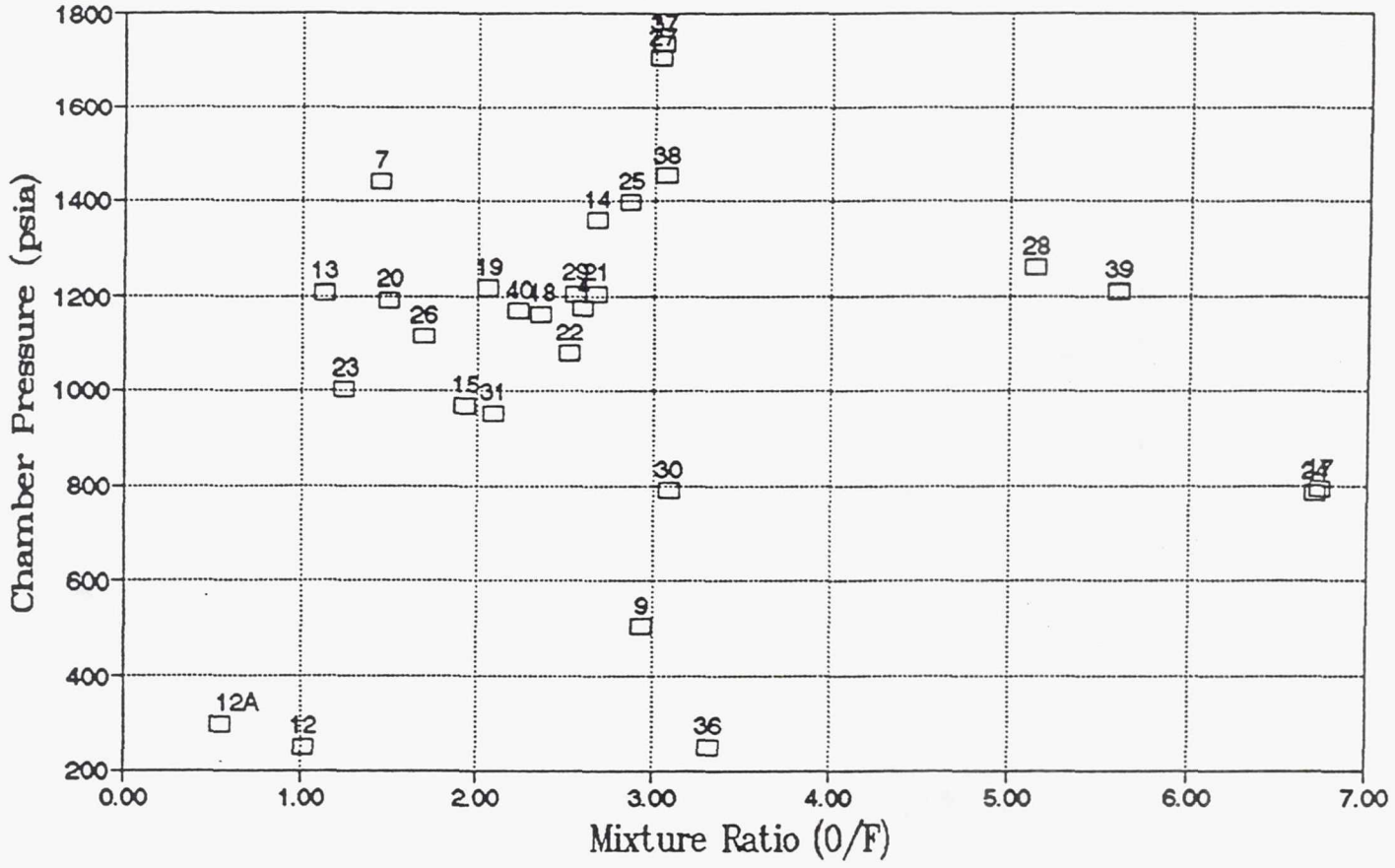

Figure 61. Test Operating Conditions

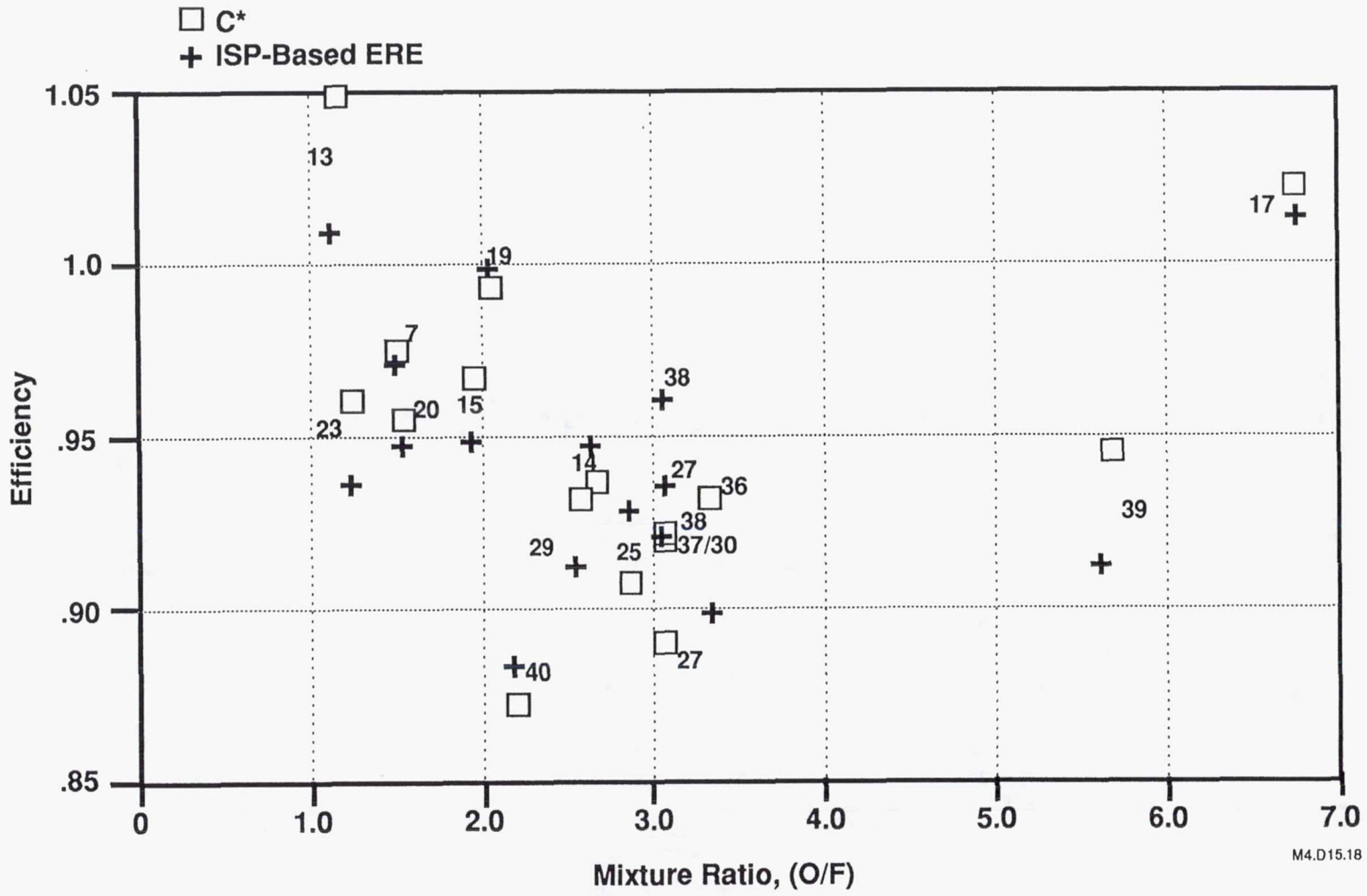

Figure 62. Calculated Performance Efficiency for Tests With Valid Steady-State Measurements

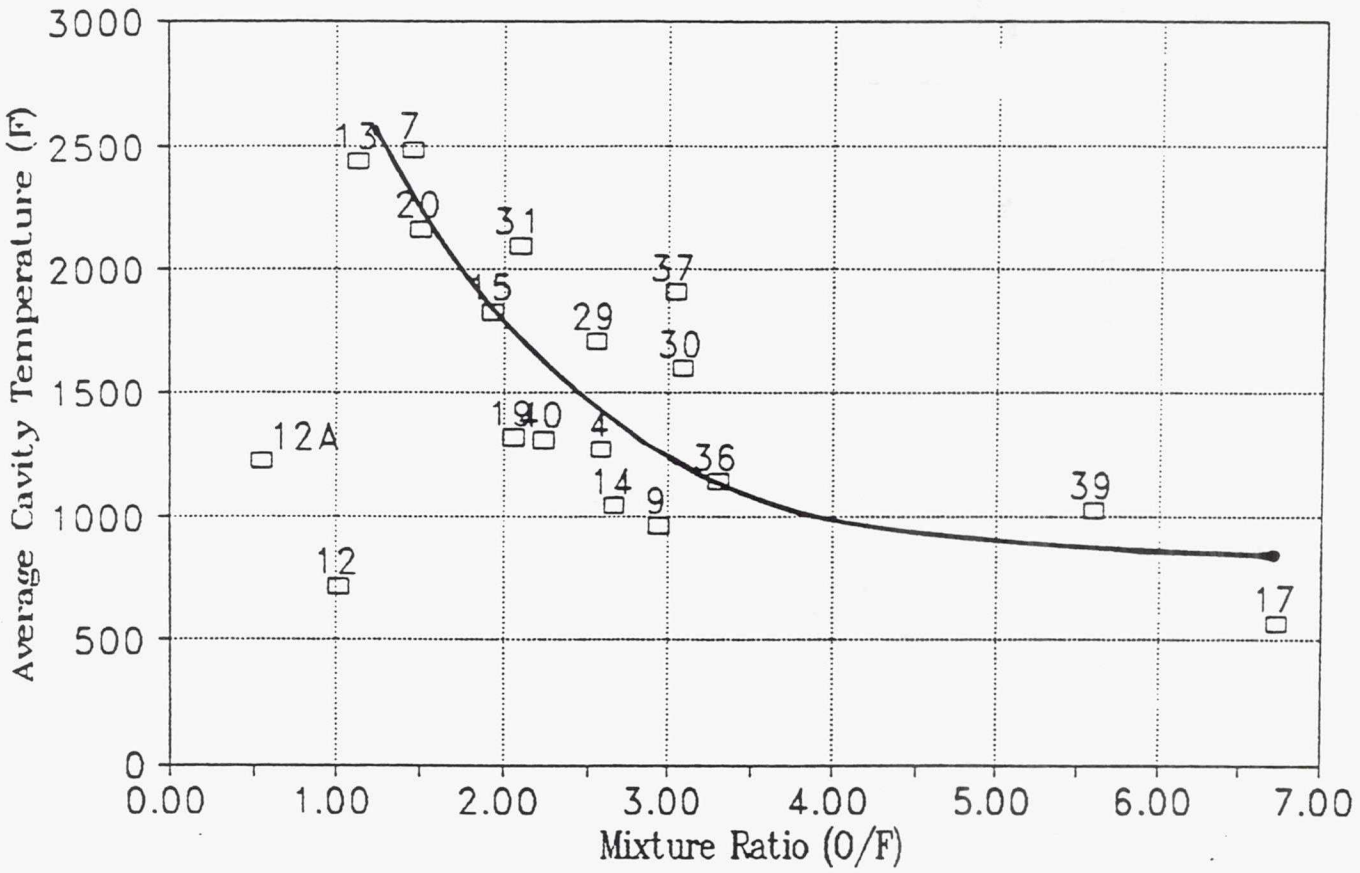

Figure 63. Average Acoustic Cavity Gas Temperature Measurements

TABLE 26. SUMMARY OF STABLE-COMBUSTION TEST RESULTS

15-Oct-91

Test No.	7	9	12	12A	13	15	17	20	23	24	31	36
Test Series	1	1	1	1	1	1	1	1	2	2	3	3
Chamber Pressure (psia)	1441	505	250	297	1210	969	792	1193	1004	788	951	249
RP-1 Manifold Pressure (psia)	2449	542	316	590	2385	1221	826	1903	1721	823	1237	258
Oxygen Manifold Pressure (psia)	1821	578	263	323	1468	1135	1061	1470	1192	1063	1177	277
RP-1 Flow Rate (lbm/s)	82.5	16.1	23.9	44.7	86.8	42.7	14.7	69.2	70.1	15.7	45.0	8.0
Oxygen Flow Rate (lbm/s)	120.0	47.3	24.2	24.3	98.0	82.4	99.2	104.1	87.4	105.2	93.9	26.4
Mixture Ratio	1.45	2.94	1.01	0.54	1.13	1.93	6.74	1.50	1.25	6.71	2.09	3.31
RP-1 Injection Delta-P (psid)	1008	37	66	293	1175	252	34	710	717	35	286	9
Oxygen Injection Delta-P (psid)	380	73	13	26	258	166	269	277	188	275	226	28
C*Efficiency	0.975	0.994	0.863	0.821	1.049	0.968	1.025	0.955	0.961	0.956	0.843	0.931
Isp Based ERE	0.972	0.987	0.792	0.781	1.010	0.951	1.015	0.948	0.937	0.947	0.663	0.899
Kistler No.	1	1	n/a	n/a	3	1	3	3	4	1.2	1.5	1
Bomb Overpressure (psid)	75	n/a	n/a	n/a	n/a	117	530	93	111	42	96	n/a
Post Bomb Frequency (Hz)	8500	n/a	n/a	n/a	3000	n/a	1867	2400	n/a	2250	n/a	n/a
Bomb Damp Time (msec)	<2	n/a	n/a	n/a	n/a	2	6	3	<2	<5	3	n/a
Decay coefficient (1/s)	n/a	n/a	n/a	n/a	n/a	n/a	-38	-666	n/a	-73	n/a	n/a

TABLE 27. SUMMARY OF UN STABLE-COMBUSTION TEST RESULTS

8-Oct-91

Test No.	4	14	18	19	21	22	25	26	27	28	29	30	37	38	39	40
Test Series	1	1	1	1	2	2	2	2	2	2	3	3	3	3	3	3
Chamber Pressure (psia)	1177	1358	1165	1220	1208	1079	1397	1118	1706	1260	1208	791	1735	1456	1213	1172
RP-1 Manifold Pressure (psia)	1479	1804	1433	1554	1467	1461	1776	1979	2242	1376	1453	894	2222	1809	1329	1569
Oxygen Manifold Pressure (psia)	1559	1918	1430	1503	1538	1610	1951	1530	2437	1814	1563	948	2432	2017	1780	1560
RP-1 Flow Rate (lbm/s)	48.2	49.2	43.0	48.8	42.7	49.8	48.3	73.2	57.0	30.5	43.9	26.3	58.3	48.4	28.6	52.8
Oxygen Flow Rate (lbm/s)	124.7	131.3	101/1	100.3	114.1	137.2	138.3	124.2	172.9	157.3	111.7	81.2	177.8	148.8	160.2	117.7
Mixture Ratio	2.59	2.67	2.35	2.06	2.67	2.75	2.86	1.70	3.03	5.15	2.55	3.09	3.05	3.07	5.60	2.23
RP-1 Injection Delta-P (psid)	302	446	268	334	259	382	379	861	536	116	245	103	487	353	116	397
Oxygen Injection Delta-P (psid)	382	560	265	283	330	531	554	412	731	554	355	157	697	561	567	388
C*Efficiency	0.801	0.932	0.978	0.994	0.934	0.836	0.908	0.736	0.890	0.904	0.927	0.919	0.918	0.920	0.945	0.874
Isp Based ERE	0.842	0.948	0.977	1.000	0.928	0.924	0.926	0.753	0.938	0.946	0.915	0.921	0.927	0.963	0.916	0.886
Kistler No.	1	1	1	1	1	1	2	1	1	1	1	1	1	1	1	5
1st Resonance Frequency (Hz)	3303	3303	3185	3185	3362	3303	3244	3126	3274	3126	3155	2949	3008	3185	2065	2772
1st Resonance Pk-to-Pk Amplitude (psid)	1205	1149	670	812	2569	2410	812	2569	1922	514	1149	363	115	1817	445	57
1st Resonance Growth Coefficient (1/s)	153	38	67	37	84	37	128	220	114	n/a	56	29	n/a	55	37	94
2nd Resonance Frequency (Hz)	6548	6548	6489	6548	6784	6725	6607	6282	6725	6400	6430	5781	4424	6430	n/a	5250
2nd Resonance Pk-to-Pk Amplitude (psid)	629	430	244	281	1990	1780	500	1817	629	574	514	57	103	574	n/a	445
2nd Resonance Growth Coefficient (1/s)	n/a	n/a	n/a	48	n/a	47	129	86	n/a	n/a	n/a	n/a	n/a	n/a	n/a	67
3rd Resonance Frequency (Hz)	9880	9910	9733	9733	10205	10087	9969	9556	9379	9497	9556	8700	n/a	9703	n/a	10500
3rd Resonance Pk-to-Pk Amplitude (psid)	727	281	230	345	1028	1359	70	961	514	430	514	63	n/a	381	n/a	325
34d Resonance Growth Coefficient (1/s)	n/a	n/a	n/a	28	n/a	52	83	15	n/a	n/a	n/a	n/a	n/a	n/a	n/a	n/a

ratio. In addition, both tables list the high-frequency pressure transducer number from which the presented stability data was obtained. The propellant injection pressure drops, calculated from the measured manifold and chamber pressures, are also listed in the tables. In addition to the operating parameters, the stable-combustion table (Table 26) lists the bomb over-pressure, damp time, and decay (or negative growth) coefficient. These values were obtained or calculated from the pressure oscillograms. In addition to the operating parameters, the unstable-combustion table (Table 27) lists the observed resonant frequencies, growth coefficients, and amplitudes of the chamber pressure oscillations. These values were obtained from plots showing the evolutions of amplitudes and frequencies and from the power spectral analyses of the chamber pressures.

All combustion instabilities were spontaneous. Although combustion perturbation bombs were used and generated over-pressures in the range of approximately 5 to 67% of the mean chamber pressure, no tests were driven unstable by the bombs. Power spectral density (PSD) analyses of chamber pressures in all unstable combustion tests showed several resonant frequencies existing simultaneously. The first resonant frequencies in most of the unstable combustion tests correspond to the 1T acoustic frequency of the combustion chamber, which is approximately 3300 Hz. Other resonant frequencies appeared to be the harmonics of the 1T mode although they may correspond to the frequencies of higher mixed mode. The resonant frequency in test number 40 observed during the early portion of steady-state operation closely matches the 2T acoustic resonant frequency of the chamber.

Comparison of the chamber pressure oscillation amplitudes between the test series (Table 26) shows stabilizing effects of the acoustic cavities. The amplitudes and growth coefficients of the chamber pressure oscillations were generally larger in test series 2 (blocked cavities) than those in the other test series (with monotuned or bituned acoustic cavities). This indicated that the bituned and monotuned cavity configurations did provide damping to the system, although it was not adequate to completely suppress the instabilities. The fact that most of the combustion instabilities were in a first tangential mode even in test configurations with monotuned and bituned acoustic cavities suggested that the acoustic cavities might not be tuned correctly for the 1T mode. Examination of the test hardware drawings revealed that the cavity configurations were different from those intended (see Figure 54). The cavity depths were too shallow to be optimally effective for the 1T mode. Calculation using the HIFI module in ROCCID showed that the effects of the as tested cavity configurations on the 1T chamber responses were indeed small (see Figure 64).

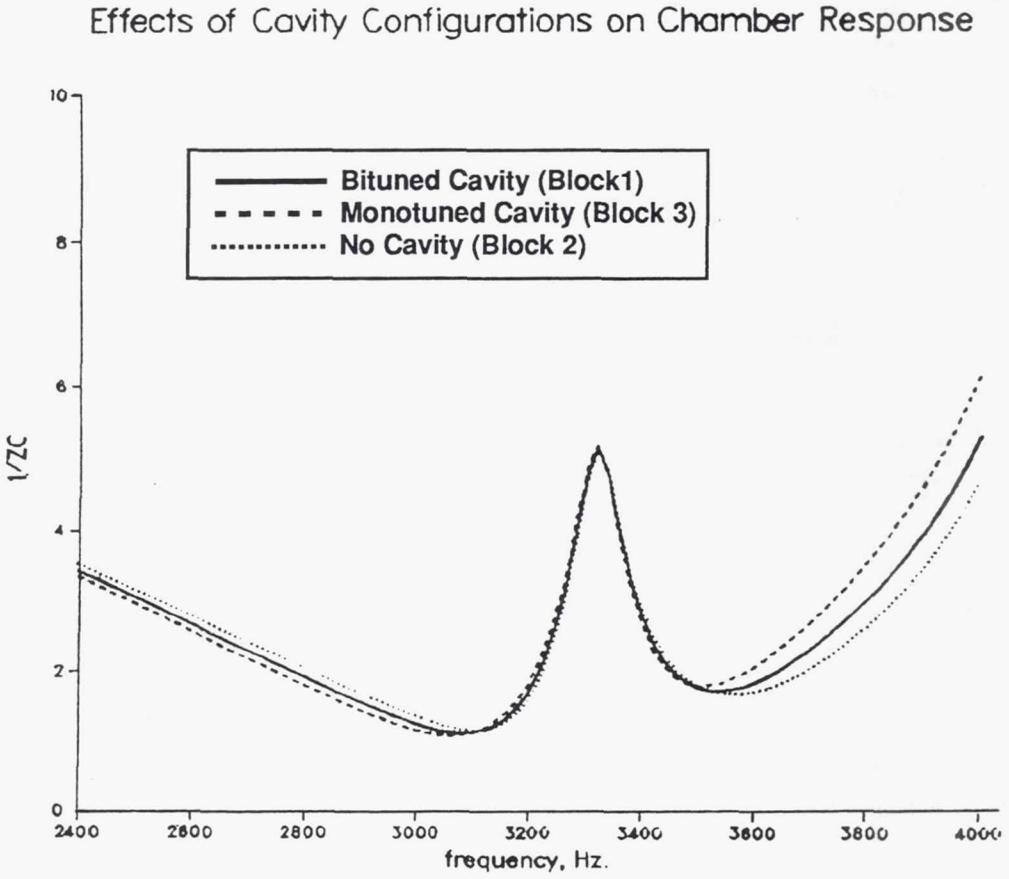

Figure 64. Calculations Show Little Effect of Actual Cavity

Figure 65 is a time series showing the oscillation component of the chamber pressure measured in a typical unstable-combustion test. The figure shows the exponential growth of the amplitude typical in a linear instability. The evolutions of the amplitude and frequency of the chamber pressure are shown in Figure 66. The power spectral density (PSD) plot, obtained for the 30 msec period during which the amplitude of the oscillations shown in the time series appear to be steady, is shown in Figure 67. The PSD plot in Figure 67 shows that the dominant frequencies were approximately 3303, 6548, and 9880 Hz. The 3303 Hz corresponds to the natural frequency of the first tangential (1T) acoustic mode of the chamber. The 6548 and 9880 Hz frequencies appeared to be the harmonics of the 1T resonant frequency although they may correspond to the natural frequencies of some higher mixed modes. Positive identification of higher mixed modes is difficult because differences in frequency values between one higher mixed mode and the next are small.

Comparison between the measurements of chamber pressure, RP-1 and oxygen manifold pressures, and accelerations shows that the high-frequency pressure transducers in the propellant manifolds and the accelerometers mounted on the outside of the combustion chamber did detect instabilities and accurately provided the values of the resonant frequencies. These instruments were demonstrated to be well-suited in supplementing the high-frequency pressure transducers in the combustion chamber in combustion stability testing.

The results shown in Figures 65 through 67 are approximately typical of all other unstable-combustion tests. A complete set of time series, amplitude and frequency evolution, and power spectral analysis of chamber pressure for all unstable tests is provided in Volume II of this report.

Waterfall plots of the chamber pressures showed that instabilities began with a 1T mode during transient start-up in tests 14, 18, 19, and 27. Approximately at the end of this start-up period a 2T mode popped up then disappeared immediately thereafter. The 2T frequency is more pronounced in the PSD plots of the chamber pressures. The waterfall and PSD plots for test 14 are shown in Figures 68 and 69 as an example. The mean chamber pressure began decaying also at this time indicating the test was being shutdown. It is speculated that if the test shutdown had been delayed a little later, the instability would have switched to the 2T

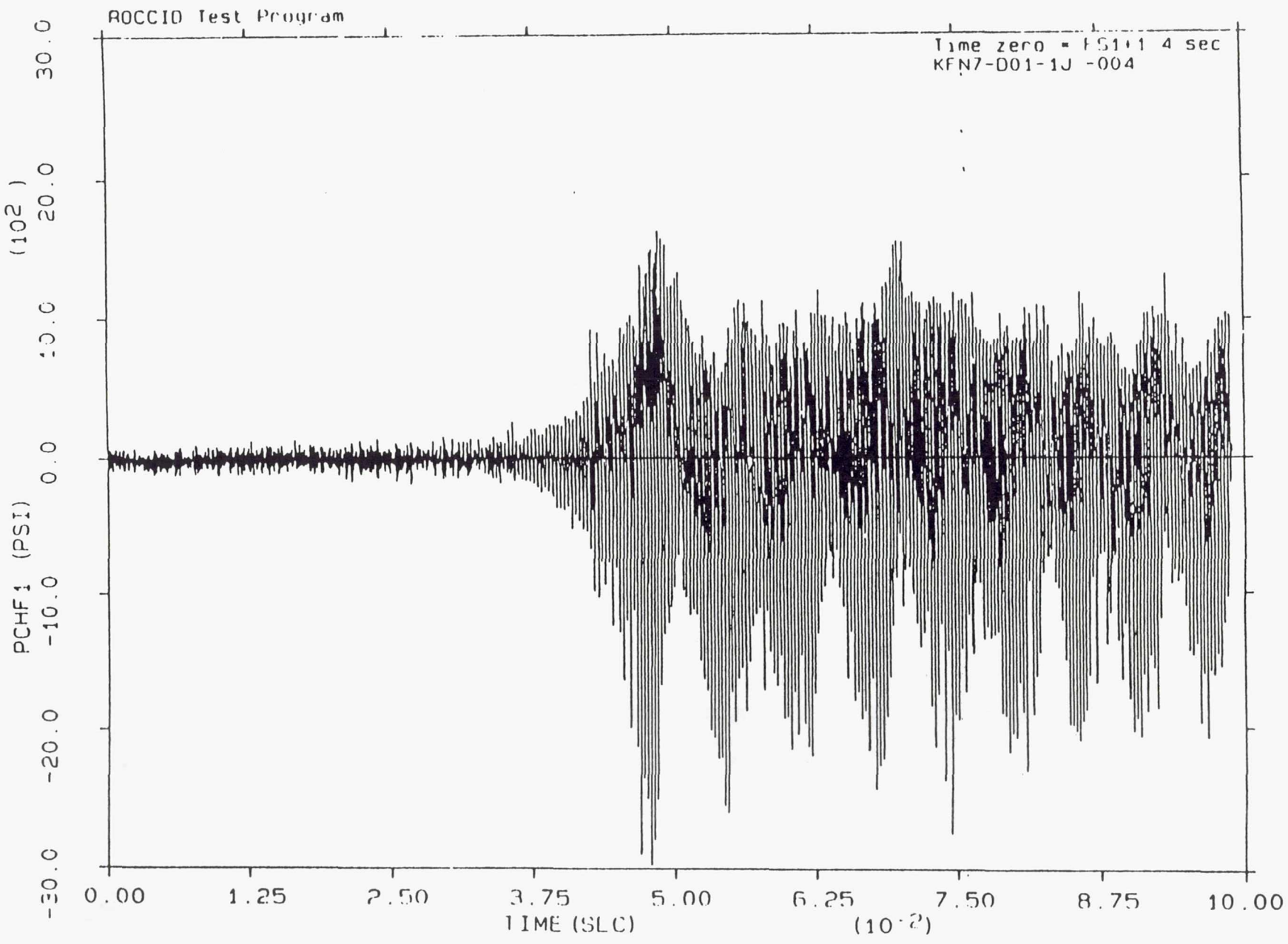

Figure 65. Oscillation Component of Chamber Pressure Measured by PCHF1

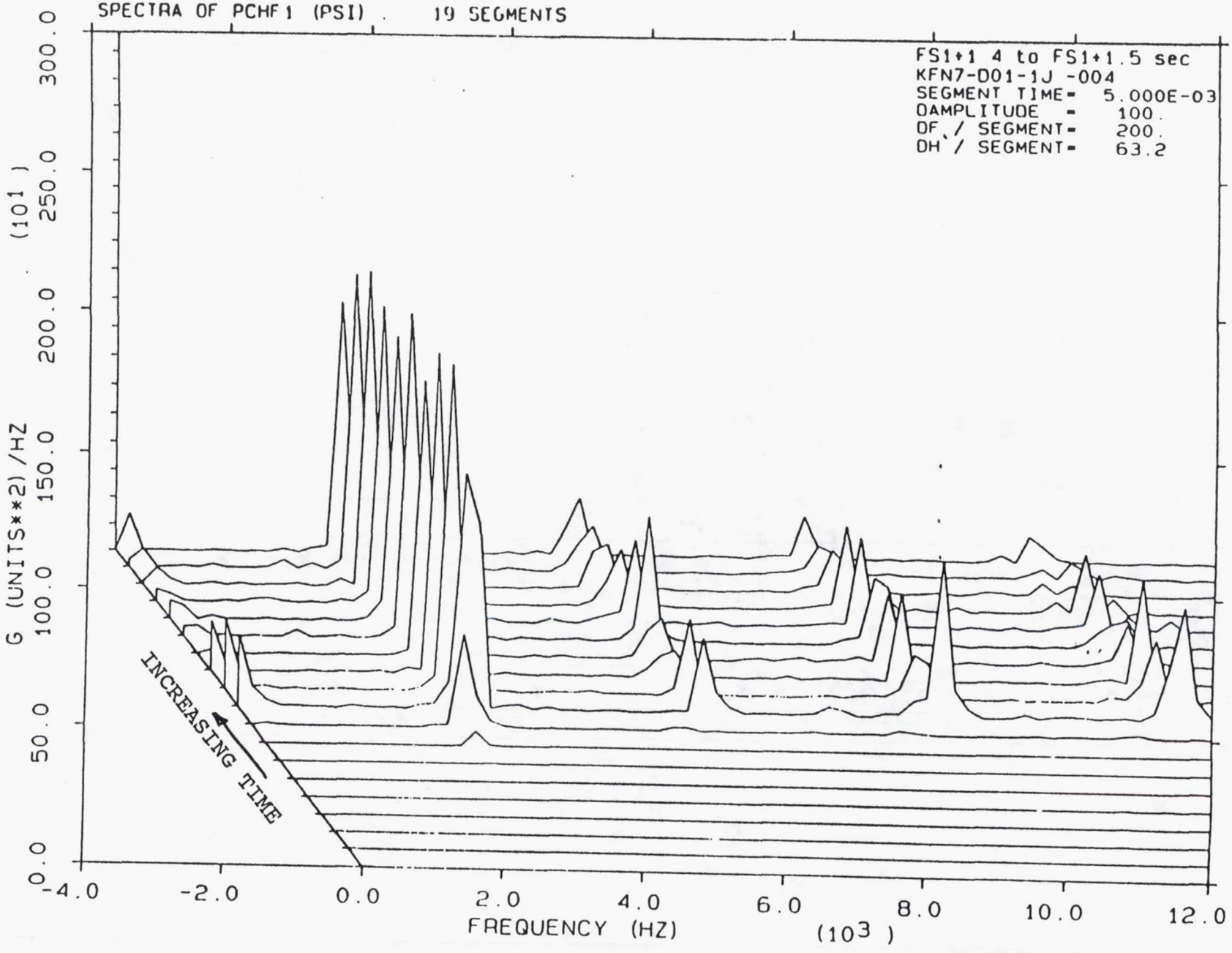

Figure 66. Evolution of the Amplitude and Frequency of PCHF1 Measured Chamber Pressure

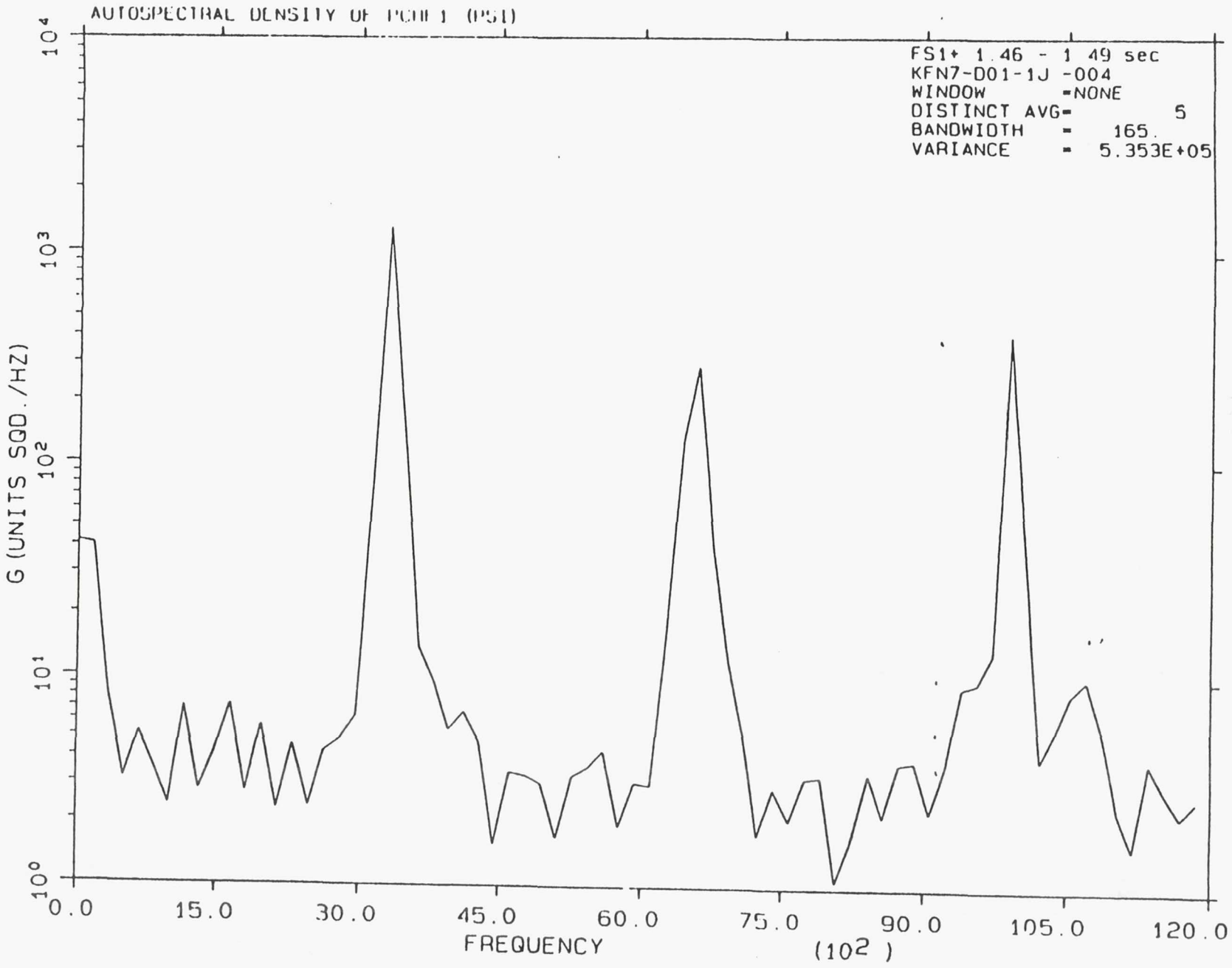

Figure 67. Power Spectral Density Analysis of PCHF1 Measured Chamber Pressure

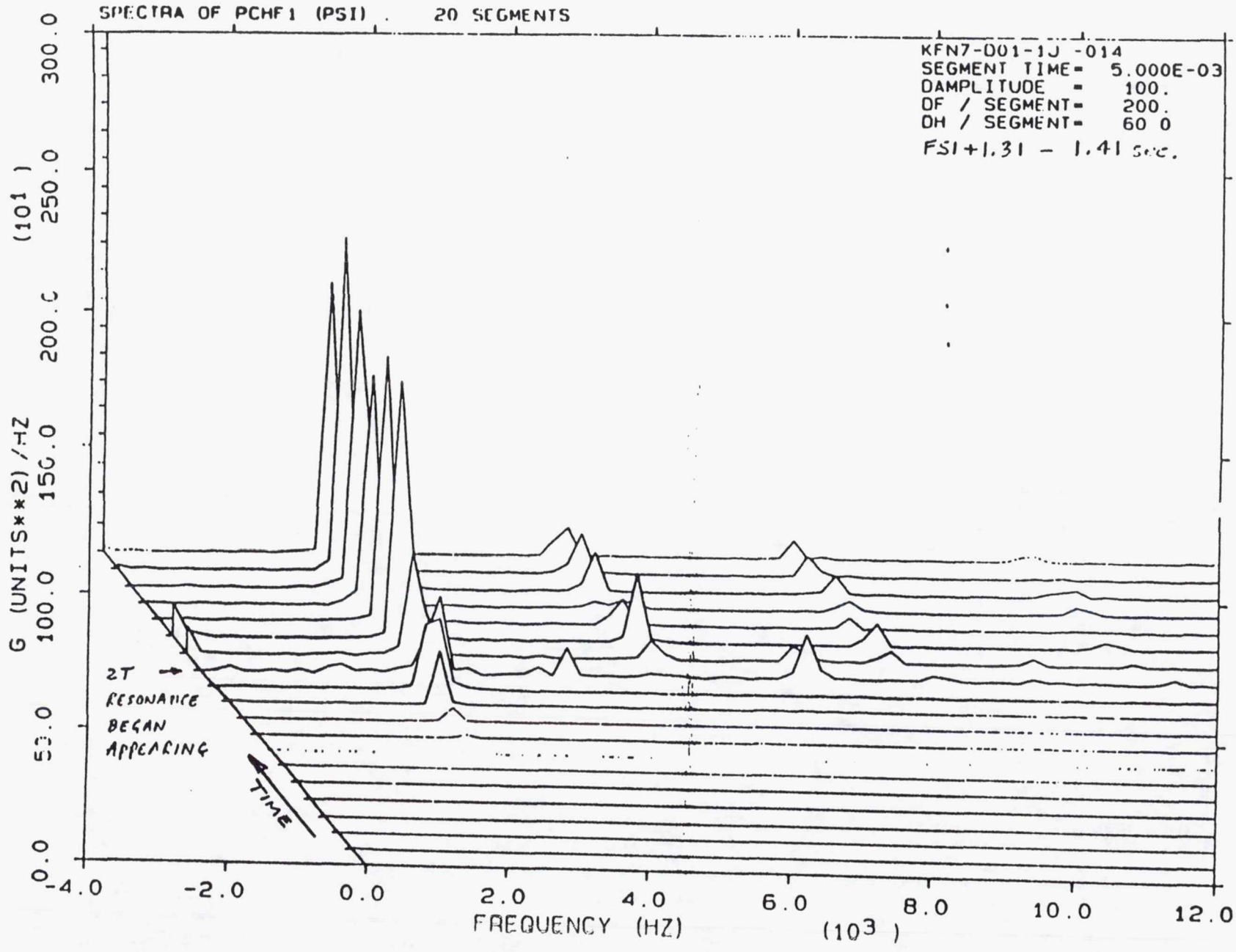

Figure 68. Waterfall Plot Shows a Resonance at 2T Frequency Appeared and Then Disappear Quickly

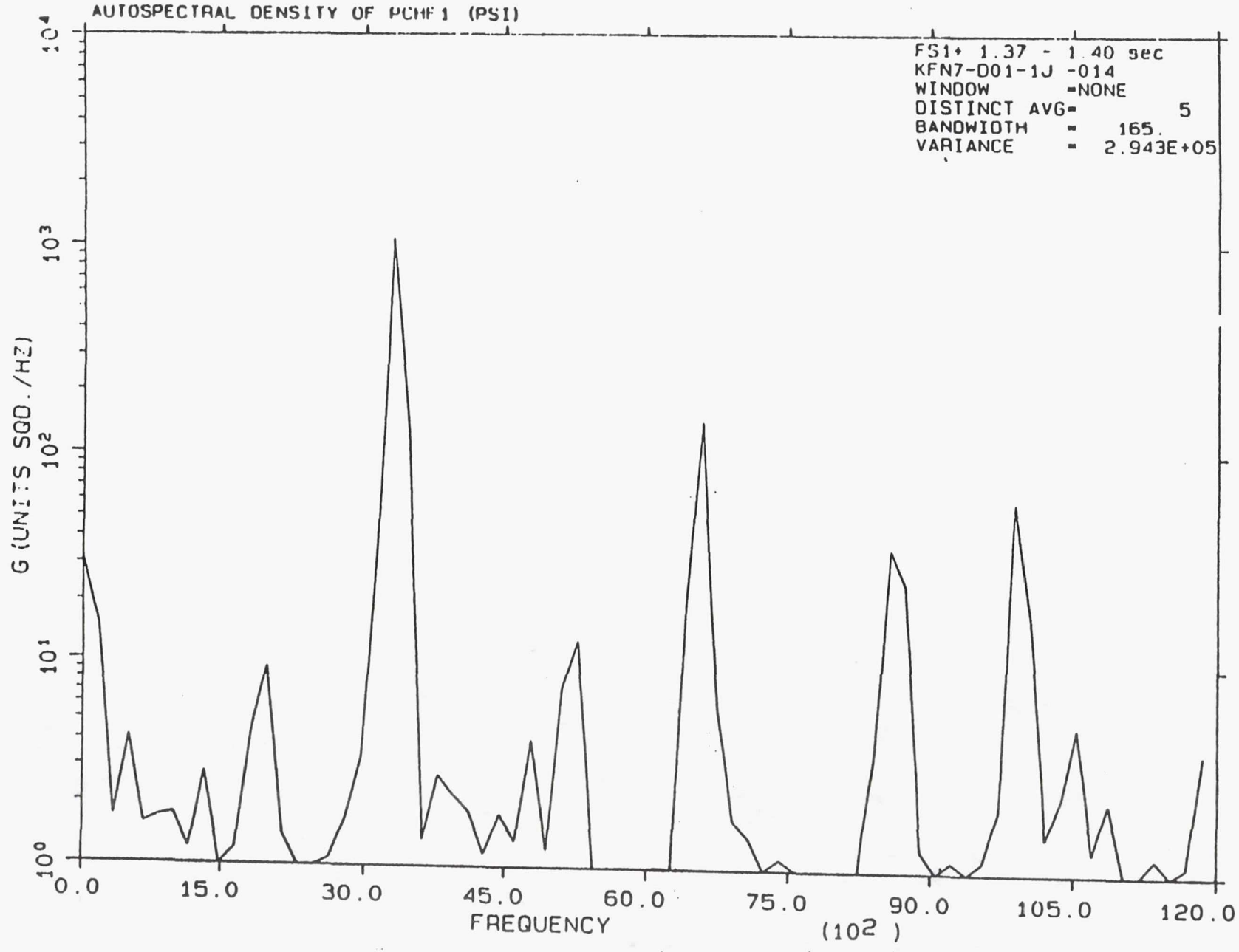

Figure 69. Power Spectral Density Analysis of Chamber Pressure Show the Existence of a 2T Resonance

mode similar to the test 40 discussed later. It should be mentioned that all spontaneous unstable-combustion tests were shutdown by the combustion stability monitor (CSM) immediately after an instability was detected in order to preclude damage to the hardware.

In test 17, the combustion was stable at the steady-state operating conditions. A large amplitude of approximately 600 psid peak-to-peak at the 1L frequency of approximately 1300 Hz, however, was seen during early start-up transient period. Figures 70 and 71 show the time series and PSD plots of the chamber pressure during that time.

In test 21, the combustion was stable during start-up transient and approximately 500 msec of steady-state operation but became unstable during shutdown transient immediately after the test termination signal (FS-2). The instability began with a 2T mode then immediately switched to a 1T mode as shown in the waterfall plot of PCHF1 (Figure 72). The PSD plot obtained for the period of time at the beginning of the instability clearly indicated the 2T frequency as shown in Figure 73. The PSD plot for a later period of time is similar to those from all other tests where combustion instabilities initiated during transient start-ups. It should be mentioned here that the injection temperature of oxygen was approximately 35 degrees higher in this test than those in all other tests. The warmer injection temperature of the oxygen appeared to have a stabilizing effect on the combustion.

In test 29, the chamber pressure oscillated with a small amplitude (with no apparent growth in amplitude) during a steady-state period of approximately 0.3 sec and then suddenly the amplitude grew larger.

In test 37, only PCHF1 indicated chamber pressure oscillation of small amplitude while all other transducers including the accelerometers were dubiously quiet. In this test, a large pressure spike that occurred during transient operation might have rendered a few or all of the high-frequency pressure transducers - and also the accelerometers although unlikely - inoperative or distorted. The oscillation measured by PCHF1 consisted of two major sinusoidal components whose peak-to-peak amplitudes and frequencies were approximately 115 psid at 3008 Hz and 103 psid at 4424 Hz. The individual amplitude of each component is less than 10 percent of the mean chamber pressure. The 10 percent value is the threshold above which engine operation is considered unstable as defined by CPIA publication 247. Therefore, this test appeared to exhibit marginal combustion stability.

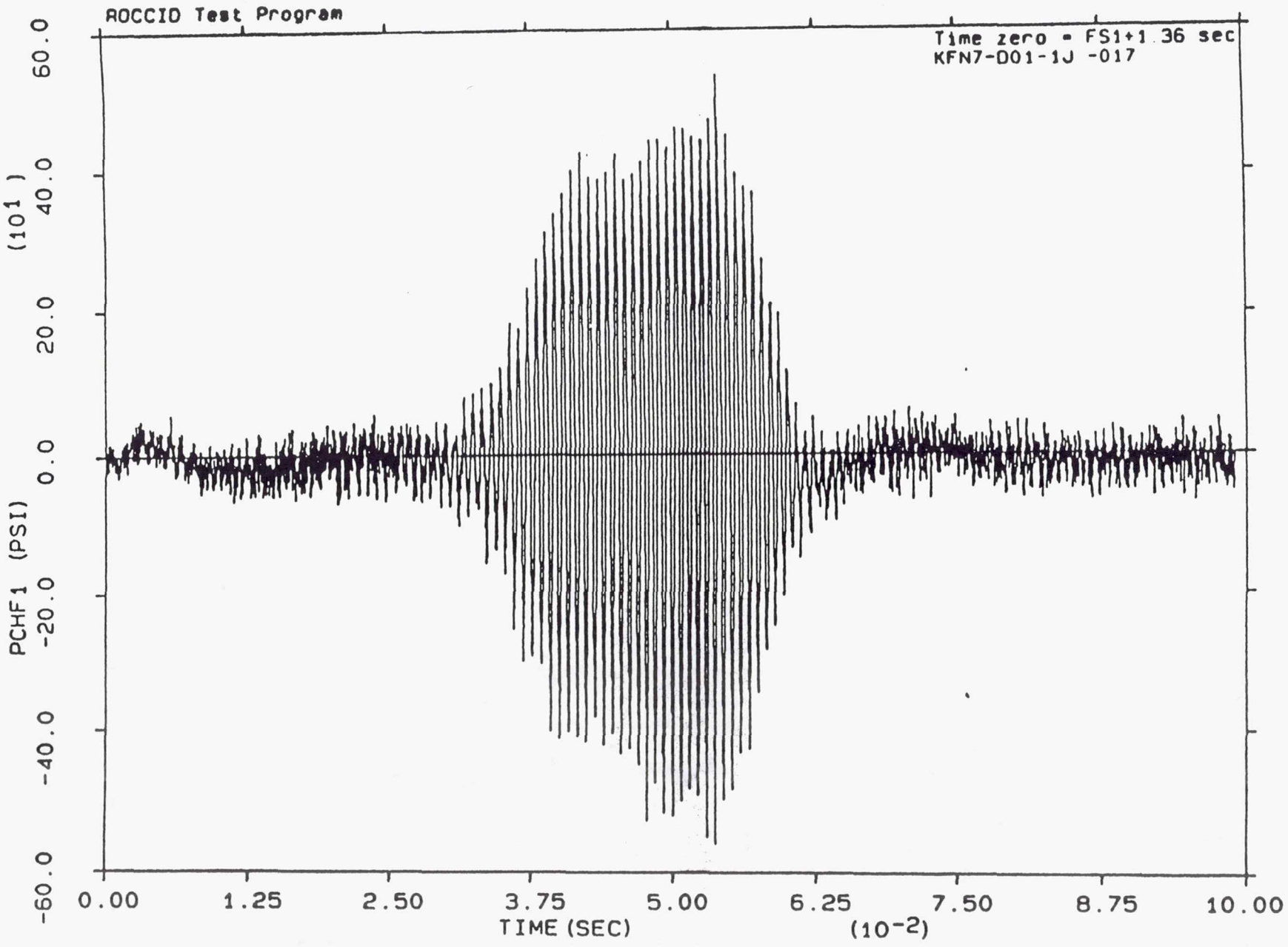

Figure 70. Chamber Pressure Oscillation With 1L Mode During Transient Start-Up of Test 17

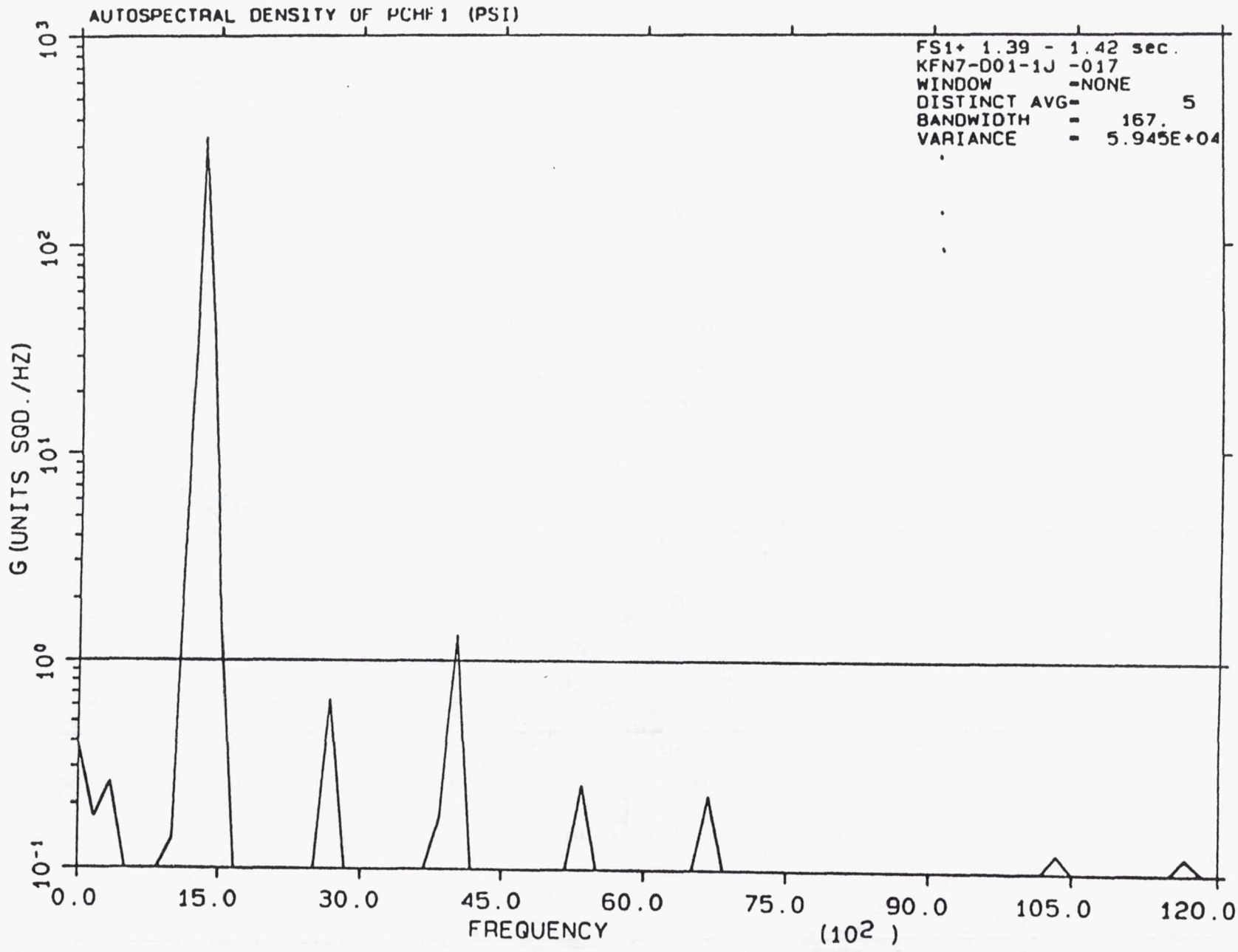

Figure 71. Power Spectral Density Analysis of Chamber Pressure During Transient Start-Up of Test 17 Showed 1L Resonant Frequency of Approximately 1300 Hz

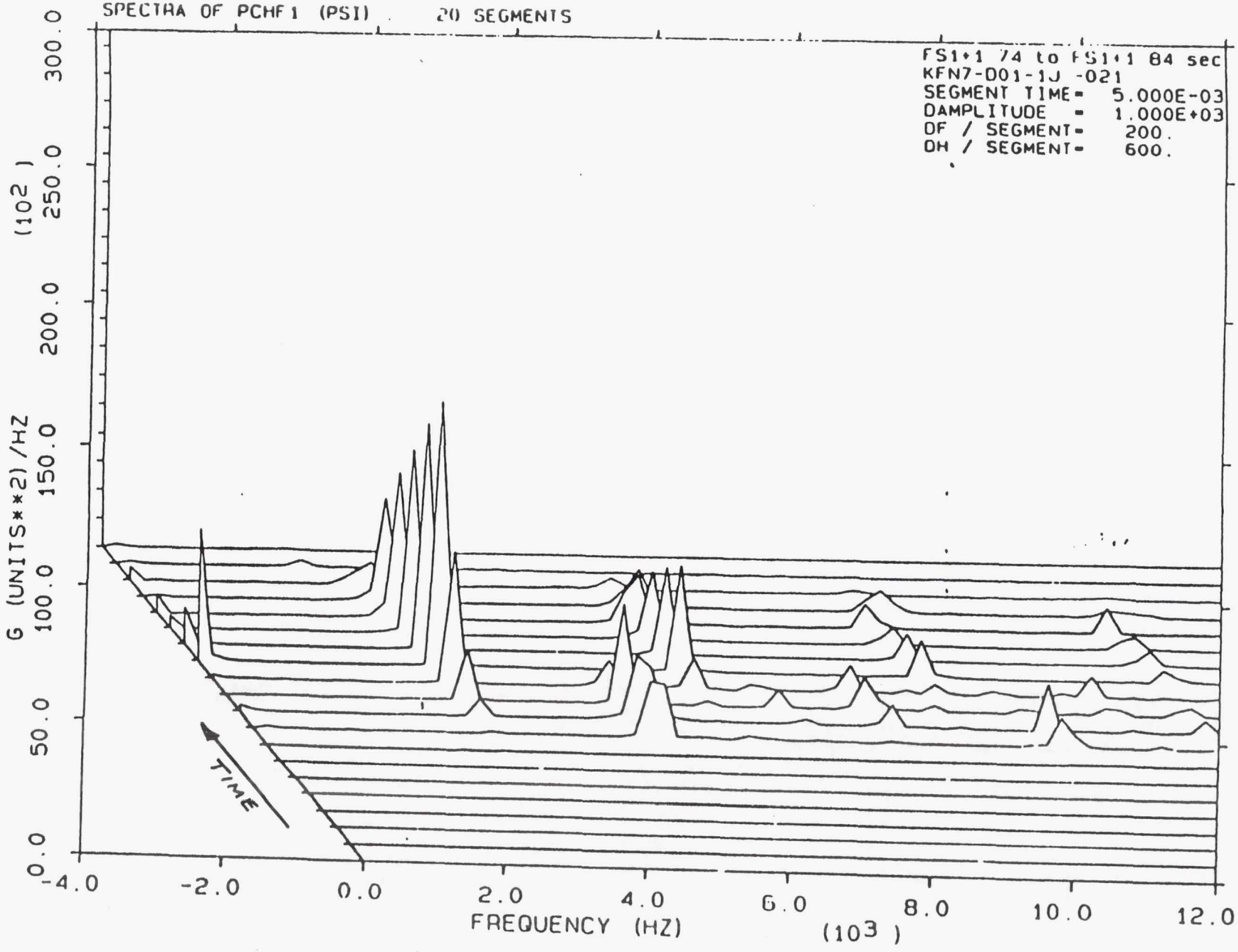

Figure 72. Evolution of the Amplitude and Frequency of Chamber Pressure in Test 21 Shows an Instability Began With a 2T Resonance Then Switched to a 1T Resonance

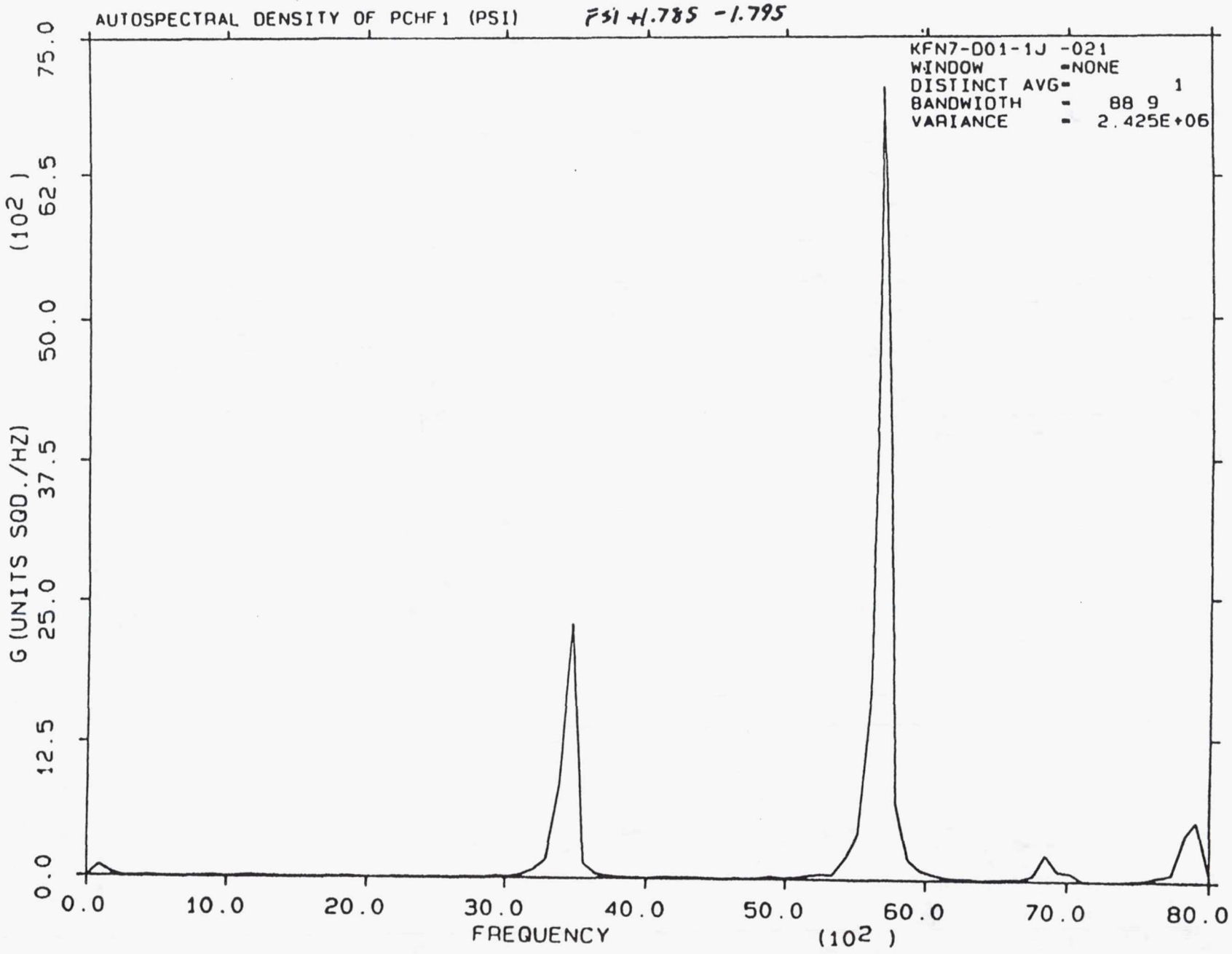

Figure 73. Power Spectral Analysis for the Early Part of Instability Indicated 2T Resonance

In test 39, the lowest resonant frequency was 2065 Hz which is significantly lower than the value of 3303 Hz commonly seen in other unstable-combustion tests. Since this frequency is not near any expected resonant mode its source is unexplained.

Test 40 is unique in that combustion instability lasted for approximately 600 msec without the test being shutdown by the CSM. The CSM did not shutdown the test because the chamber pressure transducer that provides instability information to the CSM was inoperative. In fact, all chamber pressure high-frequency transducers except PCHF1 had been damaged during this test or during earlier tests. The long duration instability in this test provided valuable data that would not be known from other tests. Figure 74 is a waterfall plot of the chamber pressure measured by PCHF1 for the entire period from the beginning of the mean chamber pressure rise to the shutdown time. A higher resolution waterfall plot for only the start-up transient period shown in Figure 75. Figure 76 shows the mean chamber pressure versus time from FS-1 for the purpose of correlating the combustion instability events shown in Figures 74 and 75 with the mean chamber pressure. Figure 74 shows that the instability began with a 1T mode at FS1+1.42 seconds which is during the transient start-up period (see Figure 76), and then switched to a 2T mode at FS1+1.45, a time that corresponds to the end of the transient start-up and the beginning of steady-state operation. The PSD analysis of PCHF1 obtained for this time period is shown in Figure 77. The figure clearly shows the dominant 2T frequency of approximately 5220 Hz. Figure 74 shows that the instability switched back to the 1T mode at FS1+1.70 sec, which is in the middle of the steady-state operation, as noted in Figure 76. At this time, the operating parameters such as chamber pressure and propellant flow rates were steady. The cavity sound speed, however, may still have been in transient as indicated by the time series of the cavity gas temperatures shown in Figure 76.

The fact that the instability mode switched from 1T to 2T at the beginning of the steady-state operation is worthwhile to emphasize. Had the test been shutdown by the CSM before achieving steady-state operation like many other tests, the instability in the 2T mode would not have been observed. More importantly, it points out the possibility that the 2T mode might have occurred in several other unstable-combustion tests if they had not been shutdown so quickly by the CSM. This is further supported by the data from test 21 where an instability was initiated during steady-state operation where it began with a 2T mode. A mean chamber pressure vs time plot for test 19, which is typical of unstable-combustion tests where the test shutdowns were initiated

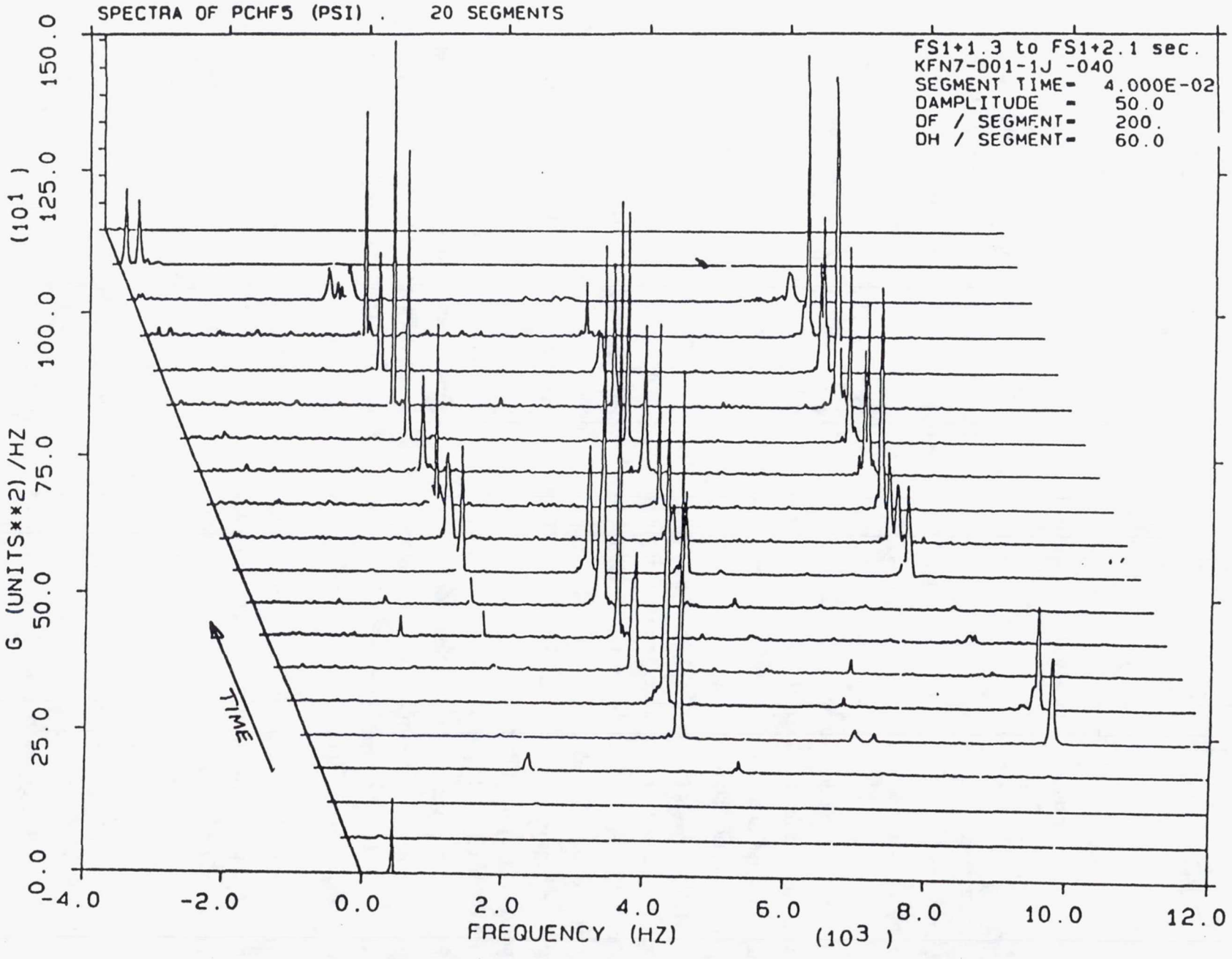

Figure 74. Evolution of the Amplitude and Frequency of Chamber Pressure in Test 40 Shows the Instability Began With a 1T Mode, Switched to a 2T Mode, Then Switched Back to the 1T Mode

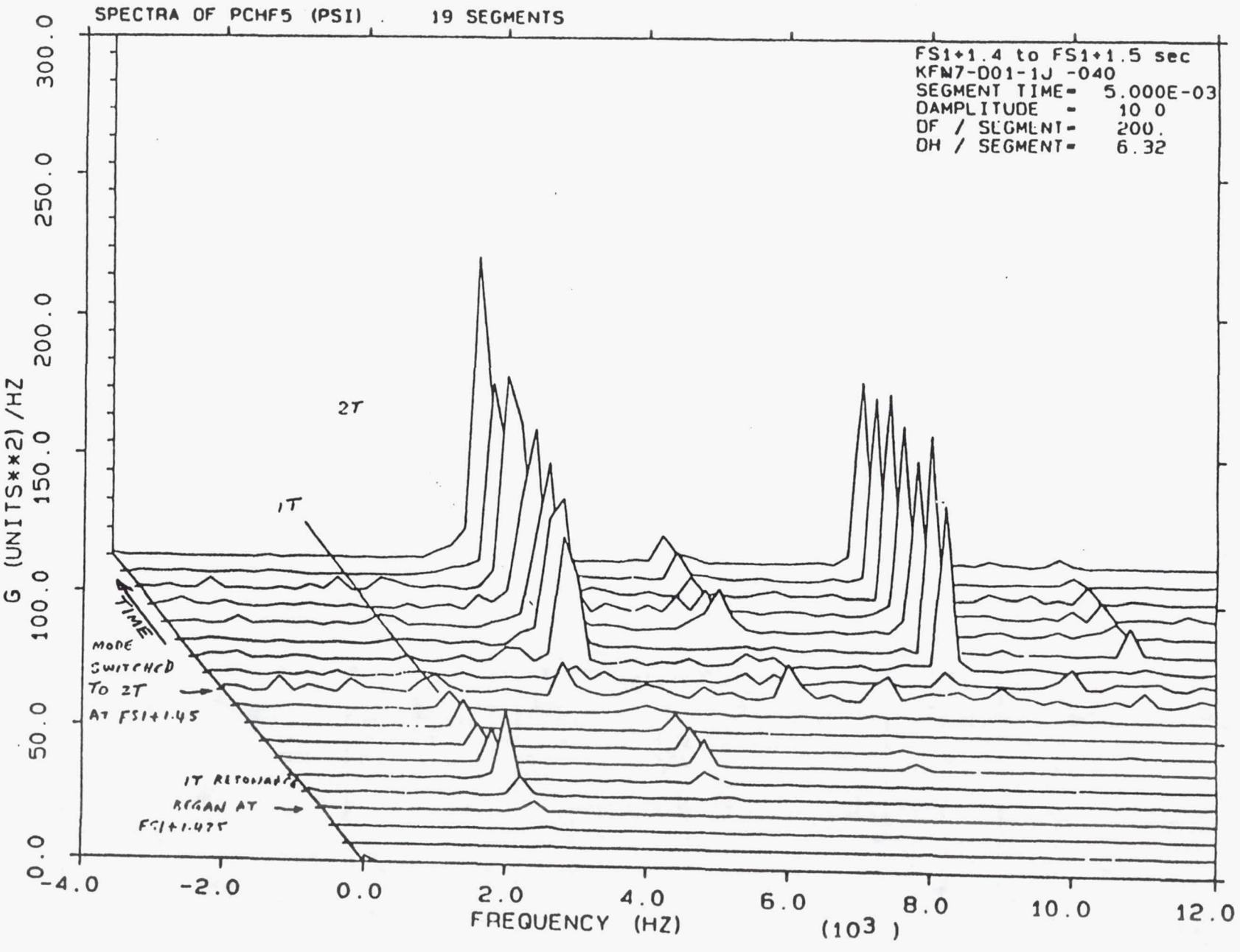

Figure 75. Higher Resolution Plot of the Evolution of the Amplitude and Frequency of Chamber Pressure in Test 40

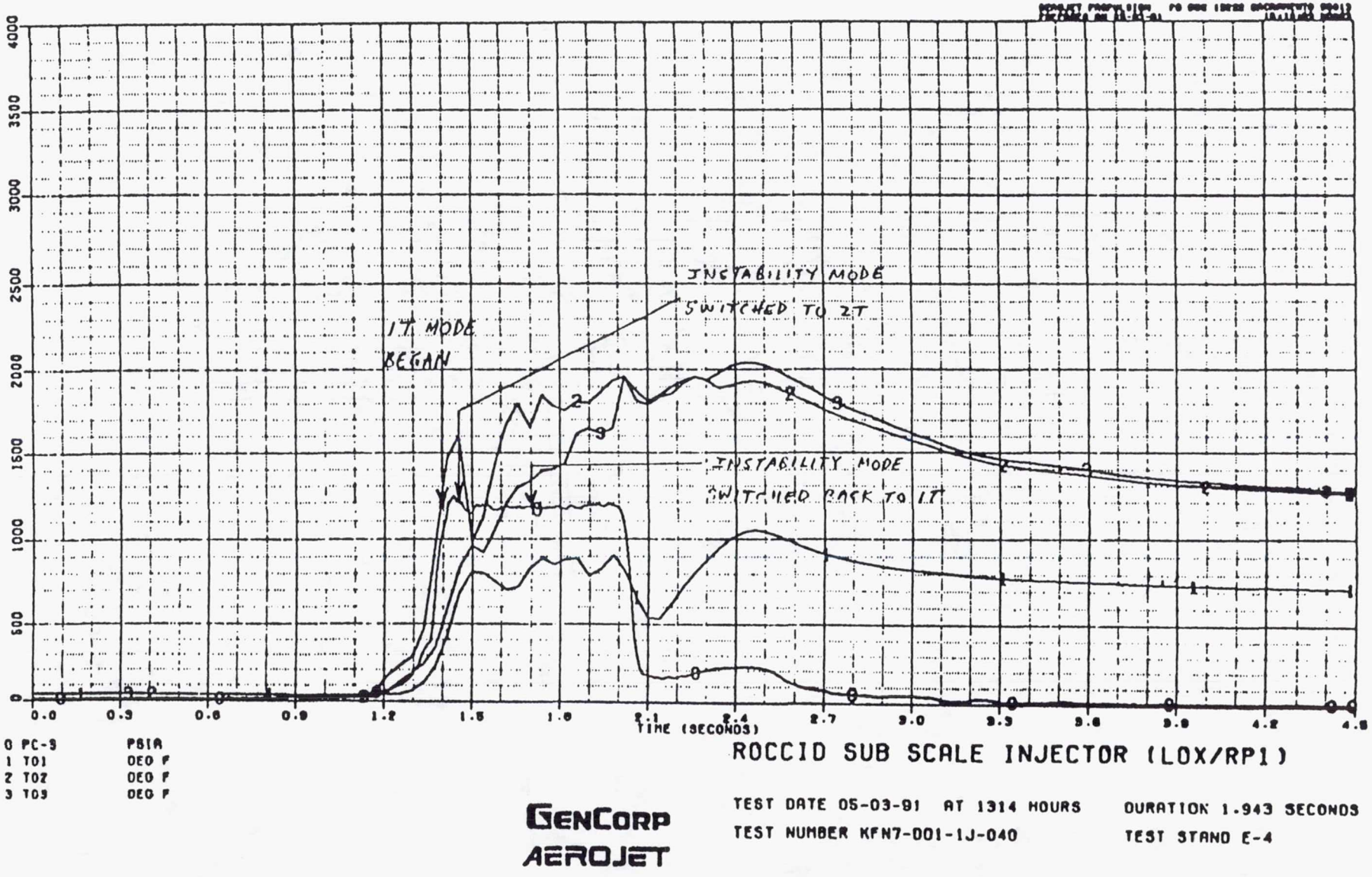

Figure 76. Mean Chamber Pressure and Cavity Temperature vs Time in Test 40

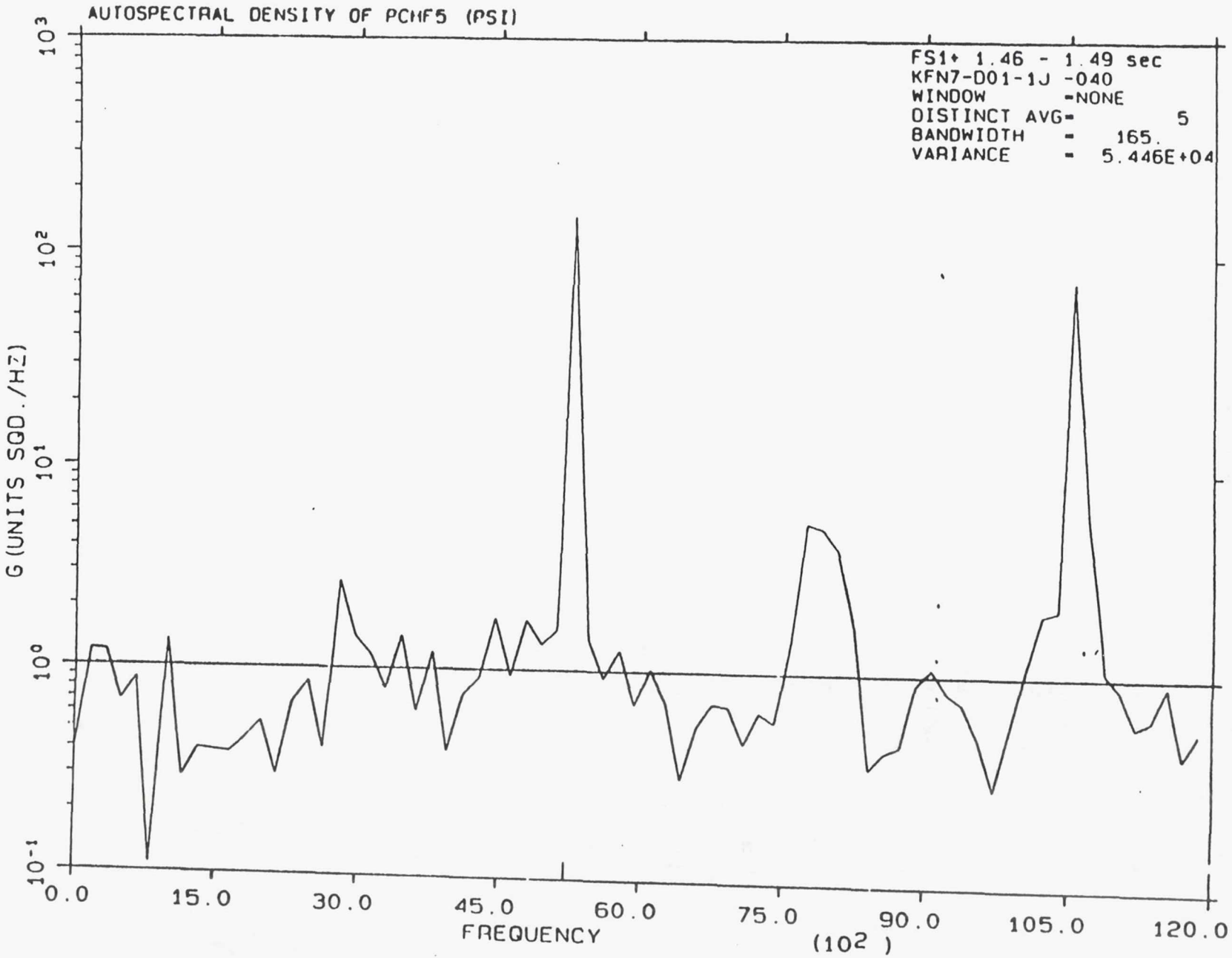

Figure 77. Power Spectral Analysis of Chamber Pressure Indicated 2T Resonance

by the CSM, is shown in Figure 78. It can be seen from the comparison between Figures 76 and 78 that there was little or no time for the 2T mode to develop in the unstable-combustion tests where the test shutdown was initiated by the CSM before steady-state operation was achieved. This is probably the reason for the extremely brief appearance or even non-existence of the 2T mode in the waterfall plots for other unstable combustion tests.

The observed combustion instabilities have been correlated with chamber pressure, mixture ratio, and injection pressure drop. The stability test results are shown as a function of chamber pressure and mixture ratio in Figure 79. The figure shows distinct areas of stable and unstable operation. The unstable region is in the area of high chamber pressure and high mixture ratio whereas the stable region is in the area of low chamber pressure and low mixture ratio. It should be noted that test 37, which could not be positively characterized as previously discussed, was considered to be unstable in this display. Although pressure oscillation amplitudes are smaller in tests with monotuned and bituned cavities than those with blocked acoustic cavities, influences of cavity configurations could not be discerned. Again, the acoustic cavities were not optimally tuned because of the previously described design/drafting error. A neutral line is estimated on Figure 79 to define the boundary of stable and unstable regions. A precise determination of the stable-unstable boundary line would require more test data. The neutral line shows that this particular test engine may operate stably at mixture ratio less than approximately 1.6 or at chamber pressures less than 650 psia. Operation at nominal chamber pressure of 1200 psia and mixture ratio of 2.80 was unstable and additional damping would be required to operate stably.

The stability test results were also correlated as a function of the fuel (DPF) and oxidizer (DPO) injector pressure drop as shown in Figure 80. This correlation also shows distinct stable and unstable regions. The unstable region is in the area of high DPO and high DPF. Again, no influences of cavity configurations are apparent from this correlation. An approximated stable-unstable boundary line is drawn on the figure. This line shows that this particular test engine may operate stably if the RP-1 injection pressure drop is less than 70 psi or if the oxygen injection pressure drop is less than 115 psi.

H. TEST ANALYSIS AND ROCCID METHODOLOGY ASSESSMENT

Predictions of the validation test hardware combustion stability and performance over a wide range of operating chamber pressure and mixture ratio were made well in advance of the validation testing. These predictions are described in Section IV.C. and IV.D. of this report

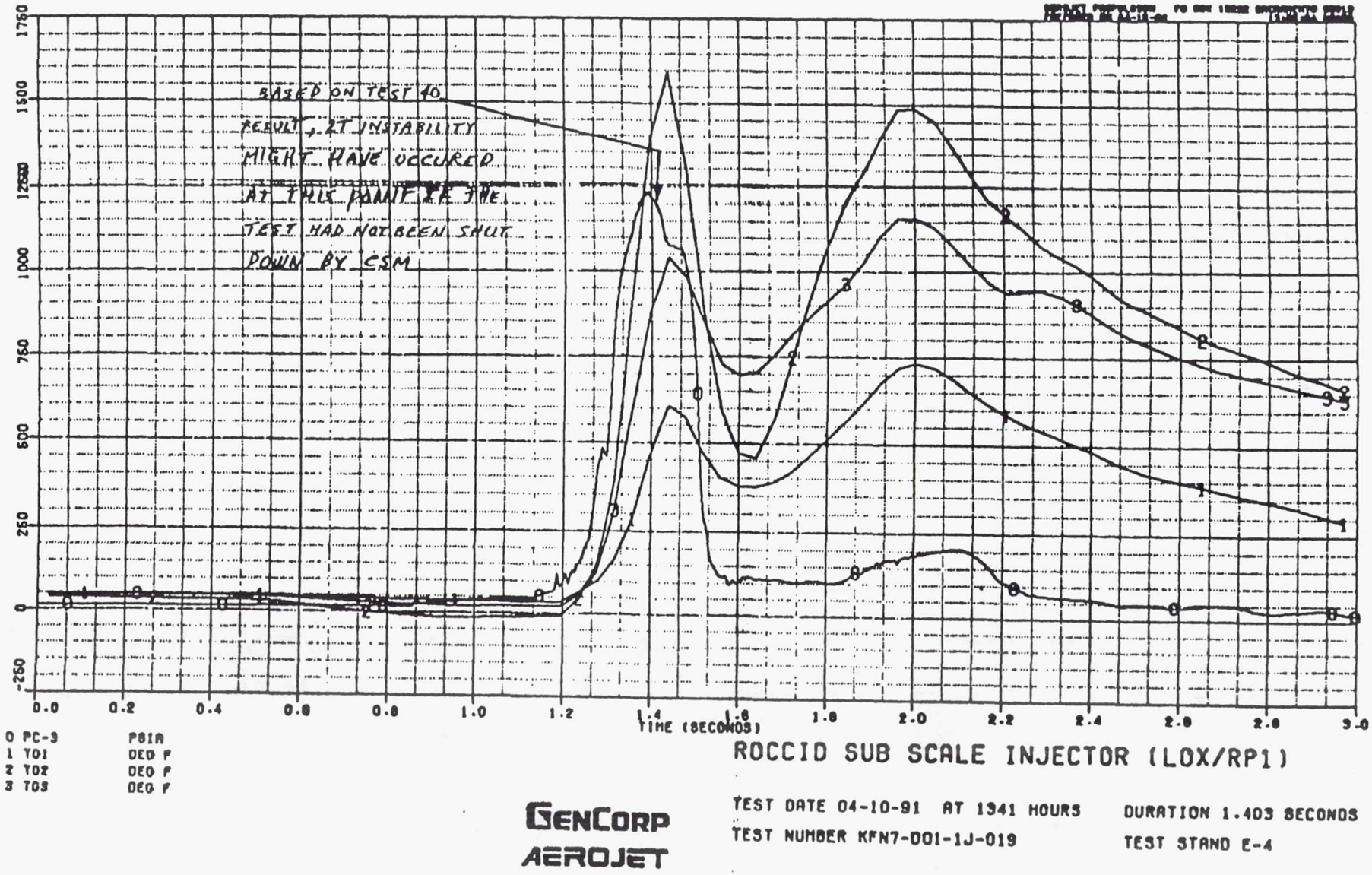

Figure 78. Mean Chamber Pressure vs Time in Test 19, Typical of Unstable-Combustion Tests Which Were Shutdown Early by CSM

open symbol: stable
solid symbol: unstable
number 1-20: test with bituned cavities
number 21-28: test with blocked cavities
number 29-40: test with a monotuned cavity

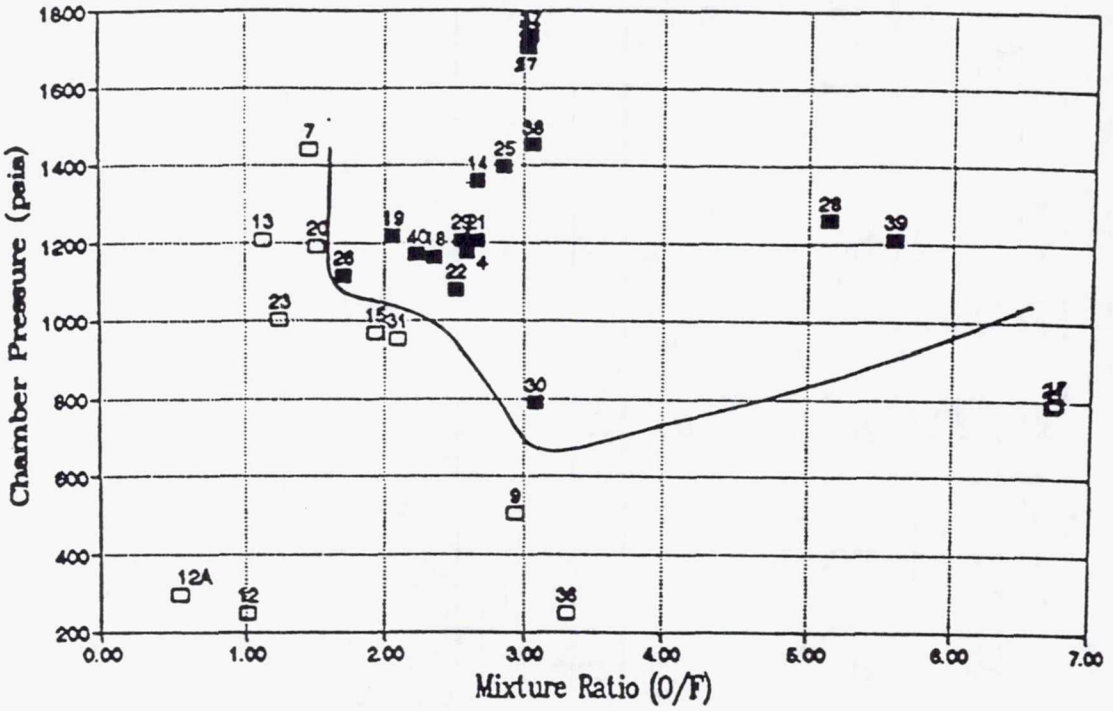

Figure 79. Pc-MR Stability Map

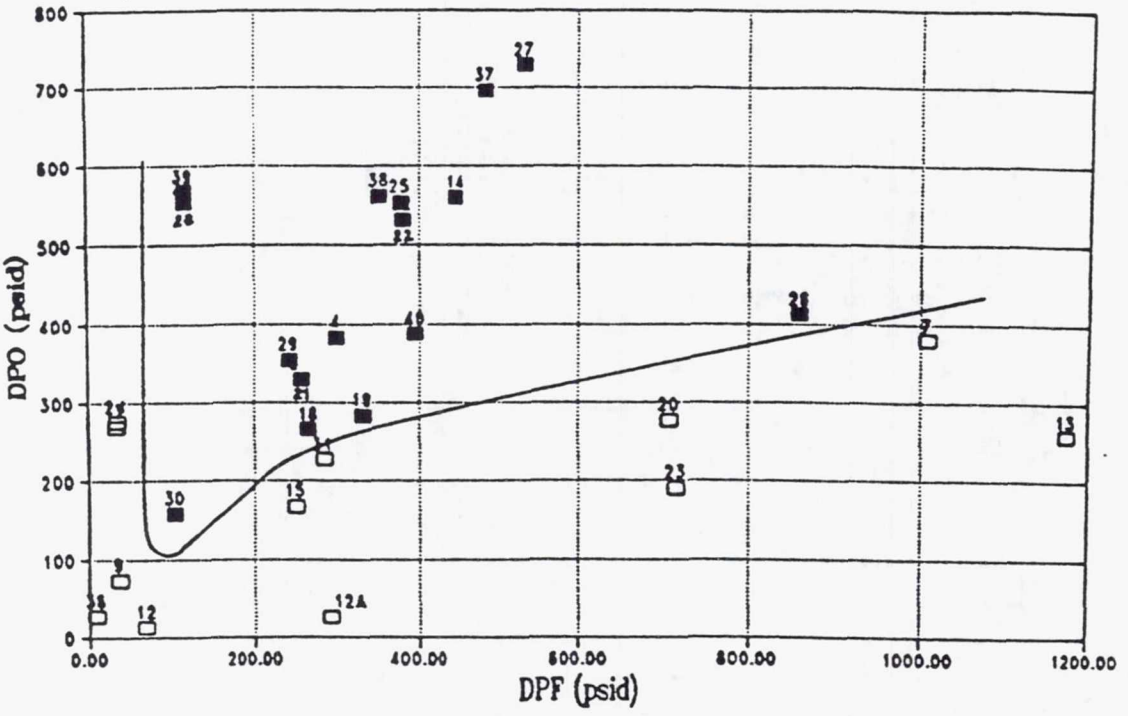

Figure 80. DOP-DFP Stability Map

and in great detail in references 14, 15, and 18. In addition, in order to provide a direct quantitative comparison of the ROCCID calculated stability and performance parameters with test measured and derived parameters, the ROCCID methodology was applied using the point analysis option for each valid test. The actual hardware design parameters, including the erroneously designed acoustic cavities, and the measured mixture ratio, chamber pressure, propellant temperatures, and chamber throat area for each test were input to ROCCID to facilitate this direct comparison.

In performing these calculations, no attempt was made to anchor any input parameters using the validation test data. Anchoring parameters from Reference 13 (Table 8 of Reference 13) and identical to those used for the pretest predictions were used in these calculations. These included a factor of 1.20 on the oxidizer dropsize, 0.08 on the atomization lengths for vaporization calculations, 0.9 for the predicted chamber sound speed and 0.925 on the overall Em predicted using Nurick's technique. In addition, the unielement Em (Em_{uni}) was determined from the correlation of cold flow test data of Reference 13.

$$Em_{uni} = 1.04 - 0.185*R + 0.042*R^2 - 3.37E\text{-}3*R^3$$

where R is the oxidizer-to-fuel momentum ratio. The concentrated combustion plane used in HIFI was assumed to be at an axial position corresponding to 80% of the total energy release. The speed of sound in the acoustic cavity was assumed equal to that in the combustion chamber since the mistakenly designed cavities had large entrance openings and shallow depths. The validity of this assumption was not extensively investigated since the test results indicated that no significant damping was obtained with the cavities installed. This assumption can be viewed as indicative of an a-priori estimate for the purposes of the ROCCID calculations.

A comparison of the predicted and measured performance in terms of C* and the thrust based energy release efficiency (ERE) is shown in Table 28. The calculated and measured C* combustion efficiencies are plotted against mixture ratio in Figure 81. The calculated and measured ERE efficiencies are plotted against mixture ratio in Figure 82. It should be noted that all data even from tests with short duration or derived measurements were plotted in the figures. Both calculation and measurement showed consistencies between C* and ERE efficiencies. The measured performance of the engine was, however, significantly lower than predicted by the ROCCID methodology.

TABLE 28. MEASURED AND PREDICTED VALIDATION ENGINE PERFORMANCE

			Calculated		Measured	
Test	Pc	Mr	Eta-C*	ERE	Eta-C*	ERE
4	1178	2.59	0.983	0.983	0.801	0.842
7	1441	1.45	0.990	0.989	0.975	0.972
9	505	2.94	0.988	0.988	0.994	0.987
12	250	1.01	0.981	0.980	0.863	0.792
13	1210	1.13	1.003	1.004	1.049	1.010
14	1460	2.67	0.985	0.985	0.932	0.948
15	969	1.93	0.980	0.981	0.968	0.951
17	795	6.74	0.991	0.991	1.025	1.015
18	1165	2.35	0.979	0.979	0.978	0.997
19	1220	2.06	0.979	0.980	0.994	1.000
20	1193	1.50	0.983	0.982	0.955	0.948
21	1222	2.67	0.984	0.984	0.934	0.928
22	1092	2.75	0.980	0.980	0.836	0.924
23	1004	1.25	1.014	1.016	0.961	0.937
24	788	6.71	0.990	0.990	0.956	0.947
25	1410	2.86	0.987	0.987	0.908	0.926
26	1130	1.70	0.983	0.983	0.736	0.753
27	1755	3.03	0.990	0.990	0.890	0.938
28	1260	5.15	0.994	0.994	0.904	0.946
29	1208	2.55	0.982	0.982	0.927	0.915
30	791	3.09	0.991	0.990	0.919	0.921
31	953	2.09	0.978	0.979	0.843	0.663
36	249	3.31	0.990	0.990	0.931	0.899
37	1738	3.05	0.990	0.990	0.918	0.927
38	1467	3.07	0.991	0.990	0.920	0.963
39	1214	5.60	0.994	0.994	0.945	0.916
40	1180	2.23	0.978	0.978	0.874	0.886

Note: Efficiencies greater than 1.00 are suspect and are probably the result of interpolation accuracies for calculated values or test measurement accuracies for measured values. See Section IV H

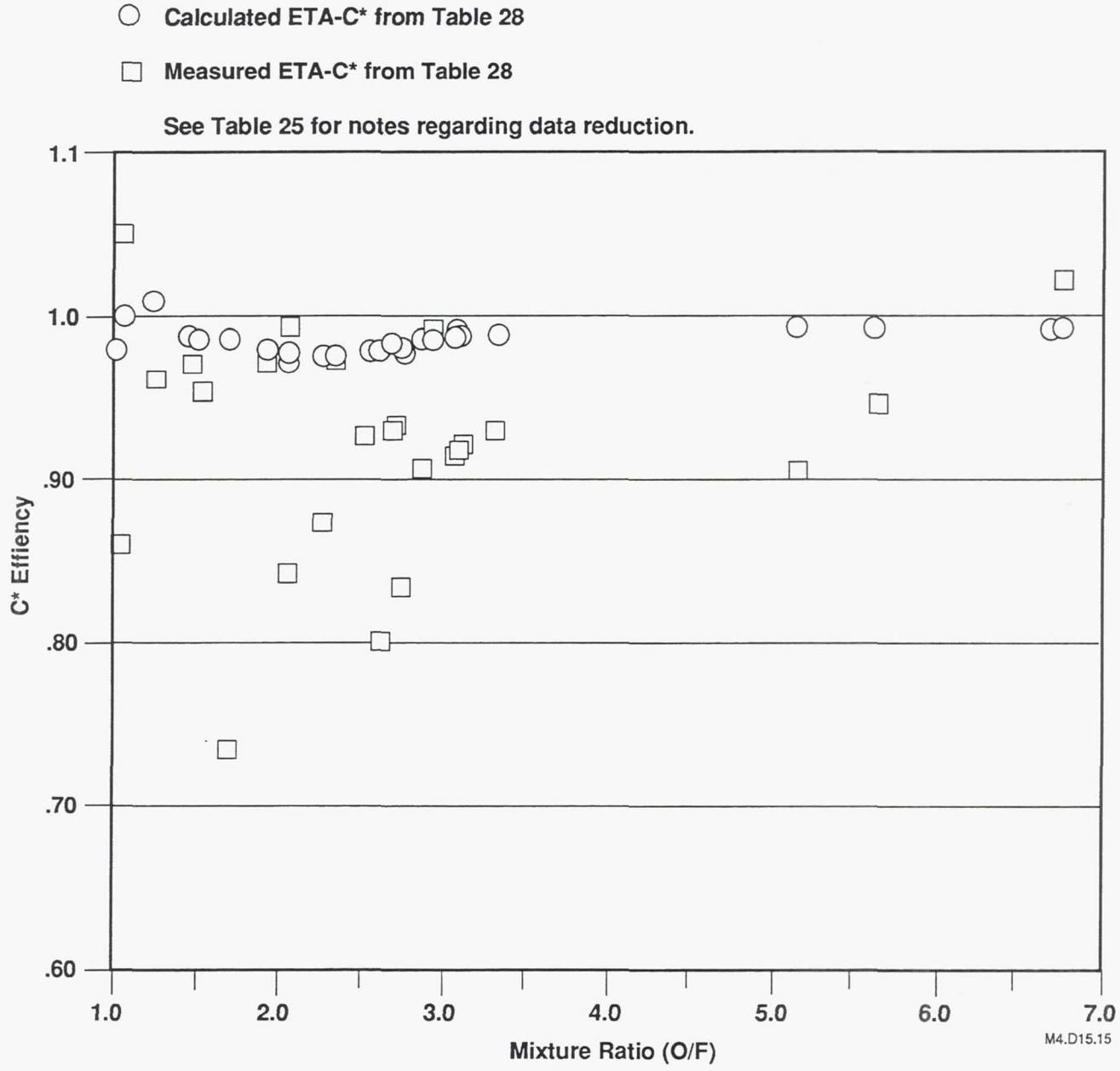

Figure 81. Comparison of Unanchored ROCCID Predictions and Test Results - C* Efficiency

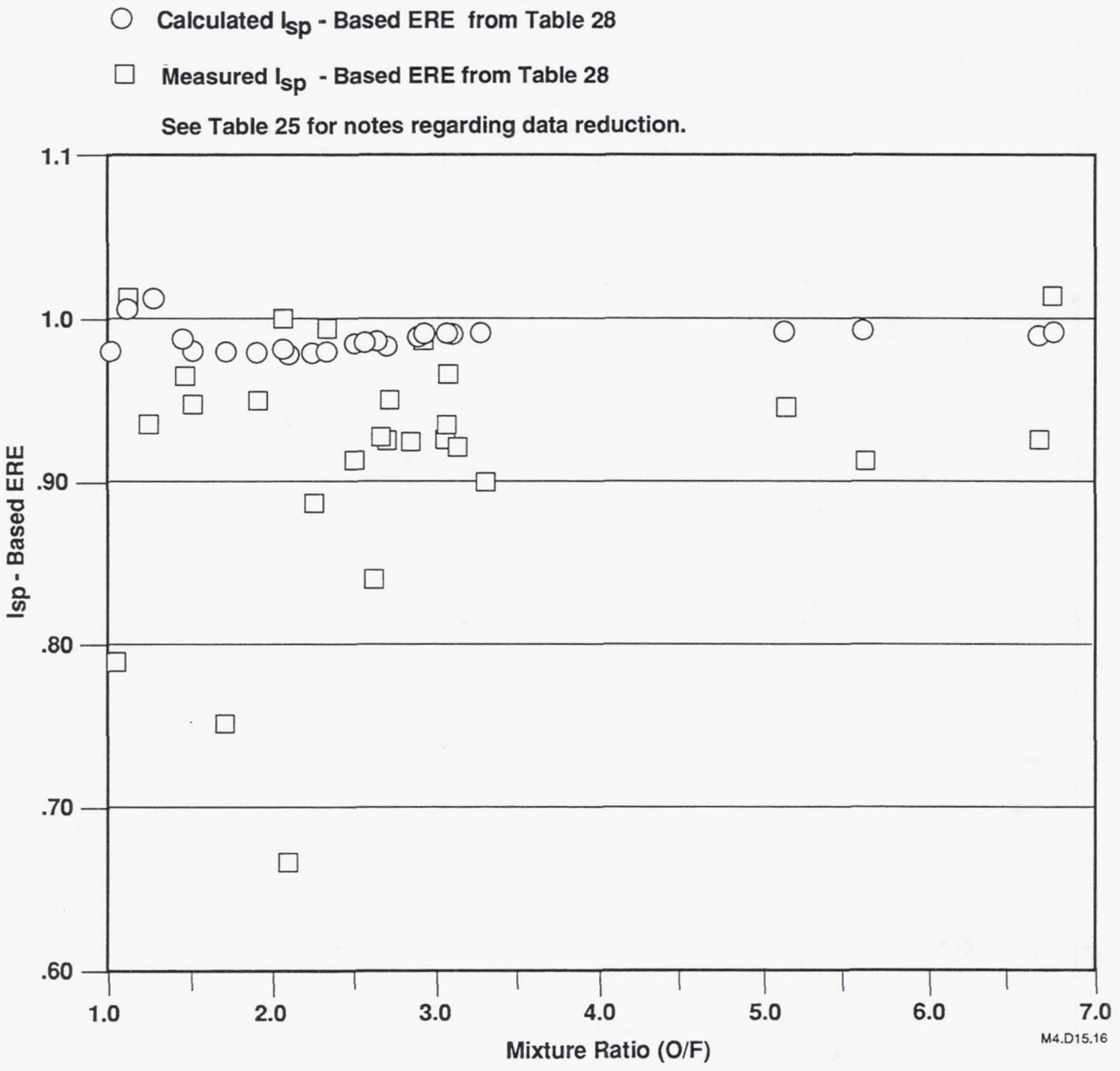

Figure 82. Comparison of Unanchored ROCCID Predictions and Test Results - ISP-Based ERE

The C* efficiency from the ROCCID point analysis ranged from a low value of 97.8% at a mixture ratio of 2.2 to a value slightly over 100% at a mixture ratio of 1.2. Efficiencies slightly greater than 100% as calculated by ROCCID resulted because of inflections in the Isp (ODE) versus mixture ratio curve as interpolated by ROCCID. No attempt was made to determine the vaidity of these inflection points. The ROCCID calculated ERE values were within 0.2% of the ROCCID calculated C* efficiencies. The measured C* efficiencies ranged from a low value of 87% at a mixture ratio of 2.9 to a value of 104.9% at a mixture ratio of 1.13. In tests with sufficient steady-state duration where accurate measurements were made, the measured C* and ERE efficiencies agreed within 2%. The largest difference between calculated and measured efficiency values is approximately 0.07 (7%). Test results showed that the efficiencies are more sensitive to mixture ratio than predicted. In addition, calculations showed that the minimum efficiency occurs at a mixture ratio of 2.2 while test results showed that the minimum efficiency occurs at a mixture ratio of 2.9. The disagreement suggested that the propellant mixing and vaporization rate might have been overpredicted.

The vaporization efficiency at near the stoichiometric mixture ratio appears reasonable based on a comparison between the predicted and measured static pressure profiles in the combustion chamber. A typical pressure profile comparison at near nominal conditions is shown on Figure 83. However, at very low or high mixture ratios the ROCCID methodology overpredicts the vaporization rate, as can be seen from the comparison between the predicted and measured chamber static pressure profiles shown on Figure 84. This overprediction is probably a result of the generalized length correlation used for vaporization estimates that were based on data and calculations assuming typical stoichiometric combustion temperatures. The ROCCID methodology should be modified to reflect the lower vaporization rates at off stoichiometric conditions either by modifying the generalized length correlation or by including a combustion temperature correction factor. Although Figure 84 indicates that the actual vaporization rates were lower than predicted in tests with low or high mixture ratios, the chamber is of sufficient length to produce a high overall performance efficiency.

The disagreement between calculated and measured performance is attributed primarily to the overprediction of mixing efficiency by the ROCCID methodology for the following reasons: 1) The performance efficiency and therefore the vaporization efficiency is high at low and high mixture ratios. The efficiencies were also high at near the nominal mixture ratio because it can be inferred from the agreement between the measured and calculated pressure

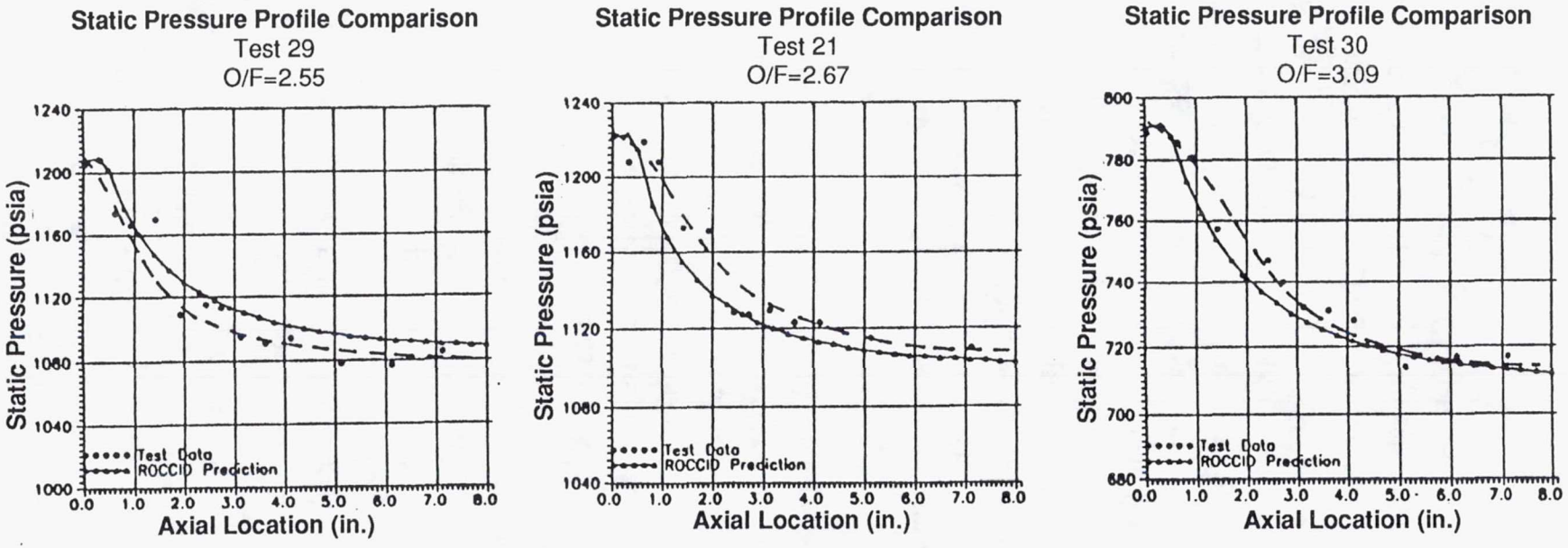

Figure 83. Good Agreement Observed Between Predicted and Measured Chamber Static Pressure Profiles at Near Stoichiometric Mixture Ratio

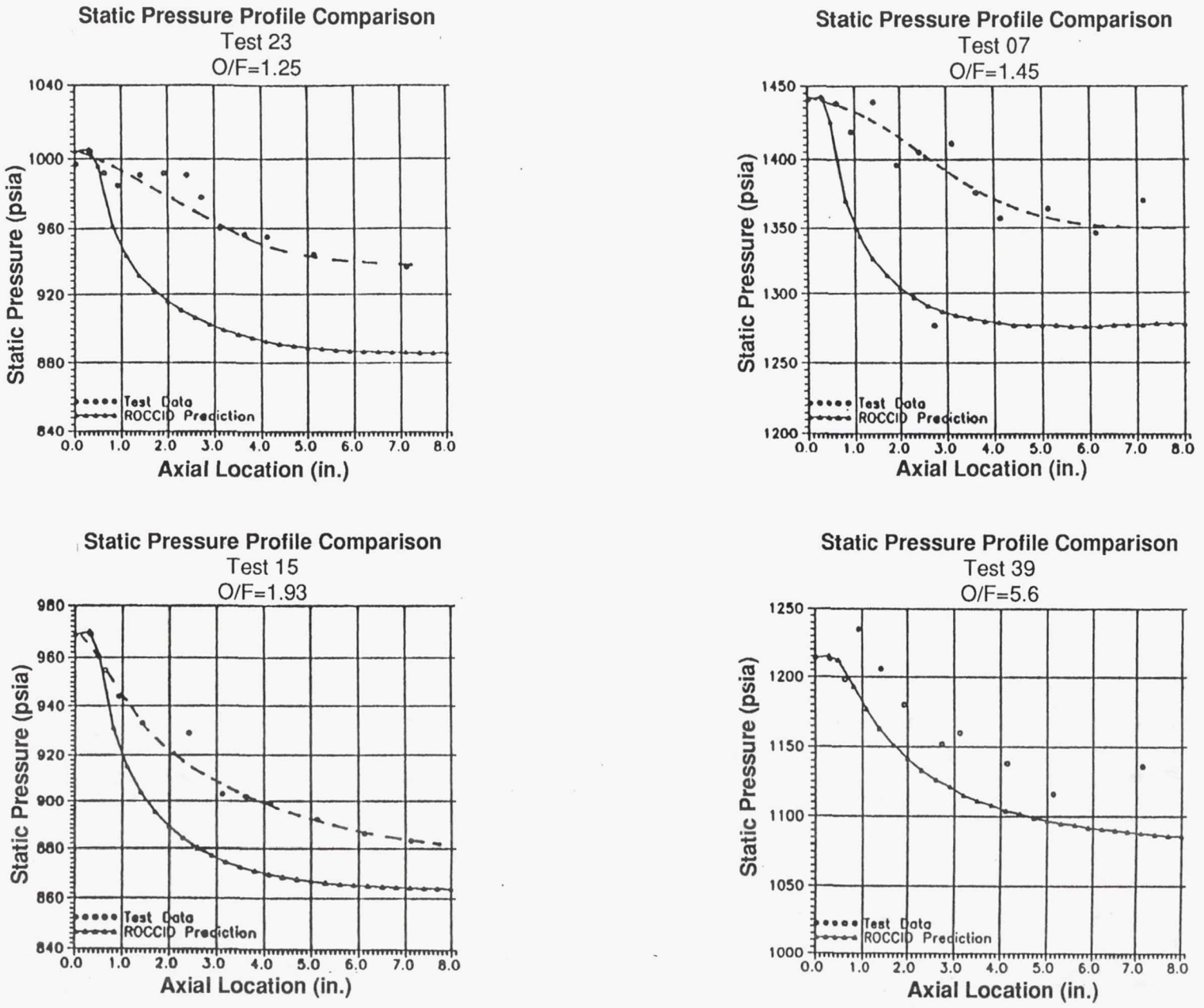

Figure 84. Poor Agreement Observed Between Predicted and Measured Chamber Static Pressure Profiles at Very Low and High Mixture Ratios

profiles and 2) Poor mixing can result in low efficiencies when the combustor is operated near the nominal mixture ratio where the values of C* and ISP are maximum, but not necessarily result in low efficiencies when the engine is operated at very low or very high mixture ratio, since performance loss in fuel lean or fuel rich stream tubes is compensated for by performance gains in stream tubes operating near to stoichiometric values.

The mixing efficiency used in the performance prediction was 0.874. This value was obtained using the DPOPMIX correlation in ROCCID with the unielement E_m of 0.77 as an input to the correlation and an anchoring factor of 0.93. The values of the unielement E_m and anchoring factor were obtained from the Reference 13. A better match of the prediction to the data is obtained if a multielement Em value of 0.75 was used in ROCCID.

The significantly finer pattern on the ROCCID engine compared to the Ref. 13 engine actually decreased propellant mixing and performance, although performance was predicted to increase with the finer pattern. Cold flow testing, shown in the photograph of Figure 57 indicates that the propellant spray fan formation from individual elements is not complete before adjacent elements begin to restrict the fans. This may cause a multielement mixing efficiency that is actually lower than the unielement mixing efficiency. To confirm this it is recommended that both unielement and multielement cold flow tests be conducted to measure the cold flow mixing efficiencies.

The spray fan formation observed from the ROCCID cold flow was used to estimate the amount of fan interaction and depict this fan overlap on the ROCCID injector pattern drawing. In addition, the Reference 13 injector pattern drawing was used to layout the estimated fan overlap from that design, using the orifice diameter ratios for the two injectors as the scaling parameter. The results are shown on Figure 85. The Reference 13 design shows good individual element fan development before intersection with adjacent fans, indicating that the presence of the adjacent fans do not restrict the fan formation and intra-element mixing. Of course, if the elements are too widely spaced, there would be no enhancement of the mixing efficiency going from a unielement to multielement configuration. The correlation currently in the DROPMIX code indicates an increase in multielement Em for a given unielement Em as the pattern fineness increases. This correlation should be used with caution for very fine patterns and an expanded element mixing data base covering a wide range of element pattern densities and element types using both cold flow and hot fire data should be generated.

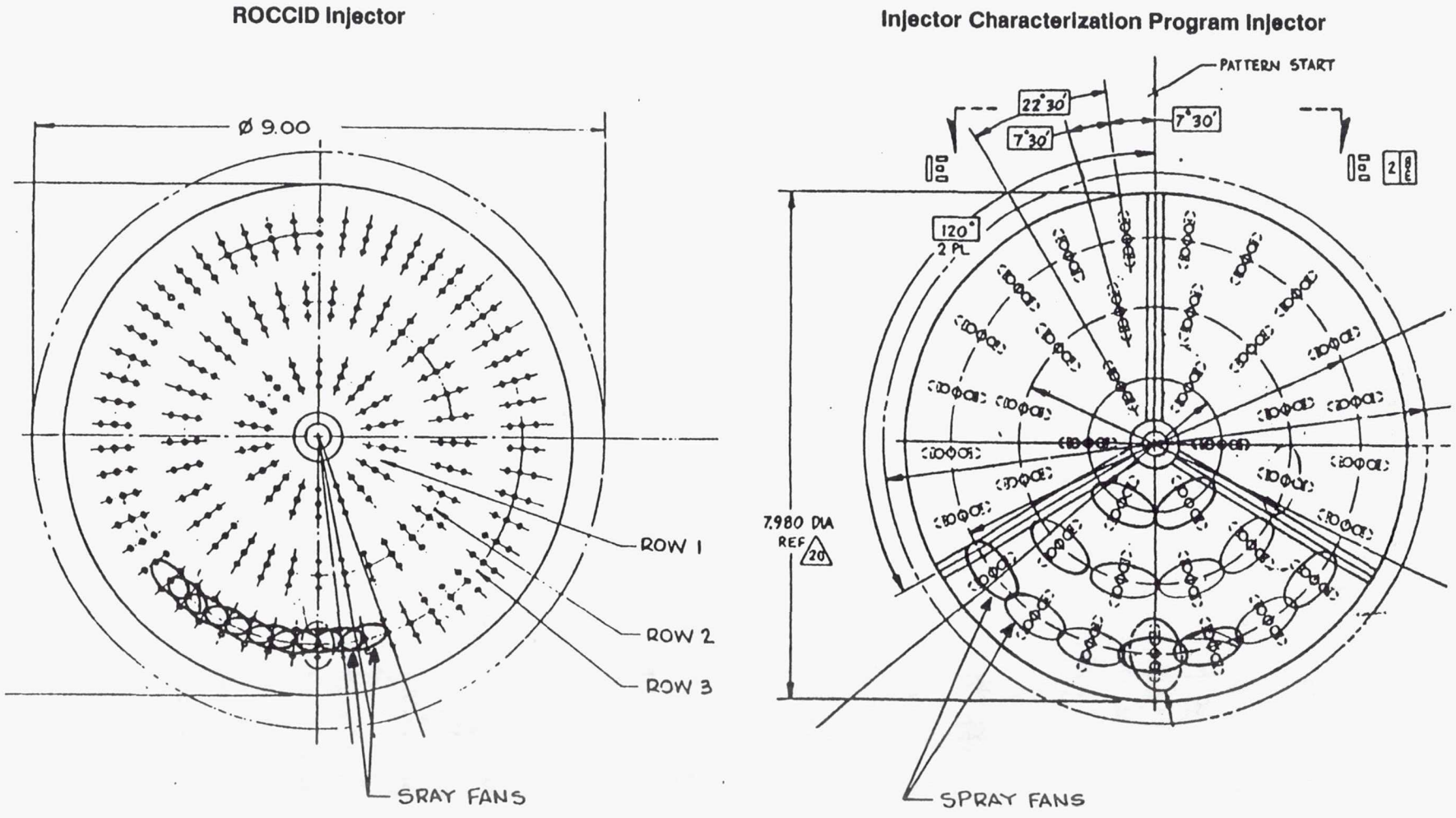

Figure 85. Comparison of ROCCID and Injector Characterization Program Engine Propellant Spray Fan Formation

Nonacoustic Stability

ROCCID calculations showed that the validation engine was chug stable at all operating conditions tested. This is in good agreement with test results. No chug instabilities were encountered in any of the tests, which covered a wide range of operating conditions. Calculated chug results are shown in Table 29. The calculated marginal chug PCs are plotted on Figure 86 for comparison with test results. Thus the ROCCID methodology is adequate in terms of defining injection pressure drop requirements.

Acoustic Stability

Acoustic stability calculated results for each test are summarized in Table 30. Test results are also shown in the table for comparison. It should be noted that the value of -2100 1/s was used for growth coefficients where the coefficients were not calculated by ROCCID because the mode is so stable.

The eleven Block 1 tests with a bituned acoustic cavity covered a range of chamber pressures from 250 to 1441 psia and mixture ratios from 0.54 to 6.74. Seven of these tests were stable and four had spontaneous first tangential mode instabilities that ranged from peak-to-peak amplitudes of 46 to 103% of the steady-state chamber pressure. Four of these stable tests had the combustion process disturbed by bombs with overpressures ranging from 5 to 67% of the mean chamber pressure. Two stable tests were low chamber pressure tests for chug stability evaluation and were not bombed and one test had a bomb intended but did not produce a measurable overpressure. The ROCCID methodology correctly predicted all of the four unstable tests but only two of the seven stable tests.

The eight Block 2 tests without an acoustic cavity had chamber pressures from 788 to 1706 psia and mixture ratios from 1.25 to 6.71. Only two of these tests were stable, the lowest and highest mixture ratio tests. These tests had bomb overpressures of 5 and 11% of the mean chamber pressure. Of the six unstable tests all were in the first tangential mode and all were correctly predicted to be unstable by the ROCCID methodology. The methodology correctly predicted, however, only one of the two stable tests.

The eight Block 3 tests with a monotuned cavity had chamber pressures from 249 to 1735 psia and mixture ratios from 2.09 to 5.60. Two of these tests were stable and six were

Table 29. ROCCID Calculated Chug Results
ROCCID Version 30-Jul-91
Date: 23-Oct-91

			Calculated Results	
Test	Pc (psia)	MR	Marginal Chug Pc (psia)	F (Hz)
4	1178	2.59	302	705
7	1441	1.45	258	608
9	505	2.94	257	645
12	250	1.01	83	744
13	1210	1.13	117	763
14	1460	2.67	288	694
15	969	1.93	280	662
17	795	6.74	76	658
18	1165	2.35	291	696
19	1220	2.06	303	704
20	1193	1.50	171	744
21	1222	2.67	274	670
22	1092	2.52	303	710
23	1004	1.25	142	759
24	788	6.71	82	681
25	1410	2.86	277	689
26	1130	1.70	269	633
27	1755	3.03	281	684
28	1260	5.15	118	683
29	1208	2.55	282	676
30	791	3.09	258	654
31	953	2.09	281	670
36	249	3.31	224	600
37	1738	3.05	257	657
38	1467	3.07	260	671
39	1214	5.60	85	651
40	1180	2.23	274	670

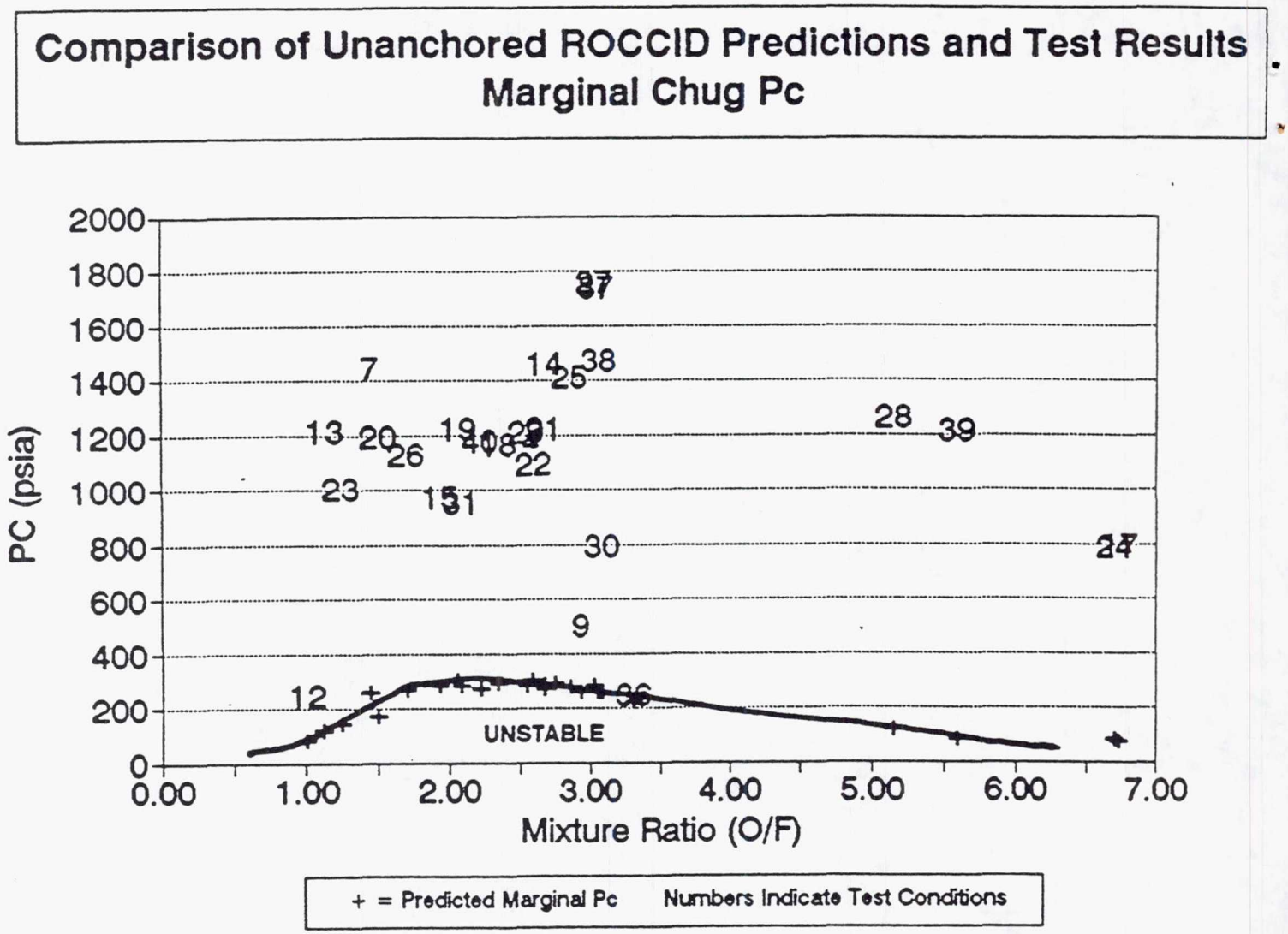

Figure 86. Comparison of Unanchored ROCCID Predictions and Test Results Marginal Chug Pc

TABLE 30.

ROCCID Version 30-JUL-91
Date: 08-OCT-91

COMPARISON BETWEEN CALCULATED RESULTS AND TEST DATA

Operating Condition			Calculated Results[3]												Test Results					
			Chug		Longitudinal		1T		2T		1R		3T		1st Resonance		2nd Resonance		3rd Resonance	
Test	Pc	Mr	Pc,psia[1]	F,Hz	Al,1/s[2]	F,Hz	Al,1/s	F,Hz	Al,1/s	F,Hz	Al,1/s	F,Hz	Al,1/s	F,Hz	Al,1/s	F,Hz	Al,1/s	F,Hz	Al,1/s	F,Hz
4	1178	2.59	302	705	-822	1441	-67	3148	156	4868	-478	5891	-2100	0	153	3303	n/a	6548	n/a	9880
7	1441	1.45	258	608	-933	1566	-267	3627	1137	5122	500	6060	-144	6104	n/a	Stable	n/a	n/a	n/a	n/a
9	505	2.94	257	645	267	1246	-2100	0	-2100	0	-2100	0	-2100	0	n/a	Stable	n/a	n/a	n/a	n/a
12	250	1.01	83	744	-2100	0	-2100	0	-2100	0	-2100	0	-2100	0	n/a	Stable	n/a	n/a	n/a	n/a
13	1210	1.13	117	763	-600	1451	-100	3004	-2100	0	-2100	0	-2100	0	n/a	Stable	n/a	n/a	n/a	n/a
14	1460	2.67	288	694	-1100	2972	278	3130	-56	5009	467	5883	-400	5926	38	3303	n/a	6548	n/a	9910
15	969	1.93	280	662	-1167	1294	200	3550	394	5068	-2100	0	-2100	0	n/a	Stable	n/a	n/a	n/a	n/a
17	795	6.74	76	658	-200	1379	100	2594	-2100	0	-2100	0	-2100	0	-38	Stable	n/a	n/a	n/a	n/a
18	1165	2.35	291	696	-867	1442	-133	3153	533	4839	-367	5867	-2100	0	67	3185	n/a	6489	n/a	9733
19	1220	2.06	303	704	-833	1461	-122	3221	336	5060	-300	6012	-507	7629	37	3185	48	6548	n/a	9733
20	1193	1.50	171	744	-867	1440	278	3224	500	5049	-267	6044	-2100	0	-666	Stable	n/a	n/a	n/a	n/a
21	1222	2.67	274	670	-1178	1535	0	3057	1000	5039	-33	6243	-2100	0	84	3362	n/a	6784	n/a	10205
22	1092	2.52	303	710	-1022	1422	78	3180	178	5086	-2100	0	-2100	0	37	3303	47	6725	n/a	10087
23	1004	1.25	142	759	-1100	1768	133	3009	-2100	0	-2100	0	-2100	0	n/a	Stable	n/a	n/a	n/a	n/a
24	788	6.71	82	681	-67	1383	-189	2647	-2100	0	-2100	0	-2100	0	-73	Stable	n/a	n/a	n/a	n/a
25	1410	2.86	277	689	-1100	2998	100	3141	533	5379	-122	6258	100	6856	128	3244	129	6607	n/a	9969
26	1130	1.70	269	633	-1122	1395	-33	3229	67	5647	133	6556	-293	7418	220	3126	86	6282	n/a	9556
27	1755	3.03	281	684	-1574	3075	0	3597	67	5103	667	6585	667	6907	114	3274	n/a	6725	n/a	9379
28	1260	5.15	118	683	-1133	2758	100	3176	667	4611	-256	5712	-2100	0	n/a	3126	n/a	6400	n/a	9497
29	1208	2.55	282	676	-933	1473	-211	3209	67	5136	133	6418	-400	6868	56	3155	n/a	6430	n/a	9556
30	791	3.09	258	654	100	1705	100	3102	-2100	0	-2100	0	-2100	0	29	2949	n/a	5781	n/a	8700
31	953	2.09	281	670	-767	1826	500	3570	233	5156	-2100	0	-2100	0	n/a	Stable	n/a	n/a	n/a	n/a
36	249	3.31	224	600	-2100	0	-2100	0	-2100	0	-2100	0	-2100	0	n/a	Stable	n/a	n/a	n/a	n/a
37	1738	3.05	257	657	-1678	3039	-100	3604	67	5382	567	6604	522	6927	n/a	3008	n/a	4424	n/a	n/a
38	1467	3.07	260	671	-1289	3034	-122	3134	26	5022	733	6213	-152	6924	55	3185	n/a	6430	n/a	9703
39	1214	5.60	85	651	-1167	2697	67	3135	533	4549	-511	5855	-2100	0	37	2065	n/a	n/a	n/a	n/a
40	1180	2.23	274	670	-933	1459	-167	3232	167	5197	300	6447	-278	7244	94	2772	67	5250	n/a	10500

(1) Chamber pressure below which chug instability is predicted for given test mixture ratio.
(2) AL is the growth coefficient calculated by ROCCID as illustrated in Figure 18.
(3) Calculated results using ROCCID as described in Section IV H.

unstable. Similar to the Block 2 comparison results, the ROCCID methodology predicted correctly all of the six unstable tests but only one of the two stable tests.

The combustion stability test result from all three test blocks are shown in Figure 87 as a function of measured chamber pressure and mixture ratio. An approximate correlation for the stable/unstable transition as a function of chamber pressure and mixture ratio is also provided and compared to the ROCCID prediction. From these results, we were not able to discern any change in this transition boundary with the use of the improperly tuned acoustic cavities. Some additional damping was evident when these acoustic cavities were used, however, based on the observed reduction in the amplitude of the instability and reduced experimental growth coefficient. Similar trends were predicted by ROCCID as noted in Table 30.

A comparison of the experimentally observed stability transition boundary (from Figure 87) to that predicted by ROCCID (1T lower boundary from Figure 35) is shown in Figure 88. From this comparison, the zone of unstable operation expected based on the ROCCID results was somewhat larger than the experimentally determined zone. Interestingly, however, a close correlation between the ROCCID prediction and the observed test results was achieved near the design mixture ratio of 2.8. This may indicate that the stability analysis models provide better predictions at mixture ratios near "nominal" values where a majority of the historical database was generated and upon which the models were developed and verified.

Although all unstable-combustion tests were correctly predicted to be unstable, the instability mode and the growth coefficients were not correctly predicted in several of the tests. The capability to predict precisely the instability modes and accurately the growth coefficients require further improvements of the component models used within ROCCID. As previously discussed in Section IV.G, early shutdown of the test by CSM after a 1T instability was detected during transient start-up provided little or no time for steady-state operation at which the instability may switch to a 2T mode similar to what was seen in test 40. This might explain the discrepancies between the calculated instability mode and test results in a few of the tests.

The discrepancies between calculated and test results are believed to result also from the use of the empirical combustion response and the chamber response model. The weakness of the models is discussed in the following paragraph.

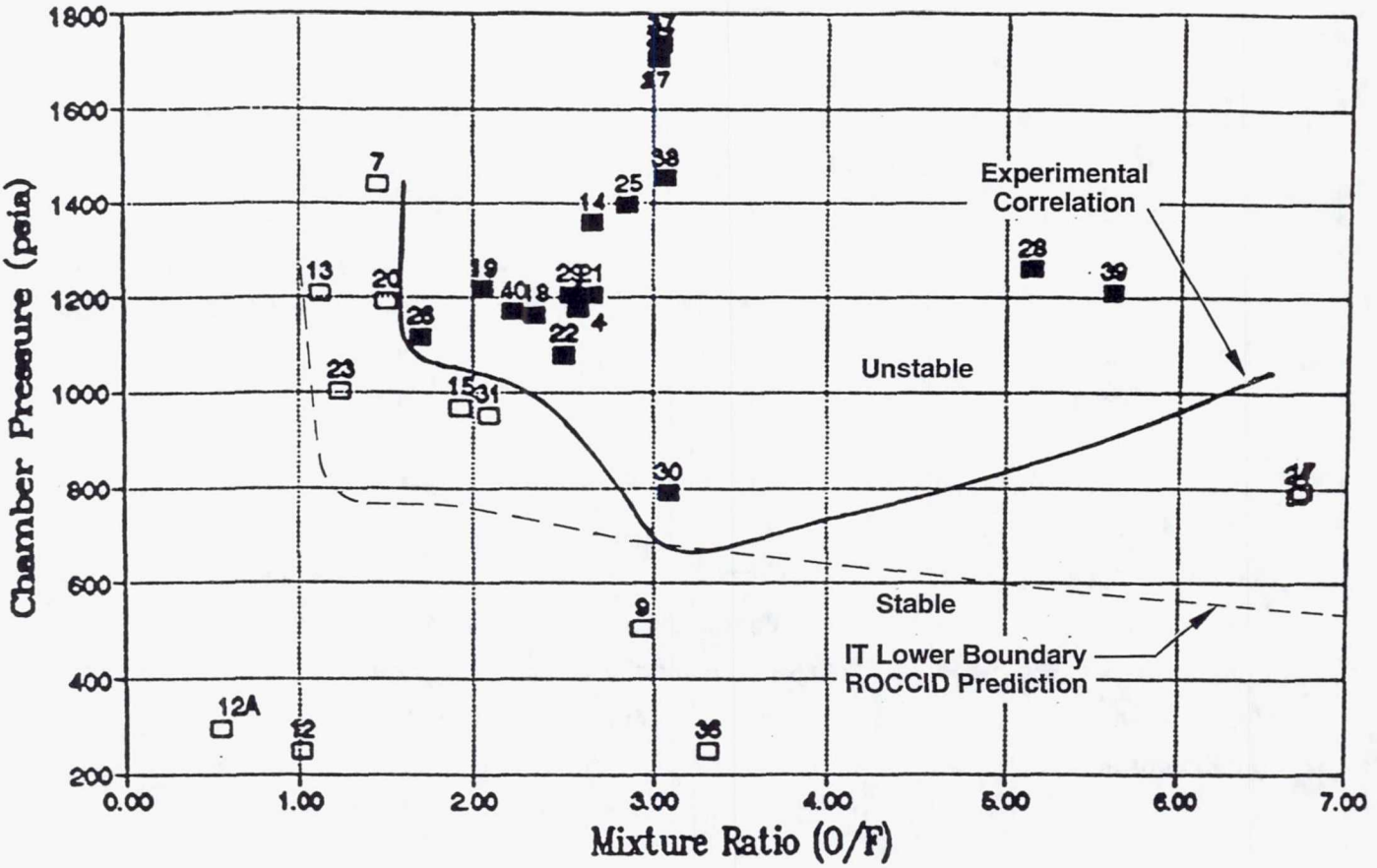

open symbol: stable
solid symbol: unstable
number 1-20: test with bituned cavities
number 21-28: test with blocked cavities
number 29-40: test with a monotuned cavity

Figure 87. ROCCID Validation Test Results Indicate Stable and Unstable Operating Regions

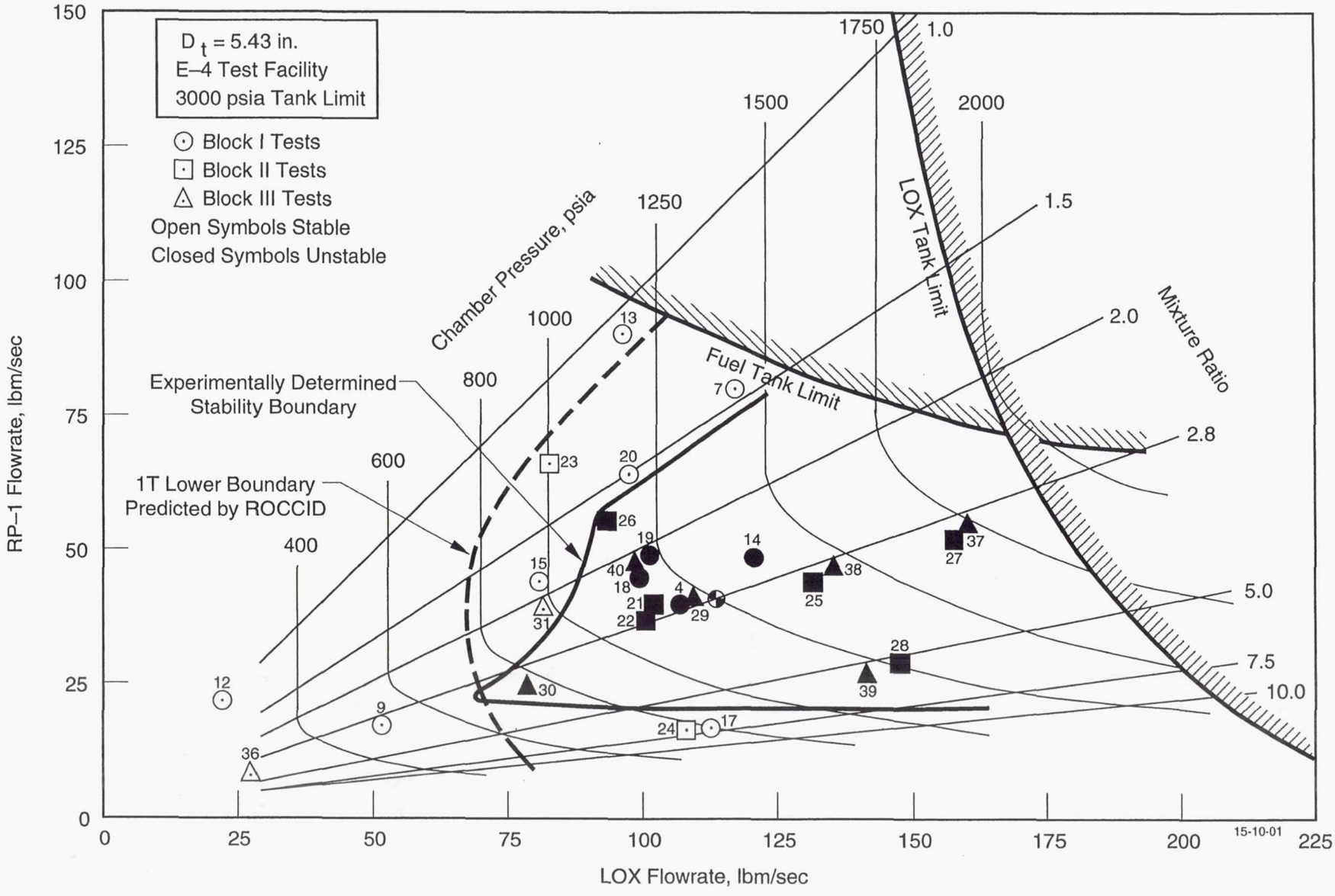

Figure 88. ROCCID Predicted a Somewhat Larger Zone of Unstable Operation Than was Observed Experimentally

The combustion response used in the predictions follow Crocco and Cheng theory, which uses to the pressure interaction index, n and a sensitive time lag, τ. The value for n was obtained using Smith and Reardon's empirical rule - by equating it to the time it takes for 20% of the controlling propellant to evaporate. The controlling propellant is defined as the propellant that is less volatile than the other. For the LOX/RP-1 propellant combination, RP-1 is the controlling propellant. The vaporization time, hence the sensitive lag, is calculated using Priem's generalized length model in ROCCID with the propellant dropsize calculated using Aerojet atomization model. Thus, the accuracy in the prediction of the combustion response depends on the accuracies of the atomization model and the vaporization model.

Interestingly, as noted earlier in this section, the propellant vaporization rate appears to be over predicted at the very low and high mixture ratios where the combustion temperature is significantly lowered. The over prediction in vaporization for the extreme mixture ratios would lead to smaller calculated values of sensitive time lags and thus a larger calculated zone of instability with respect to mixture ratio.

In spite of the relatively good correlation between the ROCCID predictions and the validation test results, determination of the combustion response remains a highly empirical and analyst dependent process. The adequacy of a pirori specification of the combustion response can be a function of the element type and design, the propellants and the available experimental data base. While some analytical approaches, such as CRP and the NASA Lewis Injection Coupling Model have been developed, their application has been relatively limited and generally involved in correlation of tested designs. Clearly, further advancement in the modeling and characterization of the combustion response is essential for improvement in the overall predictive capability of liquid propellant combustion stability.

However, since the whole sensitive time lag methodology, upon which ROCCID is based, is built upon empirical correlations and analytical approaches that have been verified, refined and/or anchored with empirical data generated over the past thirty to thirty-five years, it is not obvious that additional improvements in any specific modeling area would result in an overall improvement in the combustion stability characterization. For example, the chamber response modeling does not account for the acoustic energy damping provided by the chamber wall and the propellant spray. Improvements in this area may be able to be incorporated into the

chamber response model to make it more physically representative. Yet since, the combustion response, n, has been "backed out" from experimental results using chamber response models without the wall and spray damping considerations, its use with the improved chamber response models may actually result in a degradation in the predictive capability of the methodology.

By combining the best performance and stability models into one program and giving them a standard base for comparison, ROCCID has made it possible to rigorously evaluate the models incorporated into the program. Until better models can be developed to accurately and consistently predict the critical parameters that affect engine performance and stability, predictions by the models in ROCCID will have a large error band. Improved diagnostic equipment will permit the acquisition of better data to improve and validate the models. More mechanistic models can be incorporated into ROCCID, which require fewer assumptions in their calculations. CFD generated empirical models for portions of the combustor can also be incorporated.

V. REFERENCES

1. Muss, J.A., Nguyen, T.V. and Johnson, C.W., "User's Manual for Rocket Combustor Interactive Design (ROCCID) and Analysis Computer Program," NASA Contractor Report 187109, Contract NAS 3-25556, May 1991.

2. Breisacher, K.J. and Priem, R.J., "Analysis of 5KHz Combustion Instabilities in 40K Methane/LOX Combustion Chambers," preprared for the 25th JANNAF Combustion Conference Meeting, Huntsville, AL, October 24-28, 1988.

3. Pieper, J.L., "LOX/Hydrocarbon Rocket Engine Analytical Design Methodology Development and Validation Task 1.0 Report - Data/Stability Model Survey," Contract NAS 3-25556, April 1989.

4. "JANNAF Rocket Engine Performance Prediction and Evaluation Manual," CPIA Publication 246, April 1975.

5. Priem, R.J., and Heidmann, M.F., "Propellant Vaporization as a Design Criterion for Rocket Engine Combustion Chambers," NASA TR-R-67, 1960.

6. Nguyen, T.V., "An Improved High Frequency Combustion Stability Model," Presented at the AIAA/ASEE/ASME/SAE 24th Joint Propulsion Conference, Boston Massachusetts, July 1988.

7. Mitchell, C. et. al., "An Improved Protective Model for Injector Face Baffle," 24th JANNAF Combustion Meeting, Monterey, California, October 1987.

8. Mitchell, C.E., "Stability Design Methodology," Report AL-TR-89-041, Air Force Astronautics Laboratory, October 1989.

9. Nguyen, T.V. and Muss, J.A., "Modification of the Agosta-Hammer Vaporization Response Model for the Prediction of High Frequency Combustion Stability," 24th JANNAF Combustion Meeting, Monterey, California, 1987.

10. Muss, J.A., Nguyen, T.V., and Johnson, C.W., "User's Manual for rocket Combustor Interactive Design (ROCCID) and Analysis Computer Program," Volume I - User's Manual, NASA Contractor Report 187109, Contract NAS 3-25556, May 1991.

11. Muss, J.A., Nguyen, T.V., and Johnson, C.W., "User's Manual for Rocket Combustor Interactive Design (ROCCID) and Analysis Computer Program," Volume II - Appendices A-K, NASA Contractor Report 187110, Contract NAS 3-25556, May 1991.

V, References, (cont)

12 Jensen, R.J., Dodson, H.C., and Claflin, S.E., "LOX/Hydrocarbon NASA Lewis Combustion Instability Investigation," NASA CR-182249, 1989.

13. Pieper, J.L., "Oxygen/Hydrocarbon Injector Characterization," Final Report PL-TR-91-3029, Contract F04611-85-C-0100, Phillips Laboratory, June 1991.

14 Pieper, J.L., "LOX/Hydrocarbon Rocket Engine Analytical Design Methodology Development and Validation: Application of the Analytical Design Methodology," NAS 3-25556 Task 3.0 Report, March 1990.

15. Pieper, J.L., and Walker, R.E., "LOX/Hydrocarbon Rocket Engine Analytical Design Methodology Development and Validation: ROCCID Validation Test Plan Development," NAS 3-25556 Task 4.0 Report, June 1990.

16 Harrje, D.T., "Liquid Propellant Rocket Combustion Instability, NAS SP-194, 1972.

17. Smith, A.L., and Reardon, F.H., "The Sensitive Combustion Time Lag Theory and Its Application to Liquid Rocket Combustion Instability Problems," Vol. I Engineer's Manual, Technical Report AFRPL-TR-314, 1968.

18 Pieper, J.L., "Test Plan - LOX/Hydrocarbon Rocket Engine Analytical Design Methodology Development and Validation," Contract NAS 3-25556, August 1990.

19. Pieper, J.L., "LOX/Hydrocarbon Rocket Engine Analytical Design Methodology Development and Validation - Task 5.0 Detail Design," Contract NAS 3-25556, August 1990.

20. Pieper, J.L., "LOX/Hydrocarbon Rocket Engine Analytical Design Methodology Development and Validation - Task 6.0 Component Fabrication," Contract NAS 3-25556, June 1991.

21. Nickerson, G.R., et. al., "Two-Dimensional Kinetics (TDK) Nozzle Performance Computer Program," NAS 8-36863, prepared for NASA/MSFC by Software and Engineering Associates, Inc., March 1989.

REPORT DOCUMENTATION PAGE

Form Approved
OMB No. 0704-0188

1. AGENCY USE ONLY (*Leave blank*)	2. REPORT DATE	3. REPORT TYPE AND DATES COVERED
	May 1993	Final Contractor Report

4. TITLE AND SUBTITLE

LOX/Hydrocarbon Rocket Engine Analytical Design Methodology Development and Validation

5. FUNDING NUMBERS

WU–590–21–21
C–NAS3–25556

6. AUTHOR(S)

Jerry L. Pieper and Richard E. Walker

7. PERFORMING ORGANIZATION NAME(S) AND ADDRESS(ES)

Aerojet Propulsion Division
P.O. Box 13222
Sacramento, Claifornia 95813–6000

8. PERFORMING ORGANIZATION REPORT NUMBER

E–7828

9. SPONSORING/MONITORING AGENCY NAME(S) AND ADDRESS(ES)

National Aeronautics and Space Administration
Lewis Research Center
Cleveland, Ohio 44135–3191

10. SPONSORING/MONITORING AGENCY REPORT NUMBER

NASA CR–191058

11. SUPPLEMENTARY NOTES

Project Manager, Mark D. Klem, Space Propulsion Technology Division, (216) 977–7473.

12a. DISTRIBUTION/AVAILABILITY STATEMENT

Unclassified - Unlimited
Subject Category 20

12b. DISTRIBUTION CODE

13. ABSTRACT ***(Maximum 200 words)***

This final report includes a discussion of the work accomplished on contract NAS3-25556 during the period from December 1988 through November 1991. The objective of the program was to assemble existing performance and combustion stability models into a usable design methodology capable of designing and analyzing high-performance and stable LOX/Hydrocarbon booster engines. The methodology was then used to design a validation engine. The capabilities and validity of the methodology were demonstrated using this engine in an extensive hot-fire test program. The engine used LOX/RP-1 propellants and was tested over a range of mixture ratios, chamber pressures and acoustic damping device configurations. Although the performance was lower than the initial model predictions, the measured performance was adequate to be representative of flight type booster engines. The combustion stability testing was adequate to provide a substantial test data base, although the a-priori predictions with damping devices installed did not forecast some first tangential mode instabilities near the nominal engine operating point. Revision of some model anchoring assumptions and techniques improved the correlation with the test data. Also, recommendations for model improvement are made to further enhance the predicted capability of the model. An extensive listing of the test parameters and test data is contained in Volume II - Appendices.

14. SUBJECT TERMS

Combustion stability; Combustion efficiency; Rocket engine design; Combustion chambers; Rocket thrust chambers; Design analysis; Injectors

15. NUMBER OF PAGES
177

16. PRICE CODE
A09

17. SECURITY CLASSIFICATION OF REPORT	18. SECURITY CLASSIFICATION OF THIS PAGE	19. SECURITY CLASSIFICATION OF ABSTRACT	20. LIMITATION OF ABSTRACT
Unclassified	Unclassified	Unclassified	